# Kyoto FDEPS lectures 4-7 xi 2007
# Dynamics of oceans and atmospheres

P.B. Rhines
University of Washington

## DAY 1

- 1. rotating, stratified fluids: oceans and atmospheres
  - vorticity: a vector-tracer in classical homogeneous fluids
- geostrophic adjustment, thermal wind
- 2. wave dynamics: fundamentals, group velocity, energetics, ray theory
- potential vorticity (PV)
  - vortex stretching, Prandtl's ratio, geography of PV
- 3. Rossby waves
- 4. instability => geostrophic turbulence; subtropical gyres: dynamics, jets and gyres
- 5. meridional overturning circulations and the thermohaline circulation
- 6. Teaching young undergraduates about the global environment
- 7. Seminar: subpolar climate dynamics observed from above and below: altimetry and Seagliders

# Texture

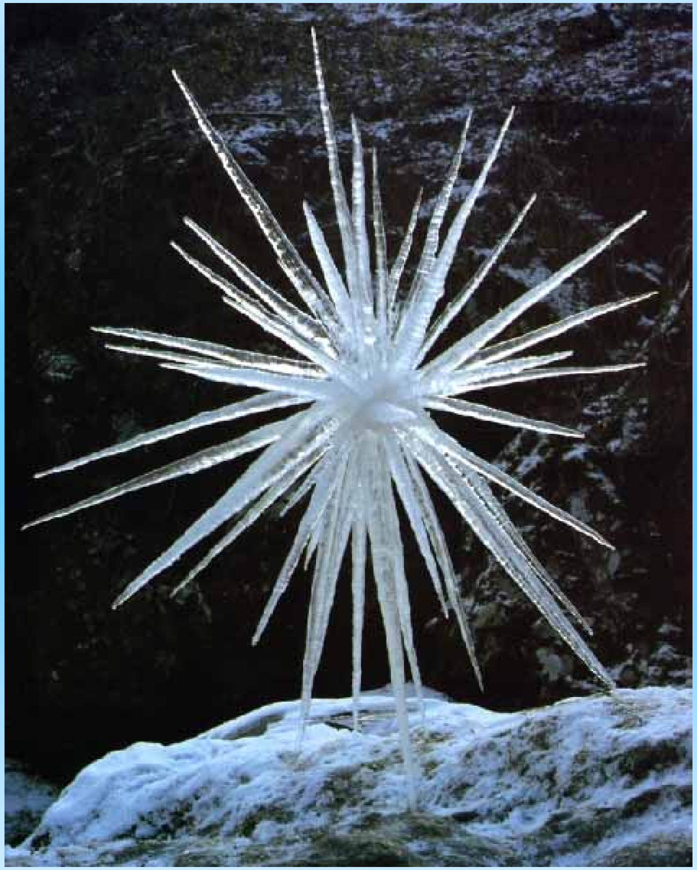

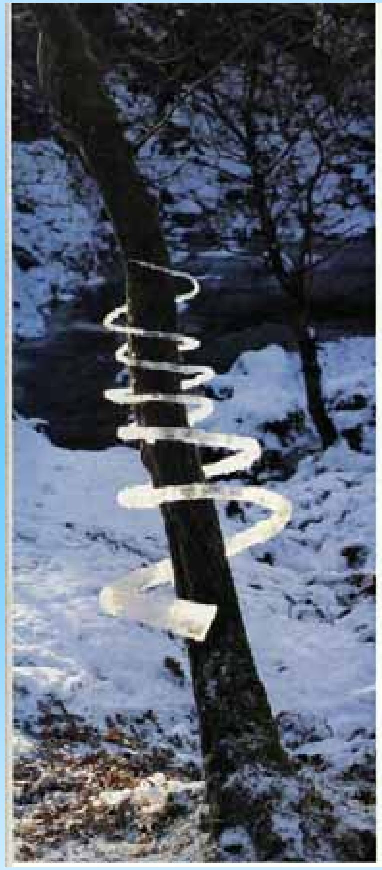

Andy Goldsworthy

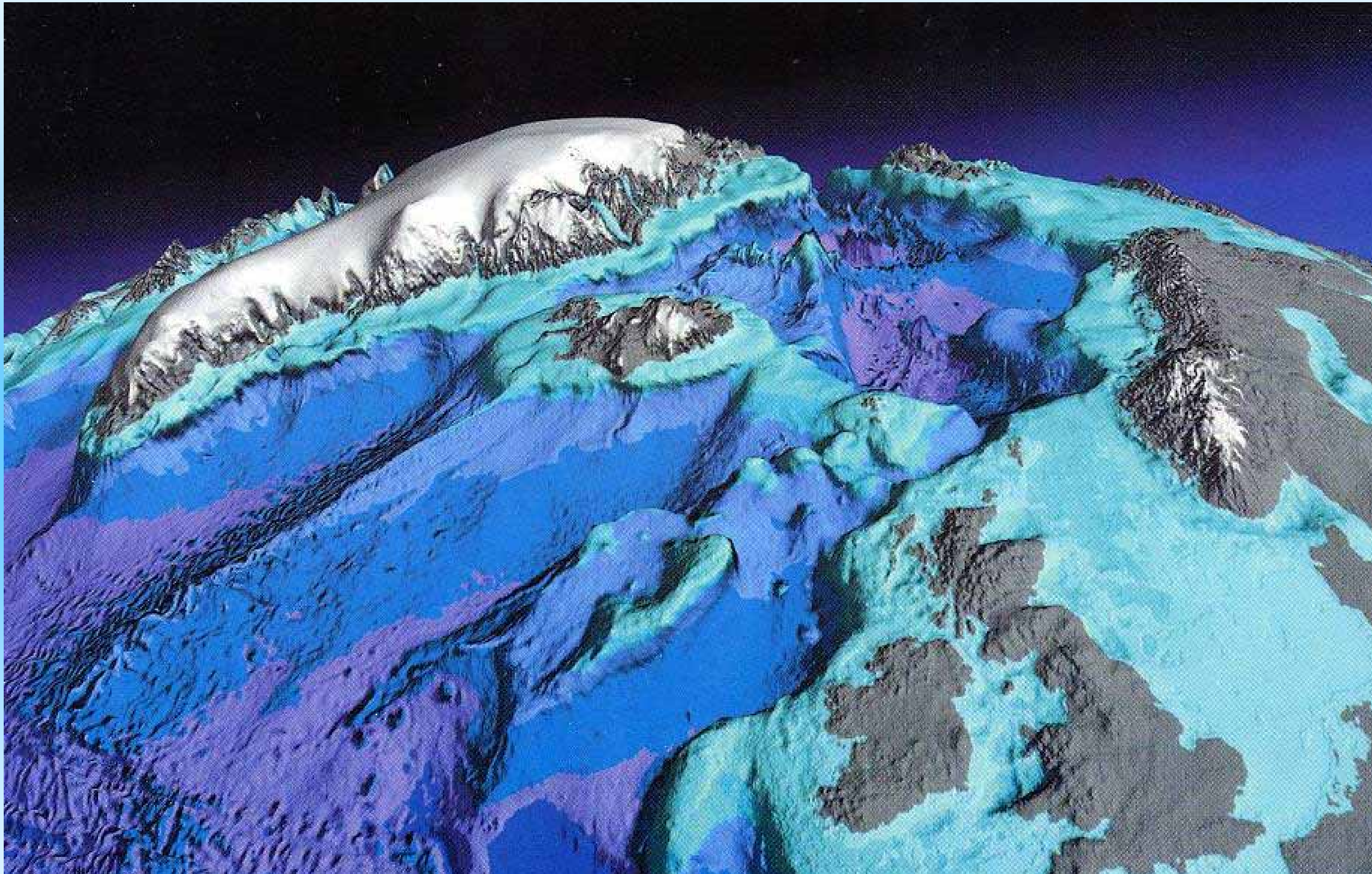

AGU, 2003

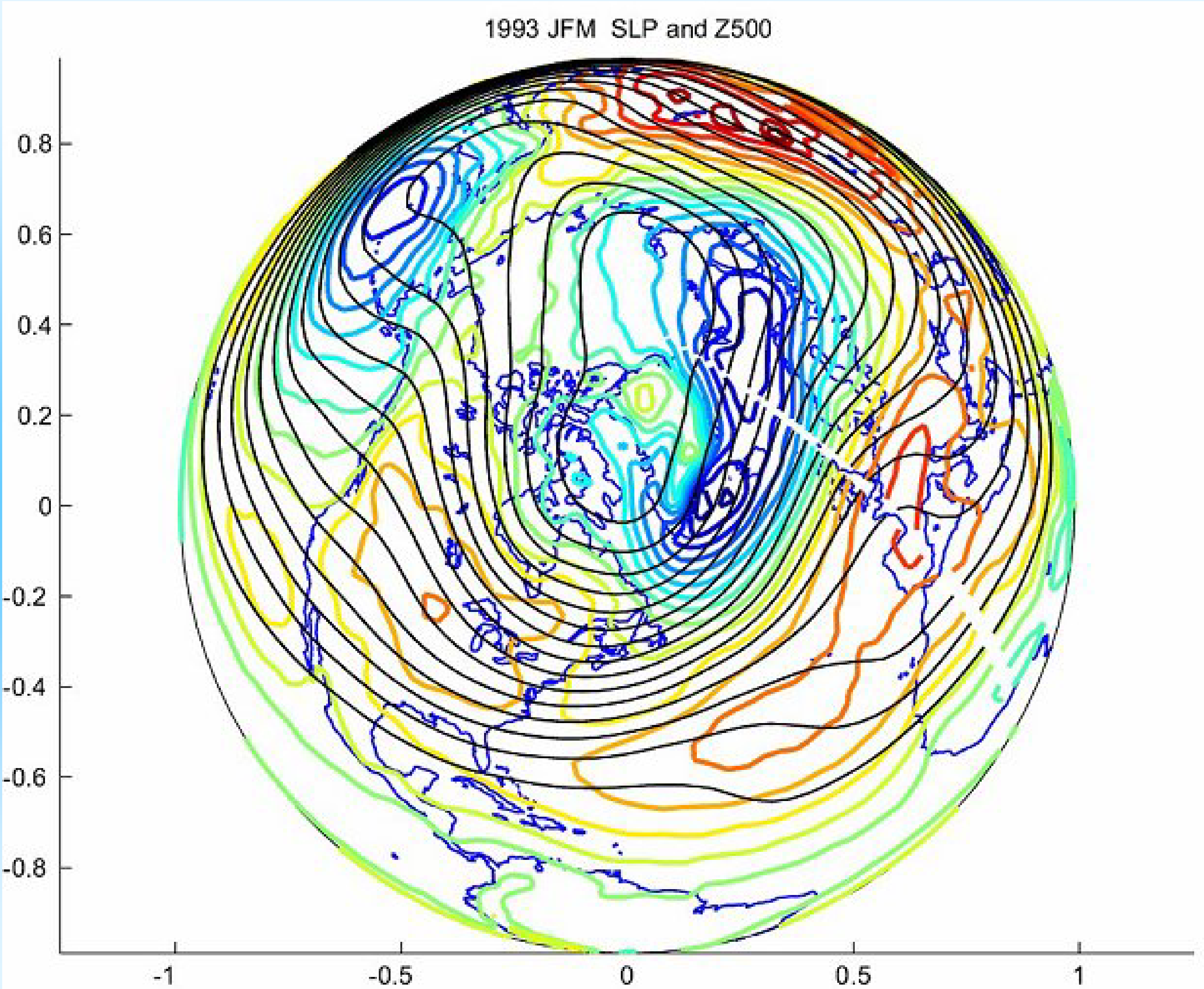
1993 JFM SLP and Z500
0.8
0.6
0.4
0.2
0
-0.2
-0.4
-0.6
-0.8
-1
-0.5
0
0.5
1

# DAY 2

# Kyoto FDEPS lectures 4-7 xi 2007
# Dynamics of oceans and atmospheres
P.B. Rhines
University of Washington

## DAY 2

- 1. rotating, stratified fluids: oceans and atmospheres
  - vorticity: a vector-tracer in classical homogeneous fluids
- geostrophic adjustment, thermal wind
- 2. wave dynamics: fundamentals, group velocity, energetics, ray theory
- potential vorticity (PV)
  - vortex stretching, Prandtl's ratio, geography of PV
- 3. Rossby waves
- 4. instability => geostrophic turbulence; subtropical gyres: dynamics, jets and gyres
- 5. meridional overturning circulations and the thermohaline circulation
- 6. Teaching young undergraduates about the global environment
- 7. Seminar: subpolar climate dynamics observed from above and below: altimetry and Seagliders

# waves: more about steady radiation, group velocity:

-2 dimensional waves from an oscillating wave source

-waves generated with a mean flow (or without mean flow but with a moving wave source)

-internal gravity waves, NH/U, Rossby waves: wave patterns and blocking

In very shallow water, undular bores occur with both gravity- and capillary nature (backward and forward of the bore front, respectively); here in a 5m channel.

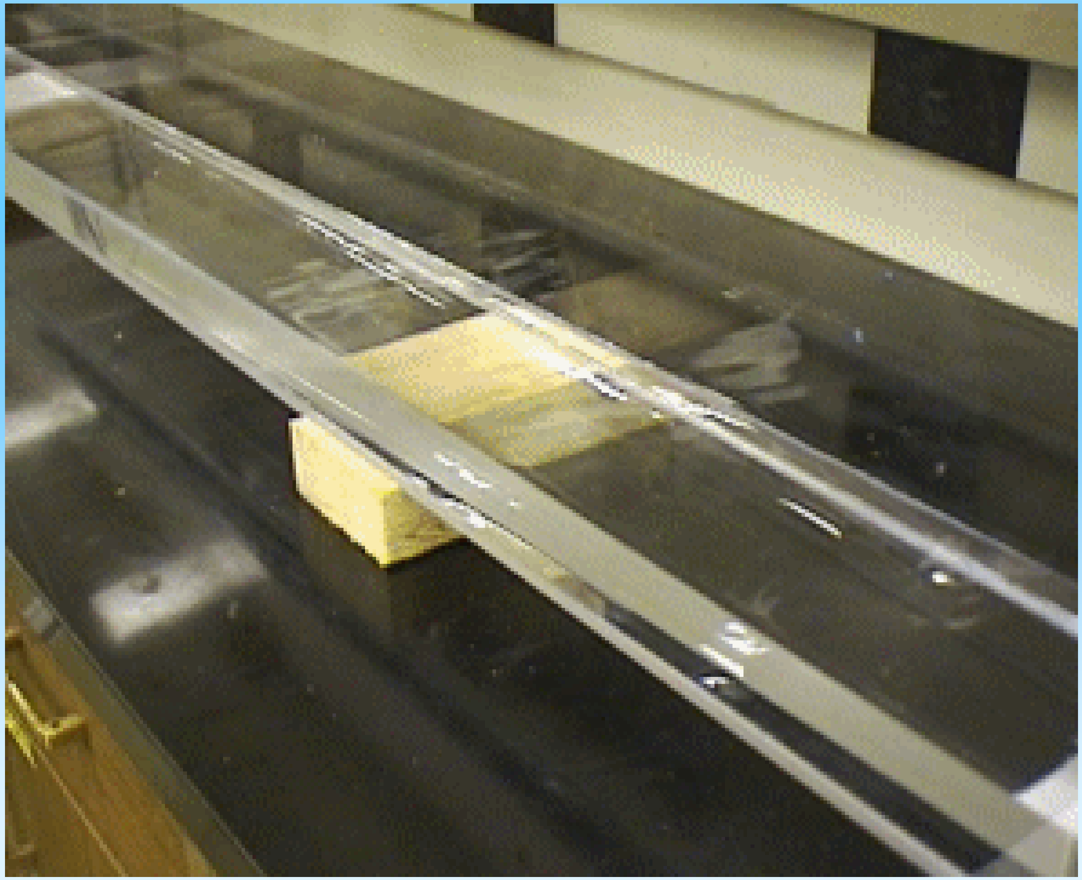

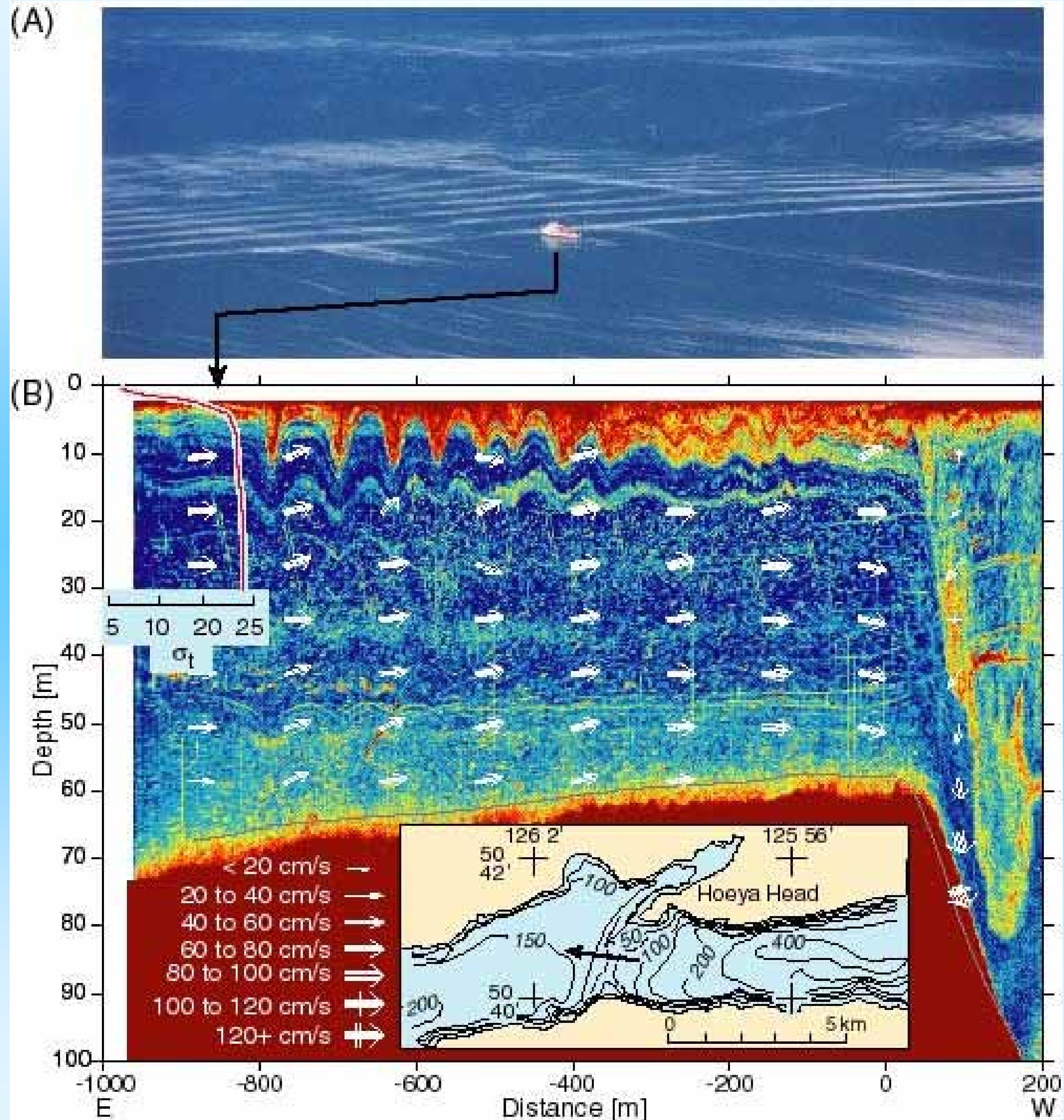
(A)
(B)
Depth [m]
0
10
20
30
40
50
60
70
80
90
100
5 10 20 25
σt
< 20 cm/s
20 to 40 cm/s
40 to 60 cm/s
60 to 80 cm/s
80 to 100 cm/s
100 to 120 cm/s
120+ cm/s
126 2'
125 56'
50 42'
50 40'
Hoeya Head
100
150
50
100
200
400
200
0
5 km
-1000
-800
-600
-400
-200
0
200
E
W
Distance [m]

# internal gravity waves: rays and modes

*Jim Renwick, GFD lab Univ of Washington*

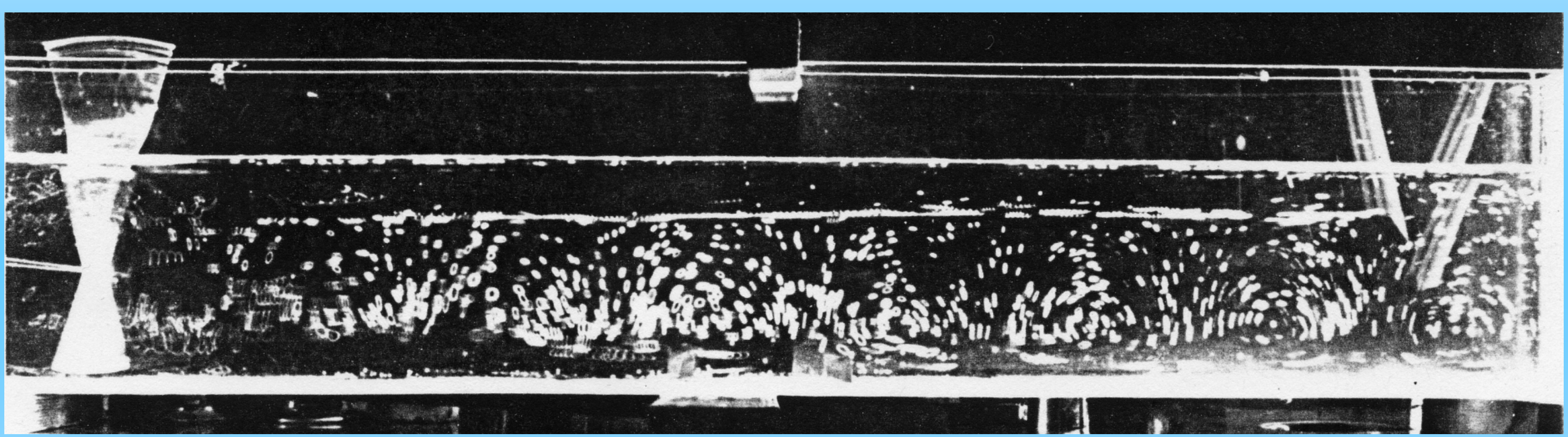

Waves: modes and rays and wave/mean-flow interaction at the base of the mixed layer

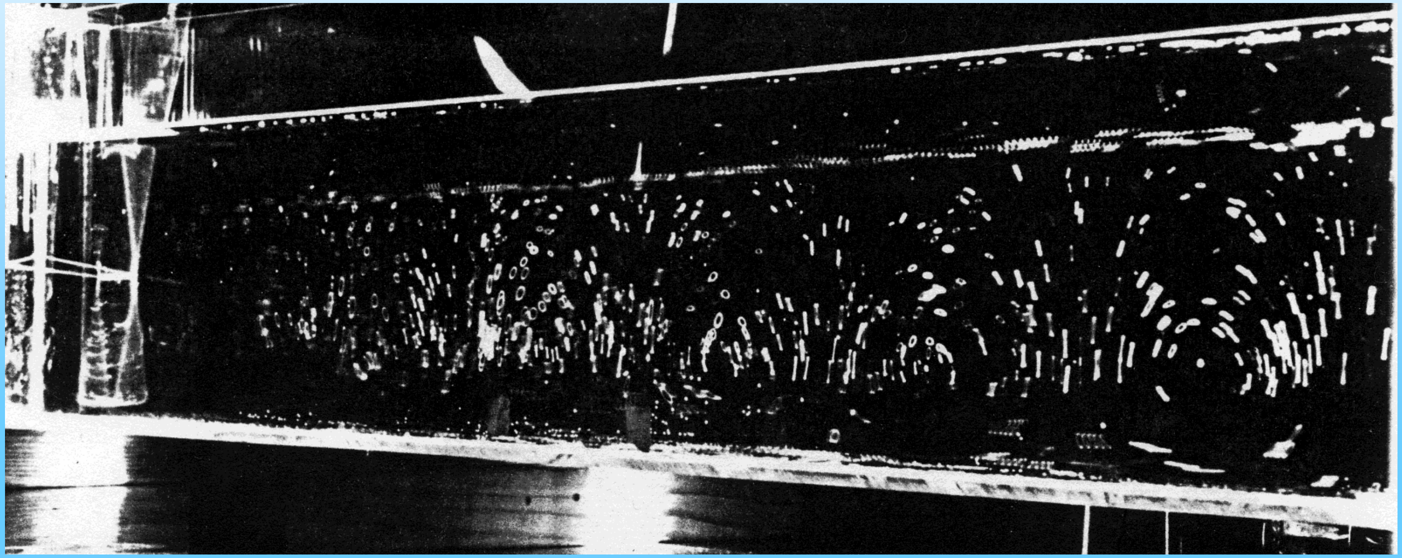

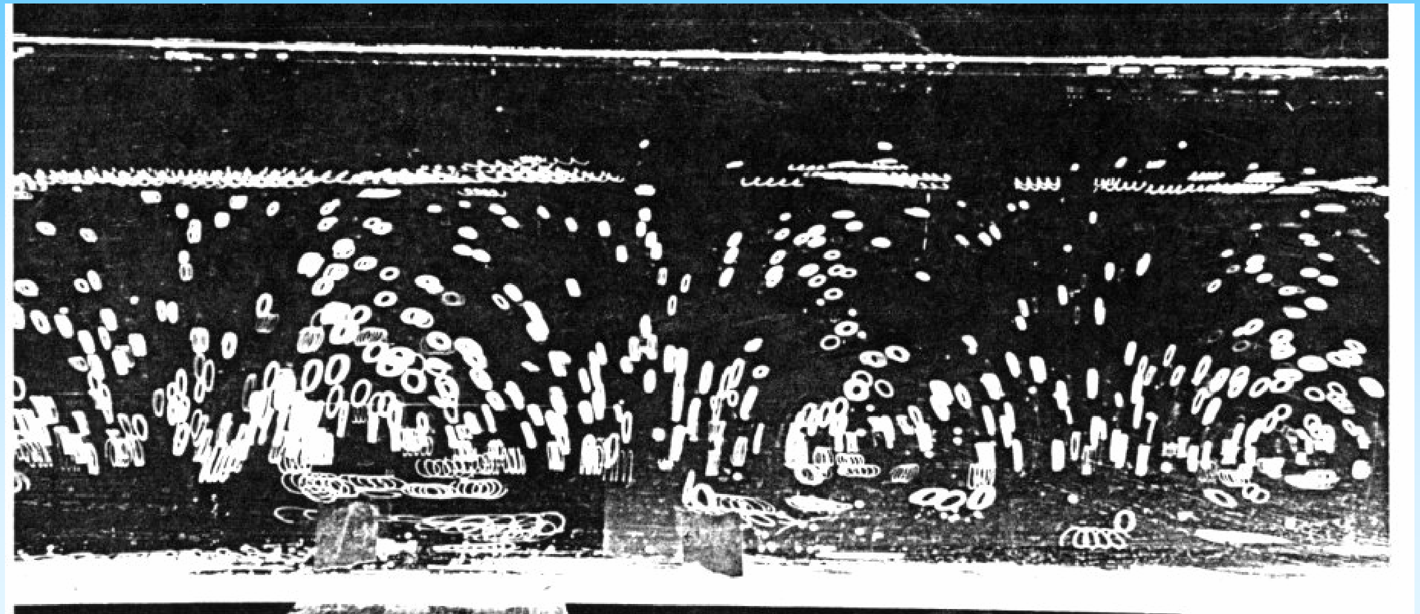

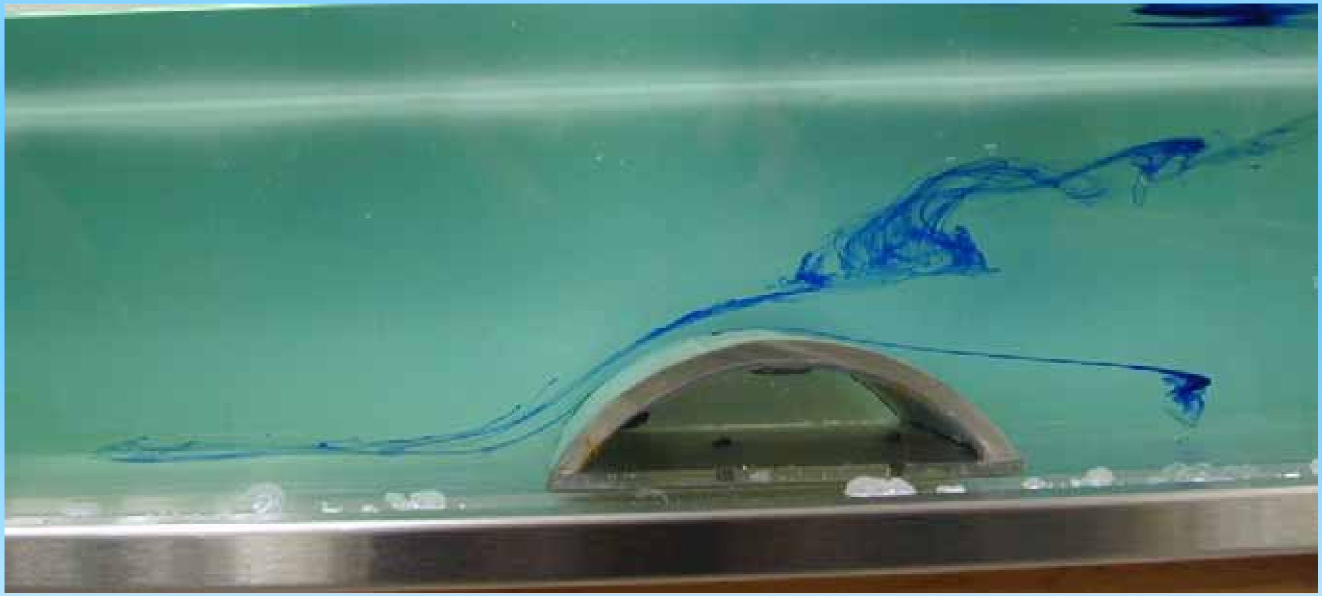

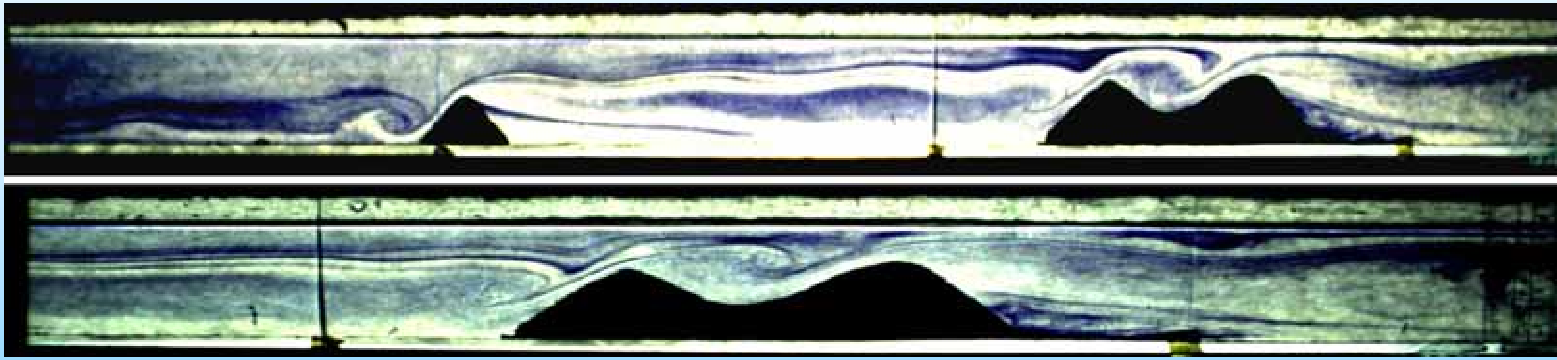

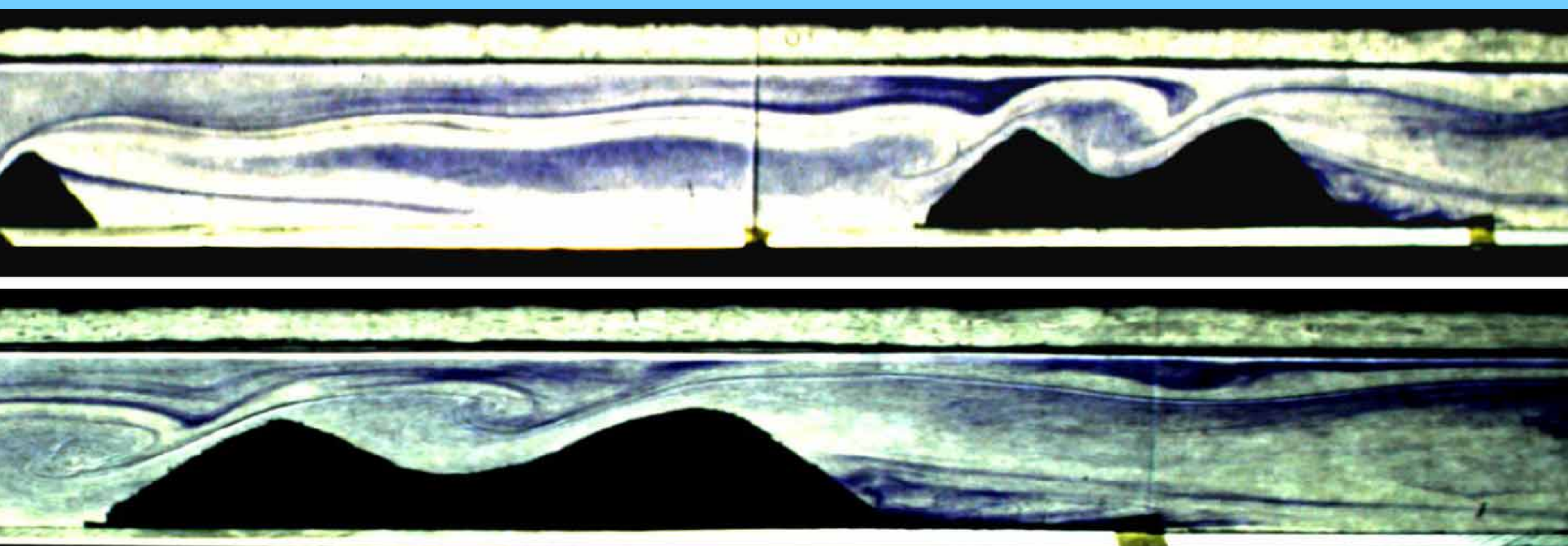

convection in a stratified fluid sends out gravity waves

# internal gravity waves driven by oscillating 2 dimensional cylinder. Viewed with shadowgraph Notice reflection at base of mixed layer

*GFD Lab, Univ of Washington*

oscillating cylinder

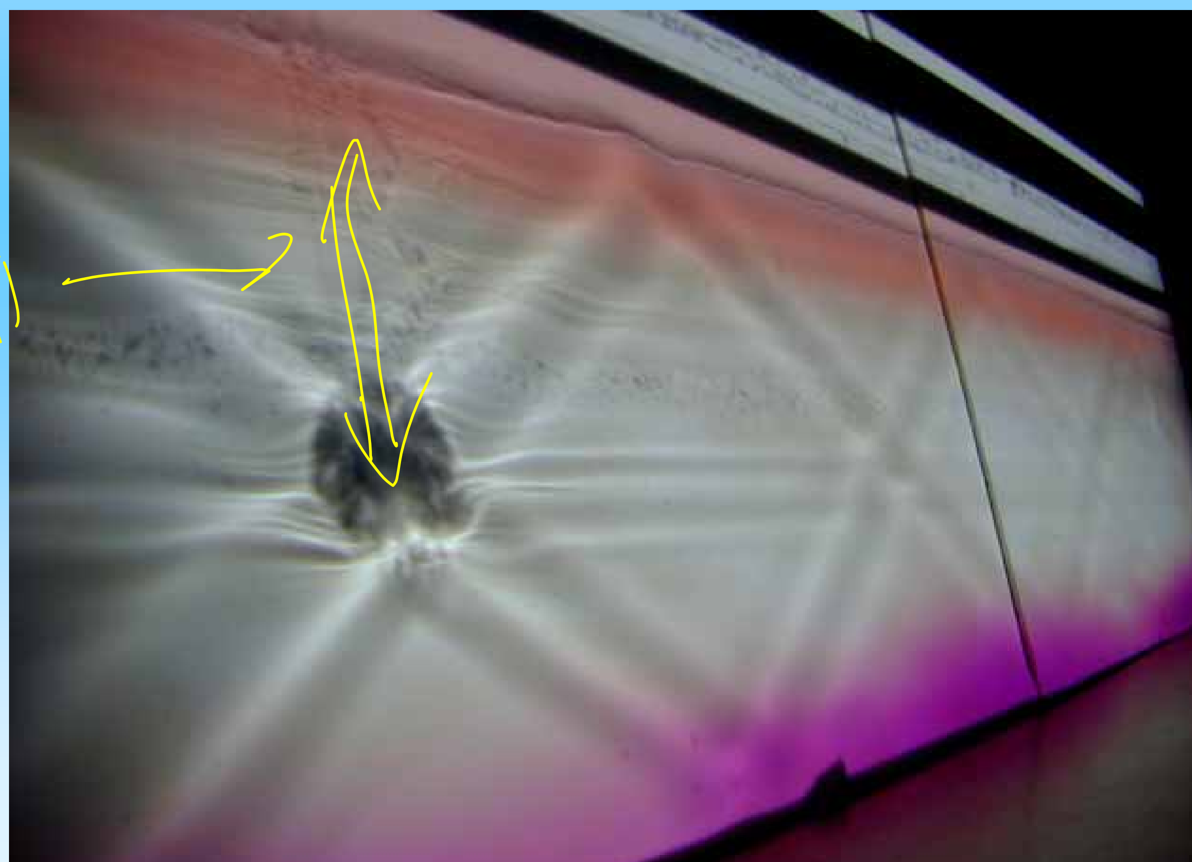

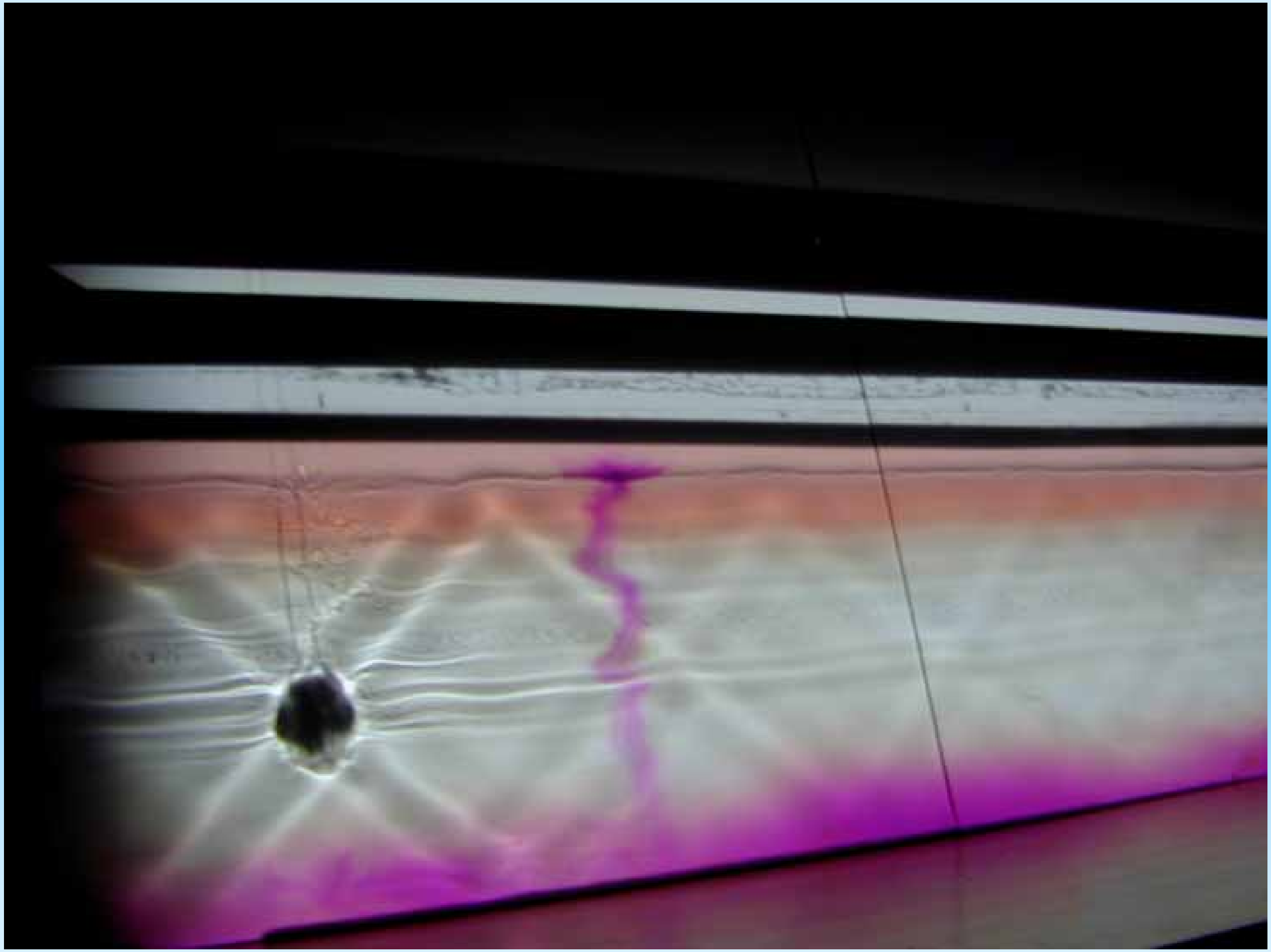

frequency close to N..some generation of harmonics and some turbulent mixing

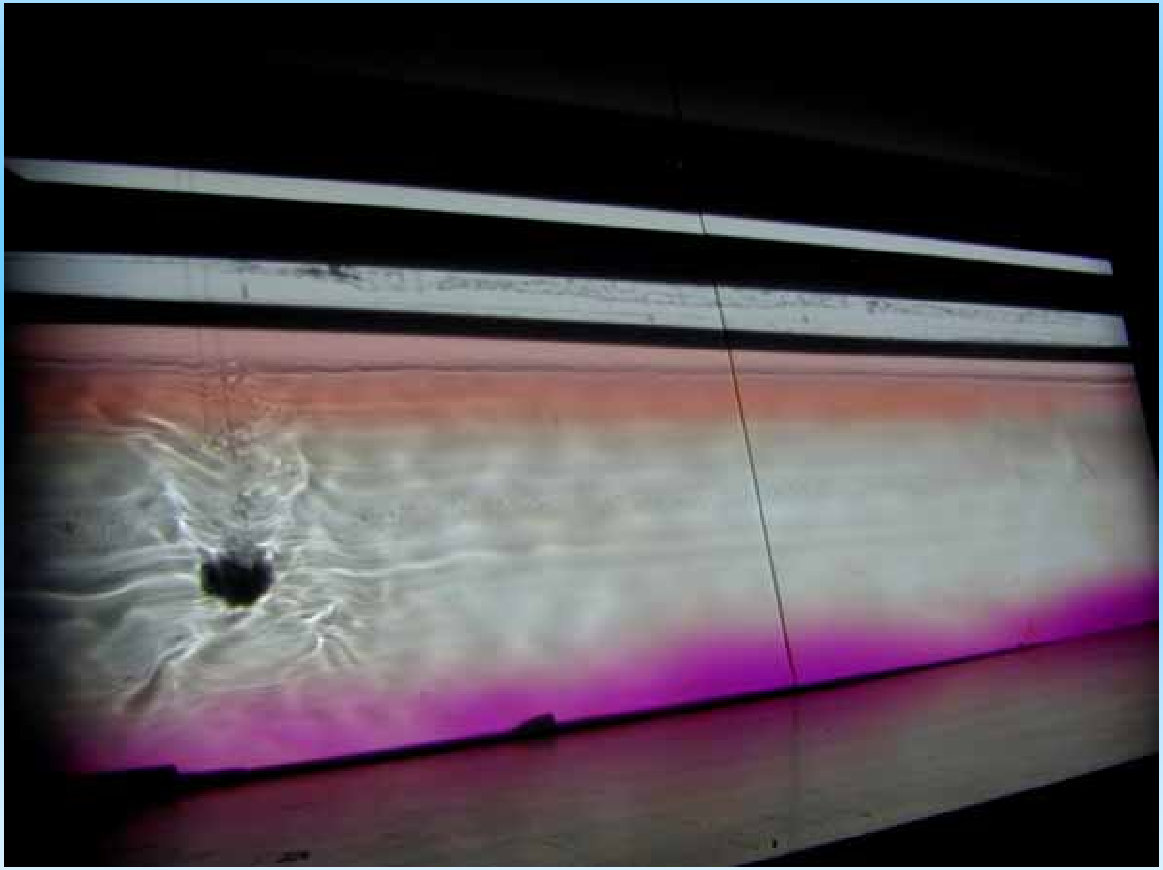

internal gravity waves: a circular cylinder moves to the right steadily, horizontally

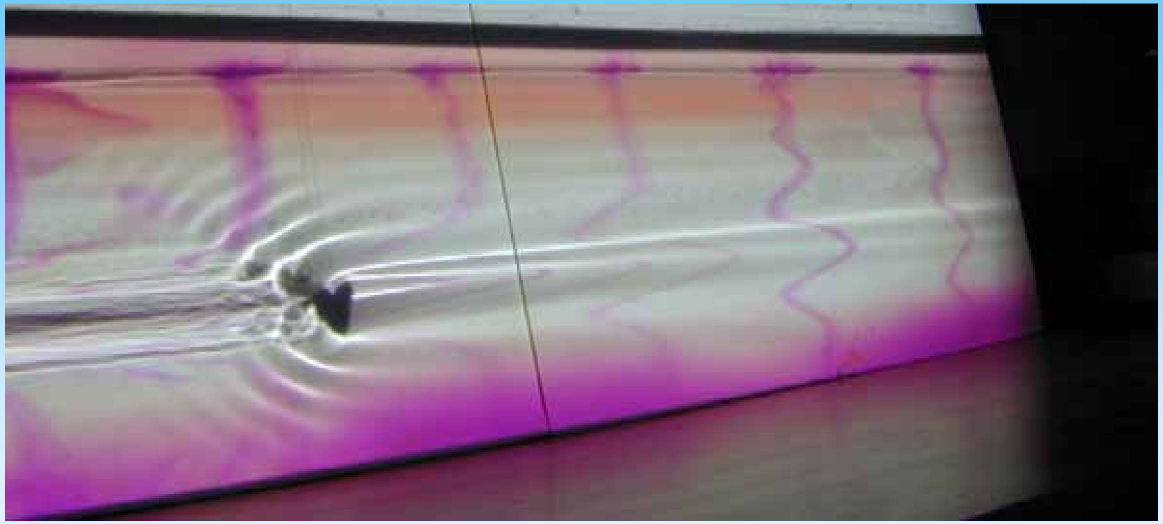

notice the fluid which is pushed ahead of the cylinder, with too little kinetic energy to rise against the stratification. In a reference frame moving with the 'mountain' this would be blocked fluid upstream of the mountain.  It is transmitted by long, low frequency gravity waves, visible in previous slide

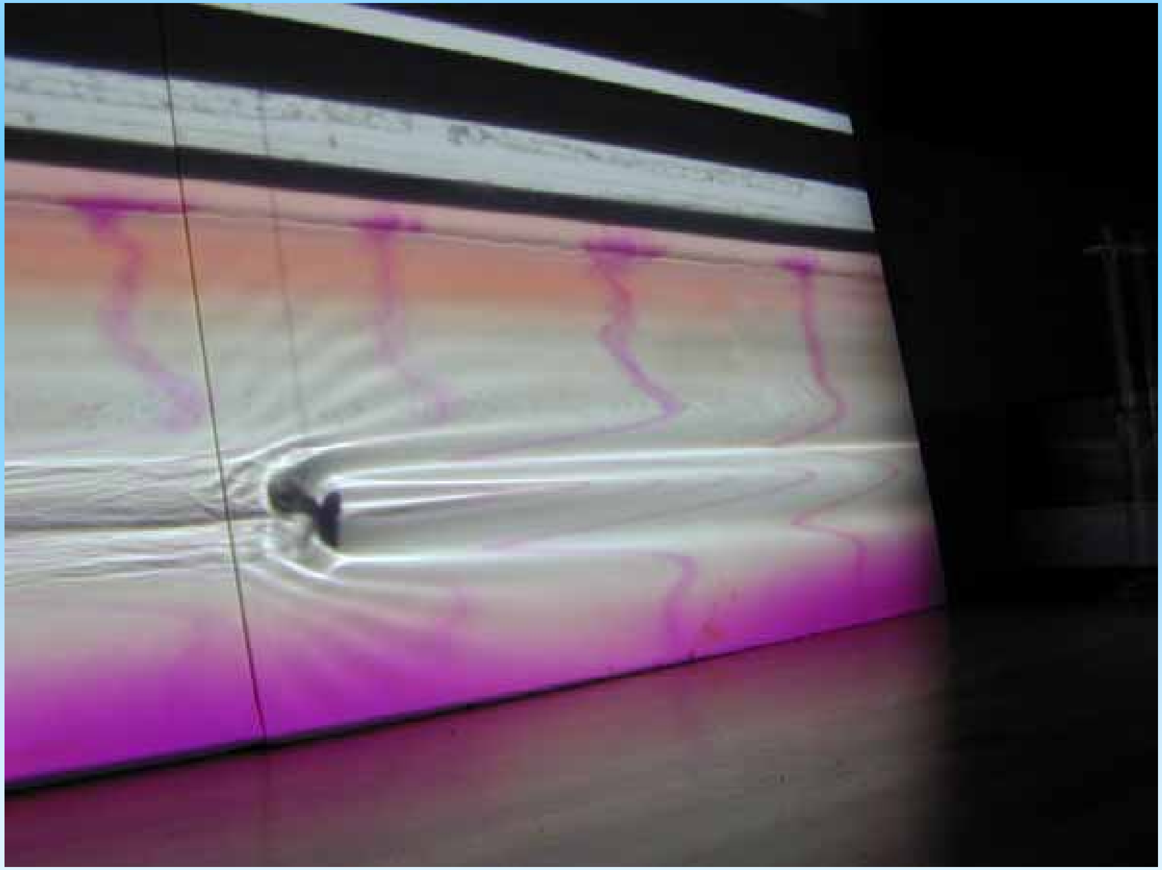

# PV dynamics (PV = potential vorticity)

uses the vorticity conservation ('vector tracer') property, but accounting for buoyancy forces

PV conservation and flux (transport); Haynes & McIntyre JAS 1996

$\beta$-effect, sphere

geostrophic adjustment in a cylinder with 2 –layer stratification. A ball of fluid is injected at the interface and allowed to 'slump' and spin. Shall we try this during the lecture?

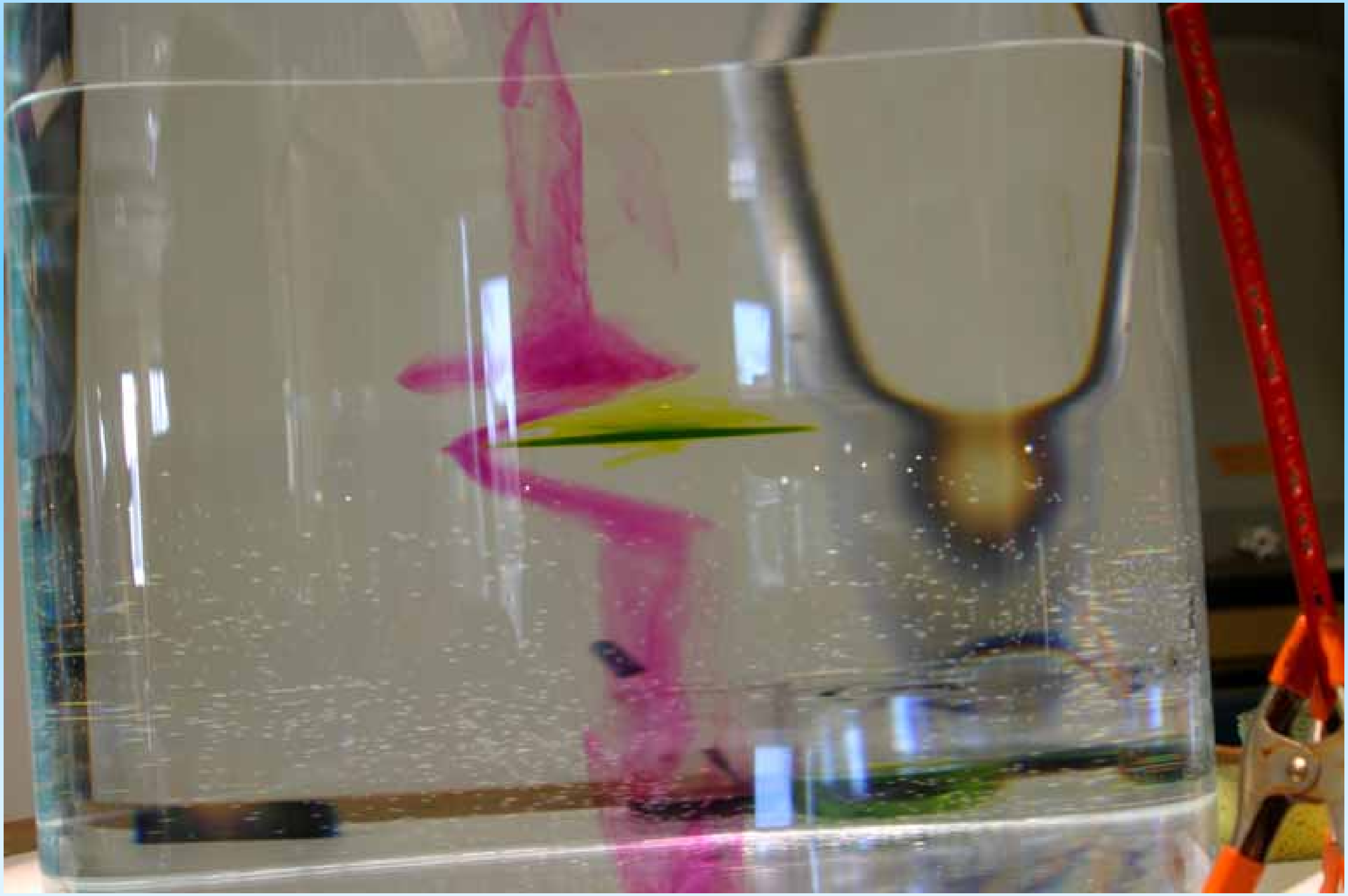

# Rossby waves

# Rossby waves (barotropic mode) evolving in x and time (left); dispersion relation (right)

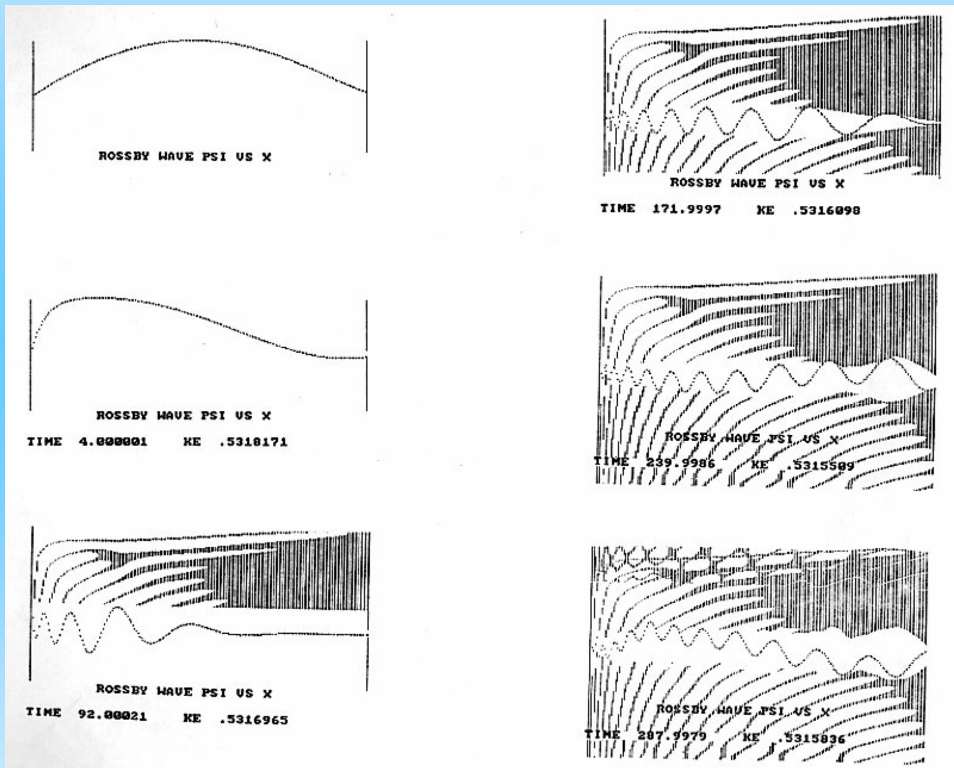


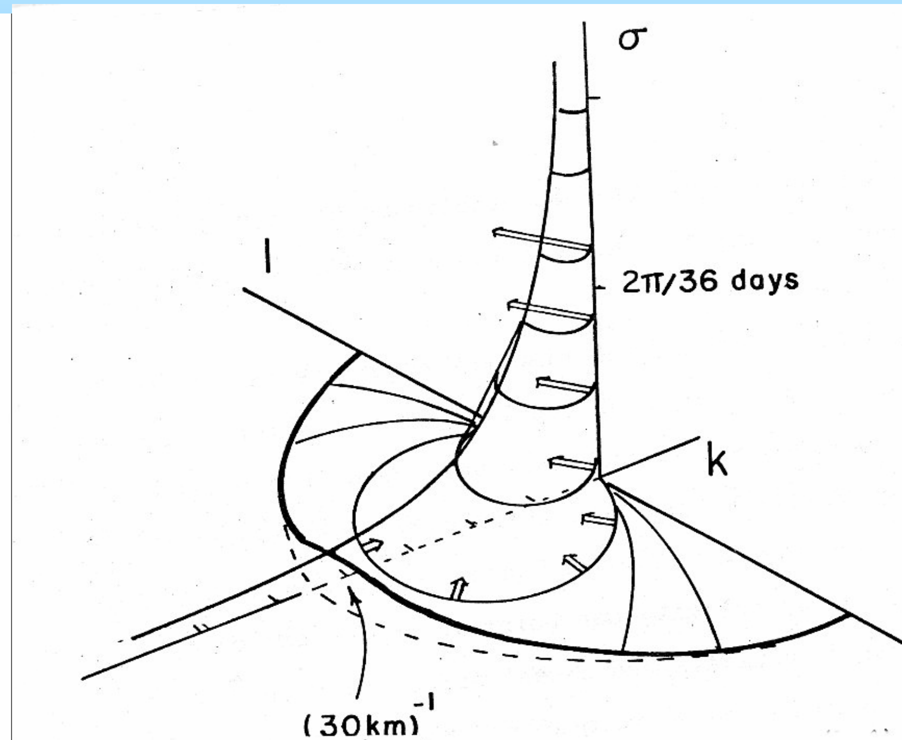

$$\nabla^2\psi_t + \beta\psi_x = \delta(x,y)\exp(-i\omega t);$$

$$\psi = \varphi(x,y)\exp(-i\kappa x - i\omega t) \quad \kappa = \beta/2\omega$$

$$\nabla^2\varphi + \kappa^2\varphi = \delta(x,y)$$

This is a Helmholtz equation for the spatial form of oscillatory waves
Geometry suggests cylindrical coordinates for which the solution is

$$\psi = \exp(-i\kappa x - i\omega t)H_0^2(\kappa r)$$

$$\psi \sim \sqrt{\frac{2}{\pi\kappa r}}\exp(-i\kappa x - i\omega t)\exp-(i\kappa r)$$

$$\sim \sqrt{\frac{2}{\pi\kappa r}}\exp(i\kappa(r+x))\exp(-i\omega t)$$

Parabolic wave crests, sweep westward.
energy flux is isotropic, yet long waves all propagate
west from forcing.
A western boundary can be simulated by an image Green function in the boundary, producing the full set of reflected Rossby waves of shorter wavelength.

If we filter the solution by making the wavemaker finite in size (say with diameter L) we pick out wavenumbers < $L^{-1}$. removing the short Rossby waves propagating east from the source.

*Low frequency waves*: fix the length scale $(k^2 + l^2)^{-1/2}$ while reducing the frequency: end up with k<<l, and group velocity pointing westward. This is the essence of westward influence, reletave to the fluid motion, on the β-plane.

# Green function for Rossby waves driven by a compact oscillating forcing

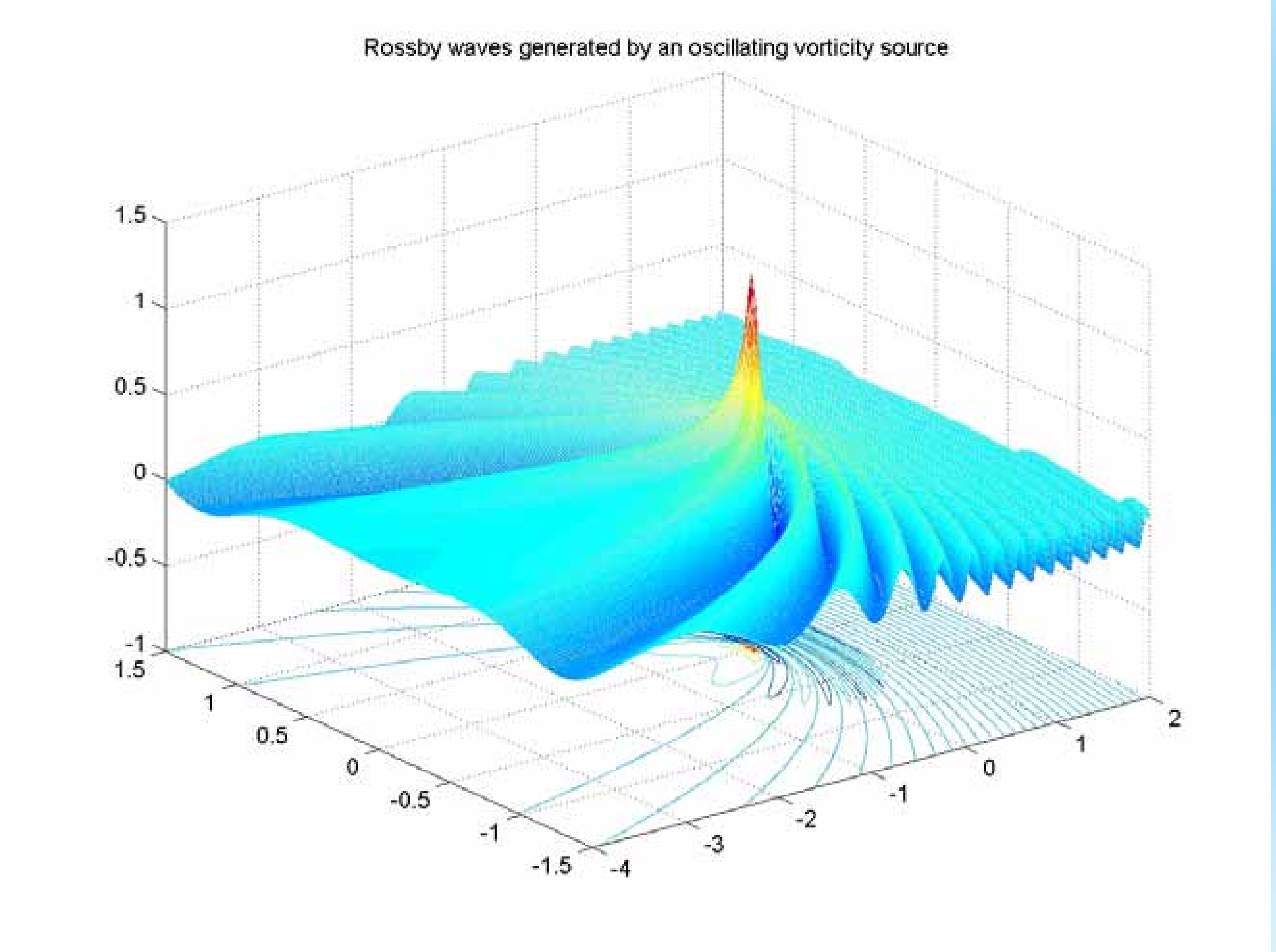

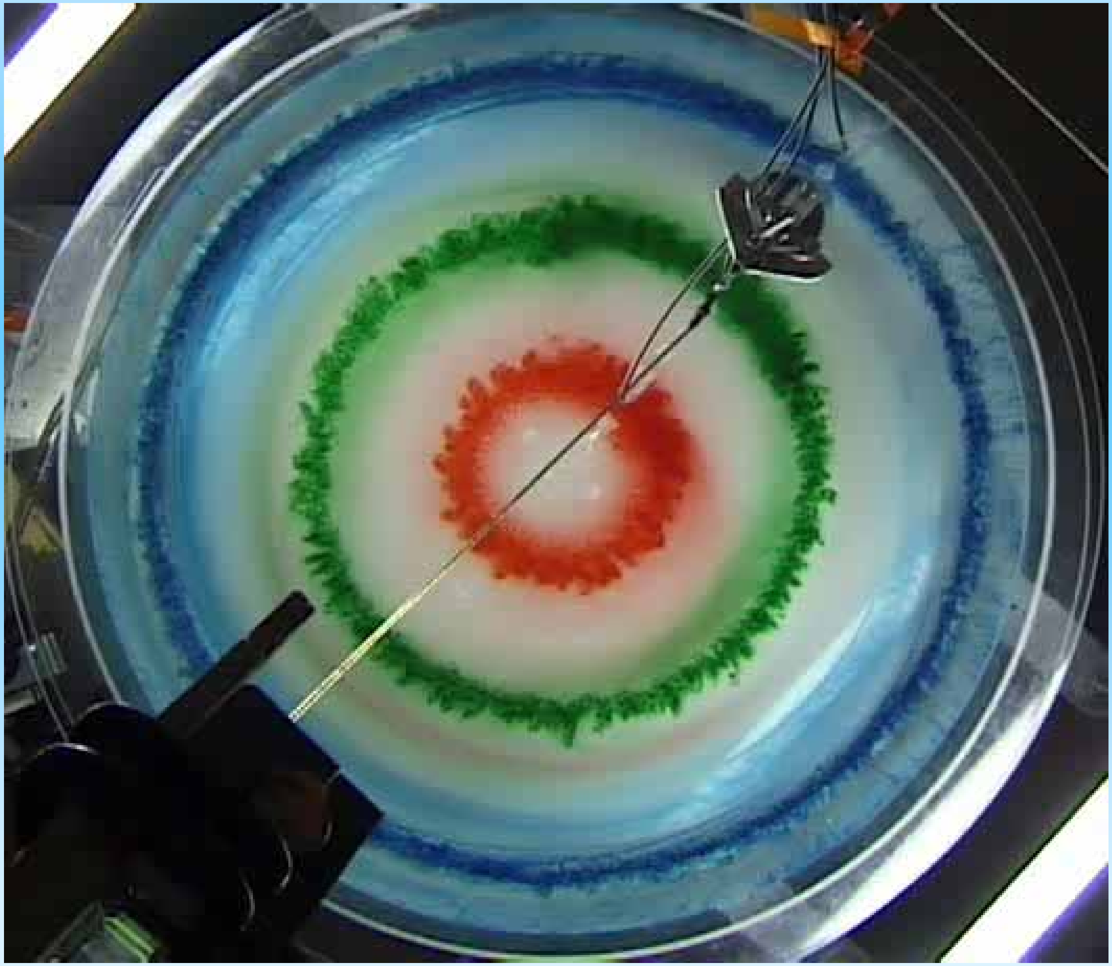

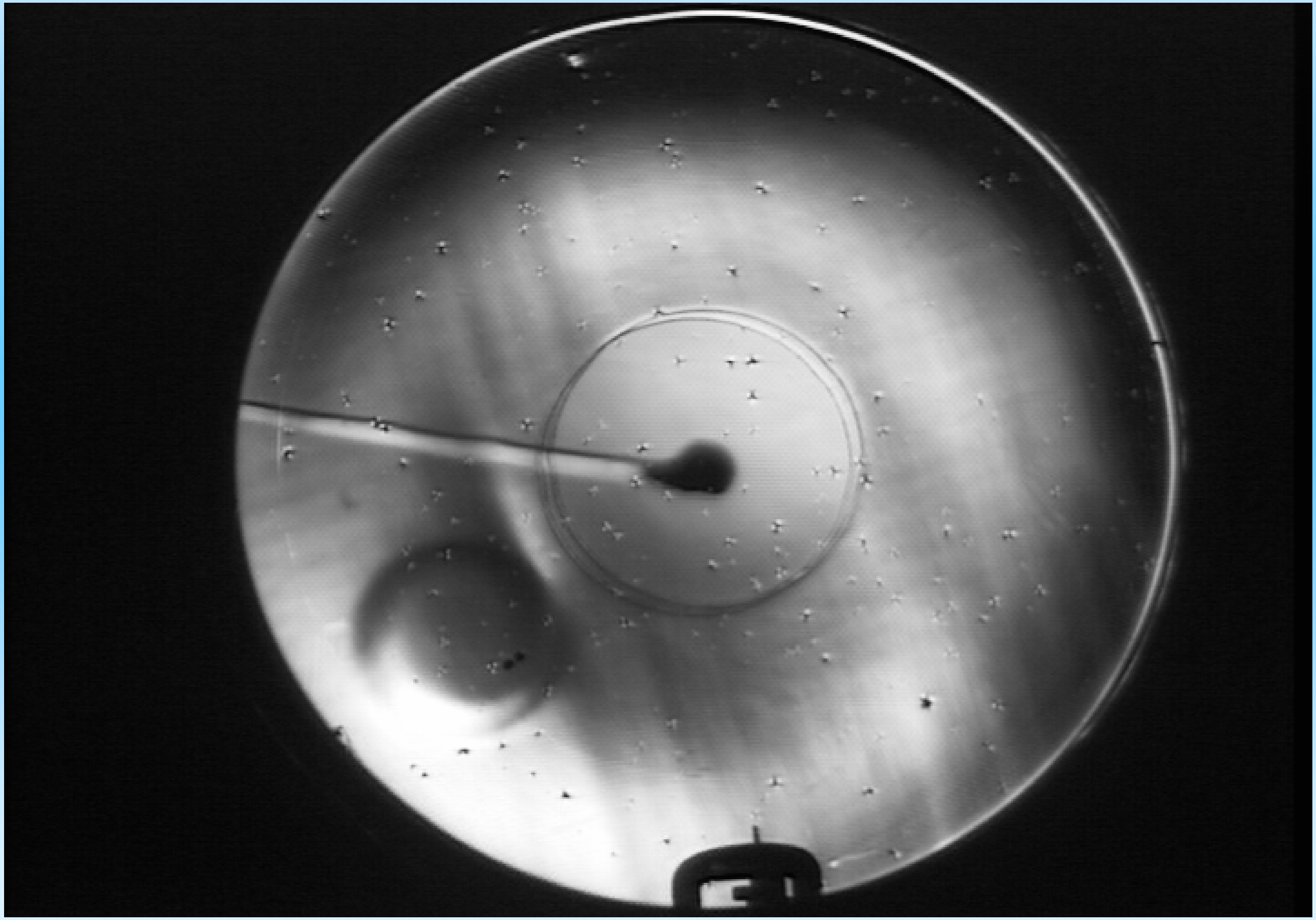

(a) (b)

(c) (d)

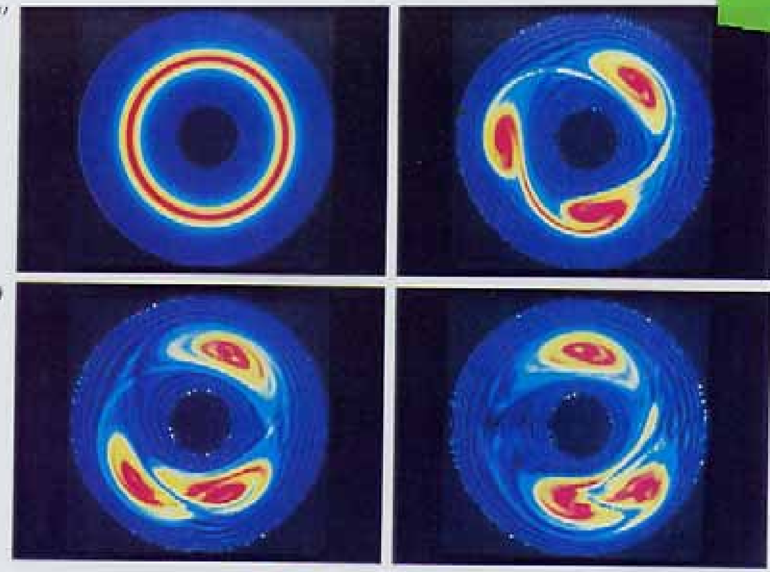

MARCUS J. FLUID MECH 1990

(e) (f)

(g) (h)

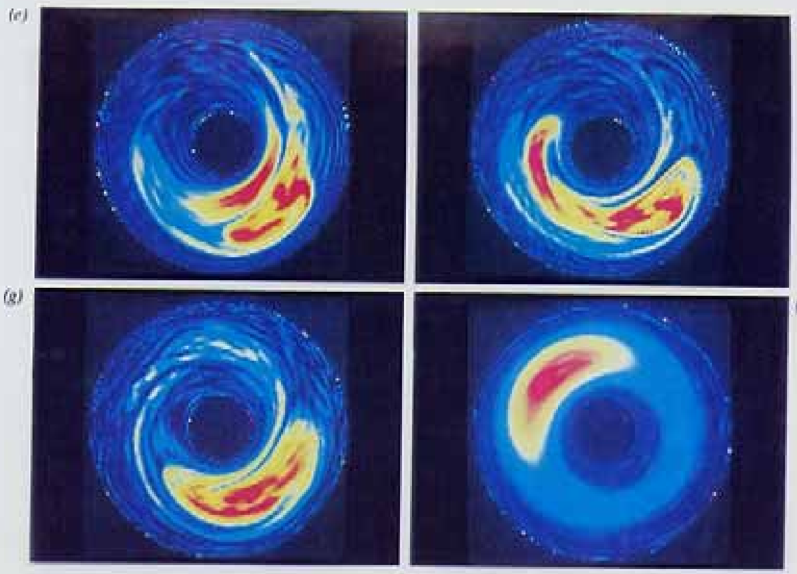

FIGURE 8. Evolution of the $\omega$ of a linearly unstable shear layer with $\delta/a = 0.28$ and with the same zonal velocity as in figure 1. The layer breaks up into a three-fold symmetric eigenmode (the most rapidly growing one). The three vortices separate from each other, merge together, and eject the irrotational (light blue and yellow) fluid entrained near the vortex centre. ($a$ – $h$) After 0, 3.34, 3.82, 4.46, 5.73, 6.21, 7.64, and 29.6 turn-around times.

**Beta plume.**

It is often interesting to let frequencies become complex, $\omega \Rightarrow \omega + i\varepsilon$. This helps to resolve difficult issues like the radiation condition (see Lighthill, *Waves in Fluids*). When do so it simulates a *steady* circulation forced by a delta function of stress curl (a 'tweak'). The relative vorticity term is now the diffusive damping of PV by linear Ekman friction

$$R\nabla^2\psi + \beta\psi_x = \delta(x,y);$$

$$\psi = \varphi(x,y)\exp(-\alpha x) \quad \alpha = \beta/2R$$
$$\nabla^2\varphi - \alpha^2\varphi = \delta(x,y)$$

$$\psi = \exp(-\alpha x - i\omega t)K_0(\alpha r)$$
$$\psi \sim \sqrt{\frac{2}{\pi\kappa r}}\exp(-\alpha(r+x))$$

The β-plume is a Rossby wave arrested by friction. It is an elongated gyre extending far west from the forcing. (As above a western boundary can be added with an image Green function, showing the exponentially narrow 'Gulf Stream' boundary current of Stommel).

This plume extends the Stommel-Arons model of the deep-ocean branch of the global MOC.

# beta plume

a steady, diffusive circulation gyre driven by a delta-function of stress curl; lop-sided, extending far to the west of the forcing as in an ‘arrested’ Rossby wave

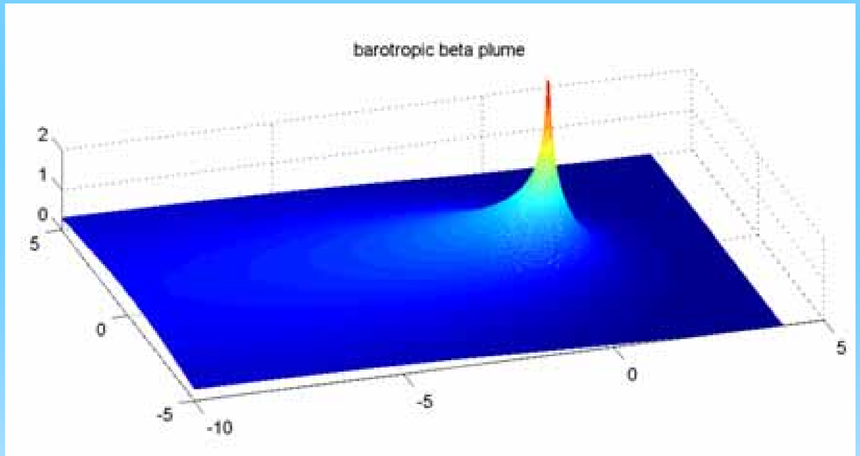


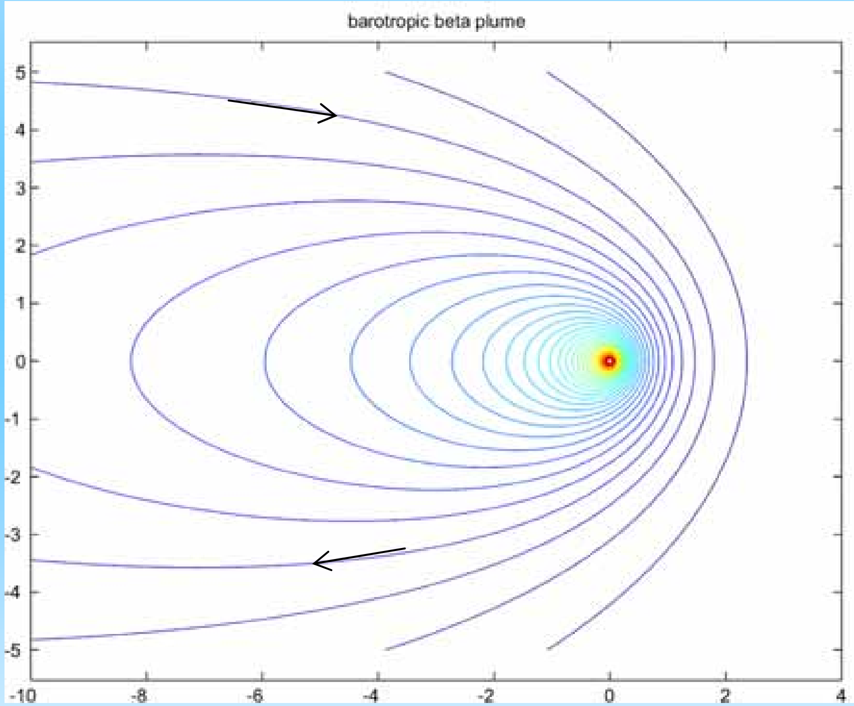

convection is simulated by diapycnal mass-flux; it drives an upper level cyclone and deep anticyclone, deep and shallow western boundary currents and a Stommel-Arons interior circulation; with continental-slope topography a deep topographic gyre competes with the simple poleward interior flow.

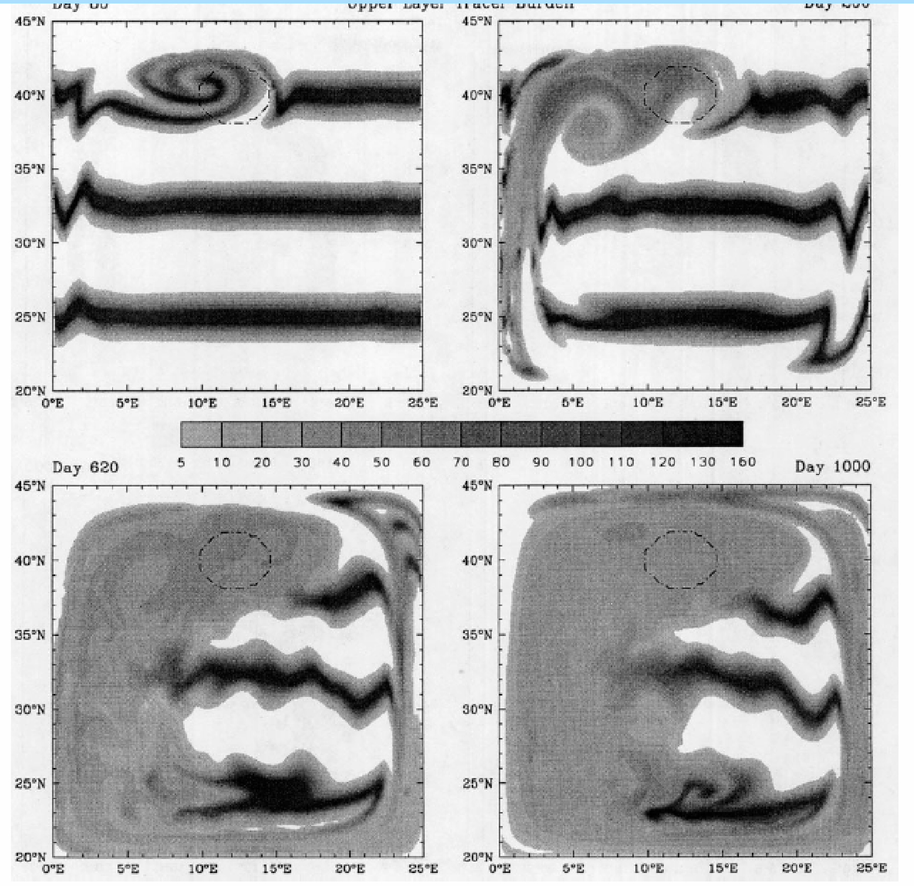


FIG. 21. Column tracer burden of the upper layer of HIAMP for days 80, 200, 620, and 1000 in arbitrary units. The dashed circles mark the forcing region.

# The β-plume:  Green function for steady, dissipative β-plane vorticity equation, 1-layer fluid

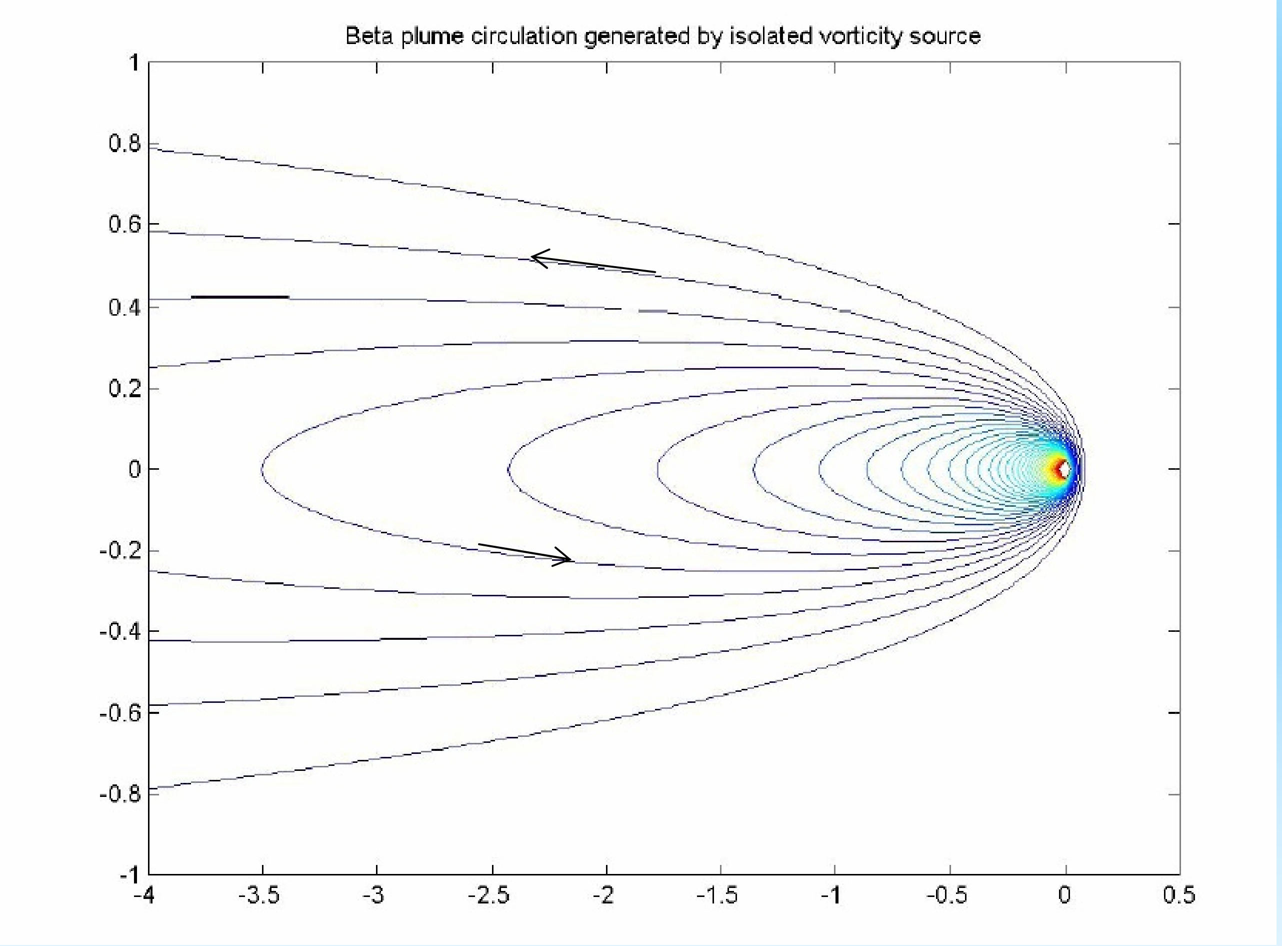

CLASSIC HOMOGENEOUS DENSITY OCEAN:

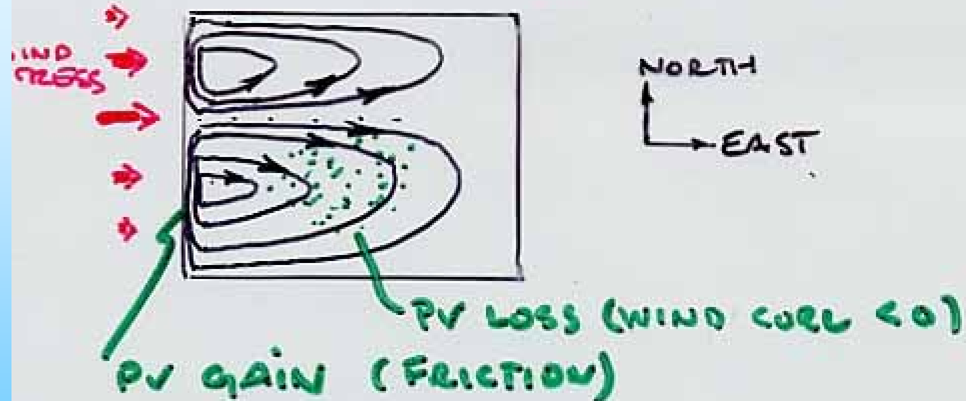


STRATIFIED OCEAN:

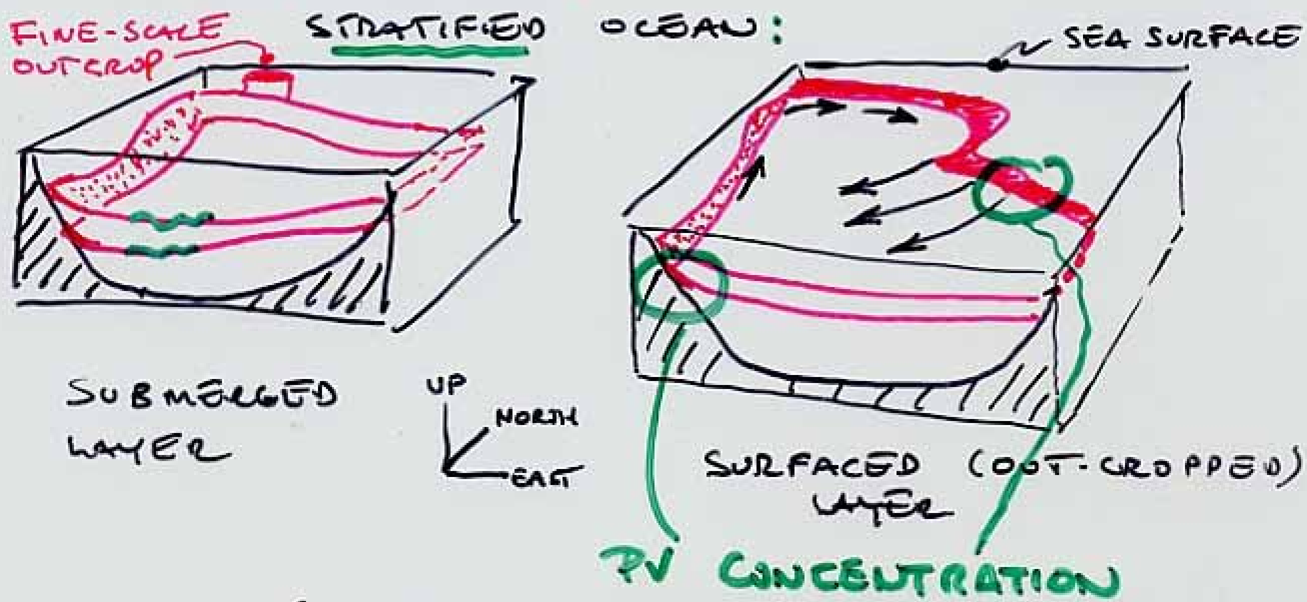


ELLIPTIC VS. HYPERBOLIC

RESPONSE TO BOUNDARY CONDITIONS

Ocean gyre simulations *Hallberg & Rhines 2000*

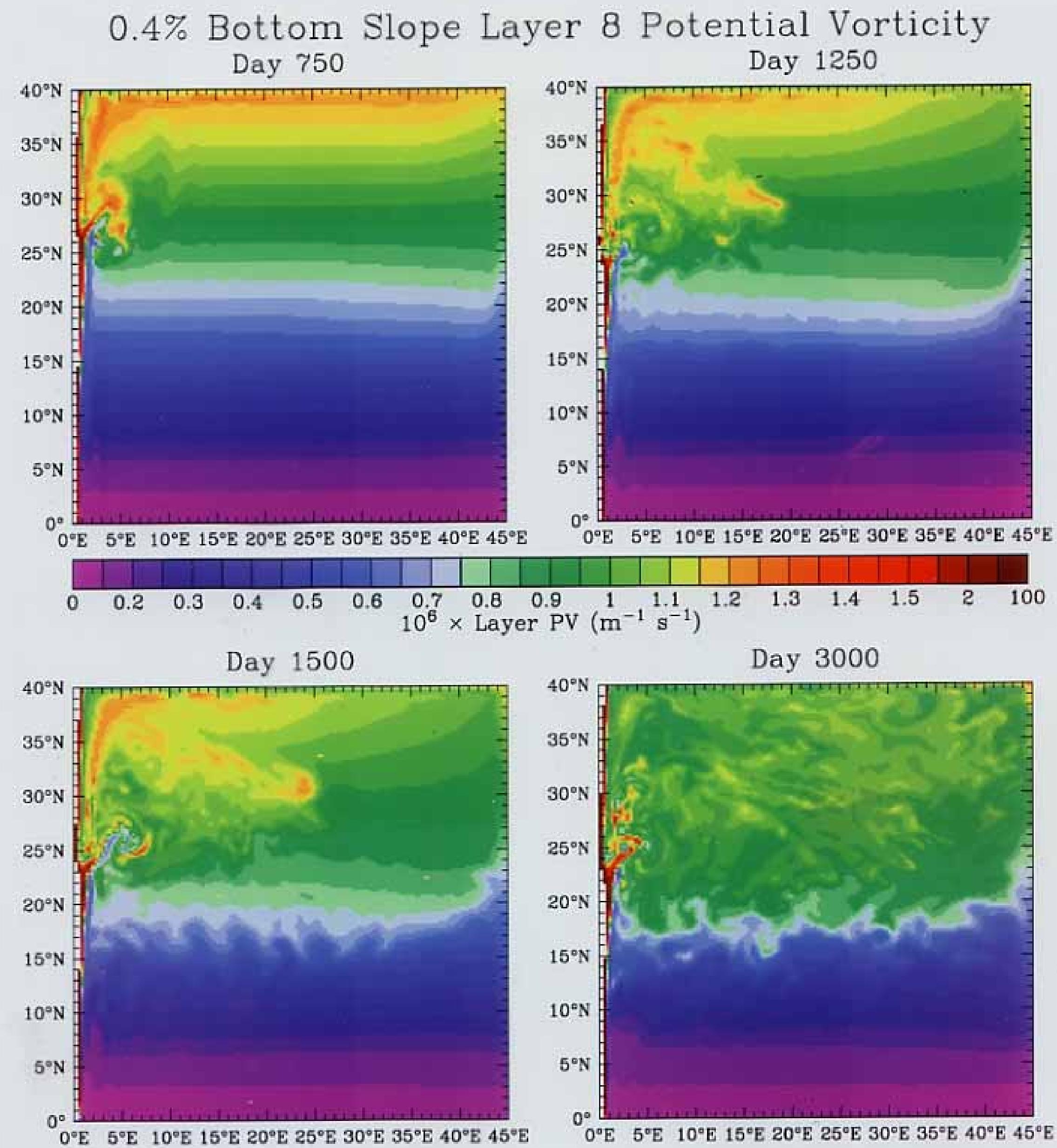

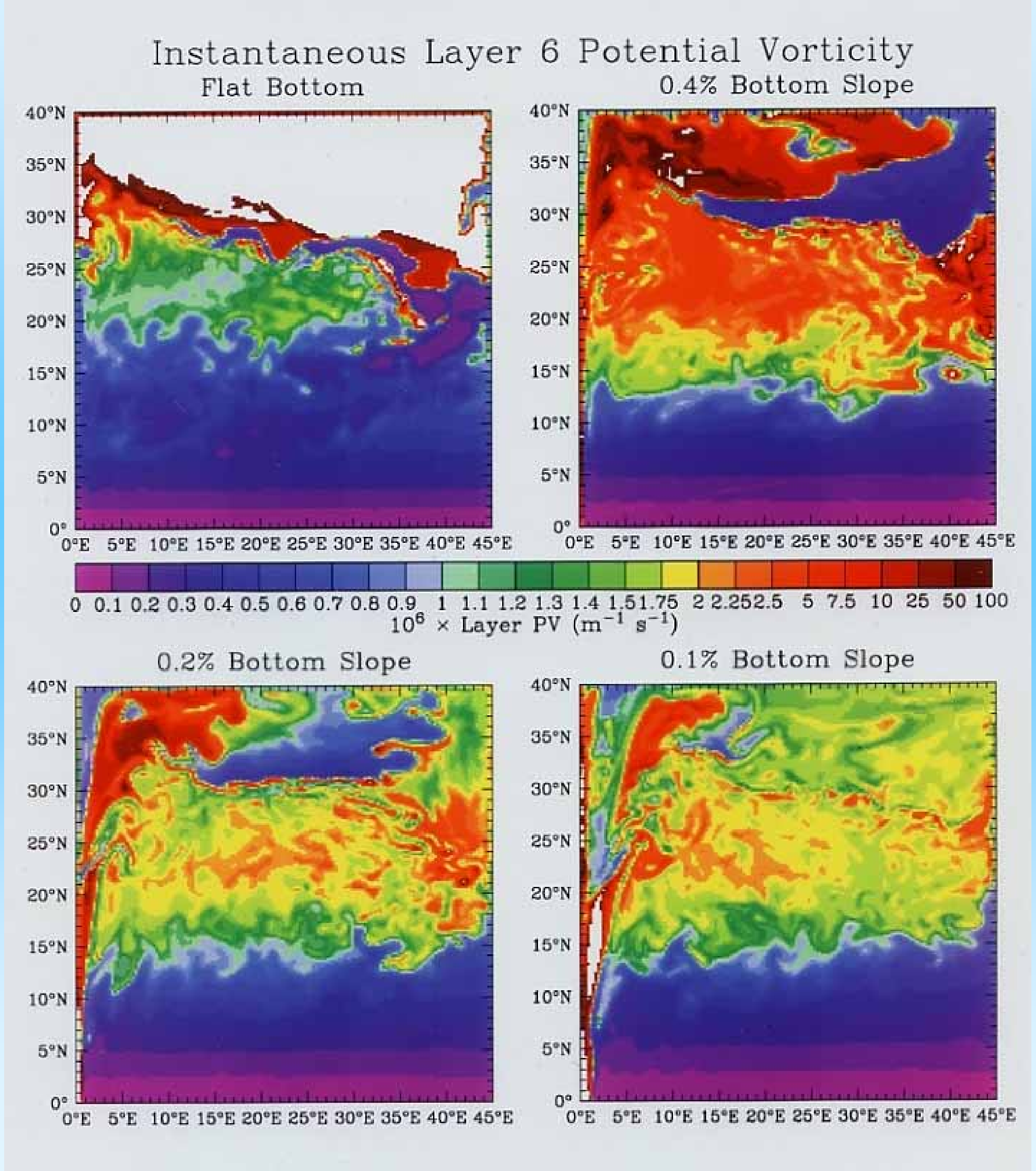

Instantaneous Layer 6 Potential Vorticity
Flat Bottom
0.4% Bottom Slope
0.2% Bottom Slope
0.1% Bottom Slope
40°N 35°N 30°N 25°N 20°N 15°N 10°N 5°N 0°
0°E 5°E 10°E 15°E 20°E 25°E 30°E 35°E 40°E 45°E
0 0.1 0.2 0.3 0.4 0.5 0.6 0.7 0.8 0.9 1 1.1 1.2 1.3 1.4 1.5 1.75 2 2.25 2.5 5 7.5 10 25 50 100
$10^6 \times$ Layer PV ($m^{-1}$ $s^{-1}$)

Subtropical gyre dynamics, thermo-dyanamics and biology

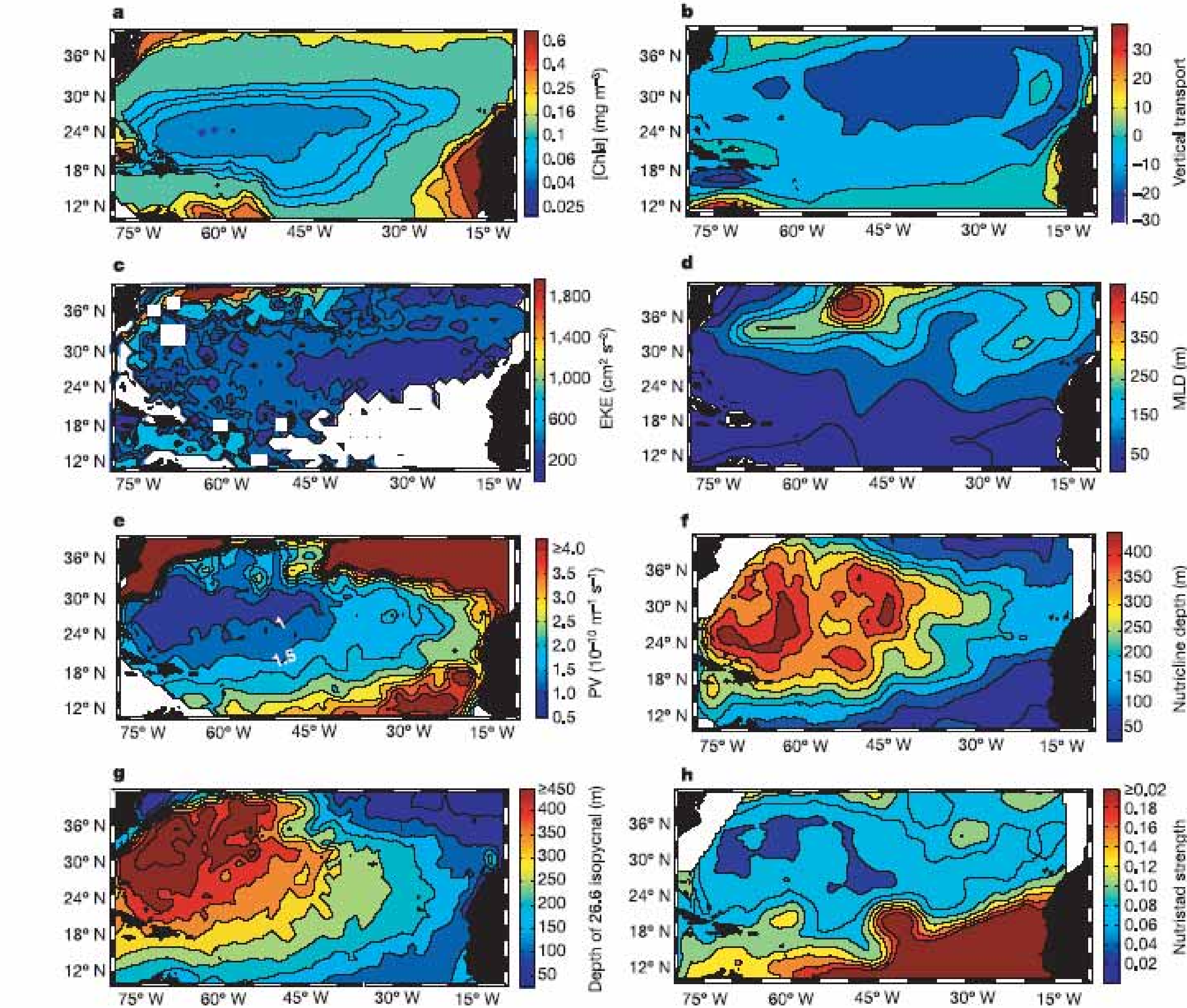


**Figure 5 | Properties of the North Atlantic subtropical gyre.** **a**, Annual mean SeaWiFS] chlorophyll *a* concentration, [Chl*a*], with a log scale for the colour axis; **b**, vertical transport calculated from the annual mean wind stress curl[25]; **c**, climatological mean eddy kinetic energy[20], EKE; **d**, climatological March mixed layer depth[26], MLD; **e**, potential vorticity on the 26.5 isopycnal, PV; **f**, nutricline depth, as defined by the depth maximum vertical nitrate gradient; **g**, depth of the 26.6 isopycnal, approximation for the base of the STMW; and **h**, the strength of the gradient at the nutricline, showing the wedge of STMW as a deplet nutristad.



*Palter, Lozier & Barber Nature 2005*

*Williams, Follows, Migillicuddy Nature 1998*

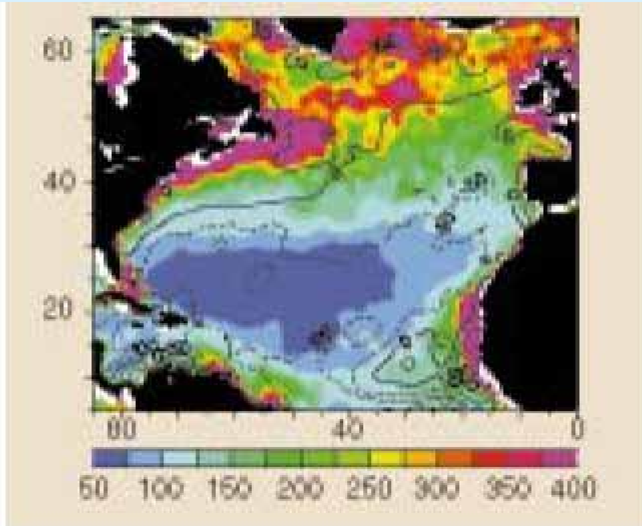


Figure 1 **Annual primary productivity (coloured values in g C $m^{-2}$ $yr^{-1}$), and upwards vertical velocity of water (contoured in m $yr^{-1}$) in the North Atlantic. Productivity reaches maximum values of 400 g C $m^{-2}$ $yr^{-1}$ where there are high levels of nutrient input from upwelling; and it has minimum values of 50 g C $m^{-2}$ $yr^{-1}$ within the subtropical gyre where there is downwelling (negative contours) and comparative nutrient depletion. Previous estimates of nutrient supply seem inadequate to account for even these low values, hence the proposal[1-3] that eddy circulation may be responsible for supplying them. (Figure derived from satellite estimates of surface chlorophyll from ref. 4, and calculations of vertical velocity at the base of the surface wind-forced boundary (Ekman) layer[6].)**

*Oschlies, Garcon Nature 1998*

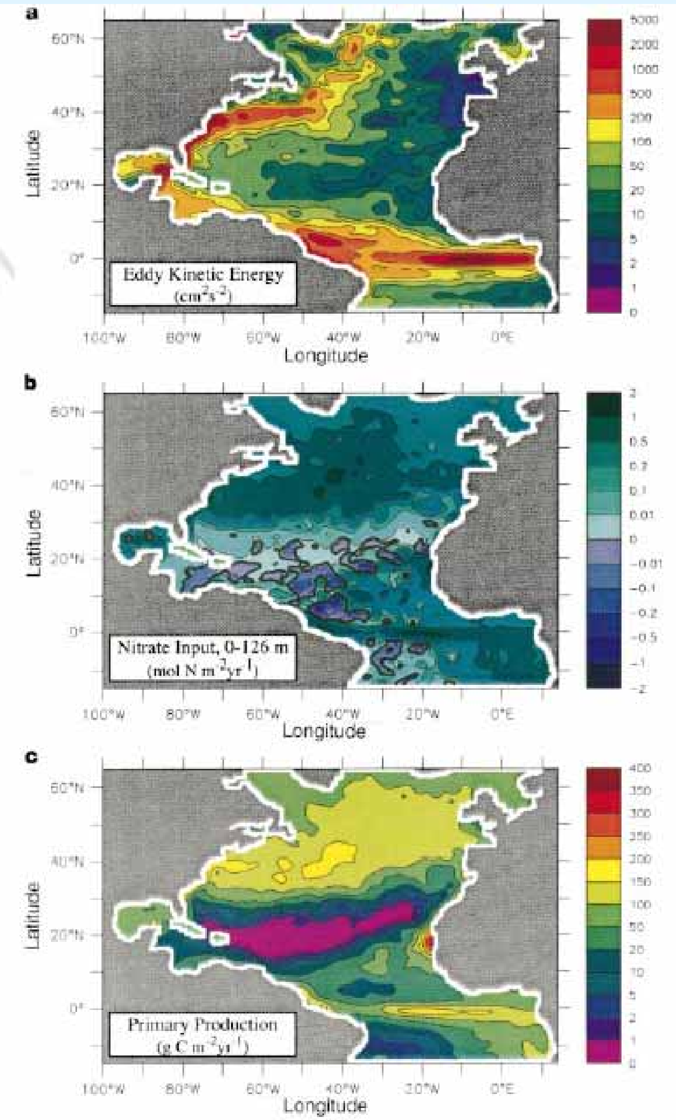


**Figure 1** Results from the assimilation experiment A. **a**, Surface eddy kinetic energy (EKE), which contains all deviations from the annual mean, computed for a depth of 60 m to avoid contamination by shallow Ekman currents (in $cm^2 s^{-2}$). **b**, Annual mean nitrate flux into the upper 126 m, which is taken as proxy for the euphotic zone (in mol N $m^{-2} yr^{-1}$). **c**, Annual mean primary production (in g C $m^{-2} yr^{-1}$). A constant ratio of C:N=6.6 was assumed to give carbon fluxes from the model. This is a rather conservative assumption[27] and will give minimal estimates of carbon fluxes.

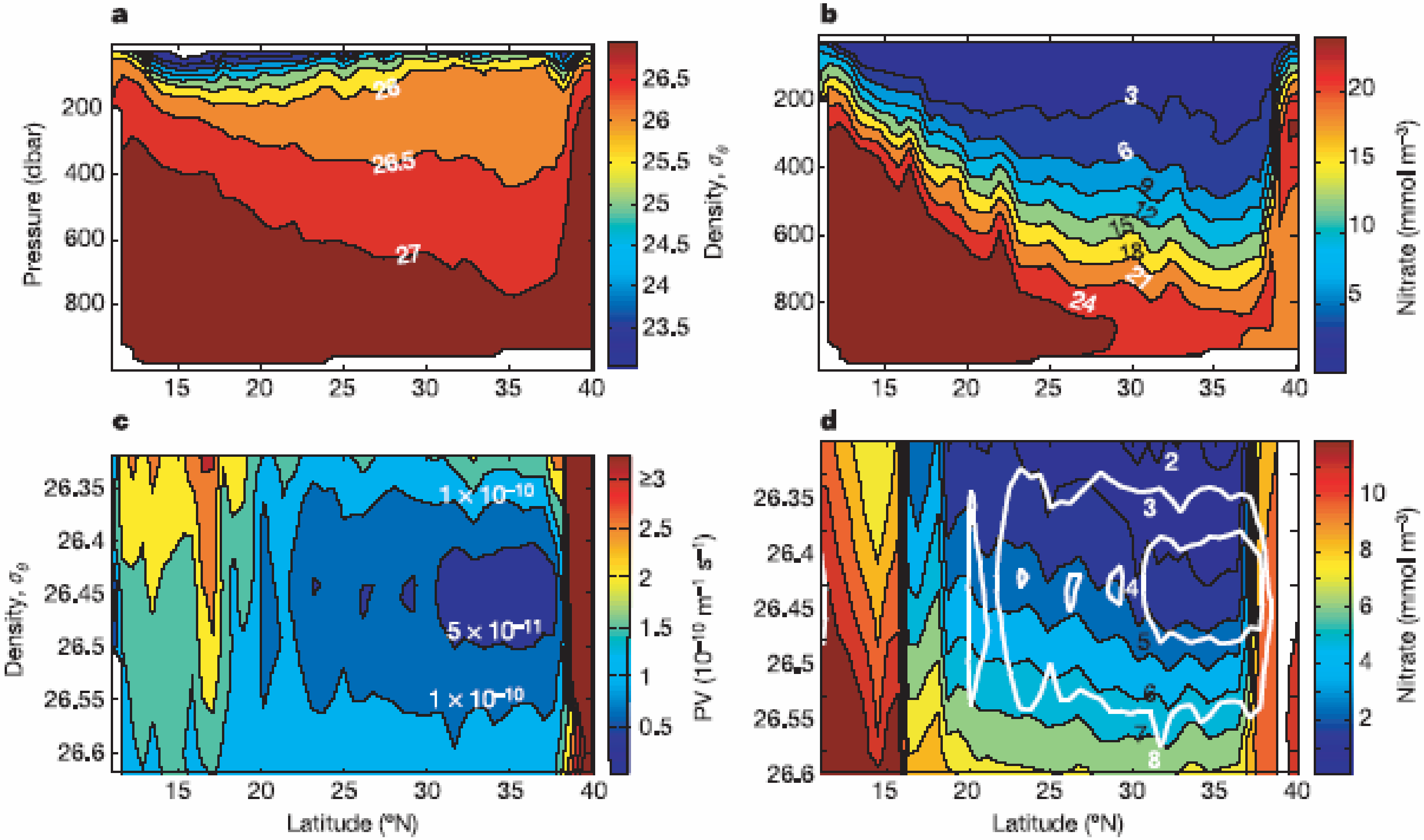


**gure 3 | Properties of WOCE section A22 in August 1997. a**, Potential nsity as a function of pressure. **b**, Nitrate as a function of pressure. Potential vorticity (PV) as a function of potential density; the low-PV aters ($\leq 1 \times 10^{-10}$ m$^{-1}$ s$^{-1}$, shaded blue) are considered the core of the STMW. **d**, Nitrate as a function of potential density. The white contour lines in **d** represent PV $= -0.5 \times 10^{-10}$ and $-1 \times 10^{-10}$ m$^{-1}$ s$^{-1}$. PV was calculated using $f/\sigma_o\ (\partial\sigma_\theta/\partial z)$, where $f$ is the Coriolis parameter, $\sigma_o$ the reference density, and $\partial\sigma_\theta/\partial z$ the vertical density gradient.

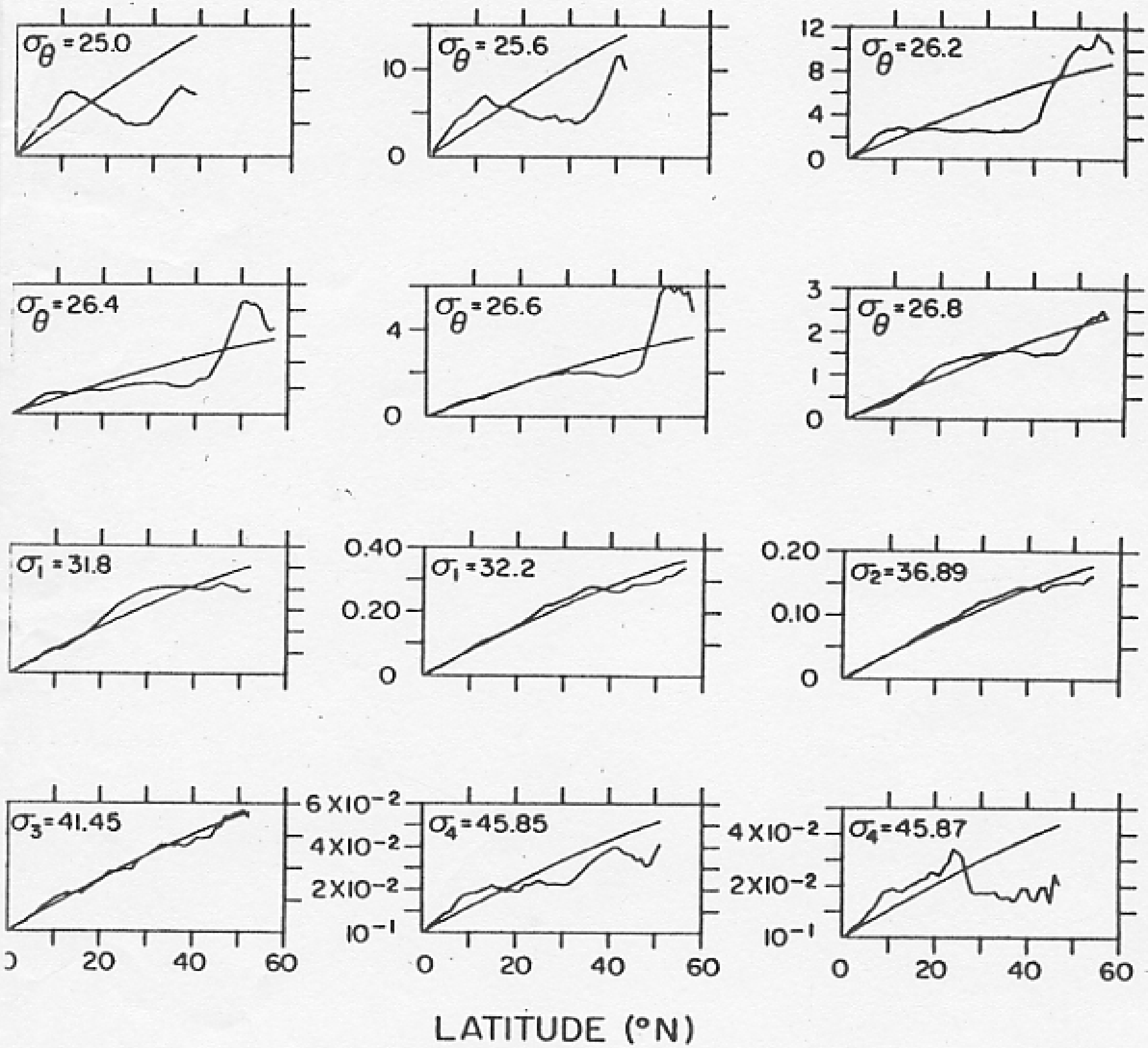


l average of potential vorticity at selected densities (jagged curves) and $\rho^{-1} f\,\partial\rho/\partial z$ based on 'ρ/∂z over the entire North Pacific for that isopycnal (smooth curves). Values are shown only :re there was at least 45° of longitudinal coverage, although the underlying smooth curve is ailable points. Vertical scales vary for each panel.

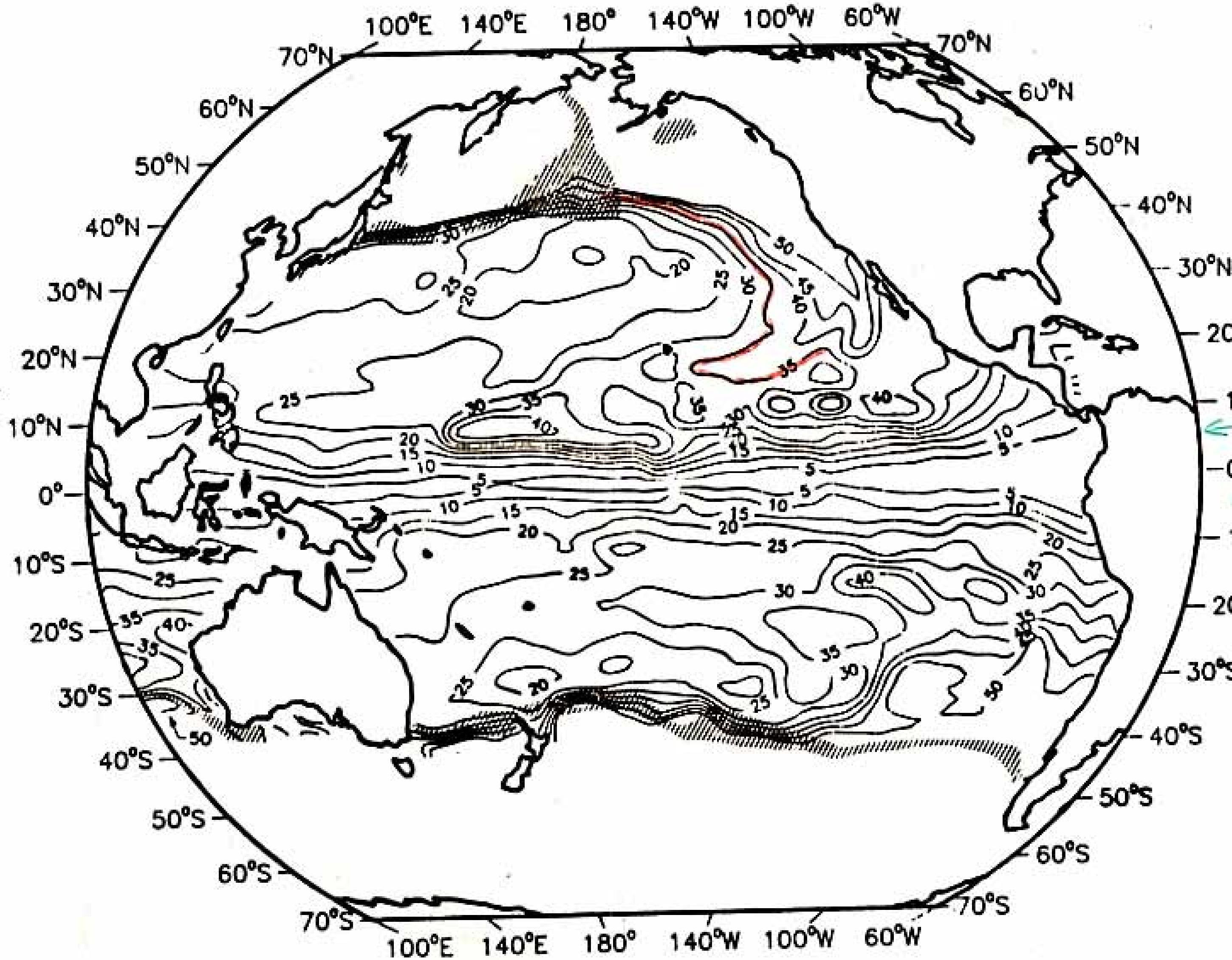


← Local source N.E.C.C.

Q. ON $\sigma_\theta = 26.5$

PACIFIC POTENTIAL VORTICITY

KEFFER 1985 J.P.O.

J. Physical Oceanography

NORTH PACIFIC OCEAN PV

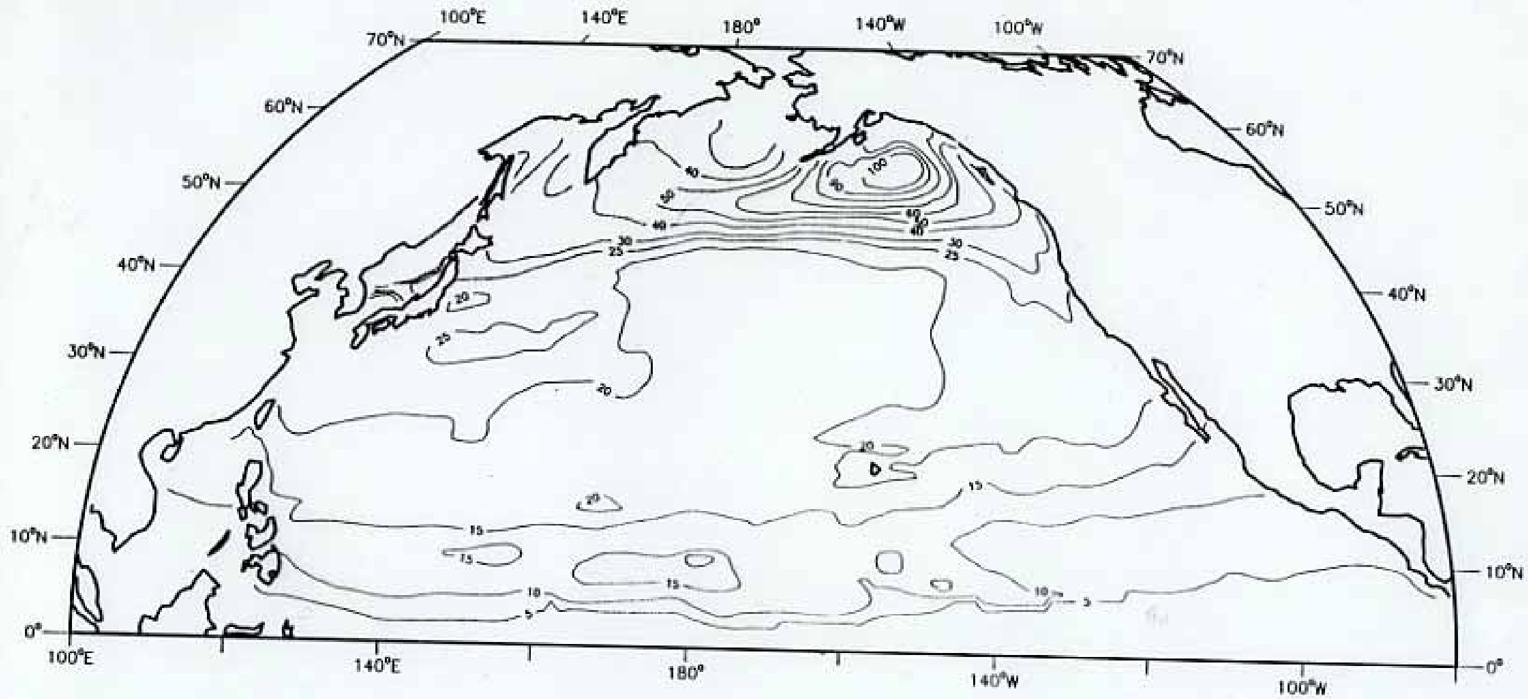


Q $(\sigma_\theta = 26.5 - 27.0)$

(TYPICALLY 200m TO 400m DEPTH)

play in the oceans, where jets flow out to sea and encounter atmospheric input of tracers, heat, and (in effect) potential vorticity. Transport and exchange with the atmosphere must be sensitive to this process of forced ventilation," in addition to the direct, but modest, injection of Ekman fluid into the geostrophic interior.

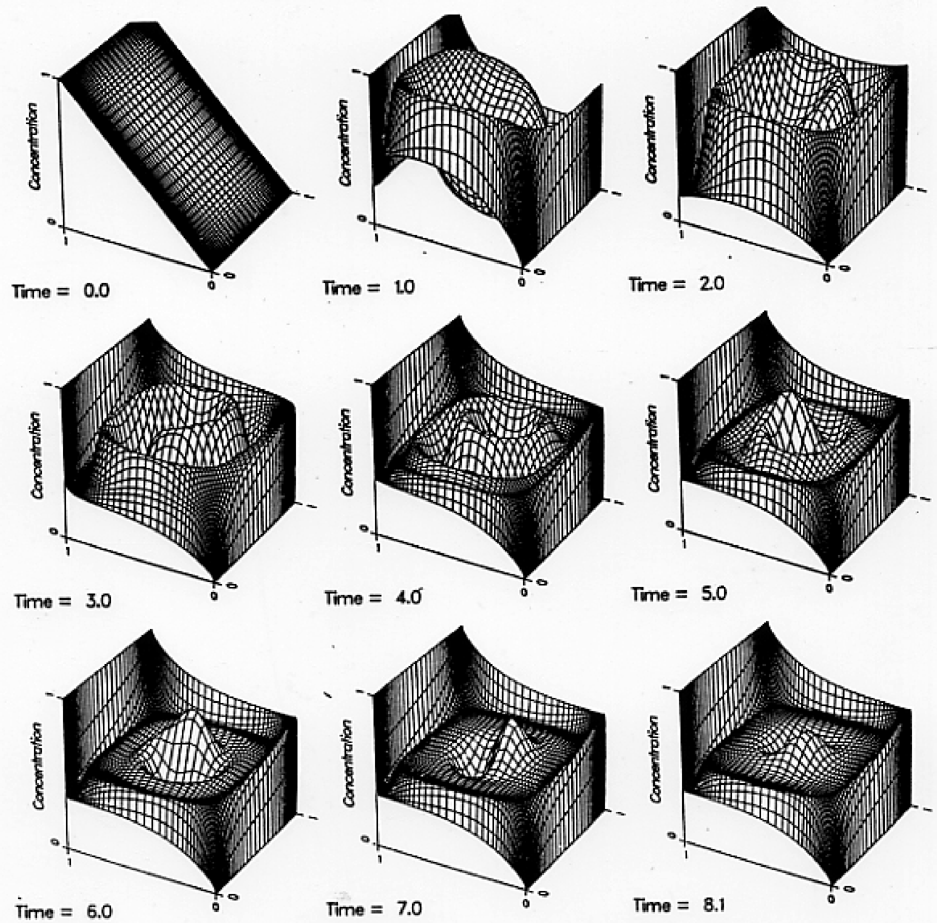


*Figure 10* The spin-up of a passive tracer in a gyre circulation with Péclet number of 2.5 × $10^3$, based on the basin scale and interior velocity (Musgrave 1985). The ridge of high values does not follow the streamlines but represents the winding up of the initial conditions. A weak diffusive spiral crossing $\psi$-lines remains in the steady state upon the homogenized plateau. The injected boundary values can be followed through the western-boundary current, but they are quickly assimilated by horizontal mixing. The large tracer flux through the system depends on thin boundary layers, which are treated with a stretched grid.

26 Jan 79

10 mbar height

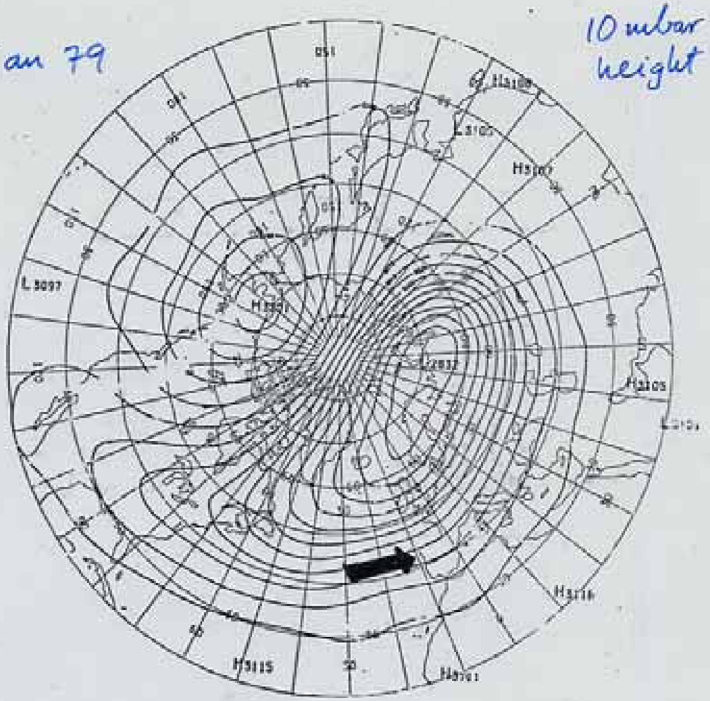

≃ streamfunction × Coriolis parameter

(Middle stratosphere, ~30 km altitude)

Max. velocity ~ 90 m $s^{-1}$, across N. pole.

Isentropic map of Rossby-Ertel potential vorticity on 850°K isentropic surface

$\rho^{-1}(2\boldsymbol{\Omega}+\nabla\times\mathbf{u})\cdot\nabla\theta$

(near 30km altitude)

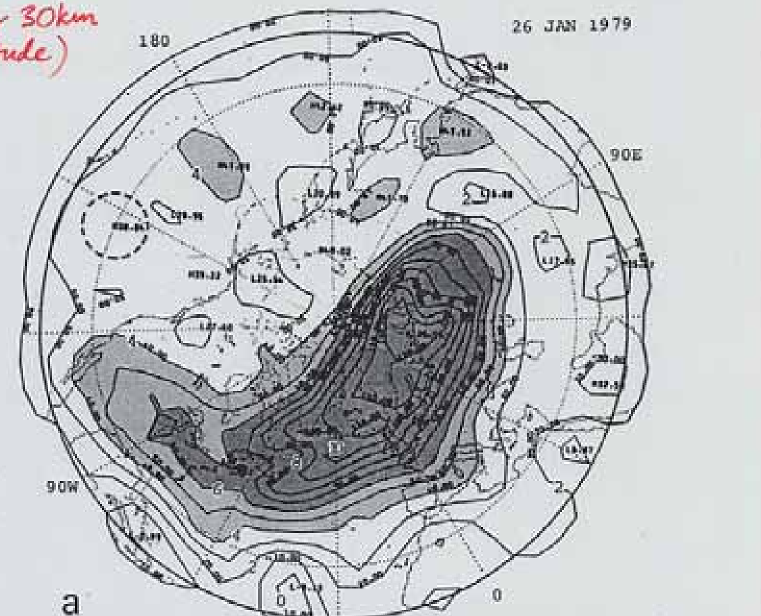


(McIntyre & Palmer 1984 J. Atmos. Terrest. Phys. **46**, 825.)

Units of PV:
Max. planetary vorticity $2\Omega$ corresponds to about 6·5 units

# Jetstreams, Storm-tracks and Subpolar Ocean gyres

Peter Rhines PO sem 2v07

in collaboration with Thomas Jung (ECMWF),
Sirpa Häkkinen (NASA Goddard Spaceflight Center),
Eric Lindahl and Alex Mendez (UW)


Wind god. Sarcophagus from 3C AD. Photo © Maicar Förlag - GML.

Jets, near and far

# The Jet-Stream Conundrum

Mark P. Baldwin, Peter B. Rhines, Huei-Ping Huang, Michael E. McIntyre

*Science, 2007*

*special issue of JAS, 2007*

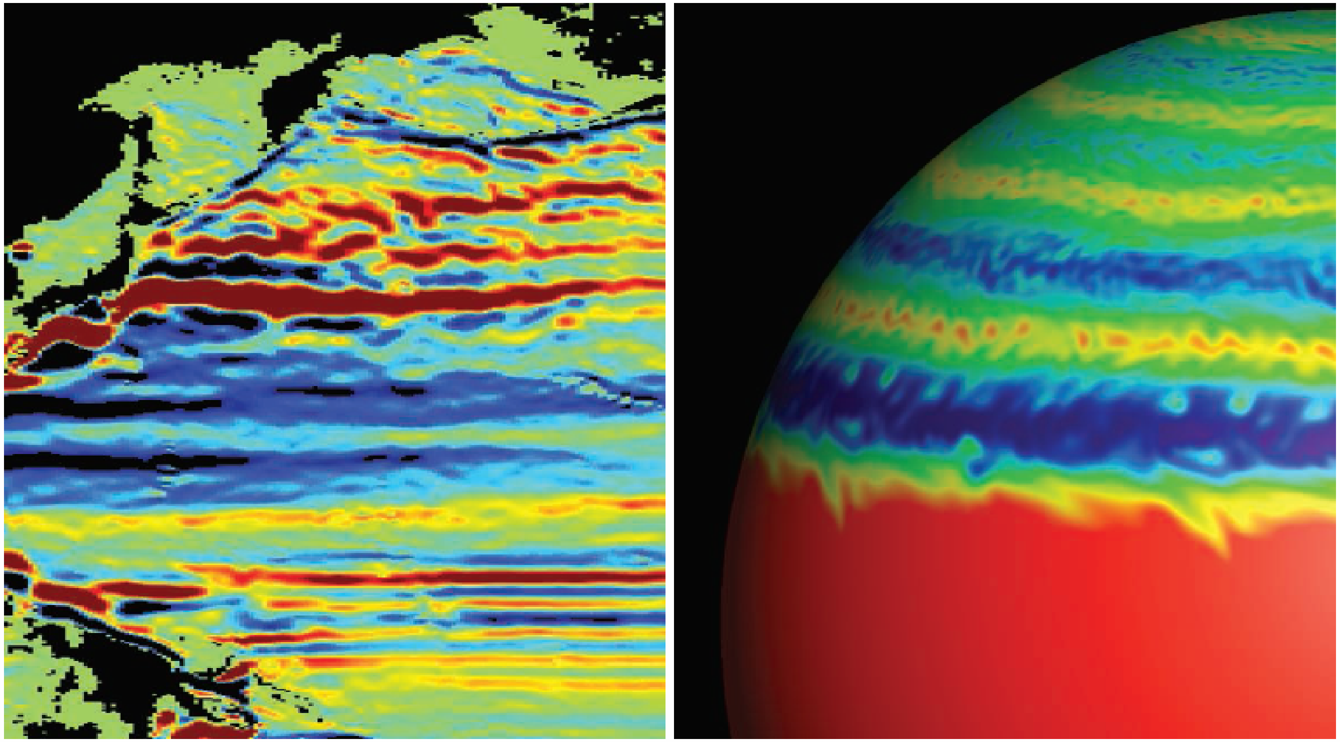

**Jets near and far. (Left)** Map of east-west current speeds at 400-m depth, simulated by an eddy-resolving ocean model. Red and blue indicate eastward and westward flows. [Adapted from Richards *et al.* (*11*)] **(Right)** Snapshot of a simulation for Jupiter, with red and blue indicating eastward and westward flows. [Adapted from Heimpel *et al.* (*16*)]

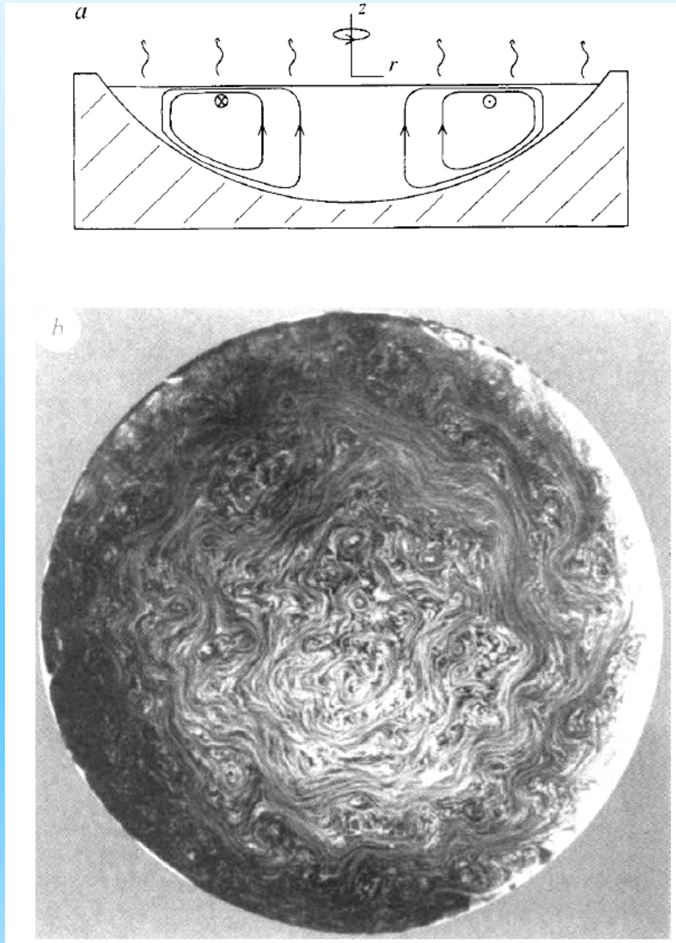


**A convective model for the zonal jets in the atmospheres of Jupiter and Saturn**


**Scott A. Condie* & Peter B. Rhines†**


*Nature, 1994*

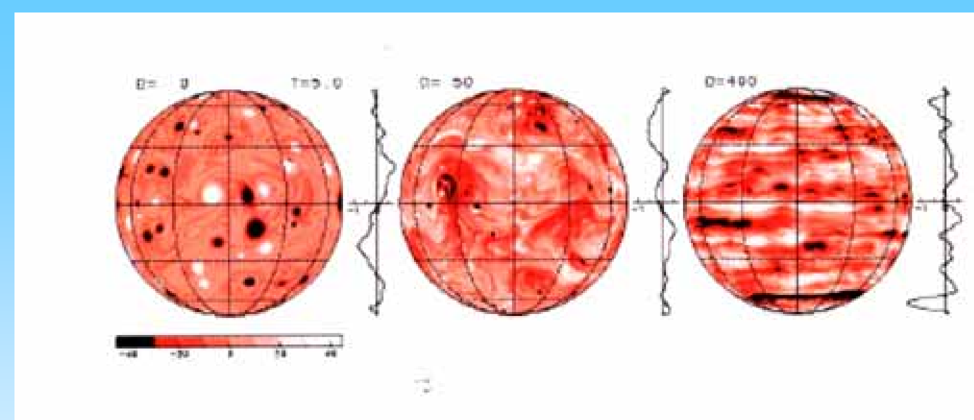

*G.P.Williams, JAS 1978 et seq.,*
*Yoden & Yamada JAS 93*

Jets, shallow and deep:

*Heimpel, Arnou & Wicht, Nature 2005*

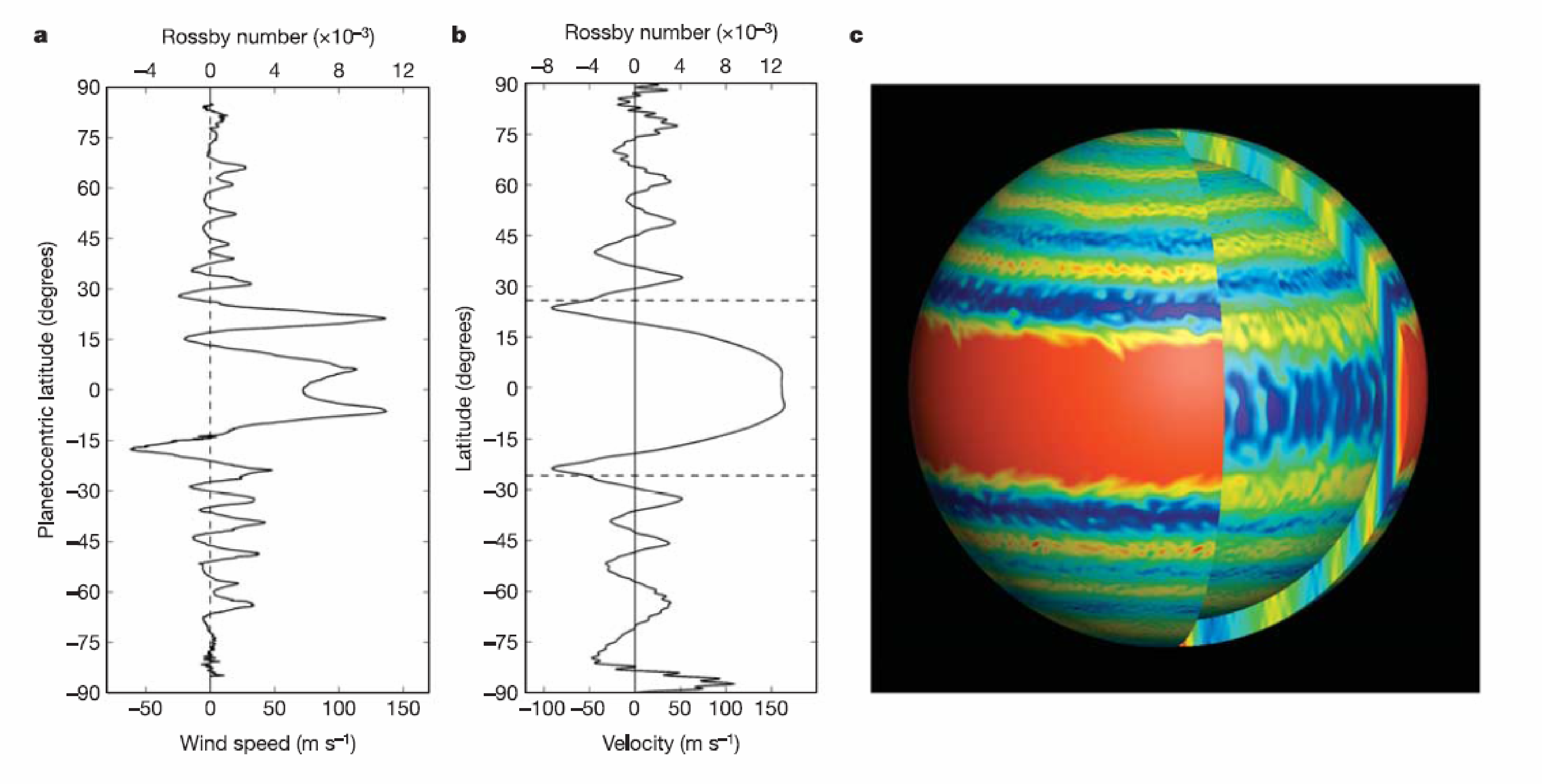

**Multiple jets of the Antarctic Circumpolar Current south of Australia**
*Sokolov & Rintoul 2007*:

**the three classic water-mass boundary fronts are fragmented into multiple filaments.**

Sea-surface height gradient, Southern Ocean, with 3 different choices of time-averaged flow

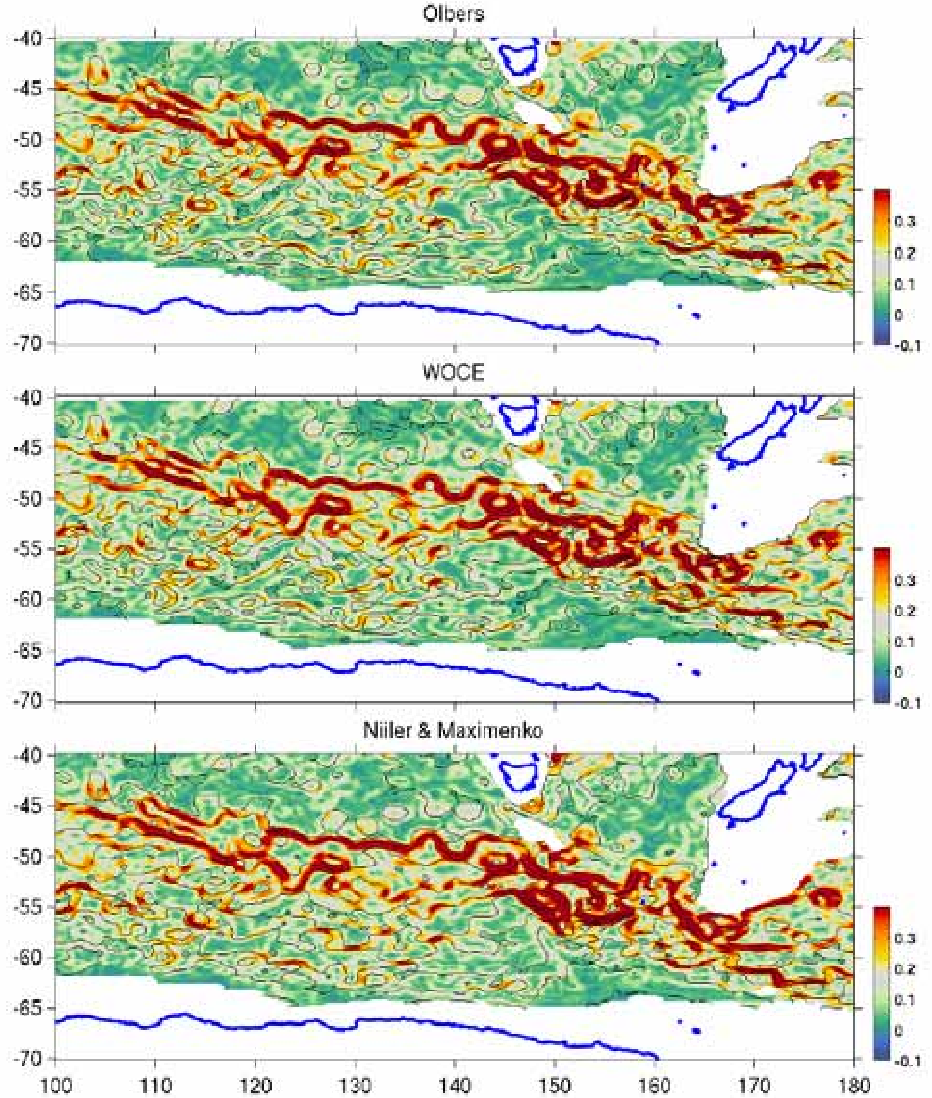


**Figure A2.** Total SSH gradient (anomaly + mean field) on 11 November 1992 using three different mean fields (color). The optimal contours $\zeta_i$ (determined from the fits to the 12-year sequence of SSH gradient maps) are overlaid on each map (black contours).

*Chelton, Schlax, Freilich & Miliff Science 2004*
4-year mean wind curl from QuikSCAT winds:

persistent topographically related ocean frontal SST=>wind stress modification

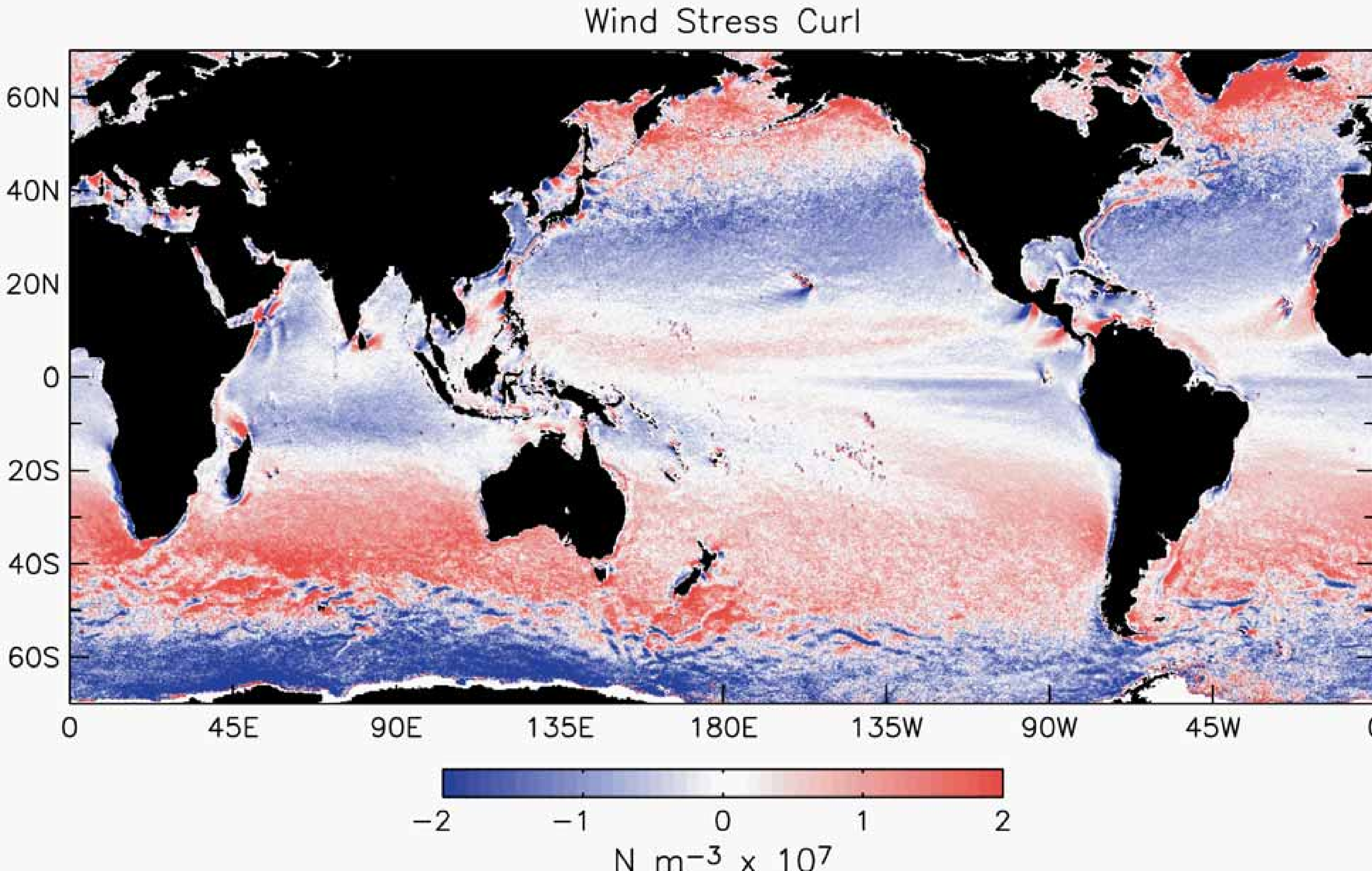

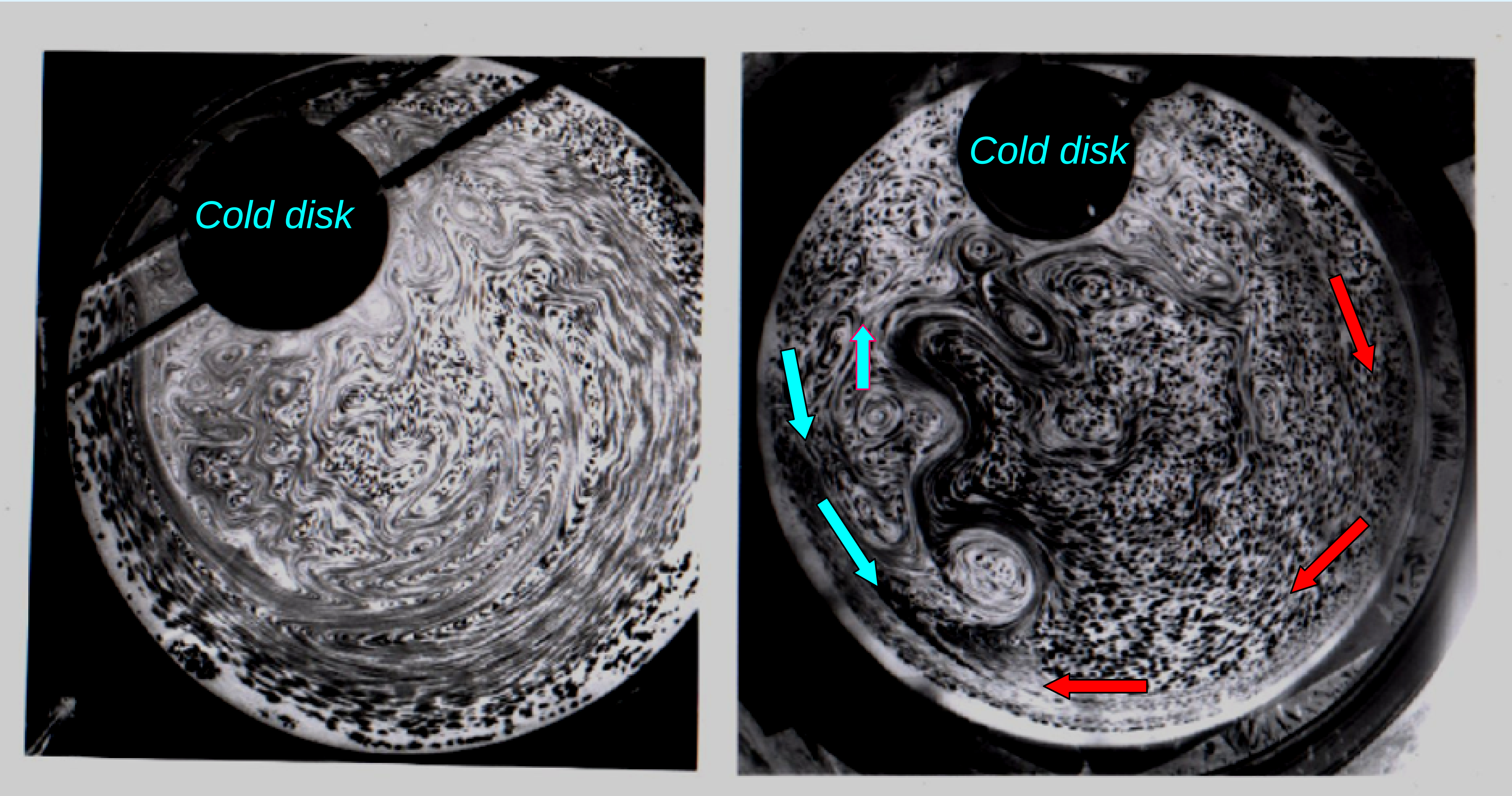


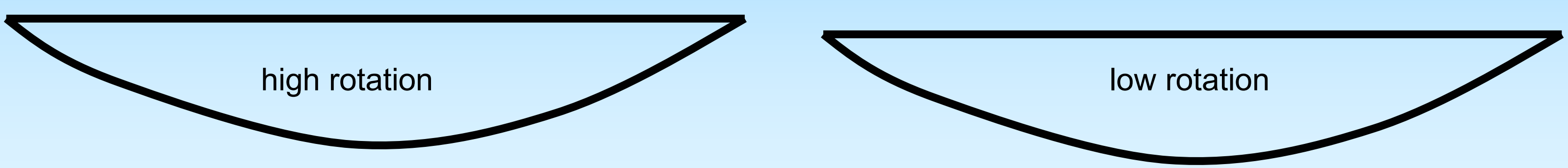


*Jets occur in rotating fluids for many reasons, here driven by thermal convection in a bowl-shaped basin. The jets in the lefthand image occur due to the very strong topographic PV gradient, at high rotation (low Rossby number). Condie & Rhines 'Topographic Hadley Cells JFM 1994; Rhines 'Jets', CHAOS 1994.*

Zonal channel with β-effect: turbulence makes jets

2-layer model,
*Thompson & Young*
*JAS to appear 2007*

Bottom friction is essential in limiting amplitude of circulation and heat flux

Local inhomogeneity generated by the spontaneous formation of zonal jets limits the traditional use of turbulent diffusivities to describe domain-averaged eddy fluxes.

$\beta\lambda^2/U=1/2$ upper, 1 lower

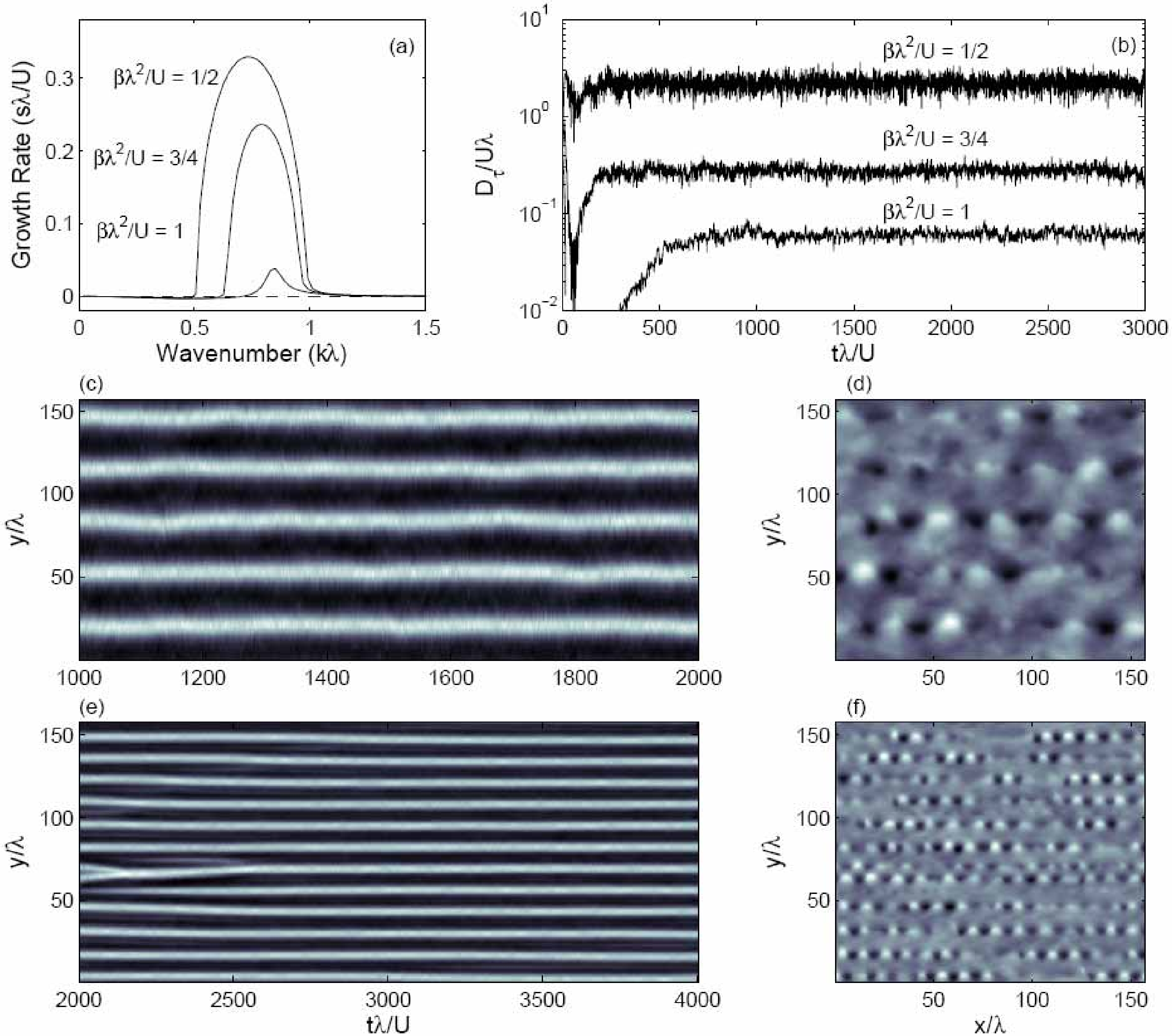

$U_1$, $U_2$ d(PV)/dy PV vs. lat

zonal velocity
and meridional
PV structure,
baroclinic instability
driven 2-layer
channel flow

. The upper layer
is more wavelike and
zonal jets are more
effective barriers to
transport at upper levels
(Greenslade & Haynes
2006). The lower layer,
on the other hand, is
more turbulent and
allows larger excursions
across the jet paths.

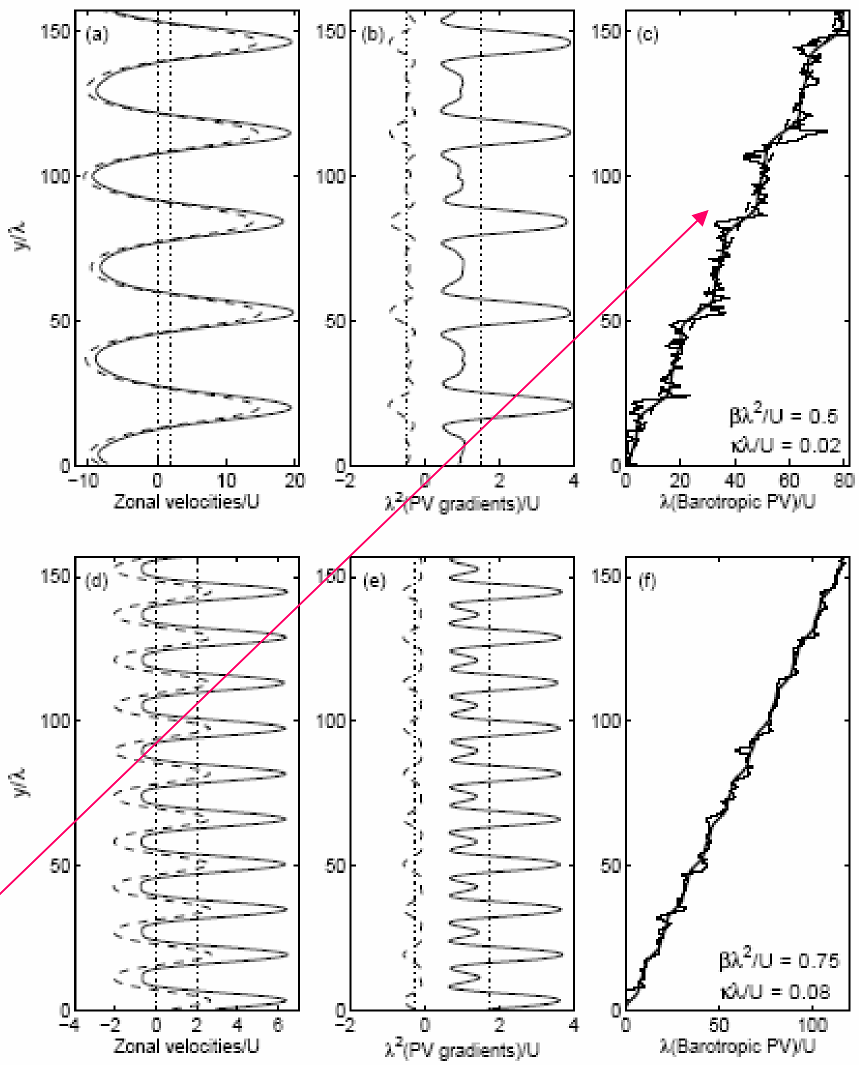


$\beta\lambda^2/U$=.5
$\kappa\lambda/U$=.02

$\beta\lambda^2/U$=.75
$\kappa\lambda/U$=.08

*PV staircase*

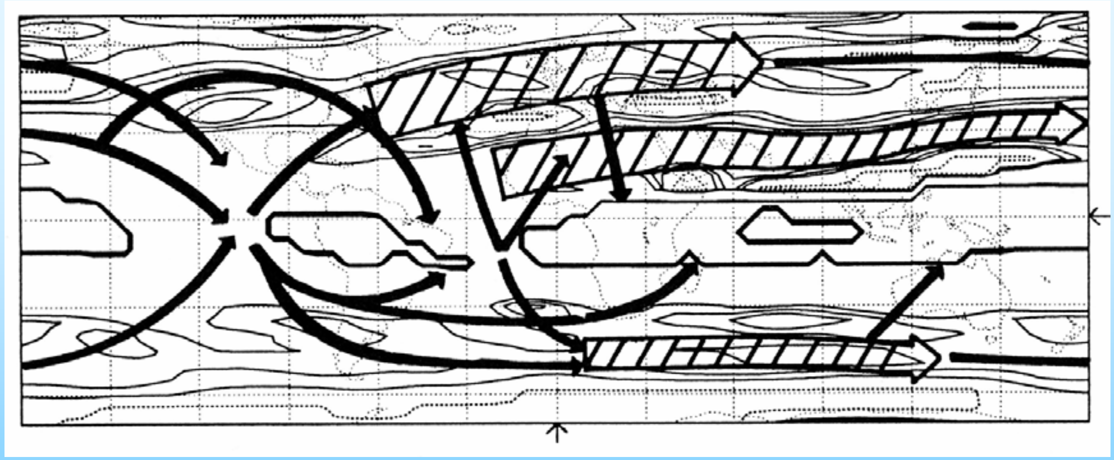

$0^0$

Hoskins+Ambrizzi
JAS 93



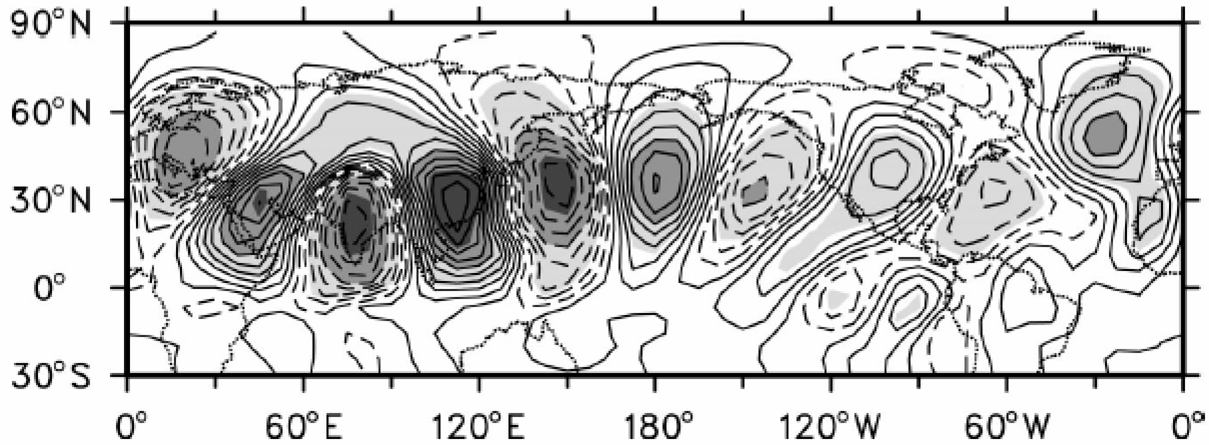


FIG. 4. One-point correlation plot for CCM3 mean Dec–Feb (DJF) 300-mb nondivergent $v$ wind component internal variability for a base point at (28.9°N, 112.5°E). Contour interval is 0.1.

*Branstator JClimate 02*

- JETS: elongated, intense, often persistent fluid flows. (from word 'jut' as jut out, Latin 'jactare', to throw or cast) .

- TRADITIONAL dynamical view: formation through baroclinic instability of a broad, tilted water- or air-mass boundary, with frontogenesis at lower boundary or tropopause.

- turbulent fluid view: stirring of potential vorticity (PV) leads to momentum flux that concentrates jets and balances with far-distant countercurrents. Spontaneous jet formation in a channel with a source of energy (wind, baroclinic instability) (*Taylor 1915, Dickinson 1969 JAS, Rhines 1977, Rhines & Holland 1979)*

- downstream development view, *Chang et al. (2004 J Clim), Hoskins & Simmons…* baroclinic wave-packets

- wavy view: Rossby wave propagation occurs on surfaces with PV gradients…due to $\beta$, topography, sloping isopycnal surfaces, velocity shear

- topographic view: strong mountainous topography is a PV anomaly that can focus broad zonal flows into intense jets and give zonal structure to principal annular modes (*e.g. Taguchi & Yoden 2002, Rhines 2007 JAS*)

Momentum transport by the waves sharpens jets, and barotropizes the mean flow. In fact, the basis of baroclinic instability lies in counter-propagating Rossby waves, one above the other, yet the basics of jet formation involve the reaction to PV stirring, which is nonlinear, perhaps turbulent

*FP Bretherton QJRMS 1966, Methven et al. QJRMS 2005,6, Rhines The Sea 1977, DAO 1979, Chaos 1994*

- Jetstream and storm track in the Atlantic:
  - concentration of meridional energy/moisture transport.
  - leap-frog exchange of meridional energy/moisture transport with oceanic MOC
  - long distance communication via the jet stream waveguide
  - role of standing wave field: **symbiosis of jets and eddies**
  - PV stirring and water mass boundaries: jet makers
  - topographic jet generation

- Atlantic subpolar ocean gyre: driven by (and driving) the atmospheric storm track and its Greenlandic focus

  - satellite altimeter view of surface circulation
    - where does the warm water flow north to reach the Nordic Seas and feed the MOC?
    - SSH : trend and eof structure showing deceleration and shrinkage of SP gyre
      - yet connection with deep MOC outflow not known
    - EKE
  - surface drifter view
    - Lagrangian and Eulerian circulation
    - ➔ hydrography, heat and fresh-water flux: the warm, saline invasion of the Nordic Seas
    - transport and transformation on the $\theta$/S plane

Southern hemisphere and northern hemisphere circulations:
(dynamic height at 1000 Hpa (colors: blue = low pressure cyclones, red=high pressure anticyclones), 300 Hpa, 30 Hpa 1993 (NH), 1996 (SH) winters, 100 days each

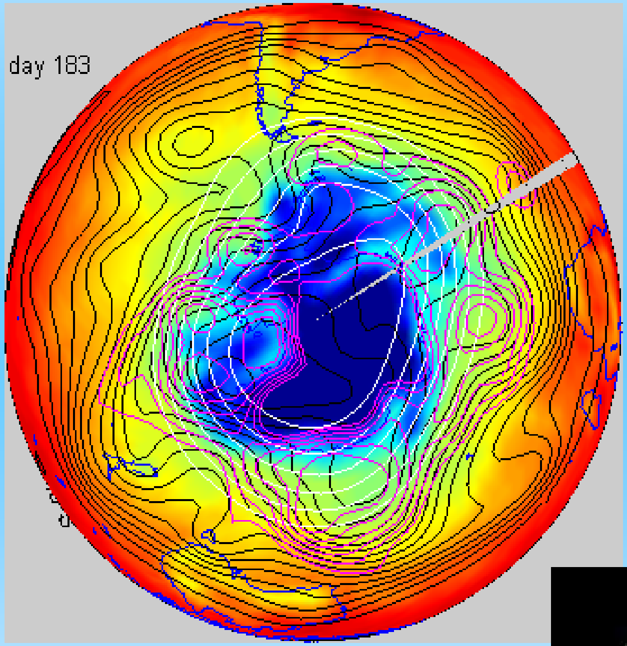


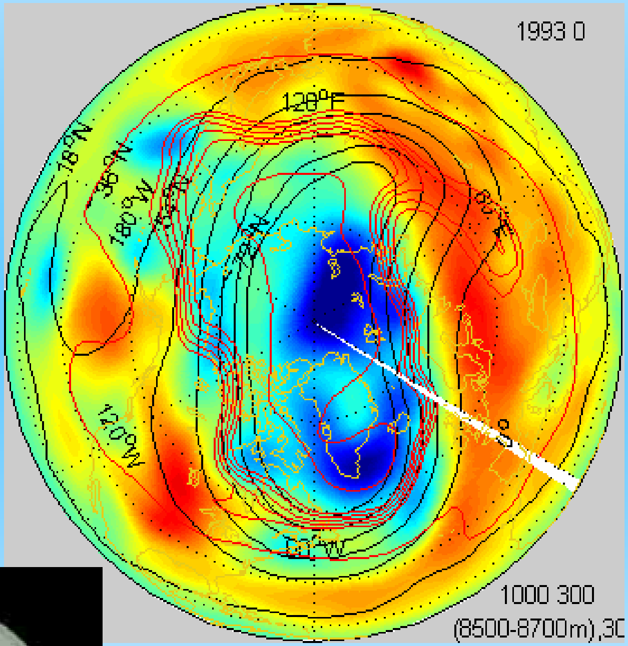


Southern hemisphere and northern hemisphere circulations:
(dynamic height at 1000 Hpa (colors: blue = low pressure cyclones, red=high pressure anticyclones), 300 Hpa, 30 Hpa 1993 (NH), 1996 (SH) winters, 100 days each

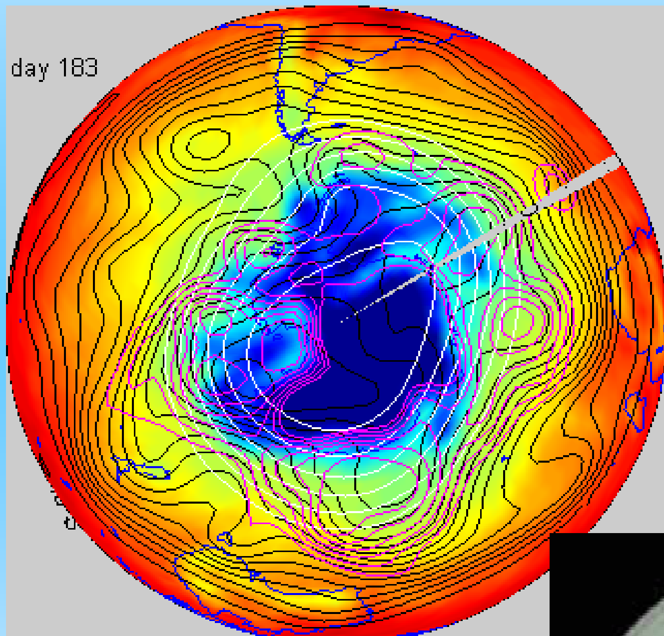


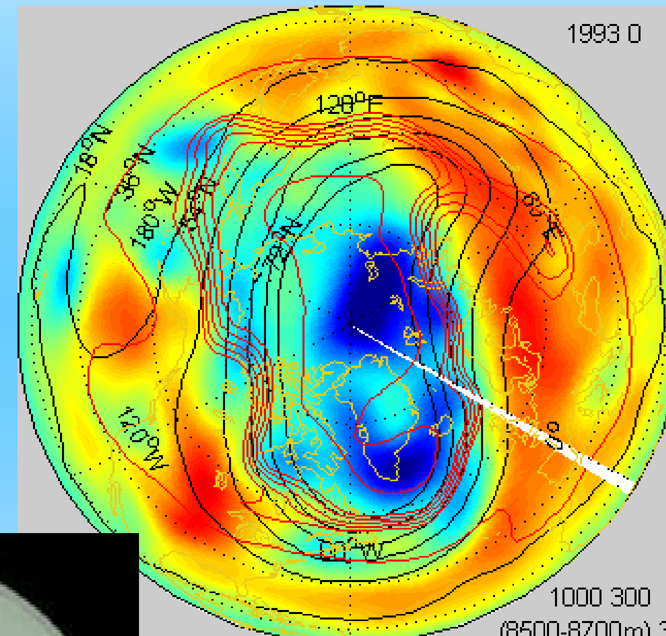


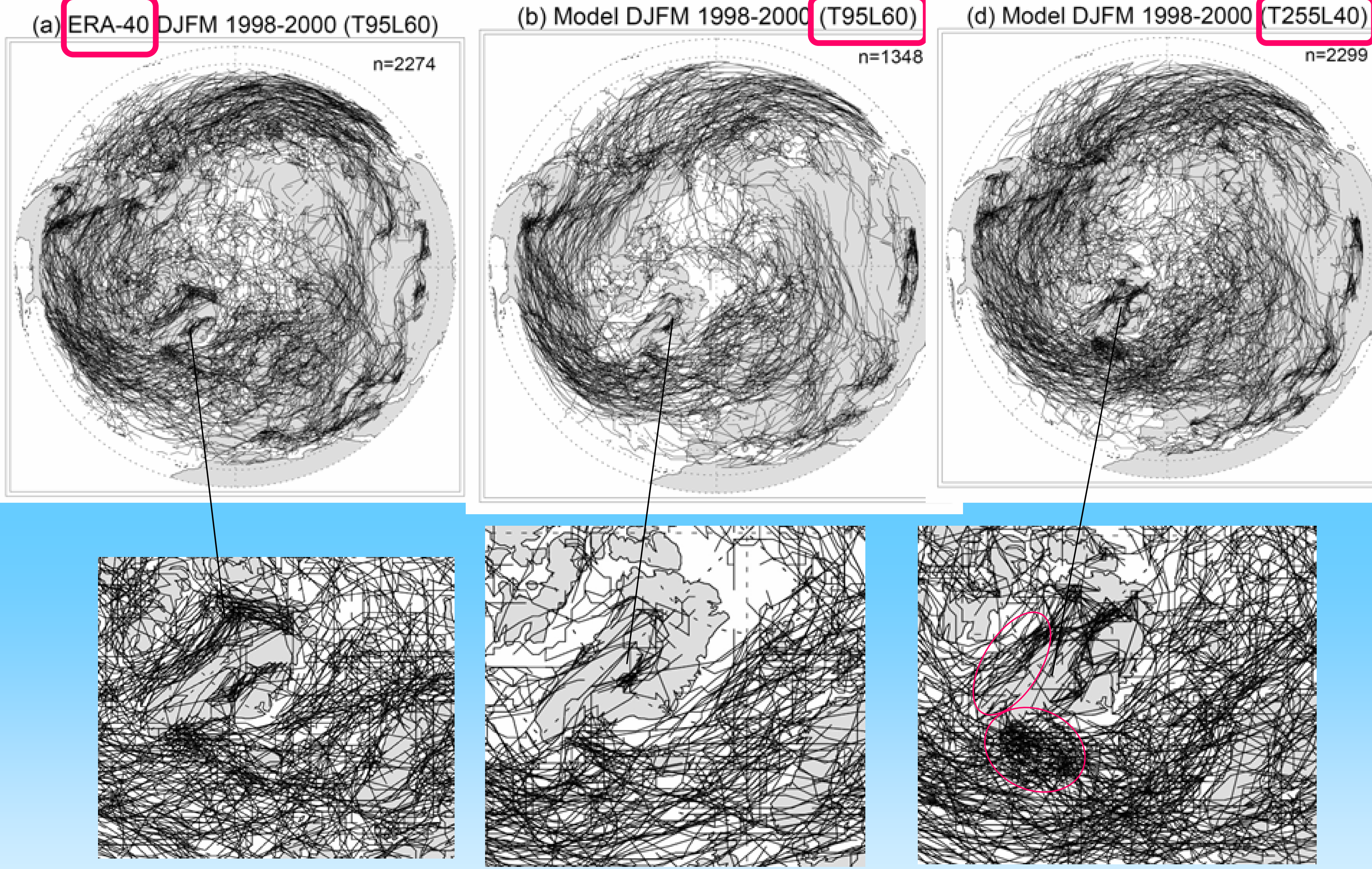


Cyclogenesis west of Greenland, lee cyclogenesis east of Cape Farewell, strong penetration of storms into the Arctic

Hoskins & Hodges
(MWR 2003)
storm tracks based
on vorticity

track density

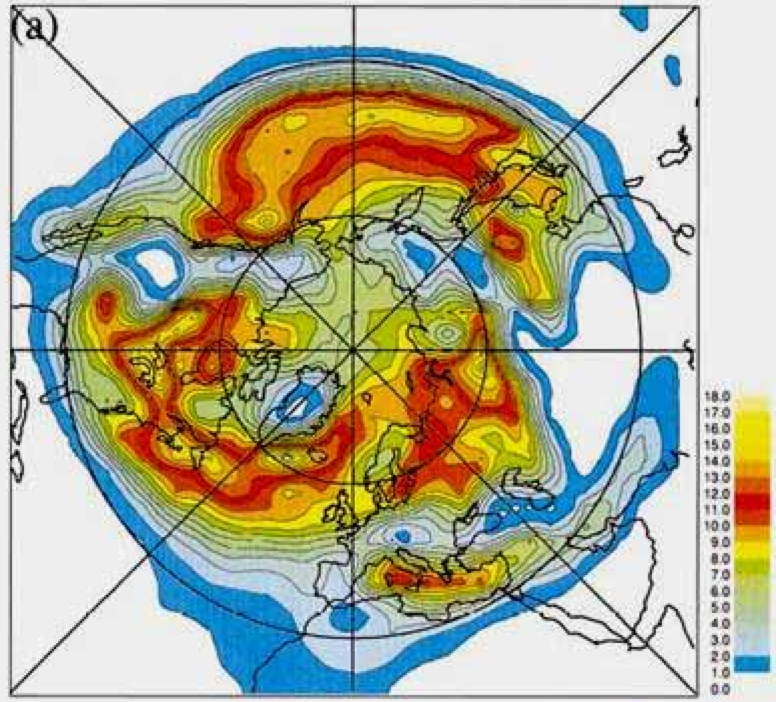


mean intensity

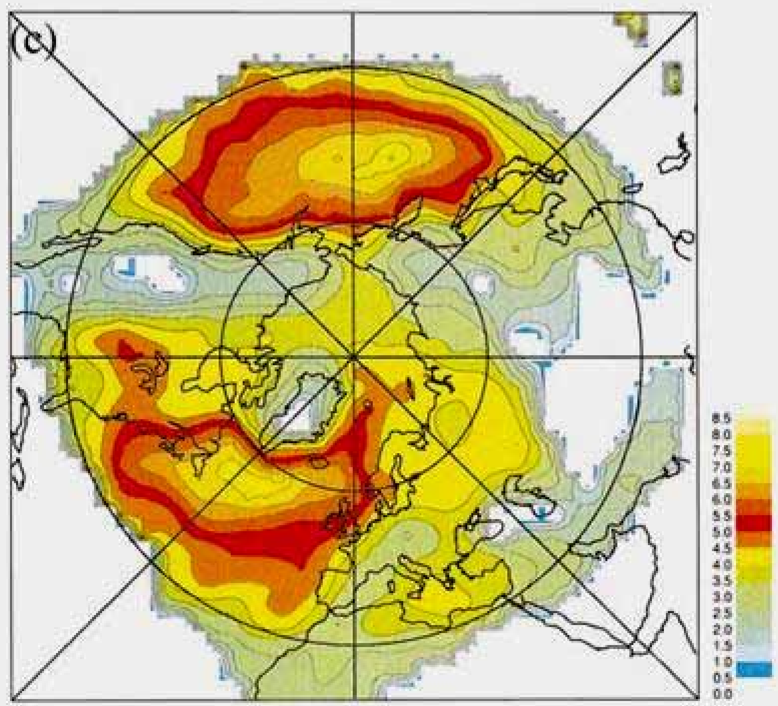

Annular modes with wavenumber-1 sinusoidal topography

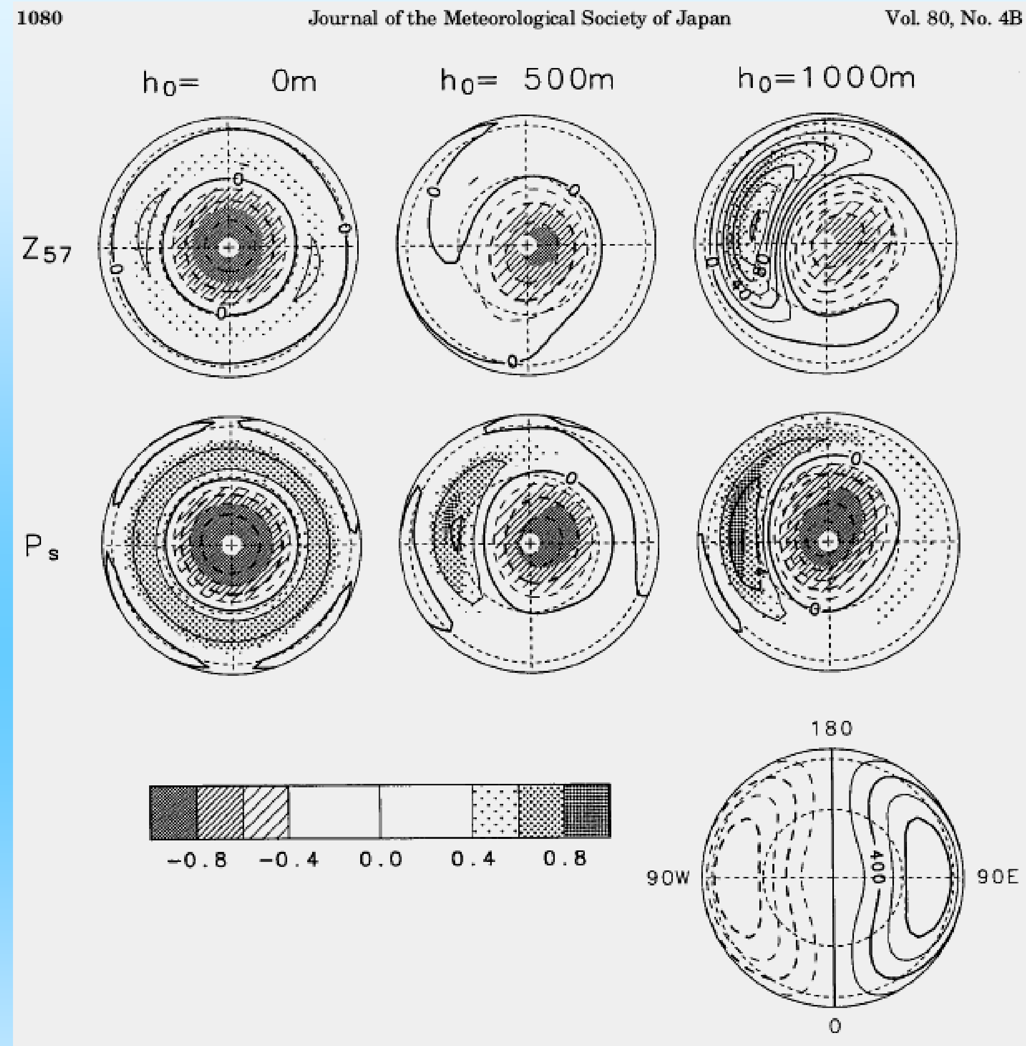

1080 Journal of the Meteorological Society of Japan Vol. 80, No. 4B



Fig. 1. Geopotential height at $p = 57$ hPa, $Z_{57}$ (top) and surface pressure, $P_s$ (middle) regressed onto the AV index in the three runs of $h_0 = 0$ m, 500 m, and 1000 m (left to right). Contour intervals are 20 m for $Z_{57}$ and 2 hPa for $P_s$. Correlations with the AV index are also shown by shades. The surface topography for $h_0 = 1000$ m is shown in the right-bottom panel, with a contour interval of 200 m. Dotted circles in each panel denote the latitudes of $\phi = 30°$N and 60°N, and outermost solid circle does $\phi = 20°$N.

*Taguchi & Yoden*
*J Met Soc Jp 2002*

kinematically, you can make a pair meandering jet by simply adding a zonal flow to a barotropic eddy train,

$$U = Az + B \cos(kx) \cos(ly)$$

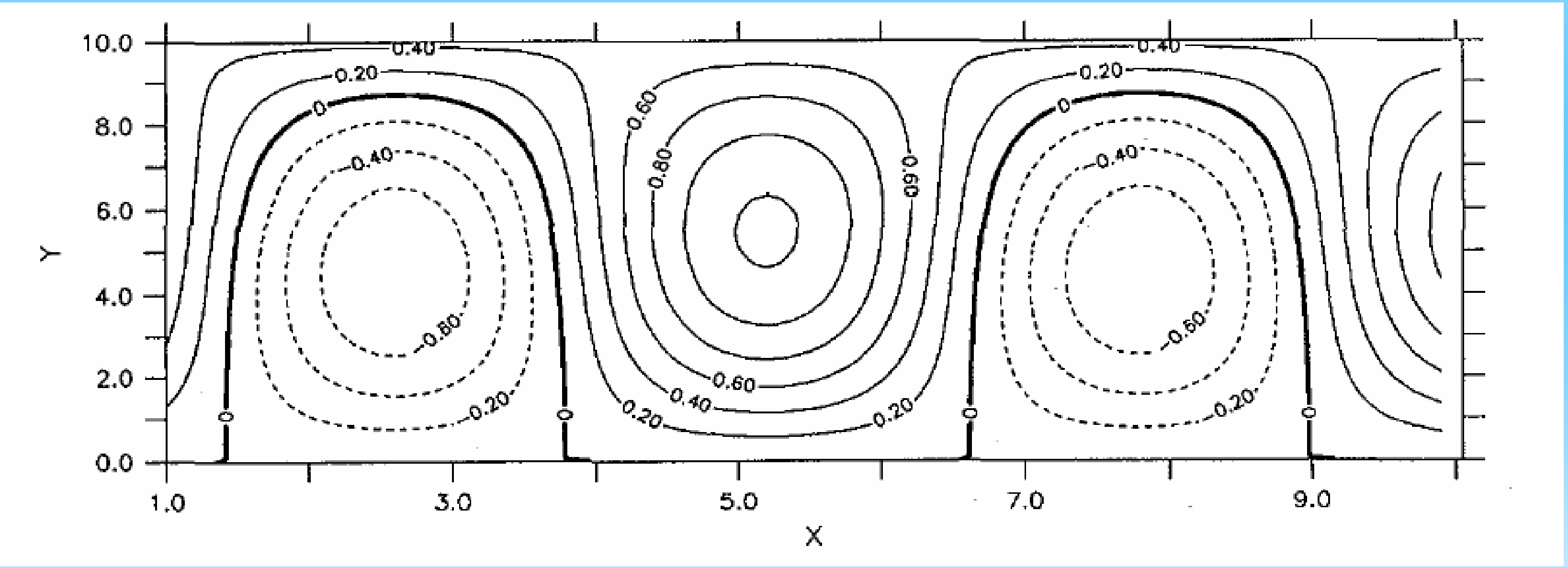

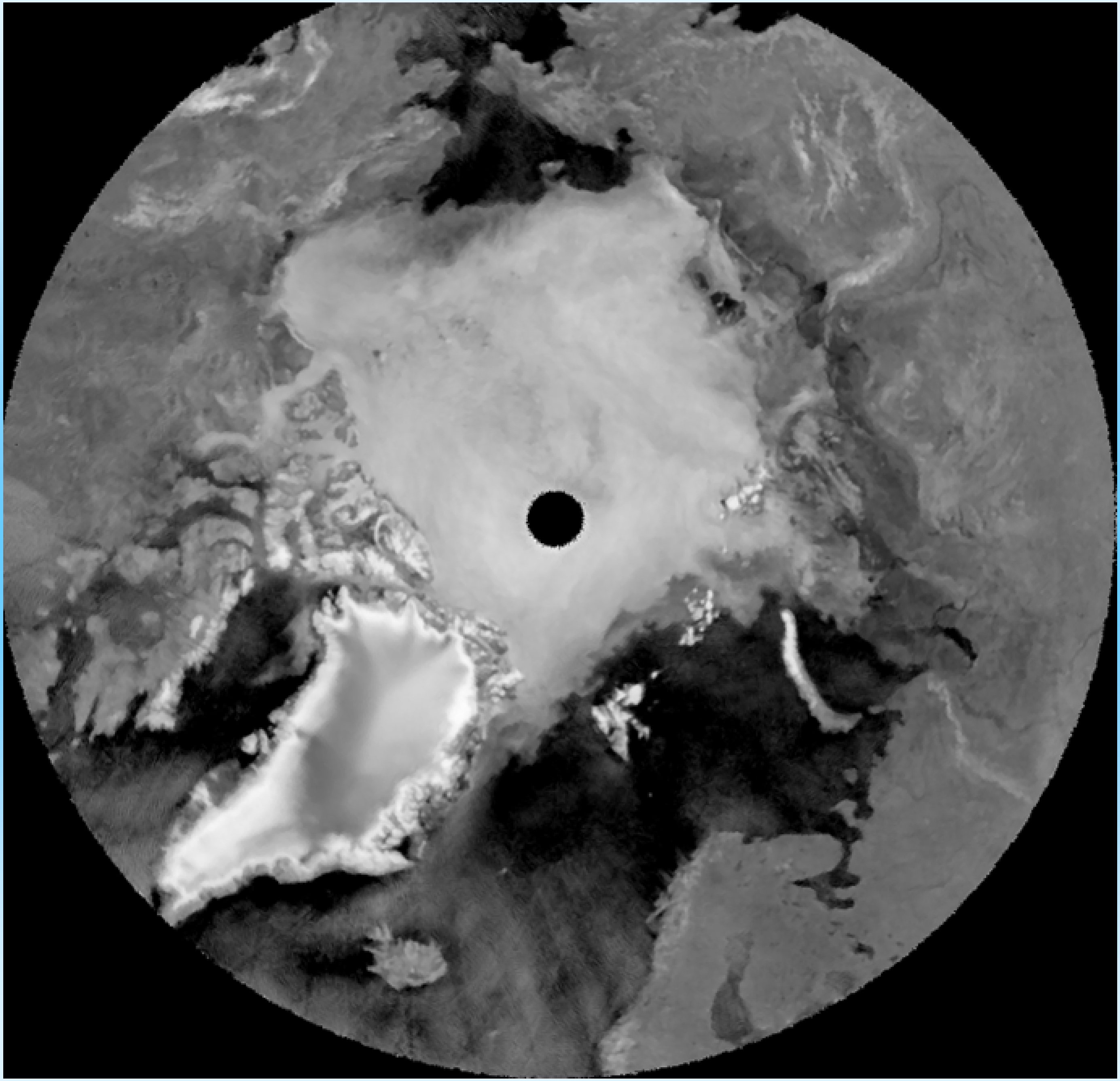

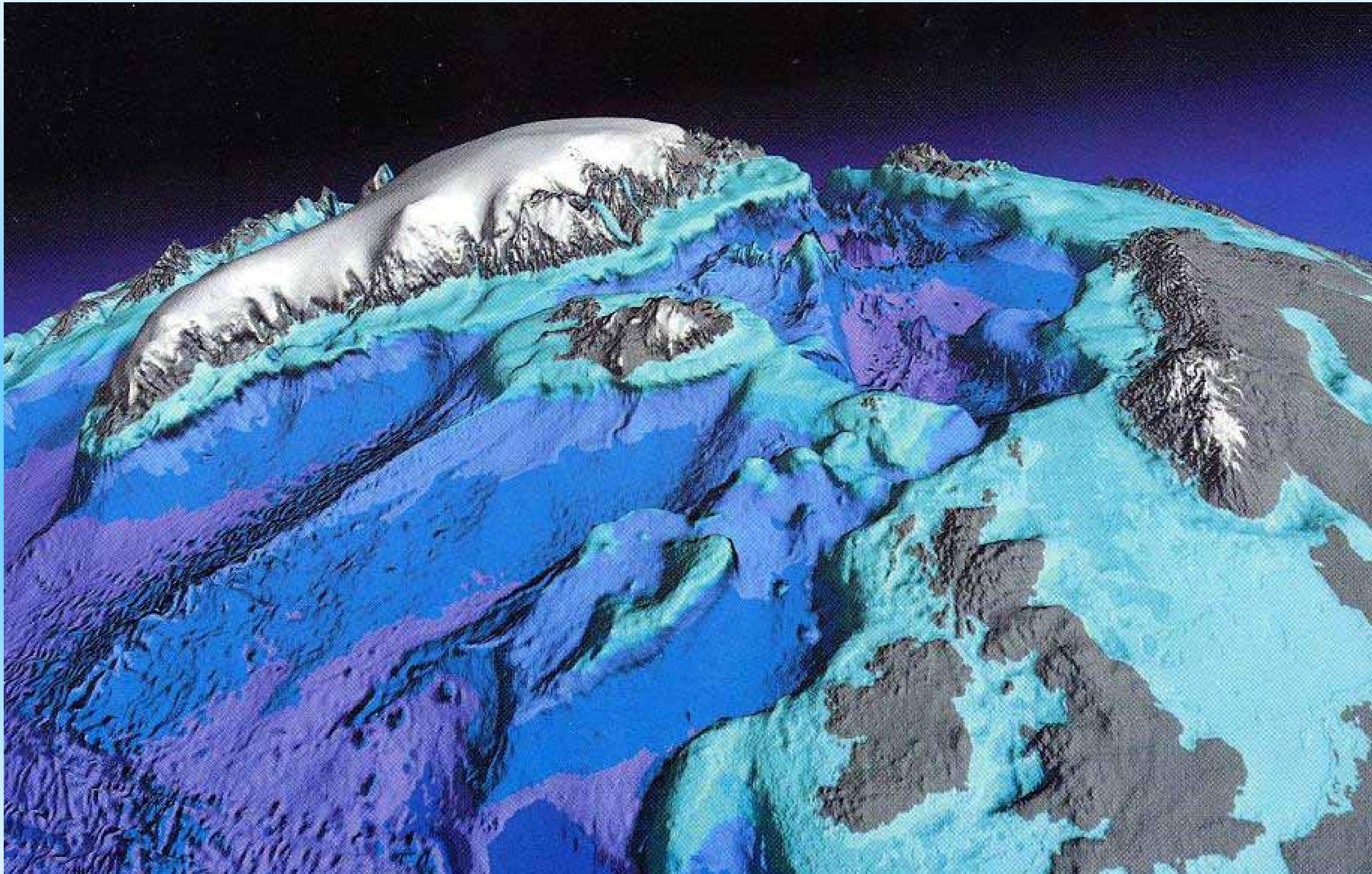

AGU, 2003

zonal wind (m/sec) at 45W with Greenland topography
JFM 1993

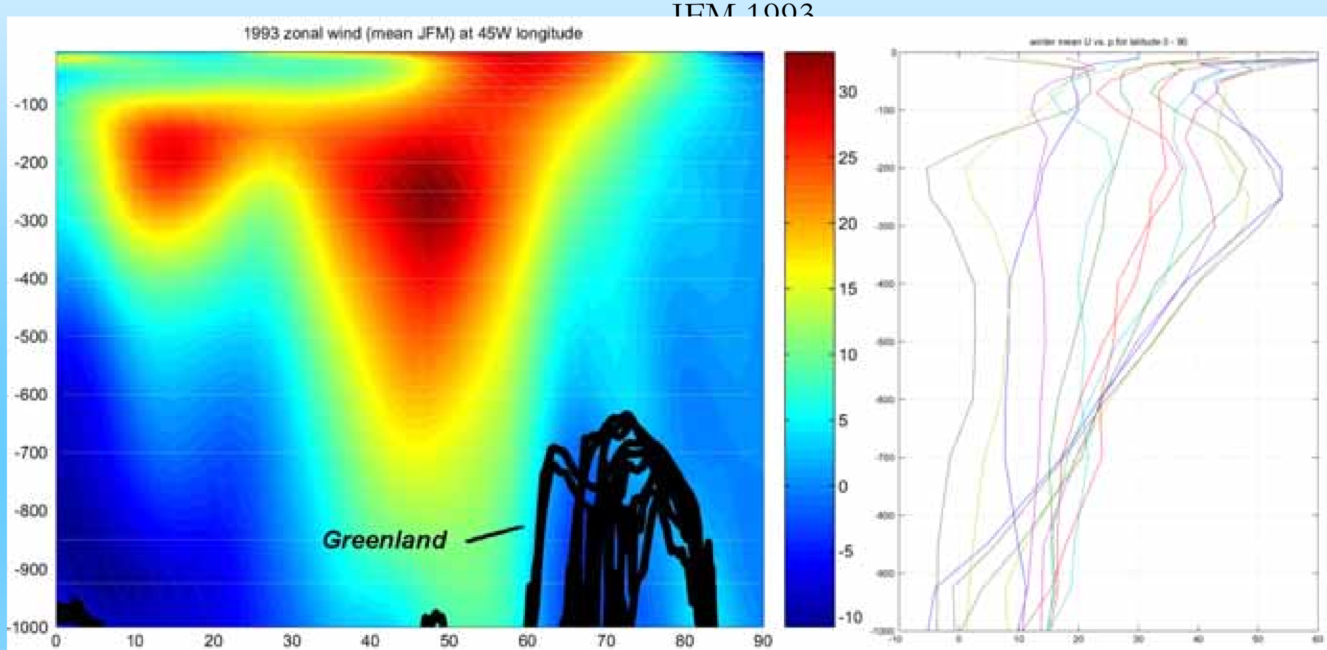


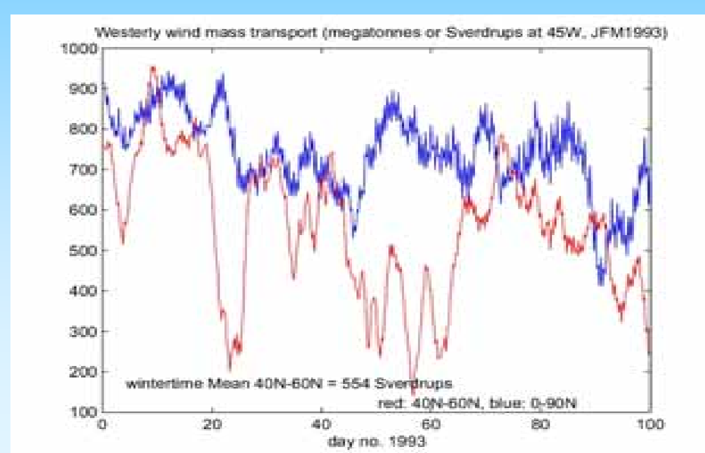


“Svairdrups”

In eddy and jet studies, the prominence of topography comes from the process of *barotropization*, the cascade of energy toward tall, nearly barotropic structures

which can be viewed as a consequence of the enstrophy cascade (the stretching of PV contours) and/or of merger of like-signed baroclinic vortices. A key issue is whether fragmentation of PV continues or is terminated during the cascade (hard-core vs. soft-and-deformable vortices).

Dissipation limited: a weak dissipation example where it plays out fully is Larichev & Held, Held & Larichev (JAS 1996, JPO 1995) β-plane channel, yet Thompson and Young (JAS 2007 in press) argue that surface dissipation is controlling, and must appear in parameterizatio
of meridional heat transport by jets

{This does not contradict the instablity of columnar vortices of scale much smaller than the deformation radius (Dritschel & Ambaum Phys. Fluids 1999)
}

*Barotropization of a two-layer zonal jet* (*Rhines, The Sea, 6, 1977*)
(as exemplified in EP flux analysis of 'baroclinic life-cycles' of the atmosphere); instability followed by eddy-eddy interaction, geostrophic turbulence cascade (taller, wider), *faster* barotropic Rossby wave radiation.

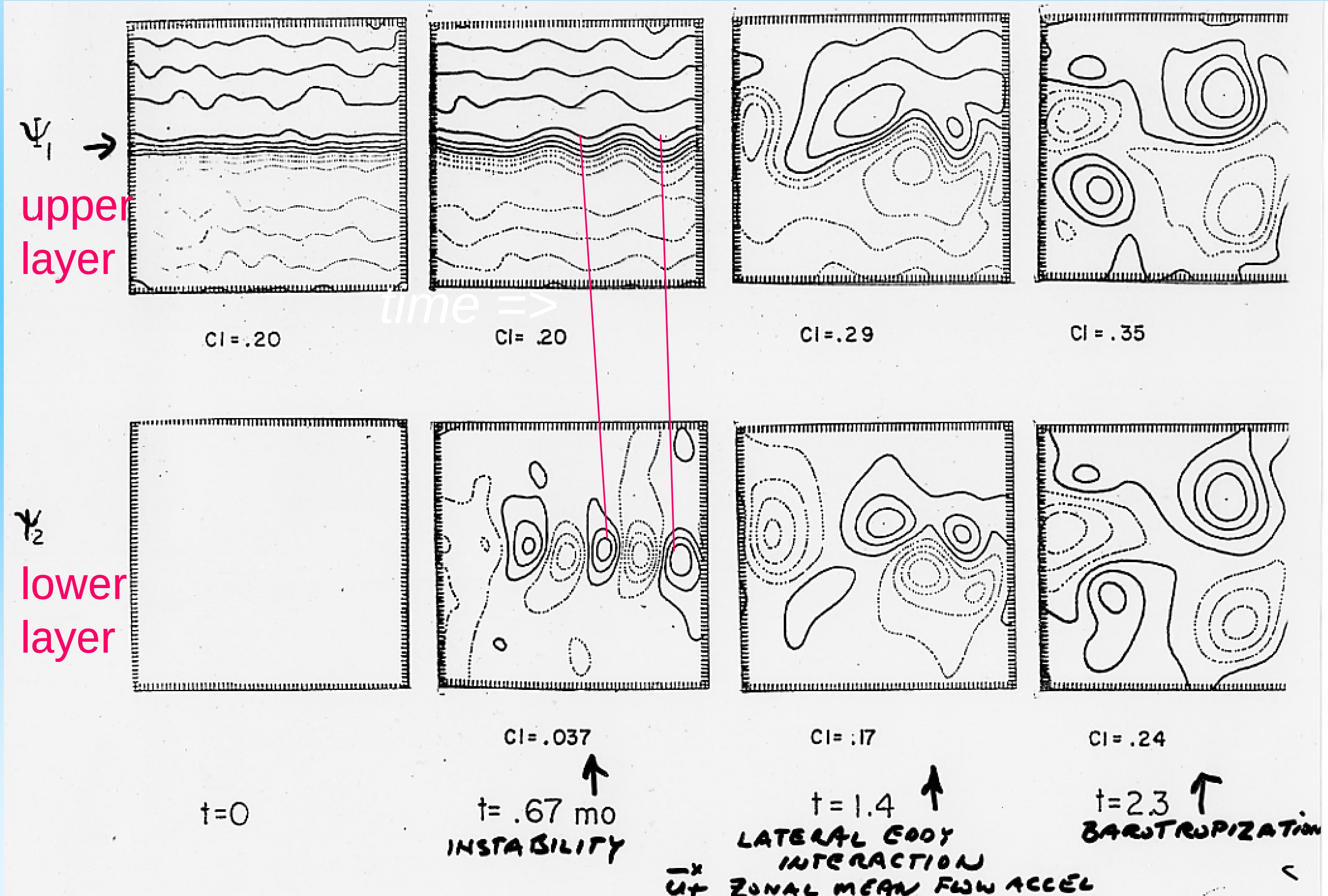

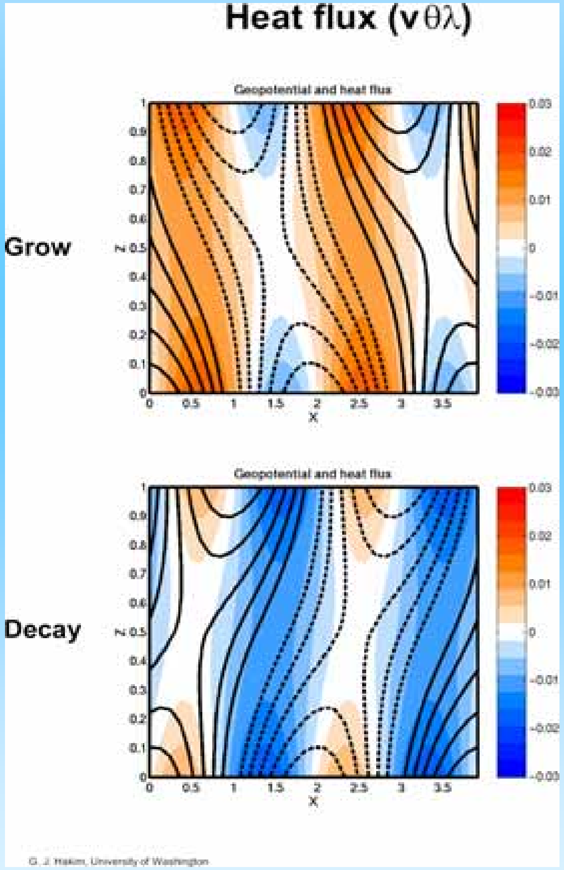


Hakim, AS542 UW

ORLANSKI + GROSS
JAS 2000

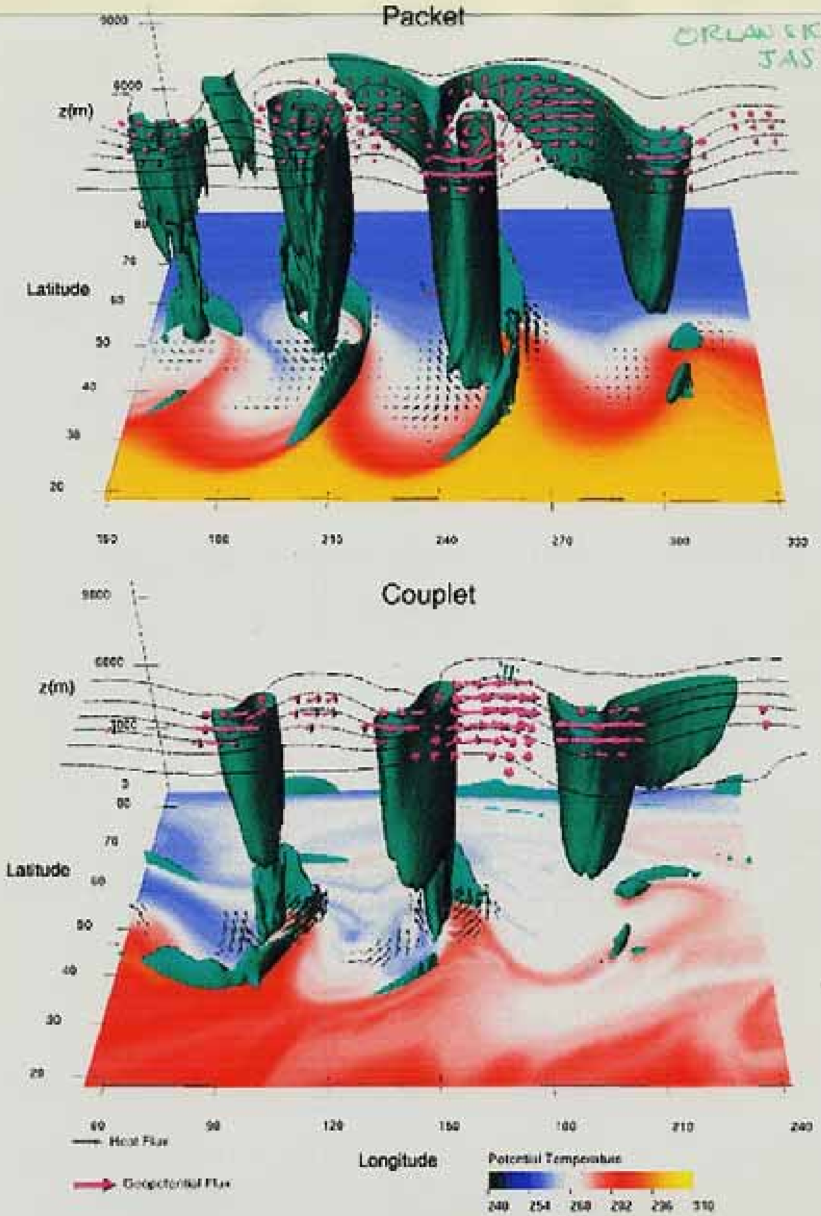


Fig. 7.1 Two distinct storm track patterns are identified: (top) the "packet" structure, in which the low-pressure center at the leading edge is organized by the geopotential

Topographic flows: we now introduce the effects of mountainous topography, which owing to the 'vertical stiffness' imparted by rotation, is greatly influential. On an f-plane, the Rossby number, U/fl, topographic height and Froude number Nh/U are key parameters.

(i) 2D stratified flow over bump of height h (buoyancy freq N upstream flow U)

Nh/U (ii) 3D stratified flow …over or around

Nh/U crit ~ 2 *(Schaer+Durran, JAS 1997)*

dispersive lee waves softens the 'sharp' hydraulic effects

(iii) f-plane rotation, unstratified: Taylor column dynamics

flows 'around' if $h/H > Ro$ ($Ro = U/fL$).

(iv) f-plane rotation weakens blocking (Nh/U crit =>3)Taylor column => Taylor cone $Nh/U > 1$ again! (independent of Ro)

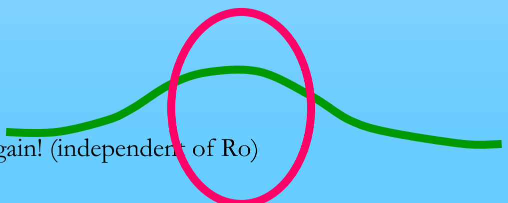

## (v) β-plane flows

-large-scale potential vorticity (PV) gradient

-contours of constant background PV (f/h = const)
bend Equatorward over a ridge, locating
a *cyclone* over its crest for very slow flow

-dispersive lee waves, semi-circular wavecrests

-hydraulic structure in some limits (planetary geostrophic)
where the waves are non-dispersive

-strong upstream blocking ('Lighthill mode') for
$\beta L^2/U > 1$

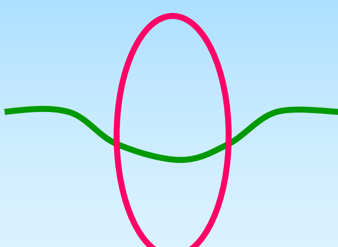

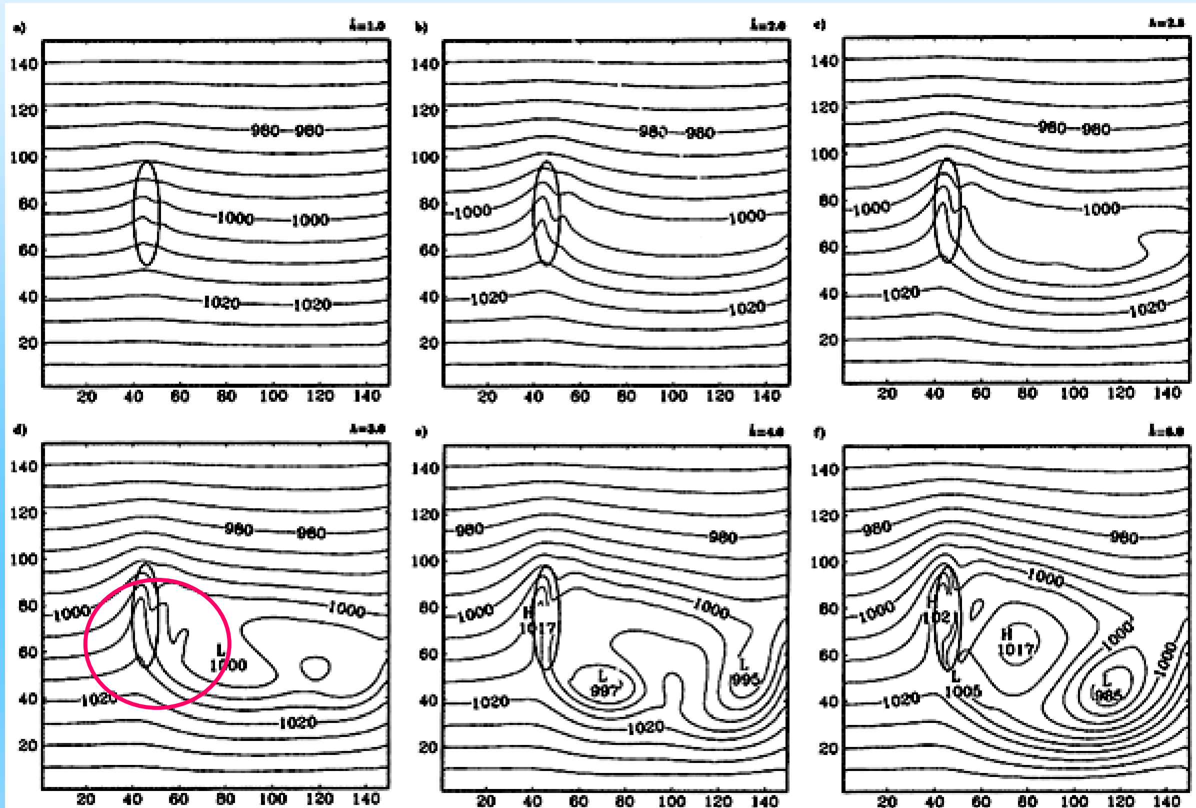

FIG. 2. The sea level pressure (hPa) for different values of $\hat{h}$, with $r = 4$ and Ro = 0.42, at $t^* = 43.2$. (a)–(f) Values of $\hat{h}$ at upper-right corner. Topography at $0.35\hat{h}$.

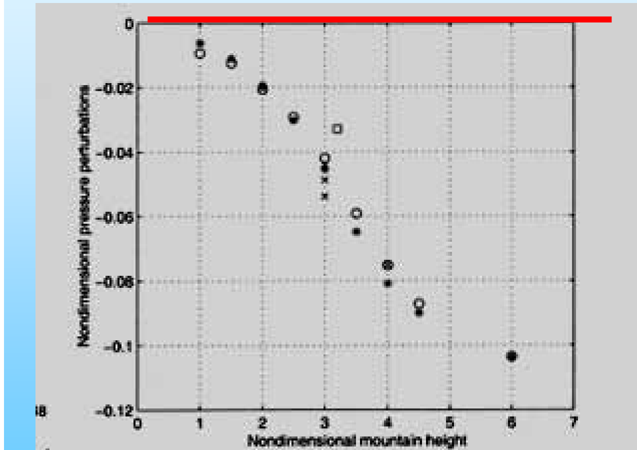


FIG. 5. Nondimensional max sea level pressure deficit downstream of the mountain as a function of $\hat{h}$. The perturbations are normalized by $\rho_o U f L_o$, where $\rho_o = 1.2$ kg m$^{-3}$. Simulations with $N = 0.01$ s$^{-1}$ and $U = 10$ m s$^{-1}$ (stars), with different combinations of $N$ and $h$ (circles), and where $U$ was varied (crosses) (see Table 1). The exgreen simulation (square).

Nh/U = 1, 2, 2.5, 3, 4, 6

*Petersen, Olaffson, Kristjannson JAS2003*

***pressure drag*** occurs when the anticyclone shifts *up*stream as wake vorticity is shed, placing the Equatorward flow over the lee downslope

*Impulse (the time-integrated force on the solid Earth)* is summed up by meridional PV flux:
<q'v'> which expresses the x-averaged force on the Eulerian fluid along a latitude circle ~ (f/H)<h'v'>

**Lee Rossby-waves in the wake of a cylindrical mountain (*McCartney JFM 1976*)**

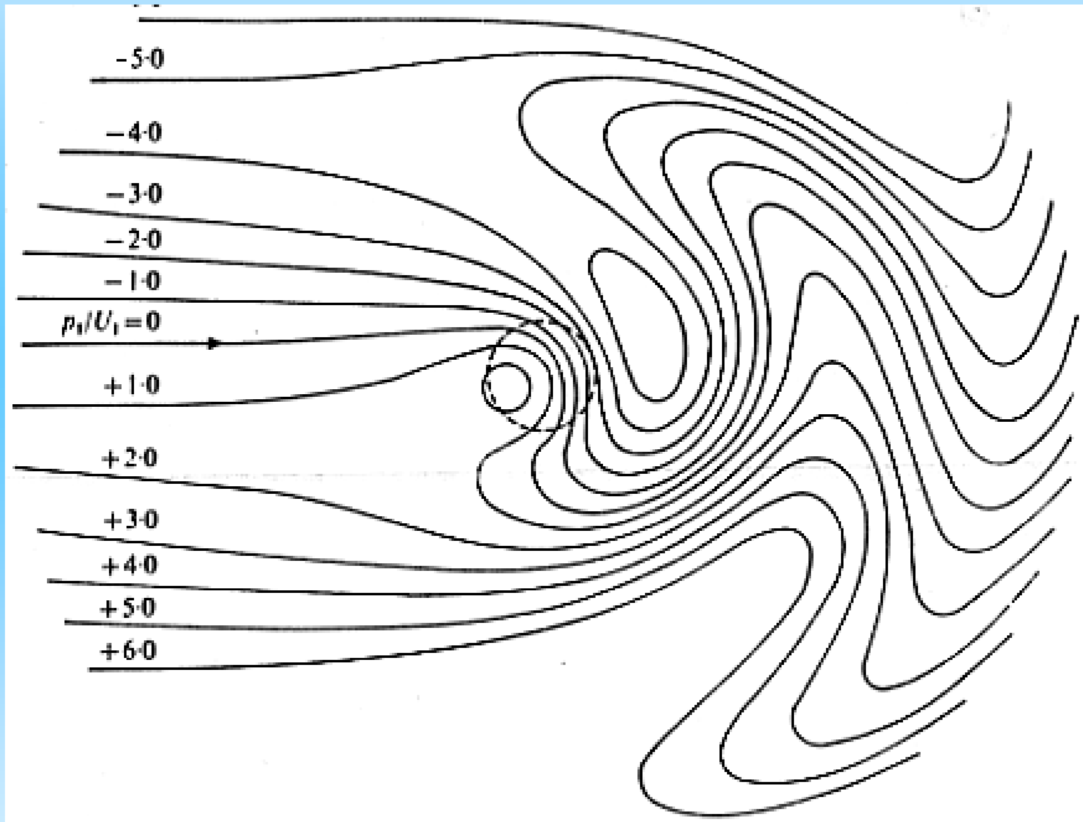


Rossby waves are ‘one-way’: their phase propagation has a westward component relative to the fluid: thus they exist as lee waves for an *eastward* flow but not a westward flow. Wave drag peaks at:

8.2 $\delta/\varepsilon$ times the ‘naive estimate’,

$$\rho f U L^2 \delta H$$

where $\delta=h/H$ is the fractional mountain height, $\varepsilon$ the Rossby number, U the mean flow, L the radius and H the total fluid depth

note strong correlation of meridional velocity and topographic height.....wave drag. Also note the beginnings of jet formation southeast of the mountain, even in the linear theory

# wavenumber diagram for Rossby waves in steady zonal westerly flow (U>0)

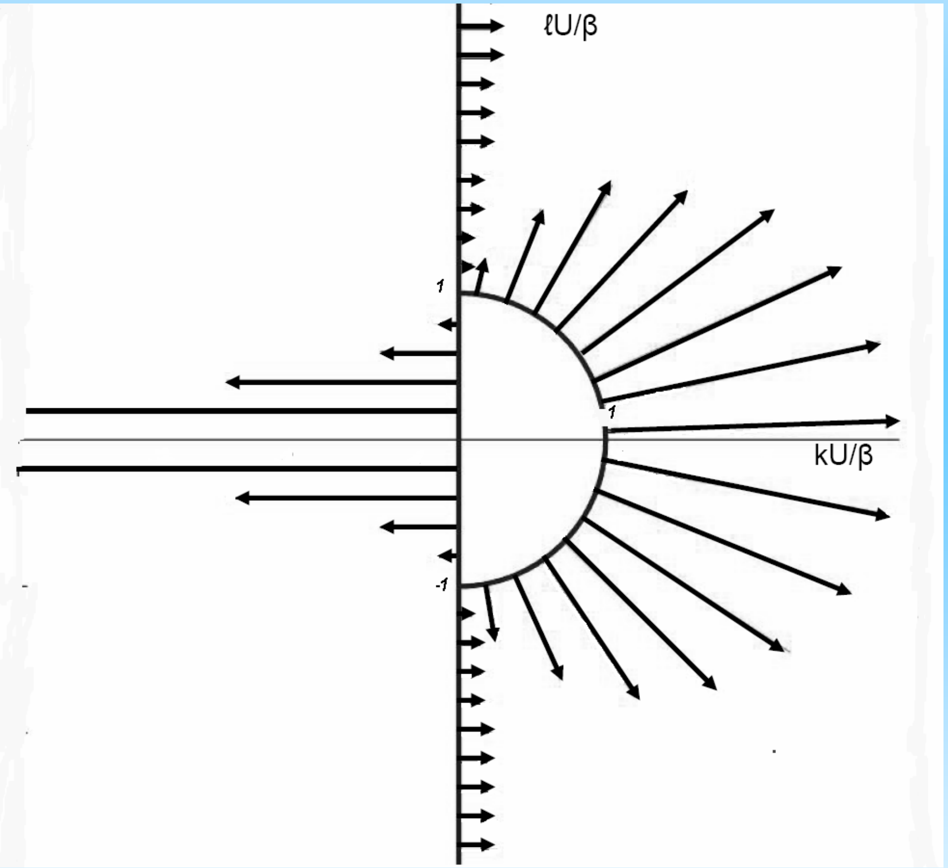

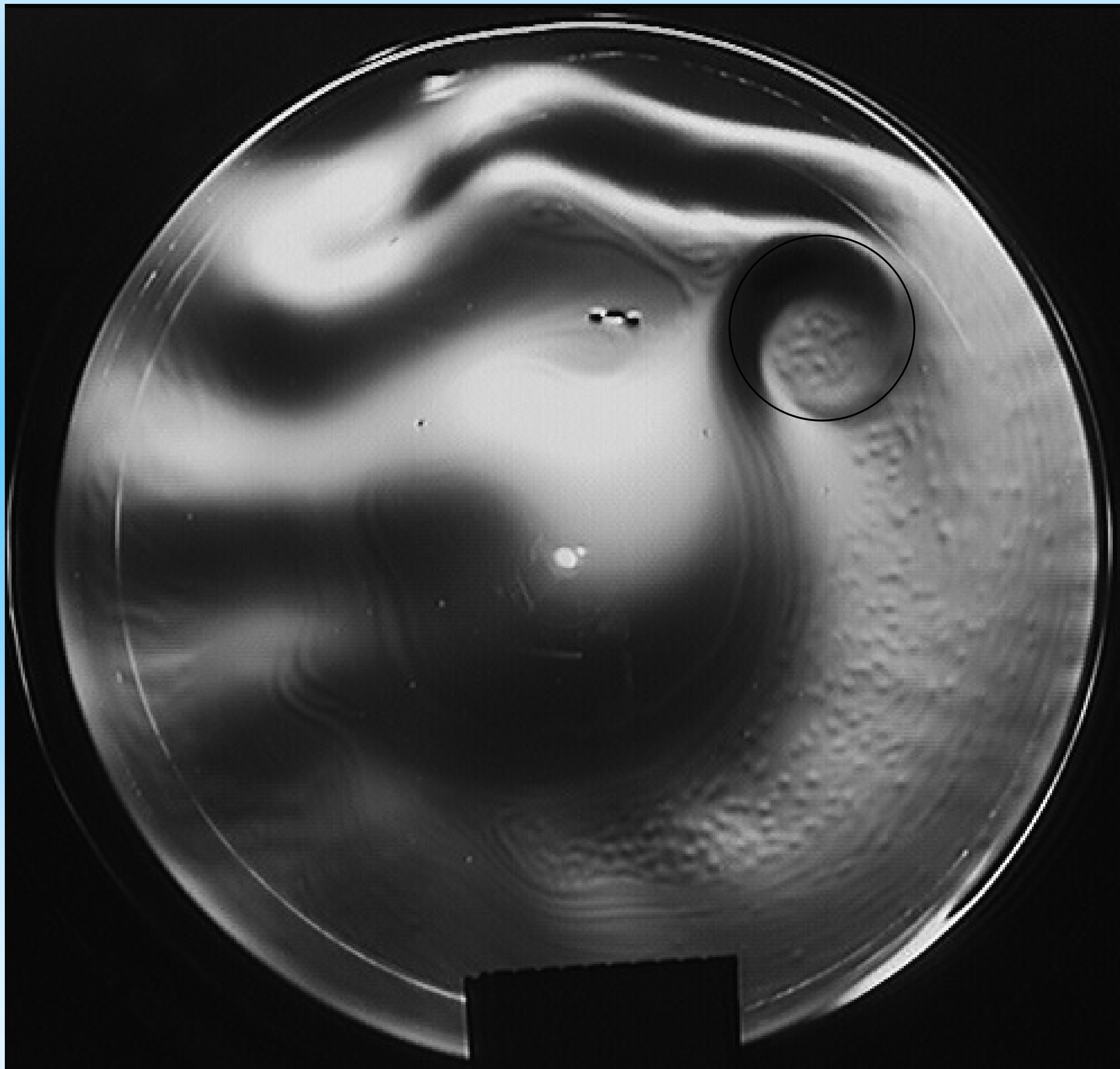

A westerly (prograde, cyclonic) zonal flow encounters a small mountain (at 2 o'clock). Rossby wave dynamics produces standing waves downwind, a convoluted lee cyclone, intense jet structure wrapping round the mountain, and a 'Lighthill block' upstream. This stagnant blocking region is (in linear, yet finite topography, theory, a Rossby wave with vanishing intrinsic frequency and upstream group velocity for merid. wavenumbers < $(\beta/U)^{1/2}$ . Note the ruddy pressure features which are fine-scale evaporative convection cells, pillar-like cyclones. The edge of the block is outlined by convective rolls.

Here the controlling parameter $\beta a^2/U > 1$ meaning that the wake is stable; smaller values of this parameter yield unstable wake and transier Rossby waves which ironically fill the hemisphere (they are not simple lee waves). See Polvani, Esler, Plumb JAS 1999 for a numerical study with some of these features.

Streak image of the same experiment (dots 2 sec apart) showing intensity of jets near mountain, lee Rossby waves and upstream block


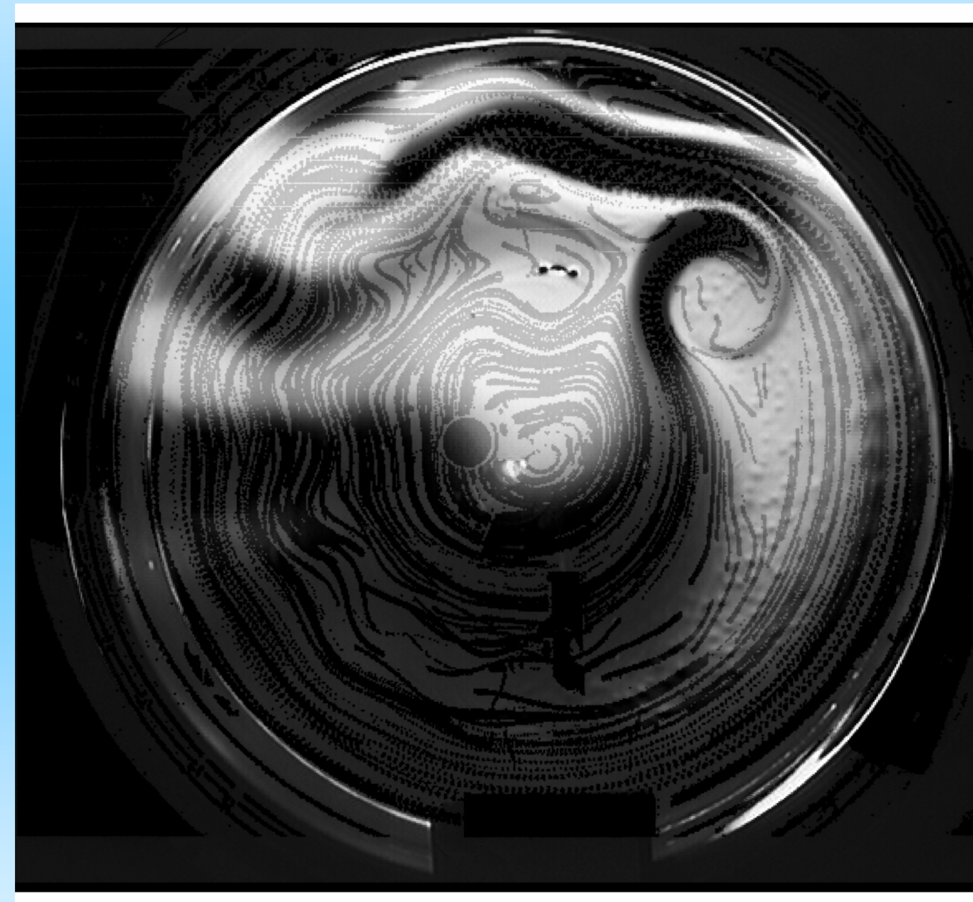

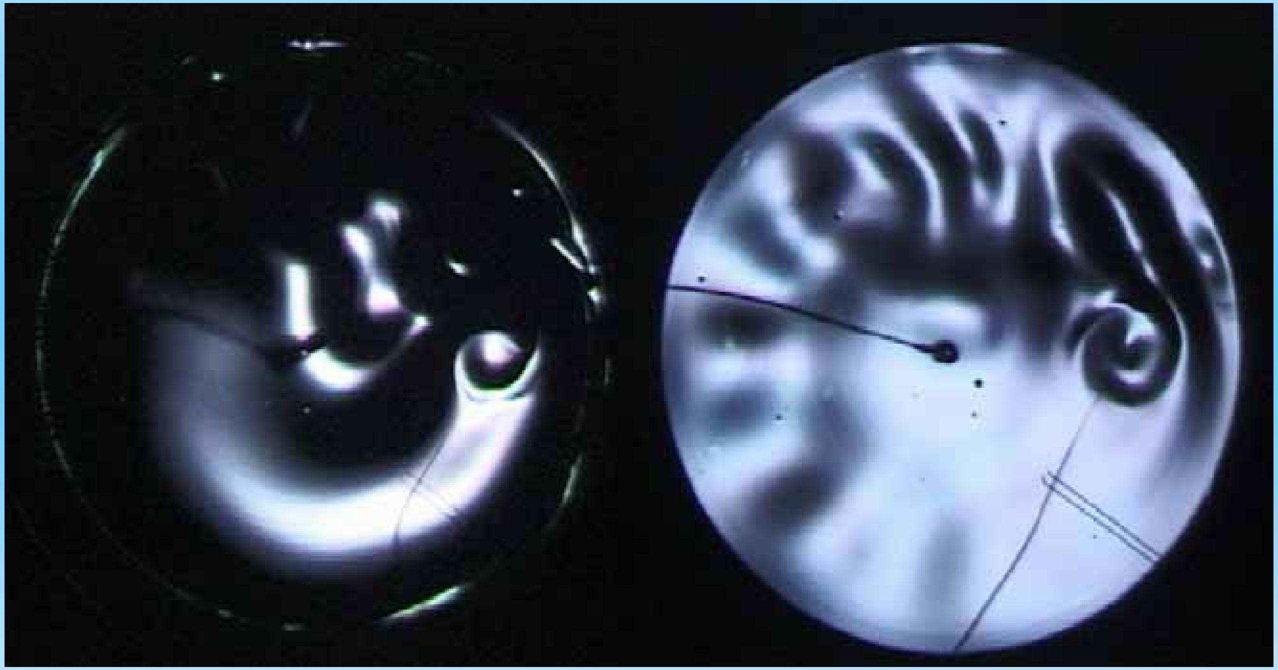

pressure field
and (stripes)
PV field



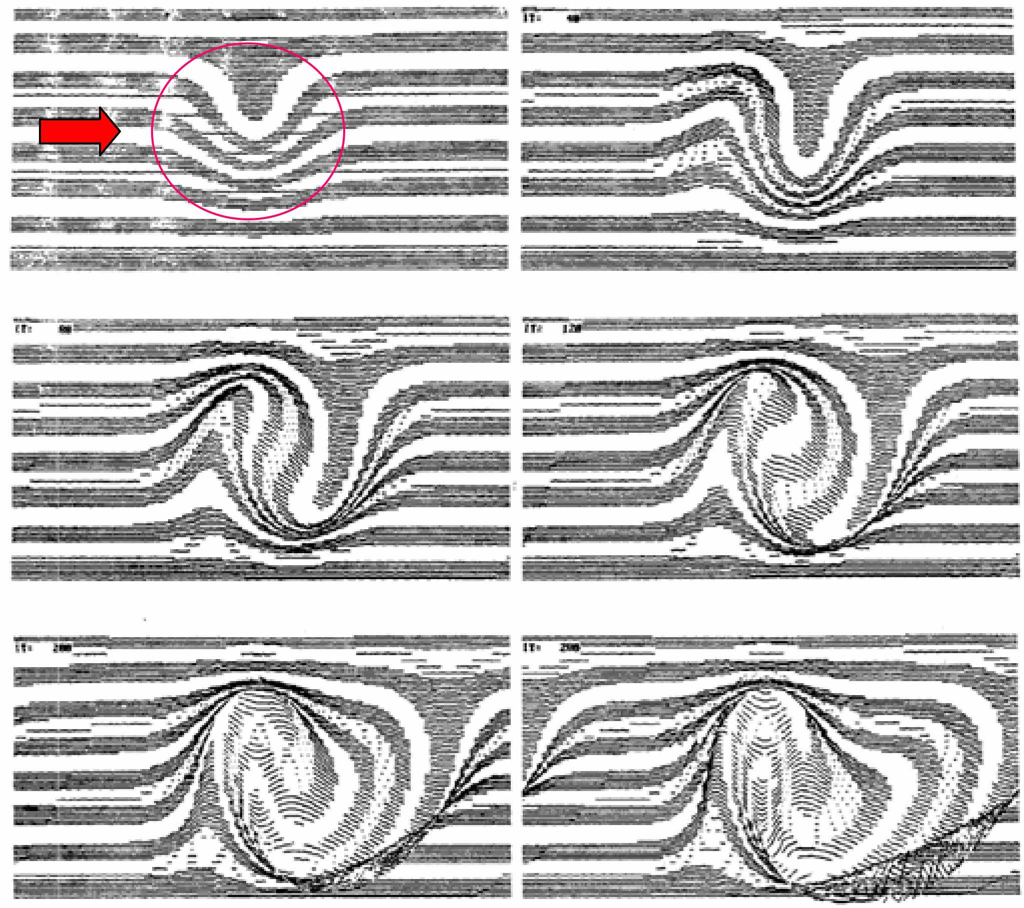

FIG. 9. *Nonlinear supercritical.* Read across, then down. Evolution of an initially uniform eastward barotropic flow over 280 days. Strong eastward flow, as in Fig. 8, except with a broader ridge (600 km half-width in the $y$-direction) and slightly faster flow (0.08 m $s^{-1}$). Potential vorticity contours, shown as bands superimposed on the interface surface plot, are wound into the region above the ridge. The slope of $\eta$ increases, and correspondingly, the velocity. The free vortex moving eastward is connected to the bound vortex above the ridge by a long trough, which draws in high potential vorticity fluid from a great distance poleward.

Planetary-geostrophic regime: exact solution by integration along time-dependent characteristics *Rhines, JPO 89*

Eastward (westerly) flow over a mountain, barotropic single layer, spherical shallow-water model; Northern Hemisphere only. Note winding of PV into spiral above topography, concentrating wake into jet. Cyclonic gyre in wake reaches north almost to Pole

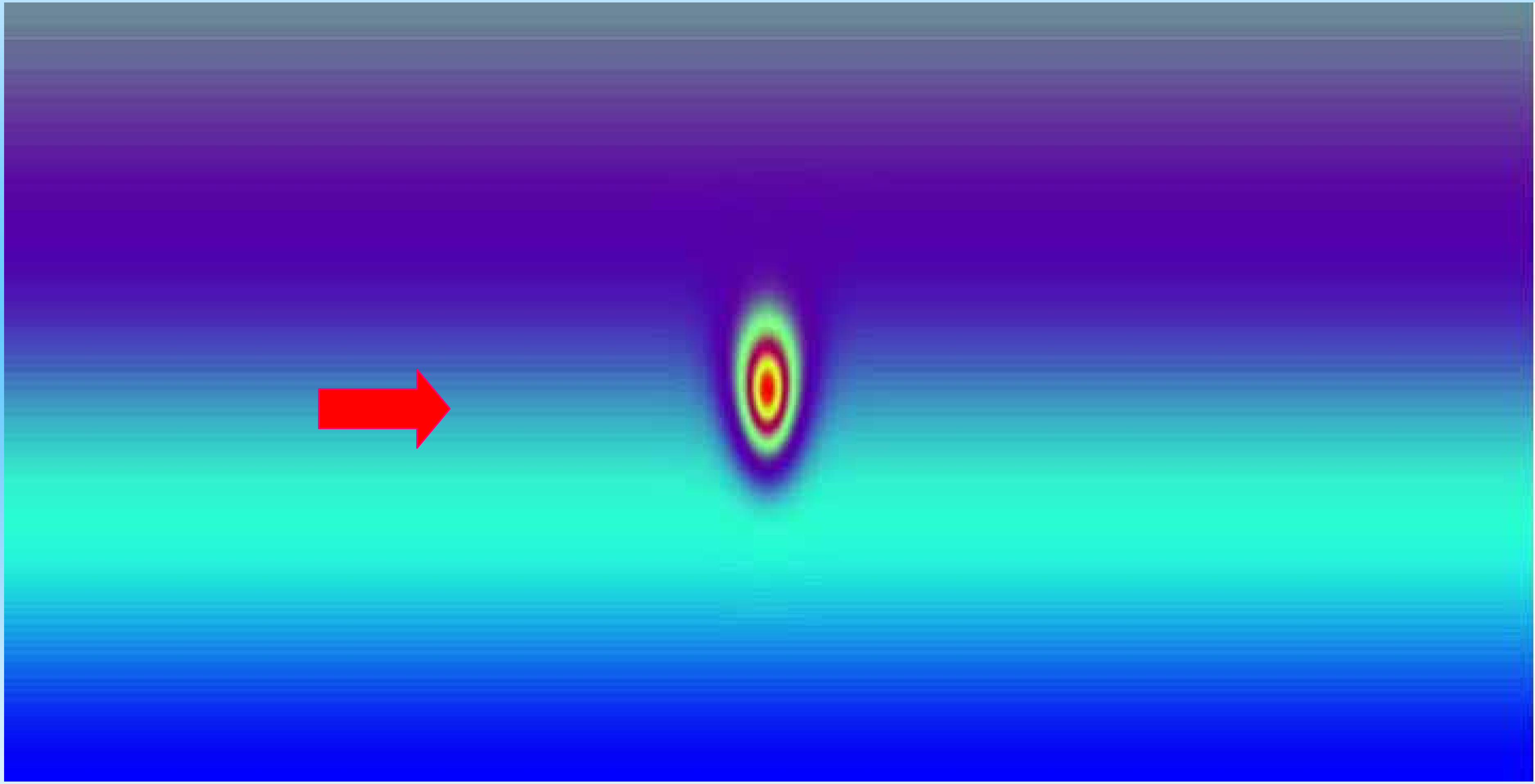

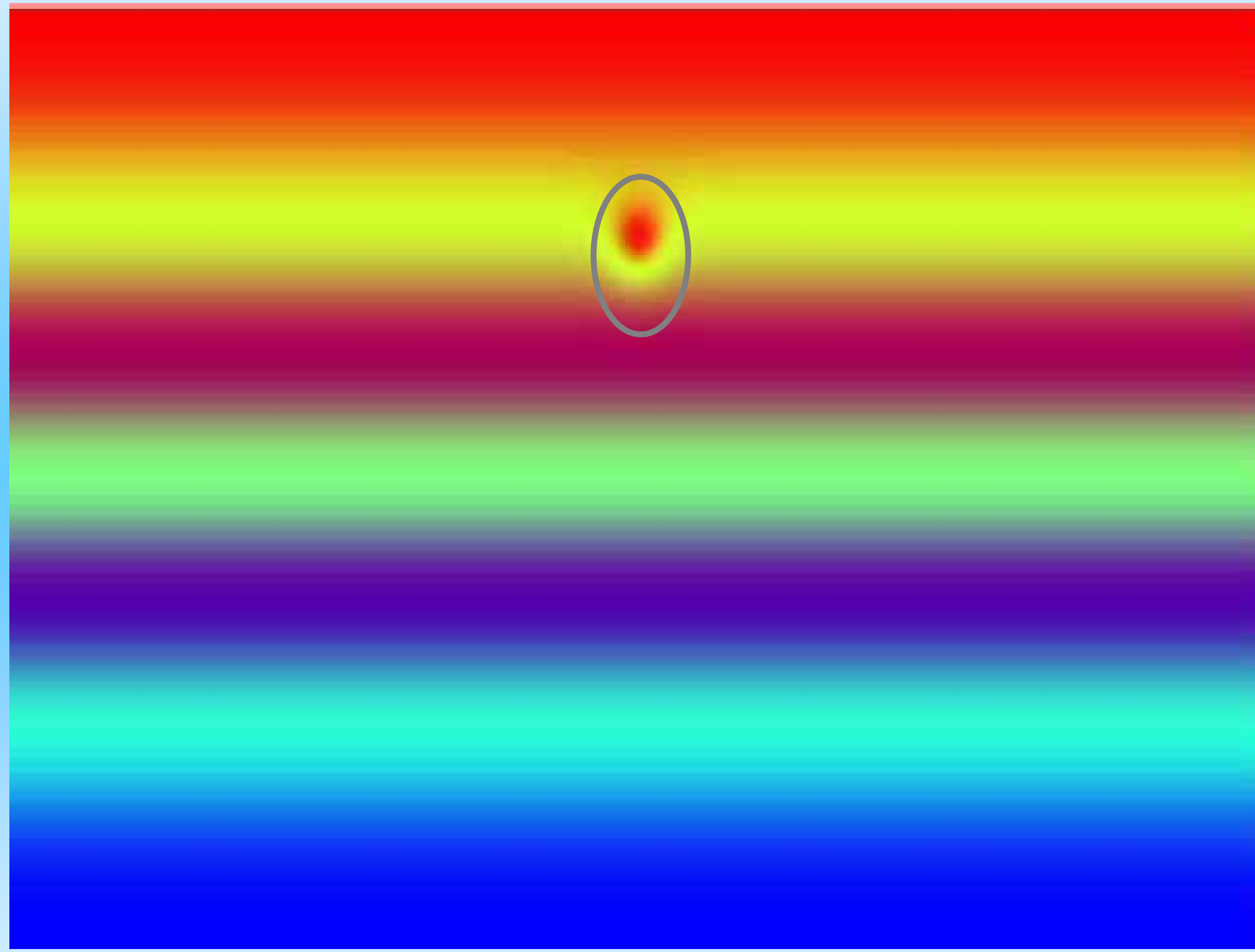

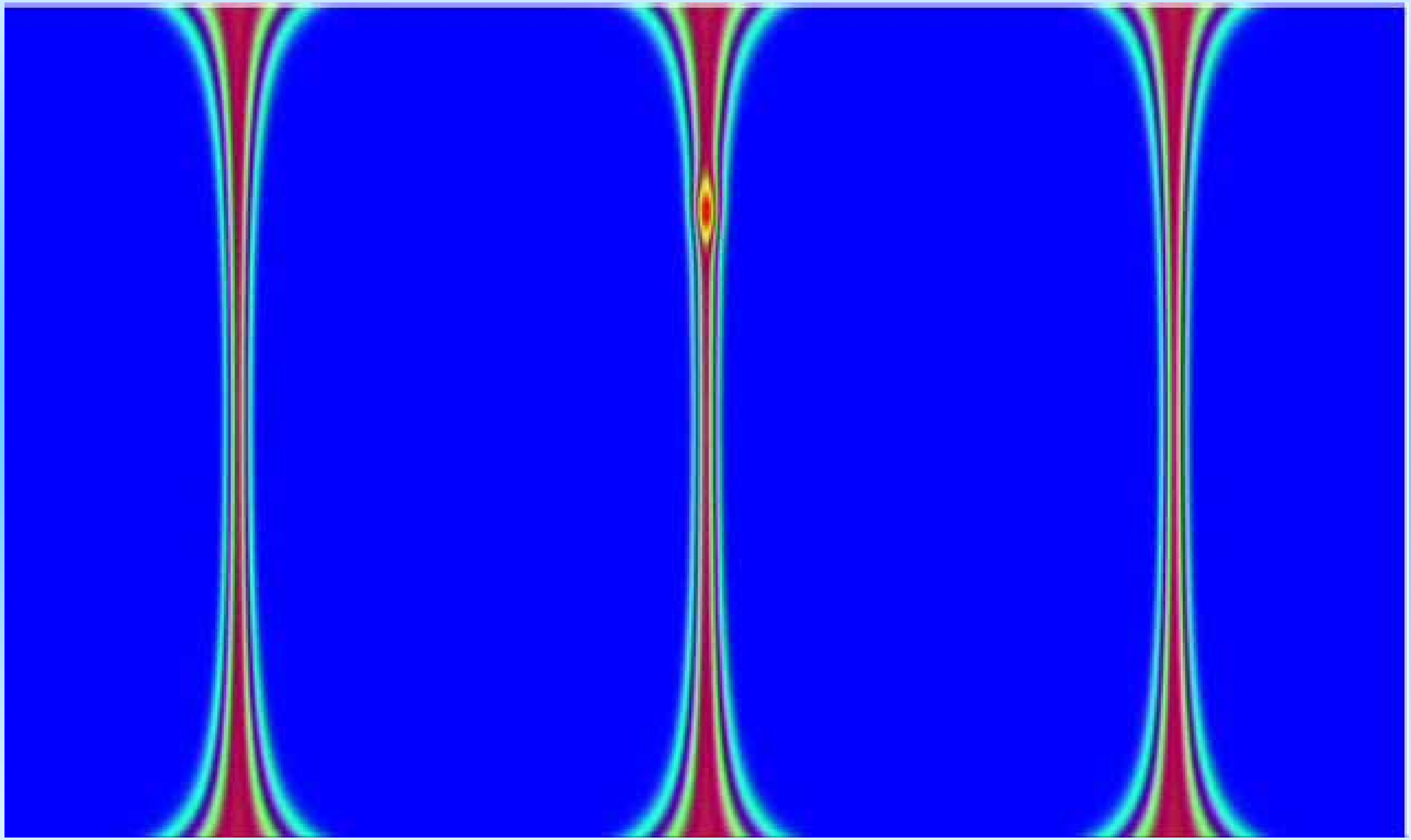

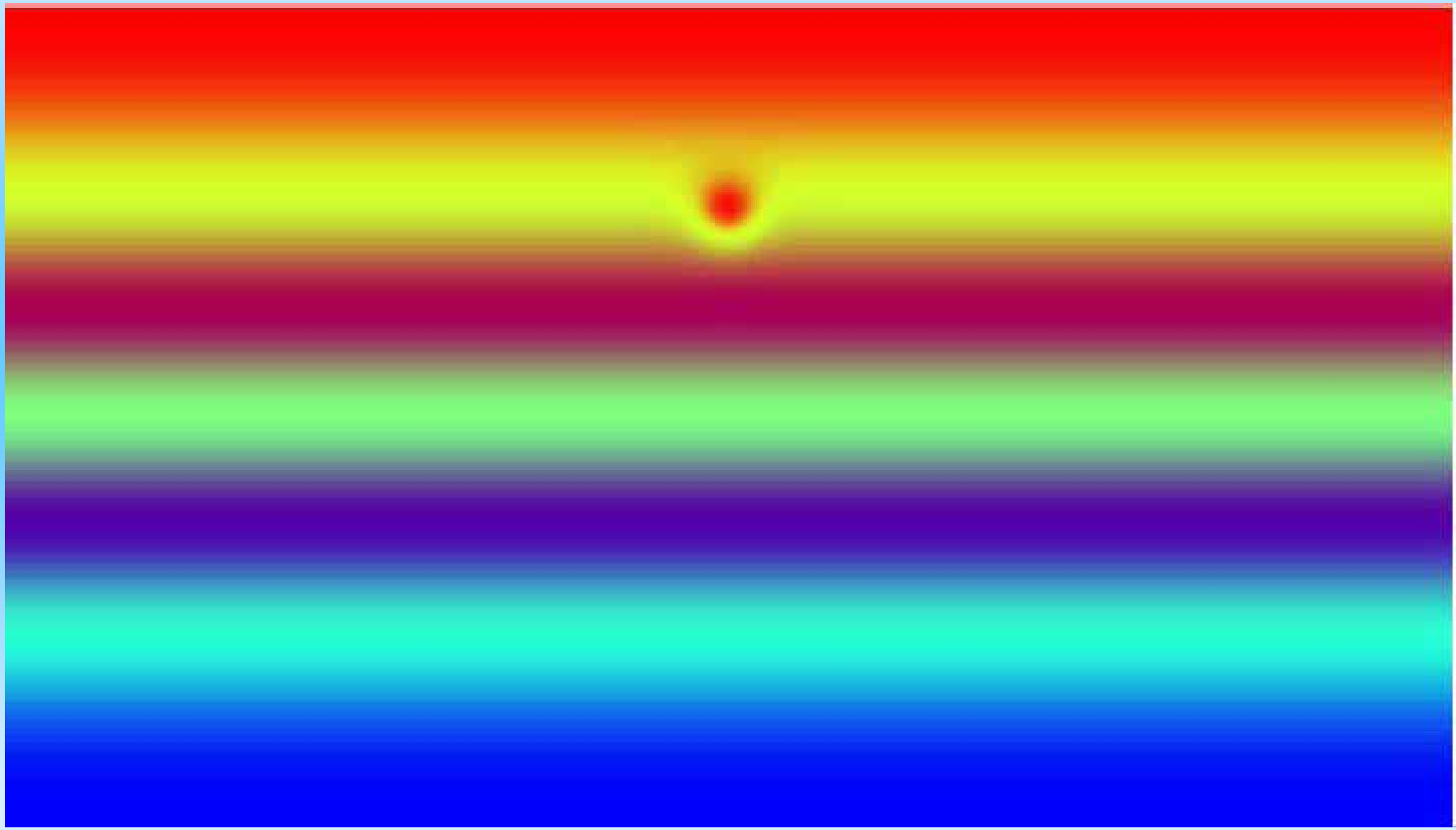

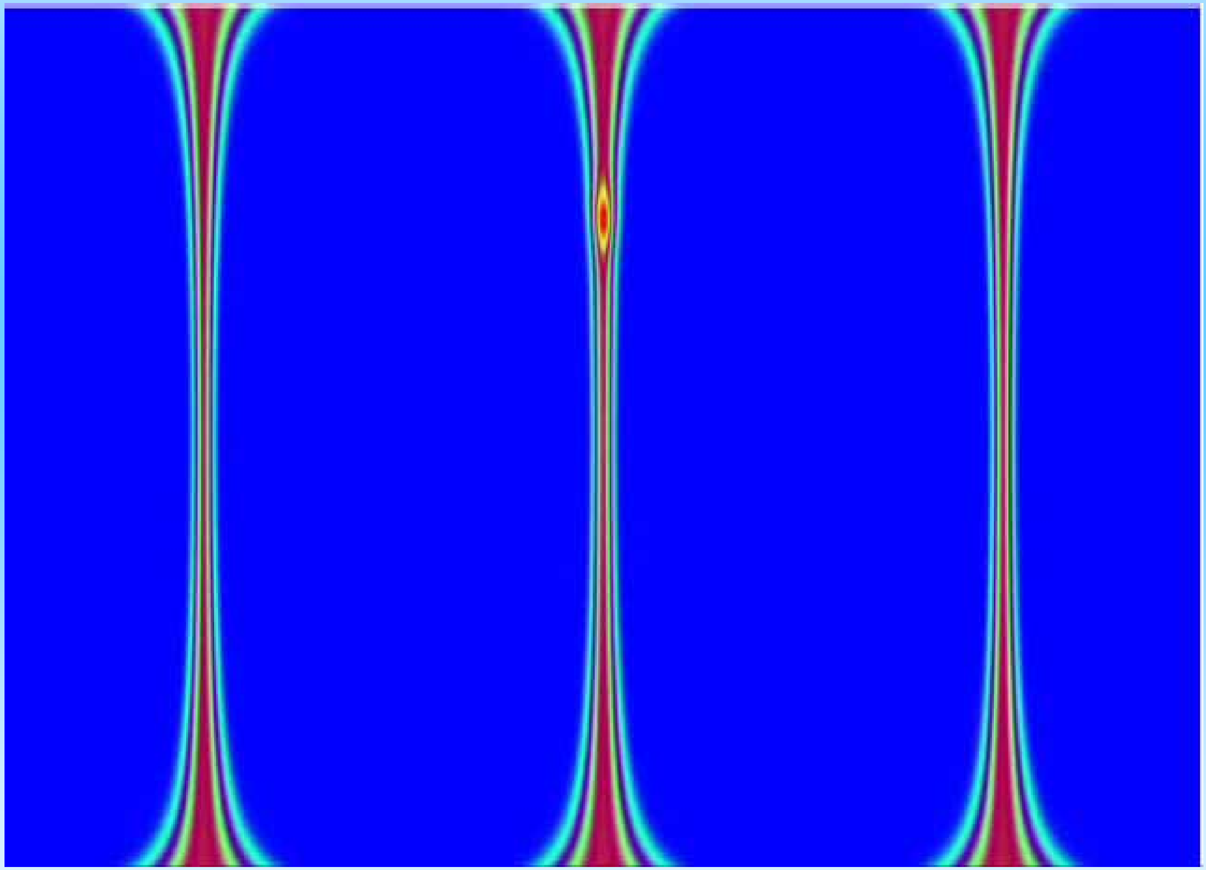

# Shallow water on a sphere: T127 model: zonally averaged zonal flow and PV: (initially uniform super-rotation). Here the blocking / wake instability parameter $\beta a^2/U$ is 0.36-1.4 depending on whether a is chosen as radius or diameter

## U(latitude)

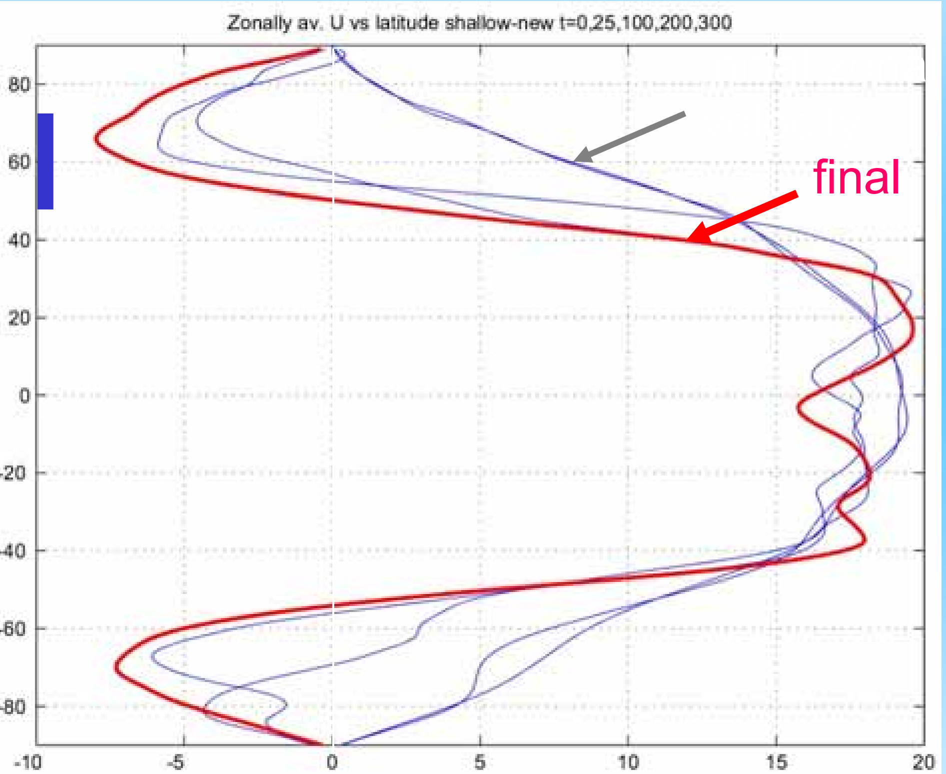


0 m sec $^{-1}$ 20

## PV

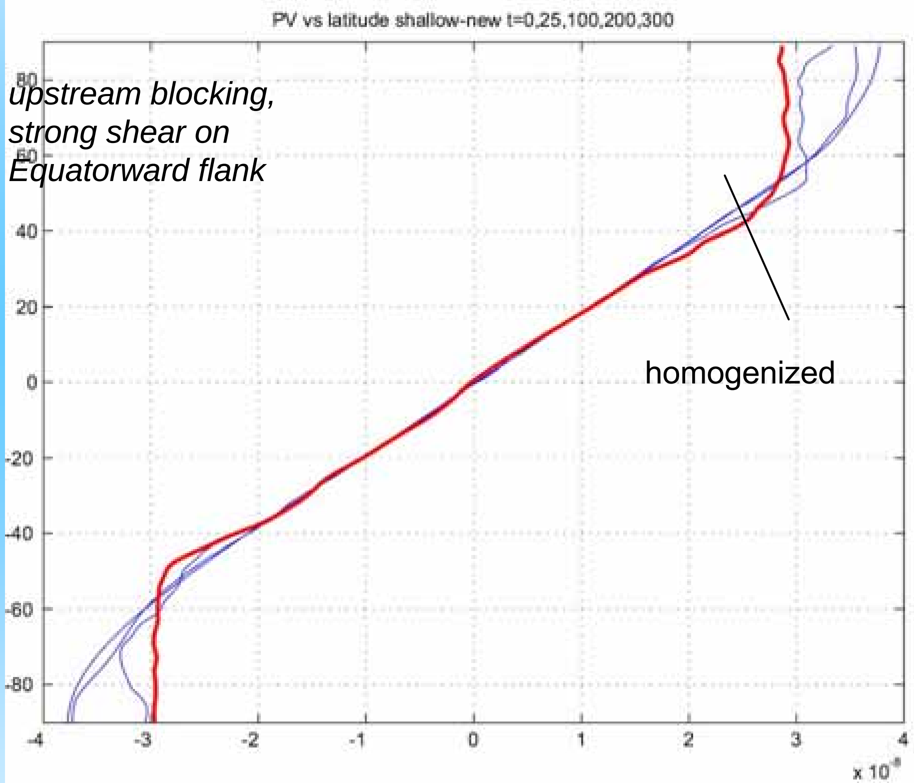


*both hemispheres are filled with wave activity; after initial linear lee Rossby wave generation, upwind blocking supresses Rossby-wave wake. There is a considerable life cycle when, as here, the frictional damping is very weak.*

# migrating critical layer produces staircase PV field
## (mountain at 60N, easterly/westerly initial zonal flow with critical layer for stationary waves)

*zonal veloc (zonal average)*

*PV*

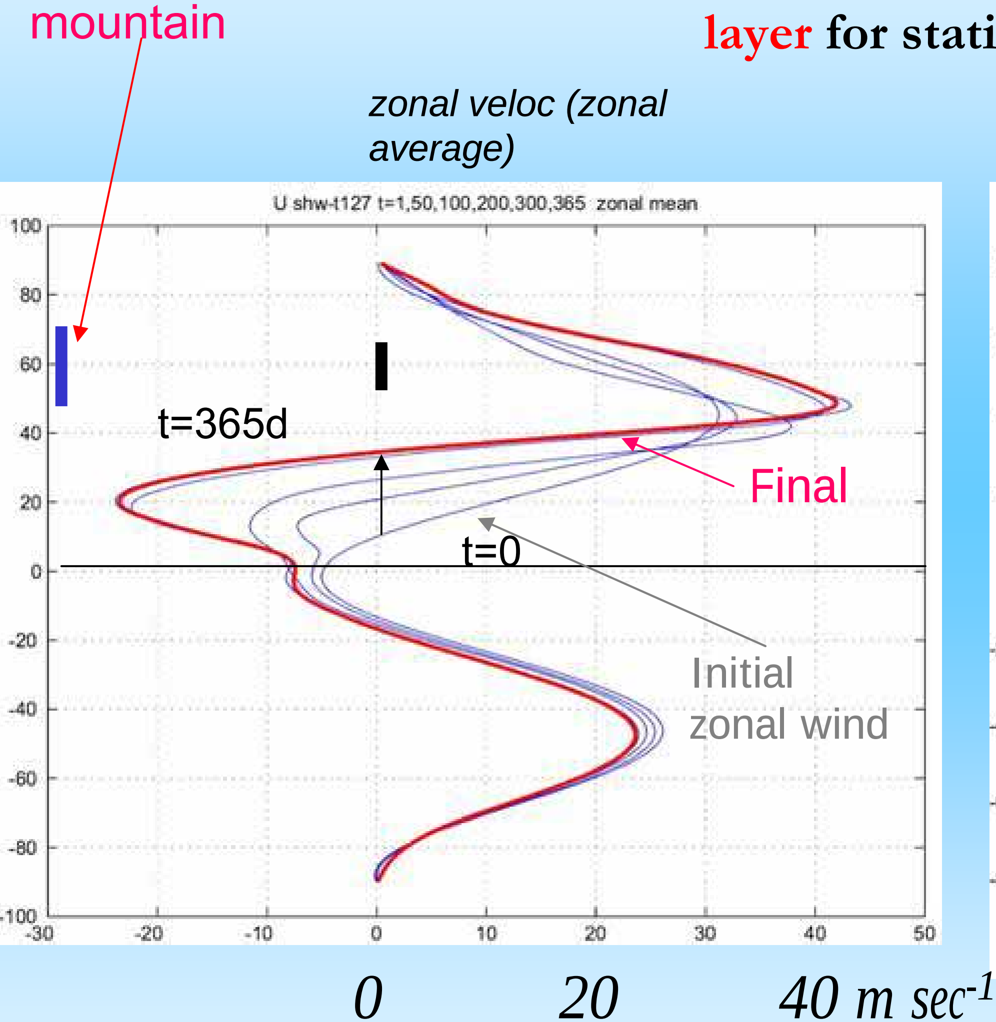


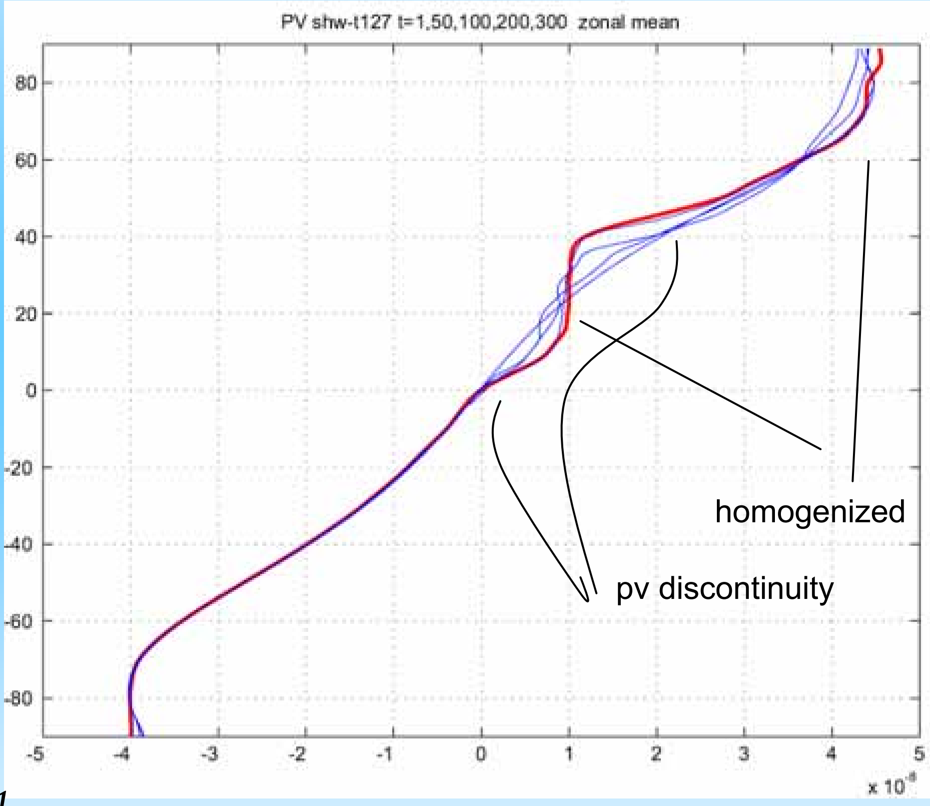


note strengthening of both eastward and westward zonal flow…particularly the westward low-latitude jet; the polar anticyclones are gone!

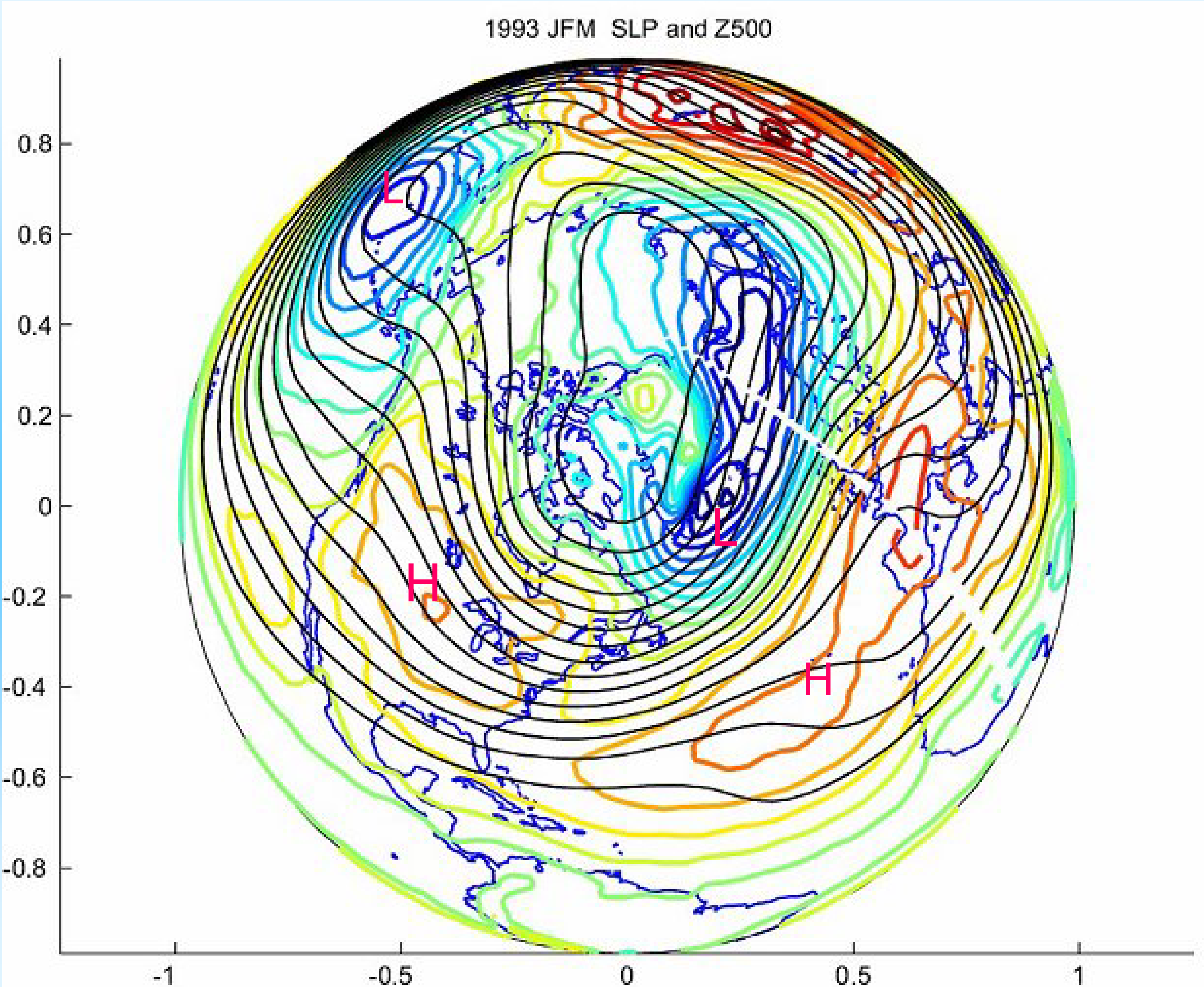

1993 JFM SLP and Z500
L
L
H
H
0.8
0.6
0.4
0.2
0
-0.2
-0.4
-0.6
-0.8
-1
-0.5
0
0.5
1

Moisture flux during high and low NAO: concentration in the high-latitude storm tracks of the ~ 2 petawatts of latent heat flux … which is ~0.7 Sverdrup (0.7 megatonnes/sec) of freshwater flux

1993 JFM 1996 JFM

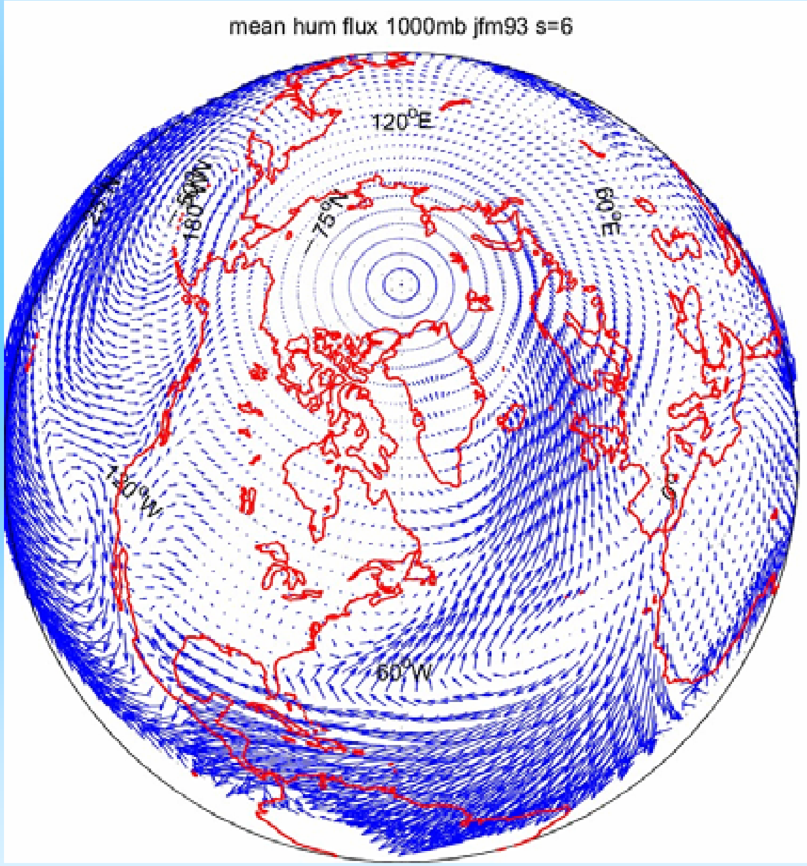


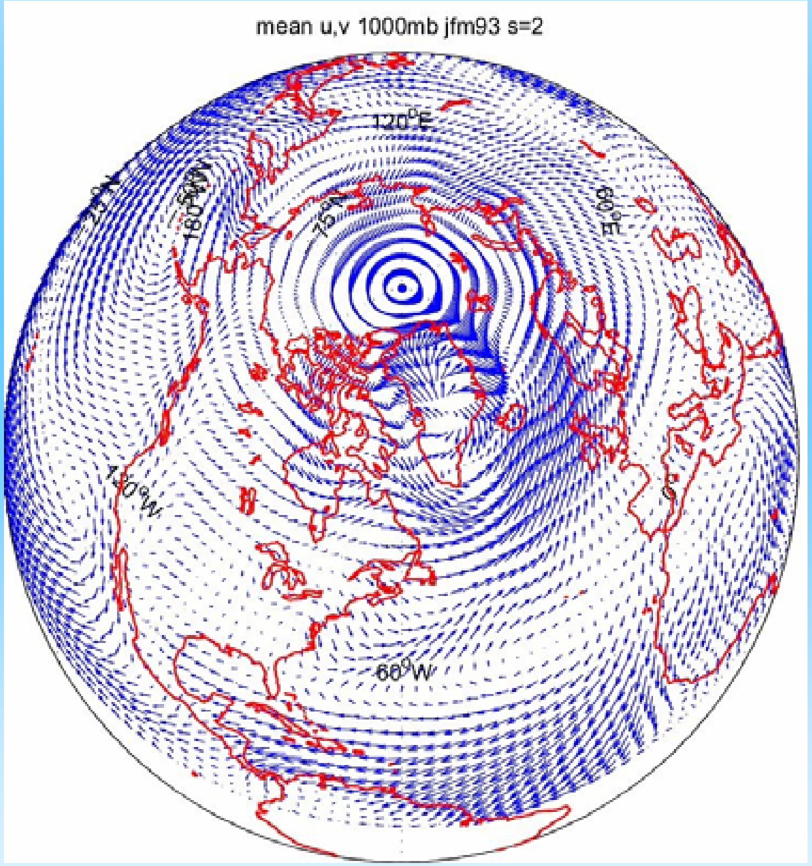

Mountain drag is associated with a strong northerly flow rounding the high ground anticyclonically, setting a lee cyclone at the *beginning* of the wake….as in a downwind-displaced f/h contour.

This is the dominant flow round the Rocky Mts. but is not characteristic of the flow round Greenland.

Role of cold-air outbreaks….

Direct thermal forcing of the wintertime Arctic forces a high latitude easterly flow and *anticyclonic* polar vortex at low levels; Rossby wave radiation from low latitude does the same.

*Cyclonic* Arctic circulation comes thermal forcing and from invasive cyclones: bodily poleward transport of PV.

# Pressure drag on Greenland

- These flows generate waves and wakes, and in doing so exert forces on the topography, with virtually equal and opposite reaction forces on the atmosphere. Taken together, the pressure drag on all the Earth's topography, plus the frictional stress at the base of the turbulent boundary layer, exerts a zonal force which changes the angular momentum of the solid Earth…the length of the day. About 90% of this pressure drag comes

from the atmosphere, the remainder from the ocean.

In this manner, our wrist-watches become virtual instruments to measure atmospheric angular momentum and the drag forces that alter it.

The length of the day varies seasonally by ~ 1 millesecond, largely due to the change in atmospheric angular momentum.

DICKEY ET AL.: ANGULAR MOMENTUM EXCHANGE—THE 1982-1983 ENSO

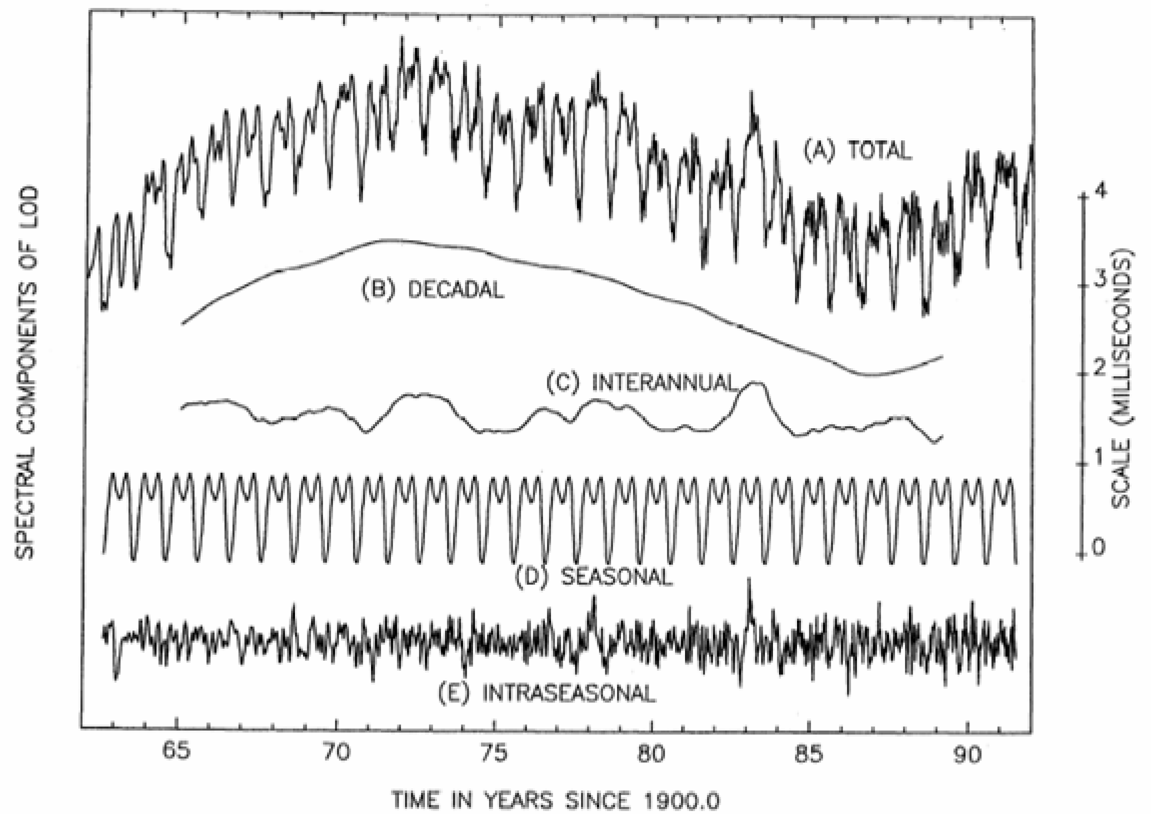


**Figure 1.** Time series of irregular fluctuations in the length-of-day $\Lambda^*(t)$ (curve A) and its decadal ($\Lambda_\alpha(t)$), interannual ($\Lambda_\beta(t)$), seasonal ($\Lambda_\gamma(t)$), and intraseasonal ($\Lambda_\delta(t)$) components (curves B, C, D, and E respectively) updated from *Hide and Dickey* [1991].

mountain pressure drag

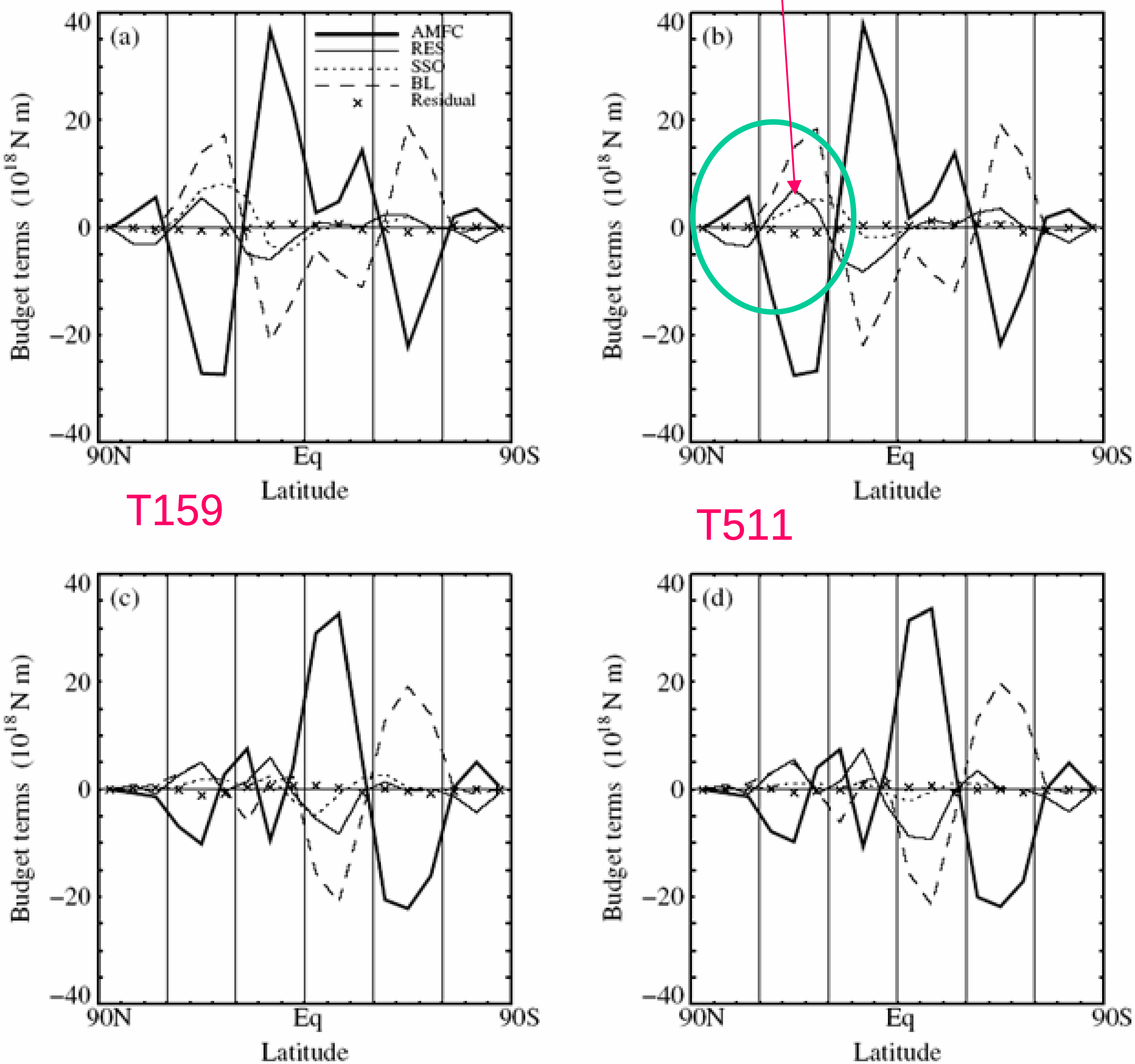


Jan 2001

July 2001

*Brown, QJRMS 2004*

igure 1. Relative angular momentum budgets for January 2001 at resolutions (a) T159 and (b) T511. In each ase the terms in the budgets (see Eq. (1) and text for definitions) have been integrated over 10° latitude bands and averaged over the first 24 hours of each of 31 forecasts. (c) and (d) are as (a) and (b), but for July 2001.

1989 JFMA:

**NAO** index **positive**

colors: 1000 HPa near-surface dynamic height (blue=low pressure, red=high)

contours:

jet stream level 300 HPa, stratosphere 30 HPa

*Synoptic storm tracks are beneath stratospheric polar vortex*

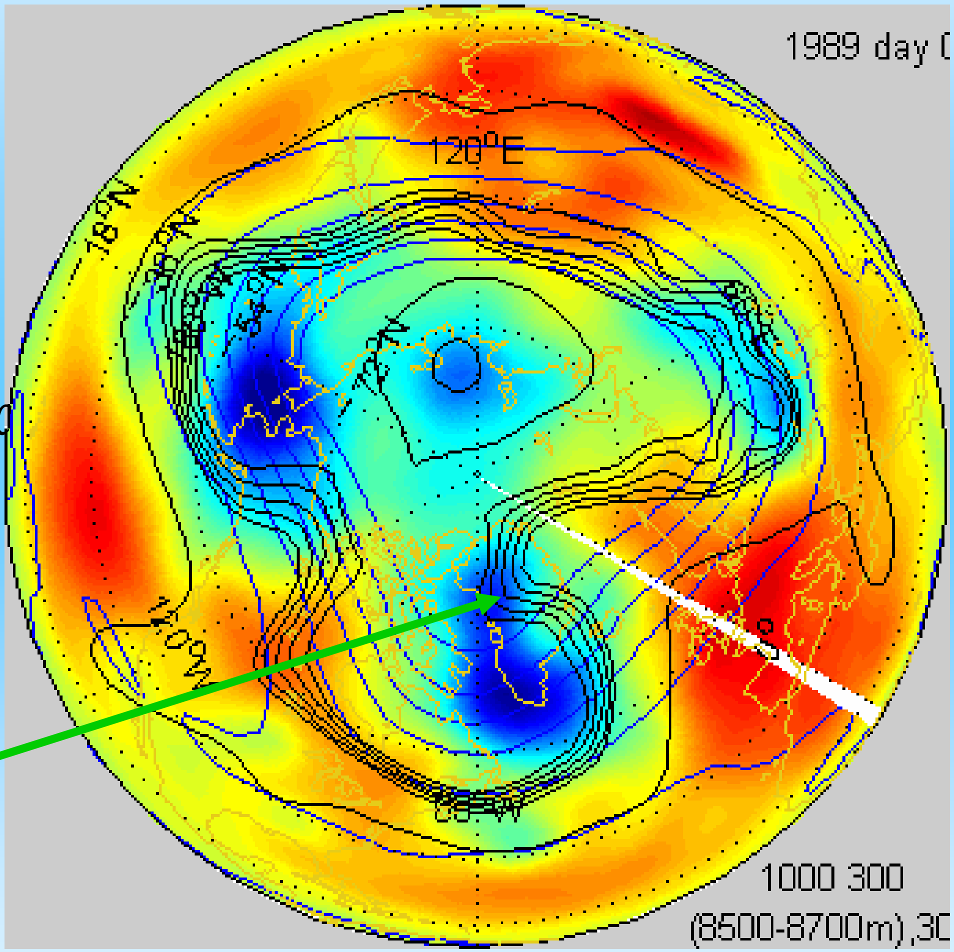

1996 JFMA (**NAO** index very **negative**)

colors: 1000 HPa
red contours: 300 HPa
black contours: 30 HPa

*Storm tracks are usually south of stratospheric polar vortex*

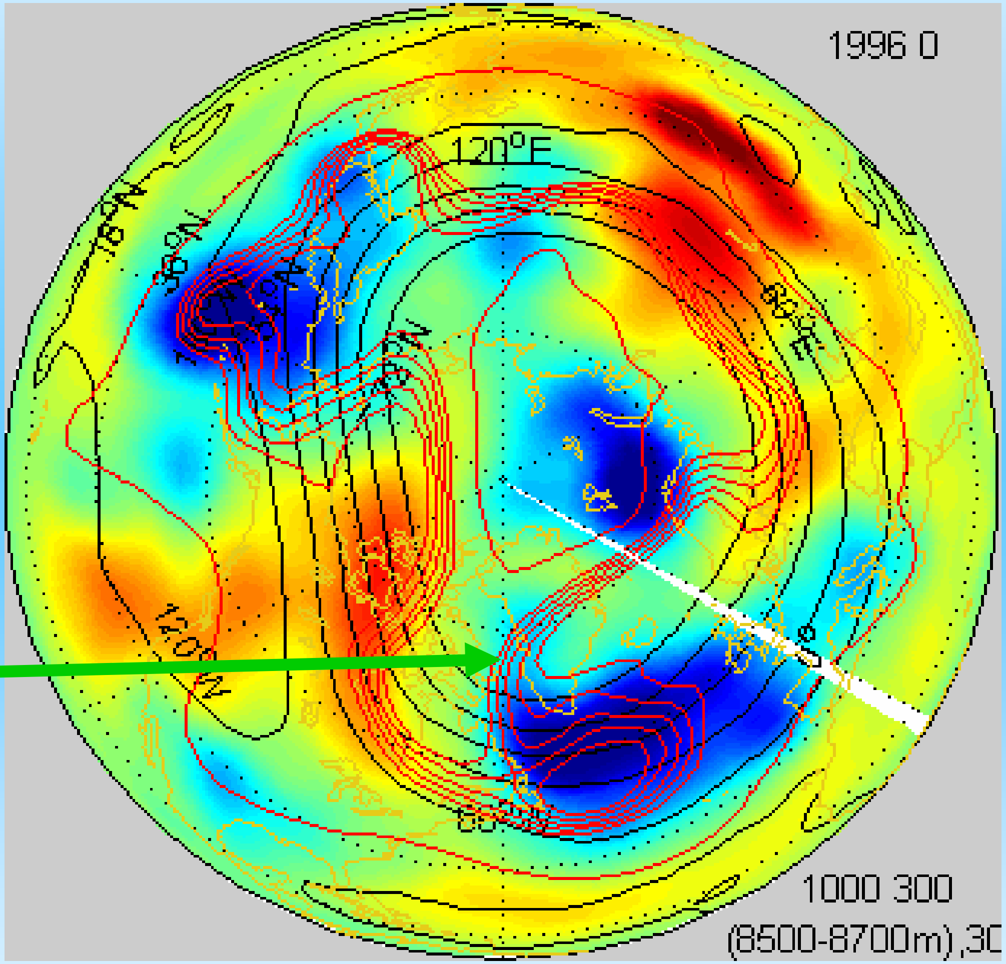


Greenland

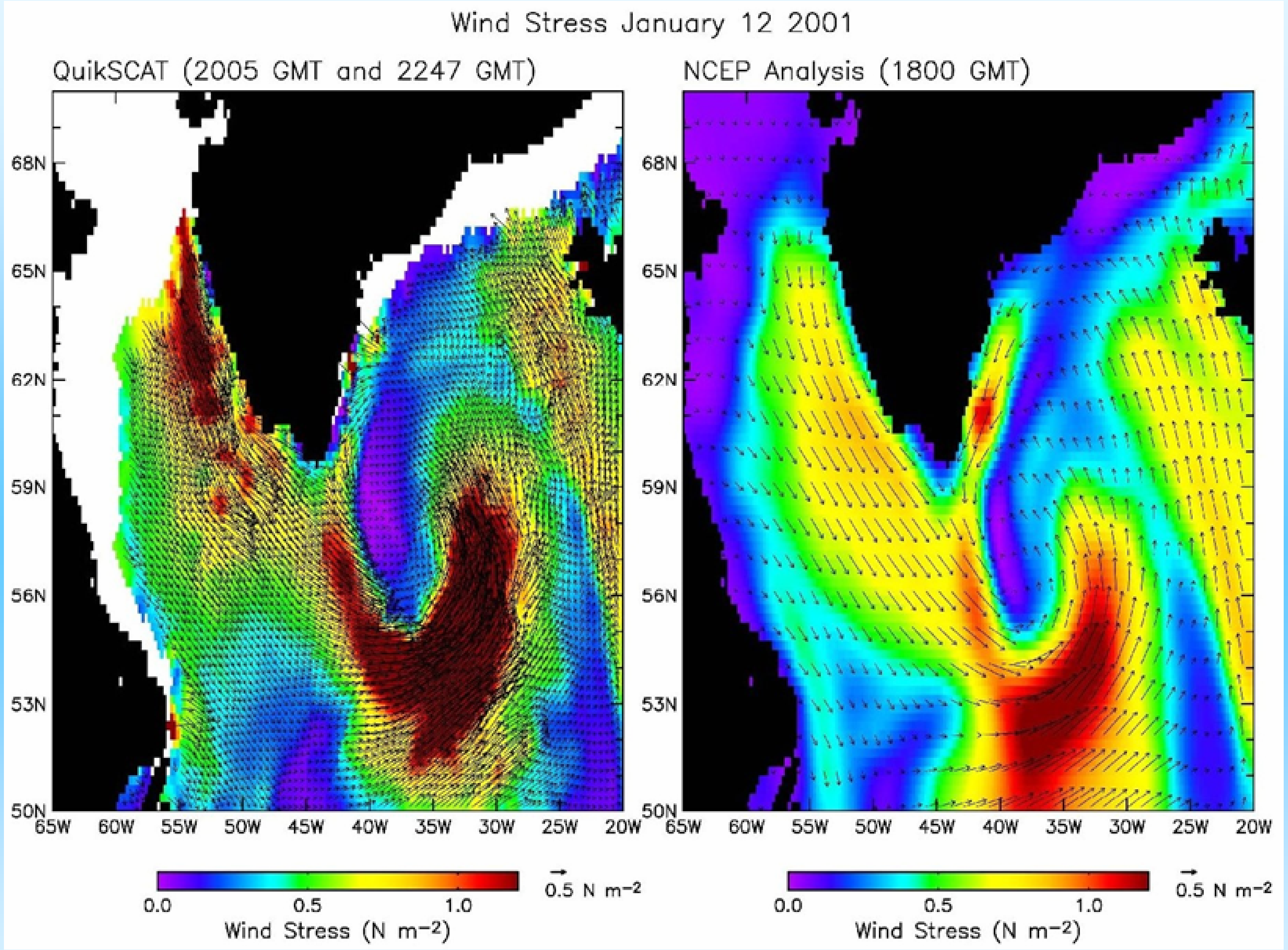


**Greenland Tip Jet:**

*Doyle & Shapiro Tellus 1999; Pickart et al. Science 2003, Moore & Renfrew J Clim 2005*

T95 T285 T799

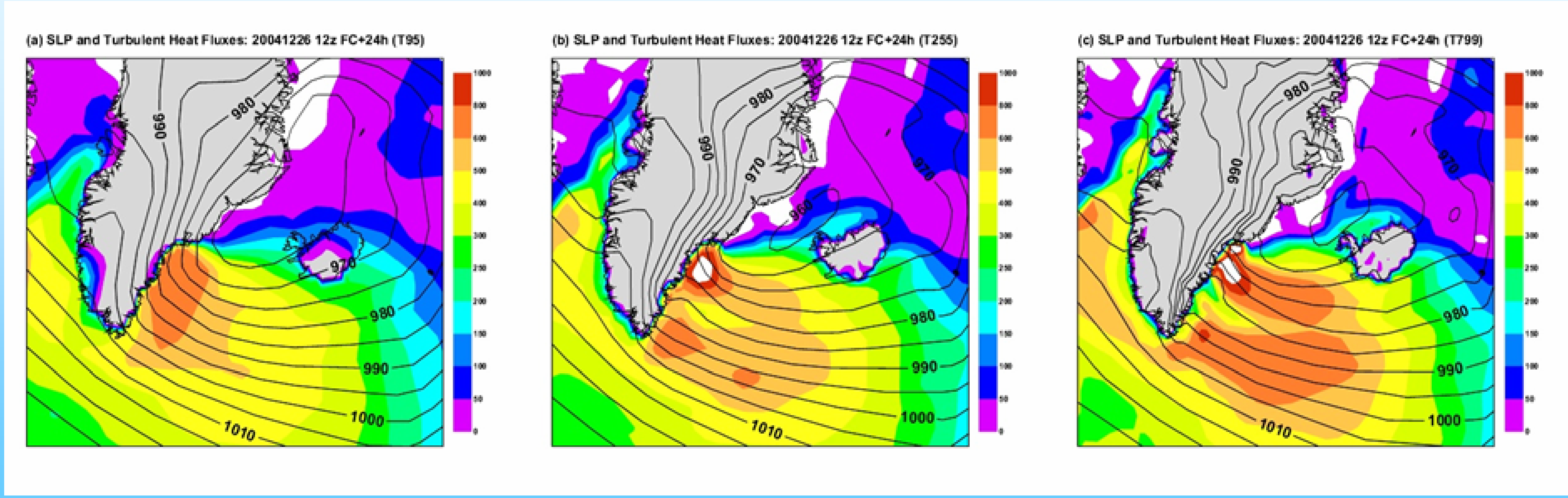


Air Sea Heat flux at various resolutions

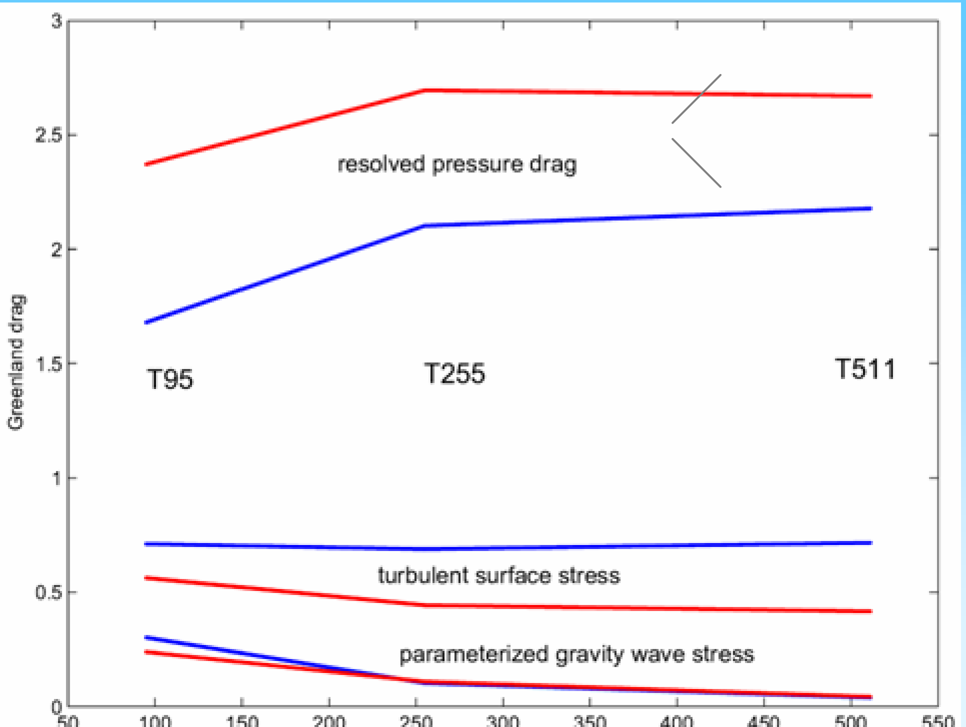


Drag at various resolutions (two case studies, 20041226, 20050207)

Interesting cyclogenesis begins to appear in Baffin Bay at high resolution.
time sequence of SLP. This is prominent in the storm track spaghetti diagram in the next slide.

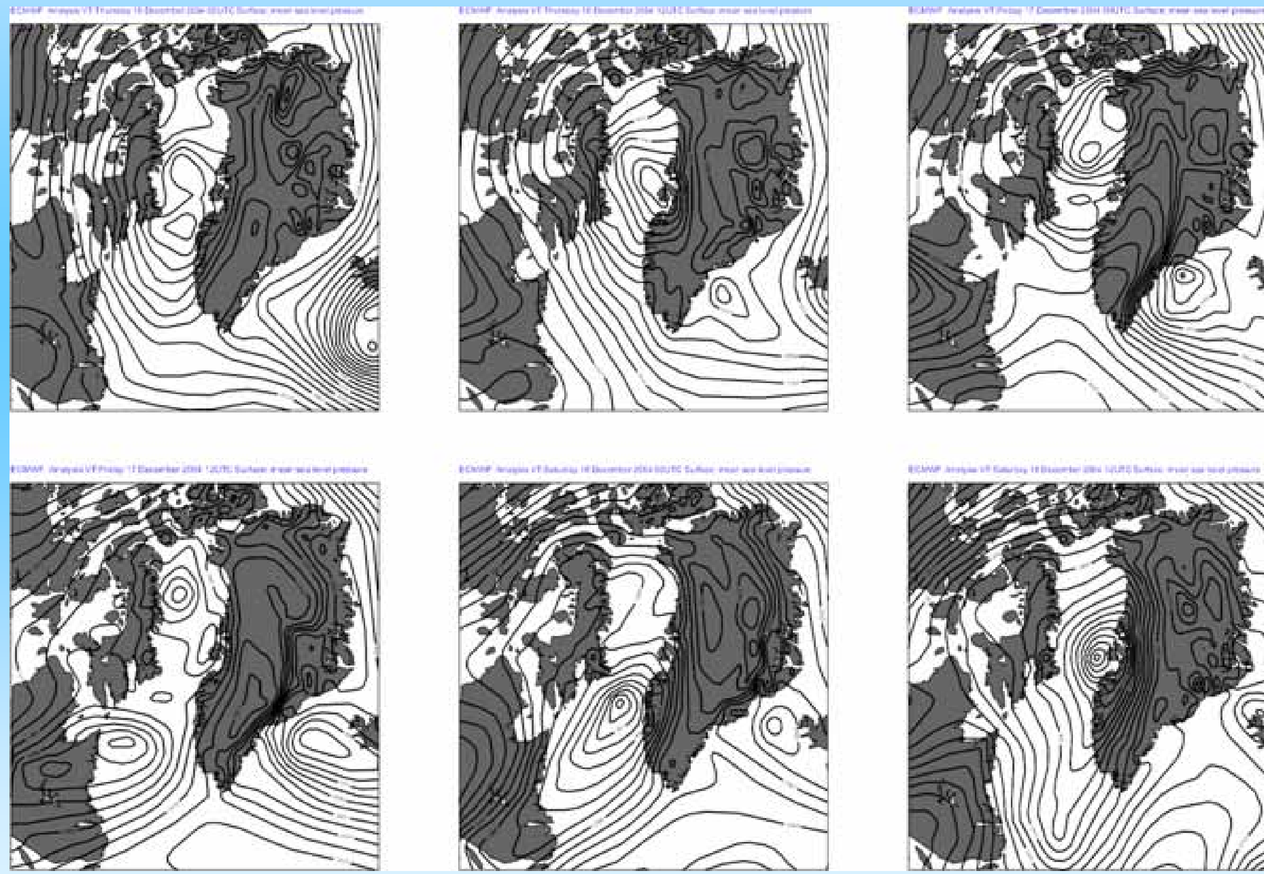

- In a series of numerical experiments at ECMWF, the flow in the Atlantic sector has been examined as a function of model resolution.

  (*Jung & Rhines, JAS 2007 in press*). Greenland's 3km high topography generates strong downslope-jet activity which spills out over the Greenland Sea; this is not resolved by typical resolutions but begins to appear at about T255. Mesoscale model simulations (e.g., of Bromwich, and Shapiro and colleagues) capture such features, but here they are present in a global simulation.

  Note the impact of resolution on the lee cyclone in the next images.

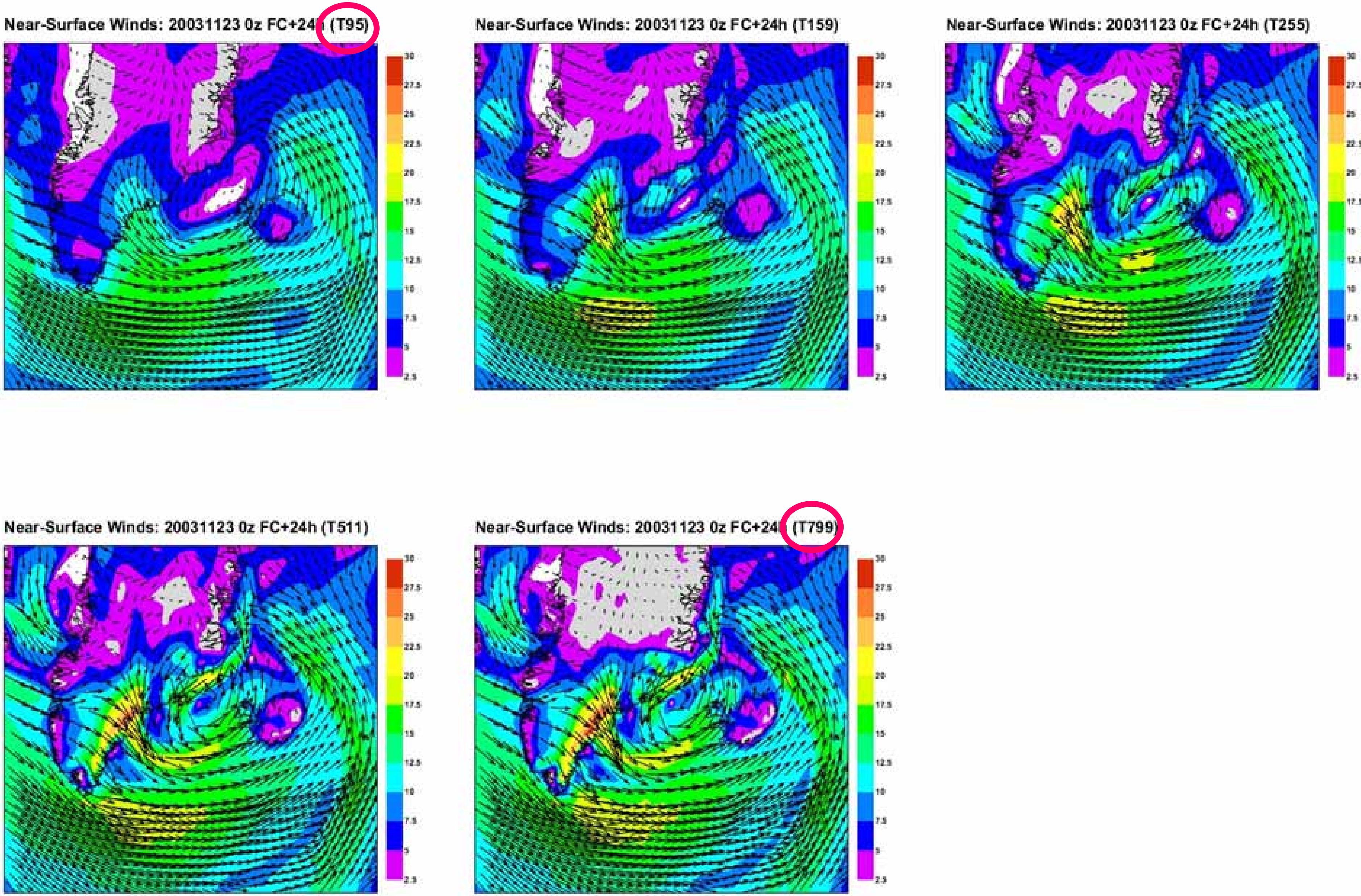


*Jung & Rhines, JAS 2007 in press*

250 HPa level case study for high drag (short integration)

T95

T255

T799

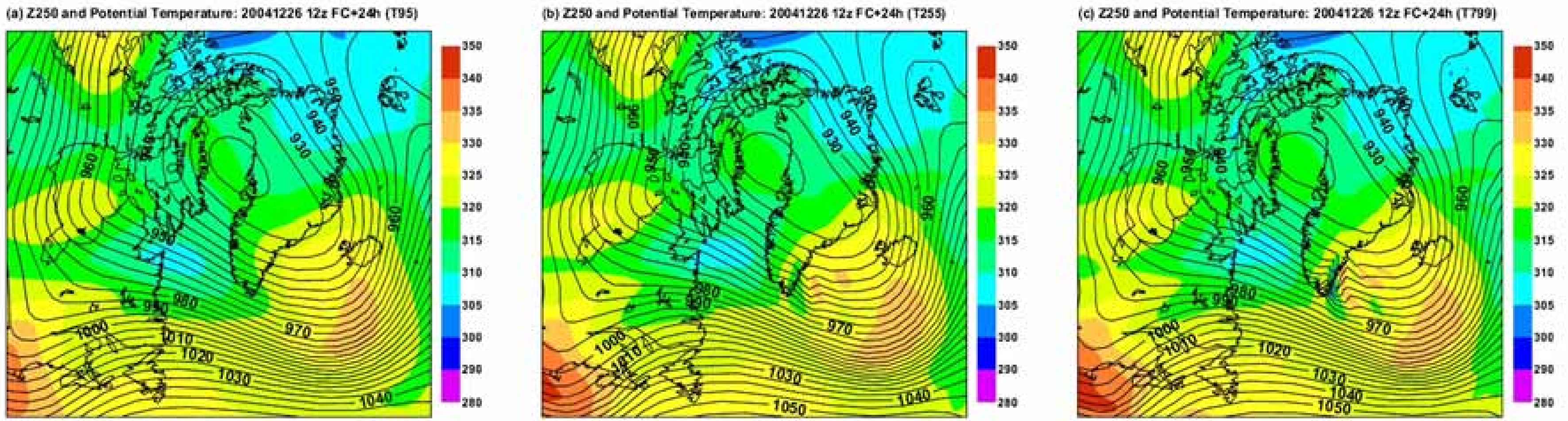

cases of cyclogenesis: resolution has a notable effect on an Eulerian measure of cyclogenesis

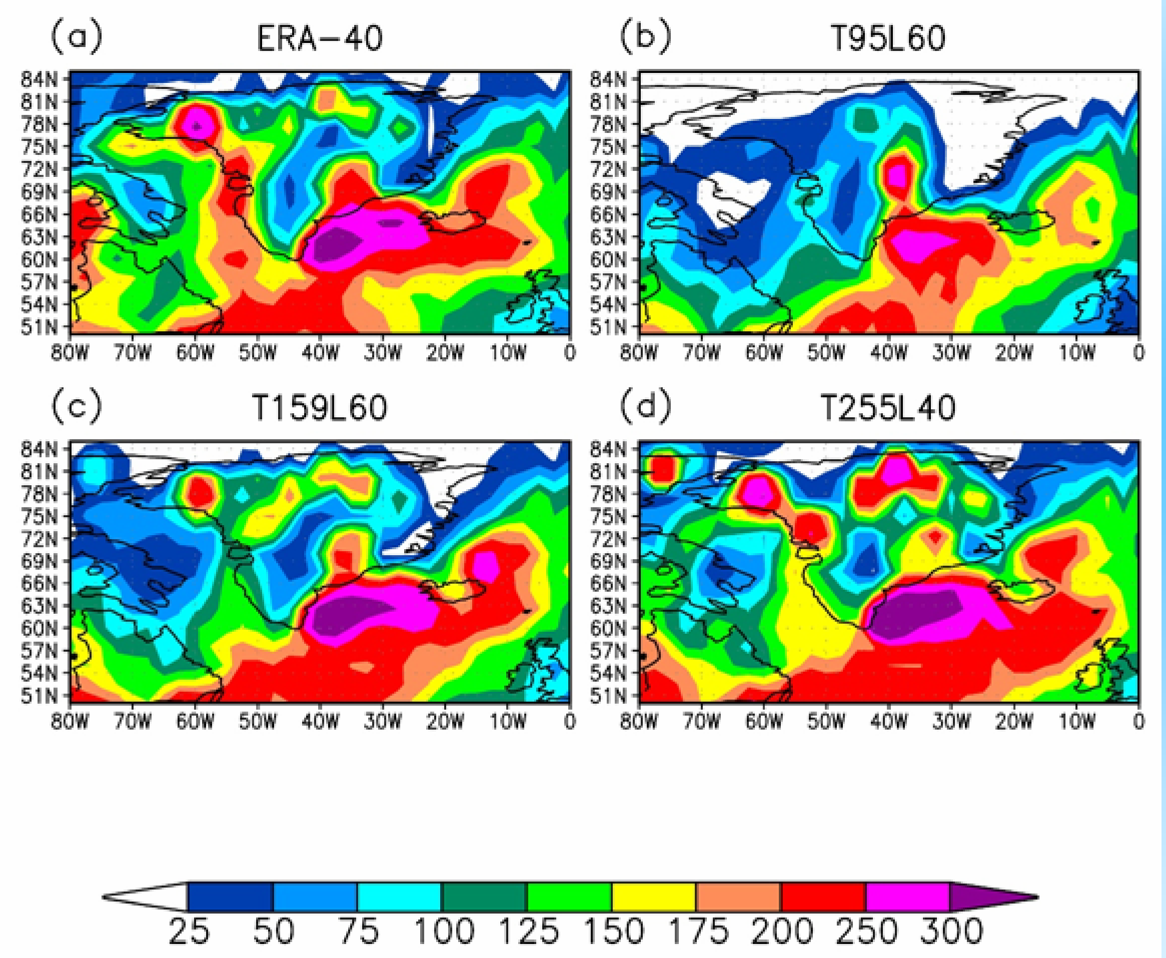

We explore the east-west component of pressure drag on Greenland.
pressure drag (red) and NAO idex
15-day smoothed

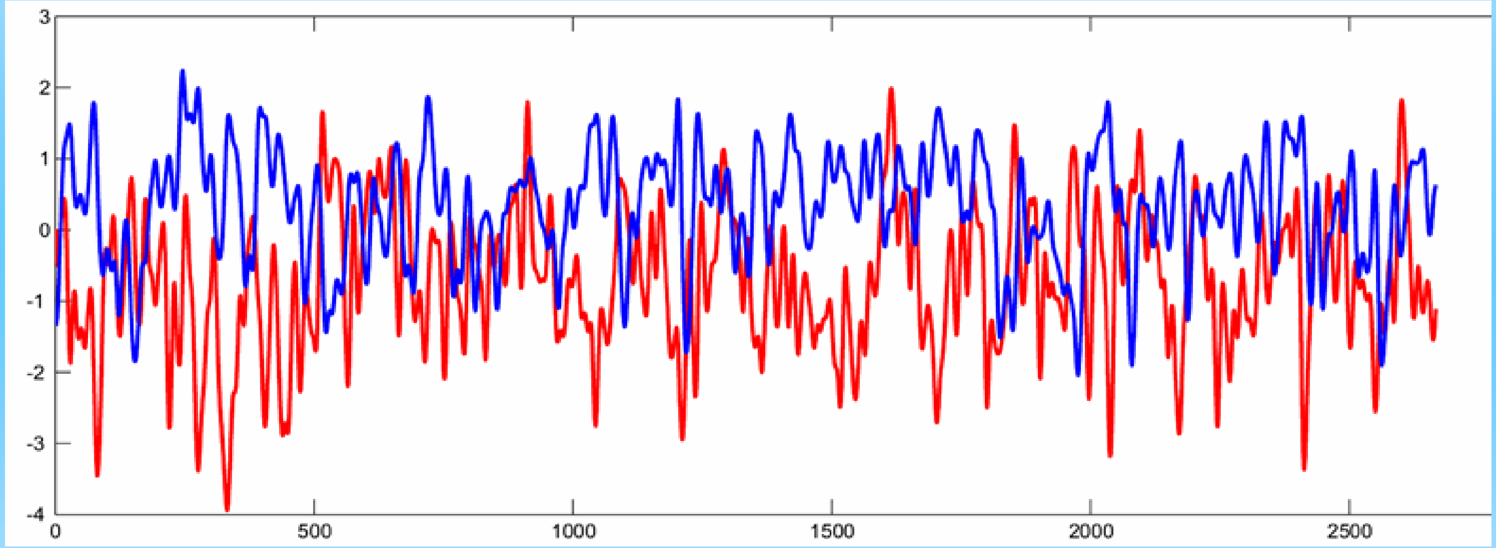


1980

2002

The 1000 HPa dynamic height fields that correspond to periods of high pressure drag on Greenland are shown next, at lags of -4, -2 , 0,+2, +4 days. The pattern is quite local, dominated by a low east of Greenland, with a lobe of high pressure farther to the southeast. West of Greenland the pressure anomaly is surprisingly small. It suggests a relation with the Atlantic storm track more than the deflection of a wind from the west, for in fact the westerly zonal flows are peaking south of this latitude.

- The next figures are animations of the northern hemisphere circulation for a high-NAO (1989) and low NAO (1996) winter, respectively. They show many things, including strong vertical interaction between clusters of cyclones and the stratospheric polar vortex. Synoptic activity is felt in the stratosphere!   A strong sudden warming is seen in 1989.

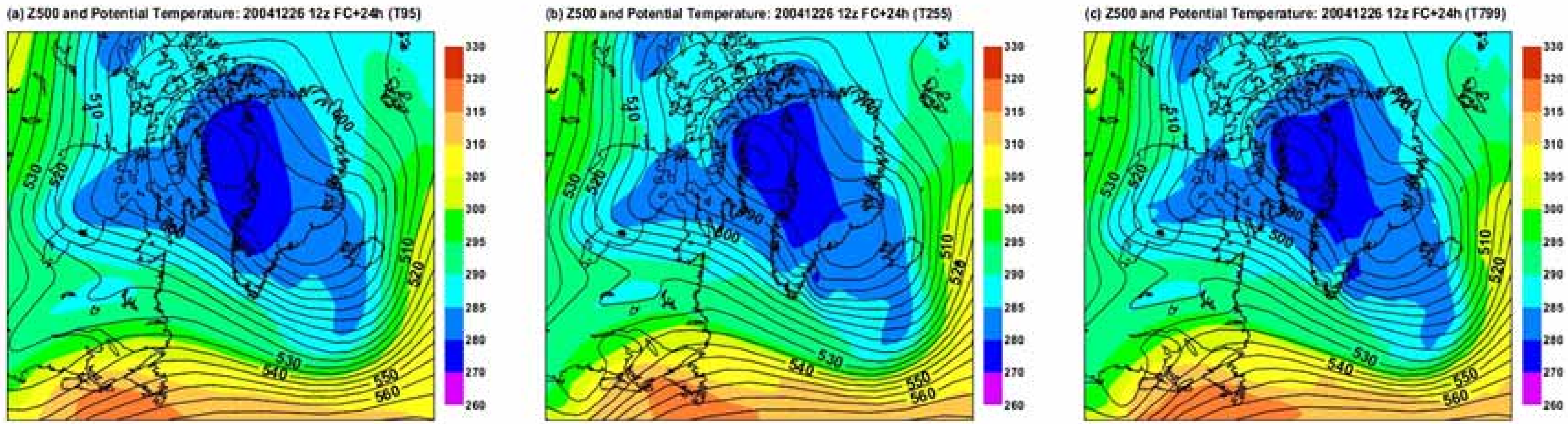
(a) Z500 and Potential Temperature: 20041226 12z FC+24h (T95)
(b) Z500 and Potential Temperature: 20041226 12z FC+24h (T255)
(c) Z500 and Potential Temperature: 20041226 12z FC+24h (T799)

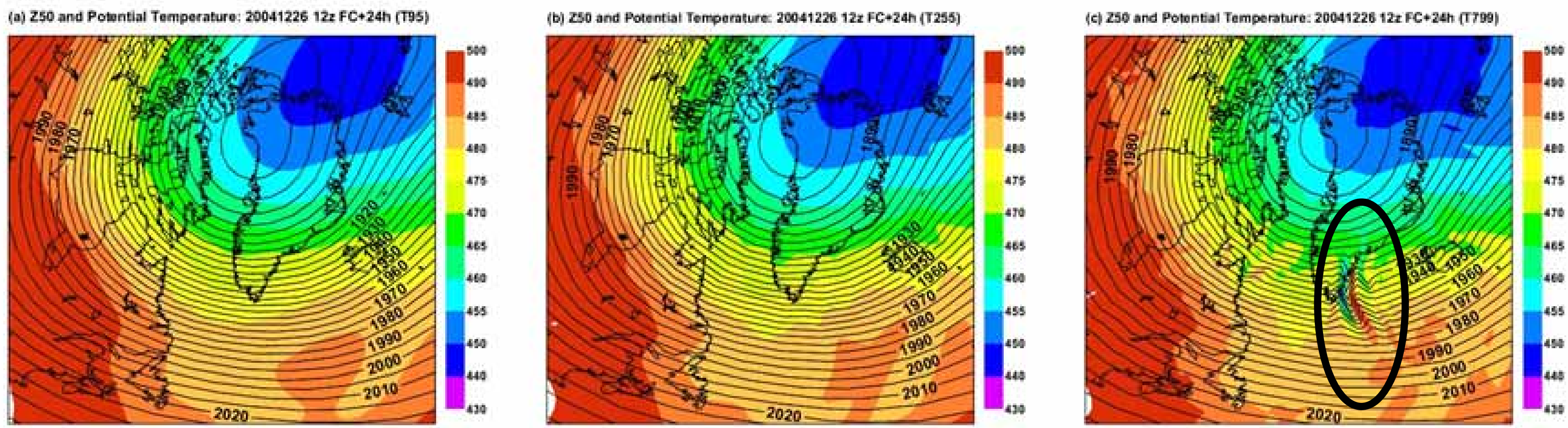
(a) Z50 and Potential Temperature: 20041226 12z FC+24h (T95)
(b) Z50 and Potential Temperature: 20041226 12z FC+24h (T255)
(c) Z50 and Potential Temperature: 20041226 12z FC+24h (T799)

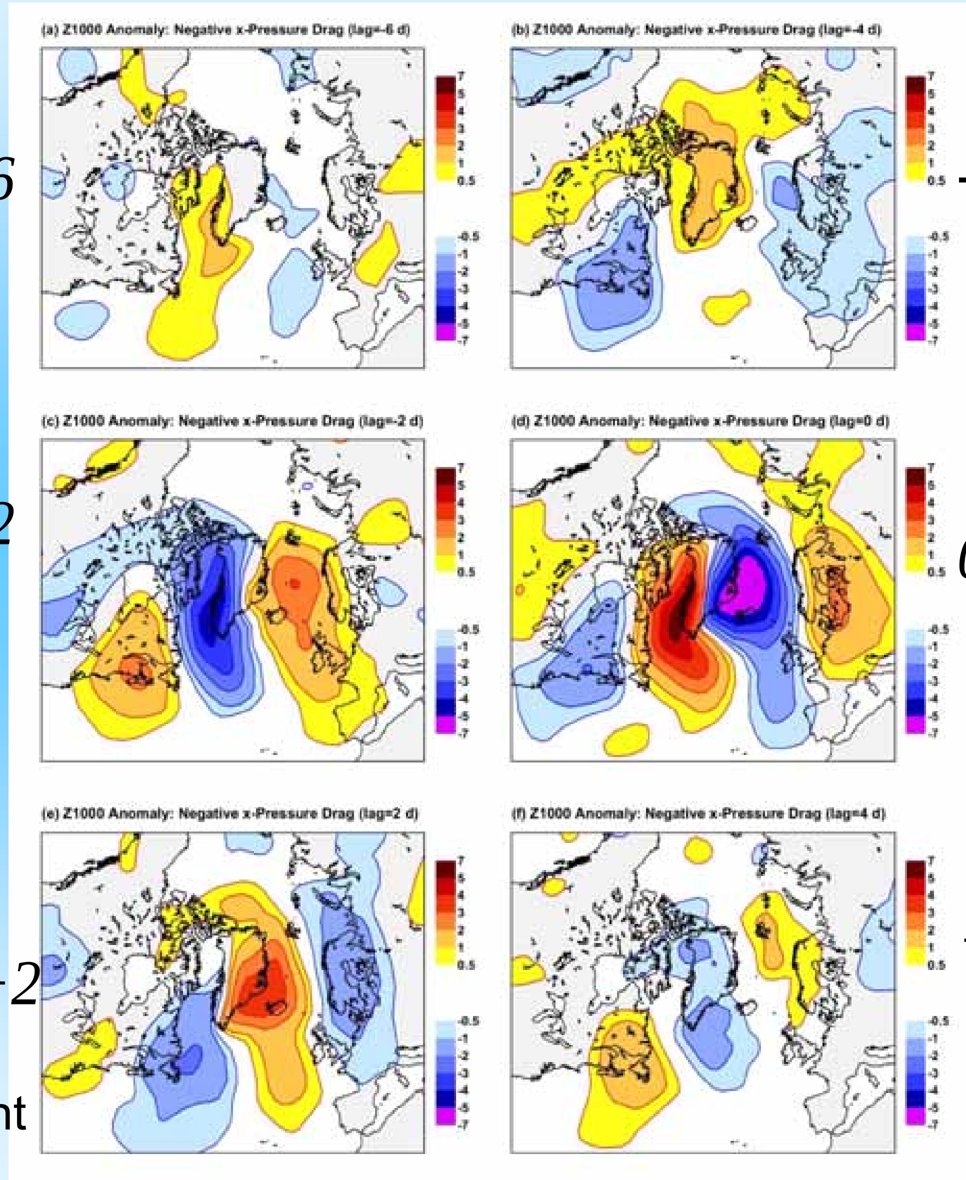


*-6*

*-4*

*-2*

*0 days lag*

*+2*

*+6*

high frequency variance composite maps: 1000 HPa level showing storm track covariant with pressure drag on Greeland

*Z50*
*stratospheric*
*polar vortex level*

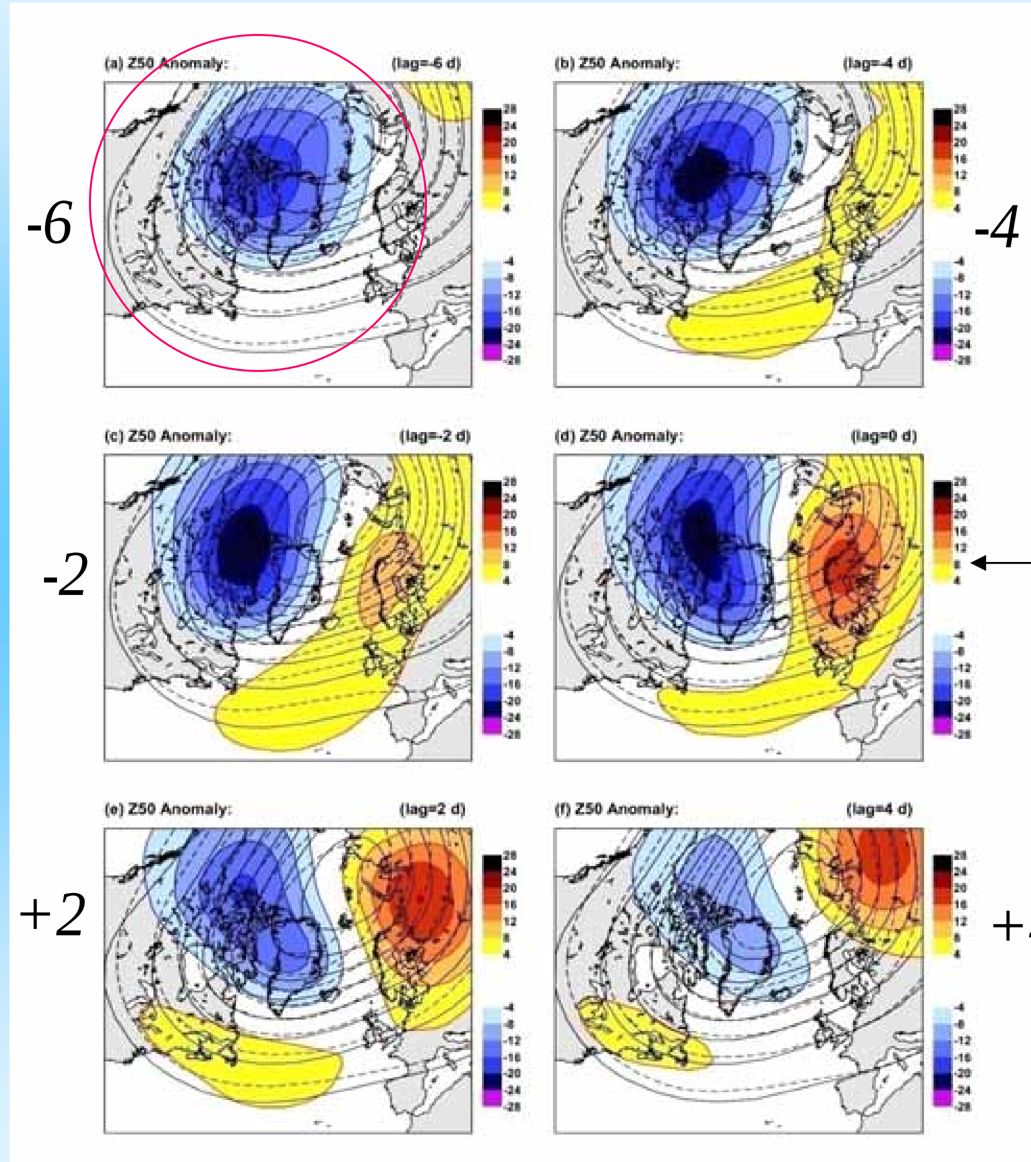


*lag 0 days*

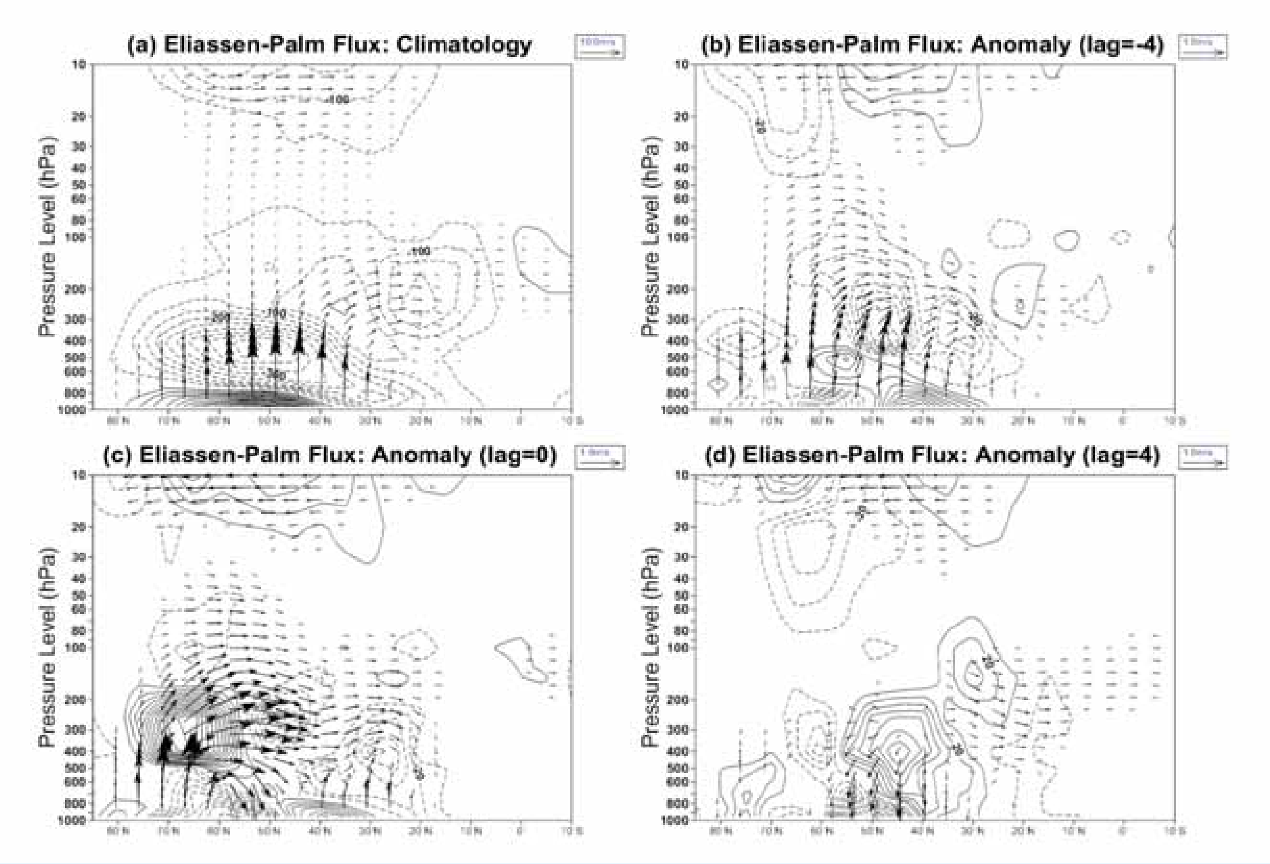

(a) Eliassen-Palm Flux: Climatology
(b) Eliassen-Palm Flux: Anomaly (lag=-4)
(c) Eliassen-Palm Flux: Anomaly (lag=0)
(d) Eliassen-Palm Flux: Anomaly (lag=4)
Pressure Level (hPa)

number of cyclones in winter…observations (ERA-40) and various model resolutions   T95 = 210 km grid; T799 = 25 km grid

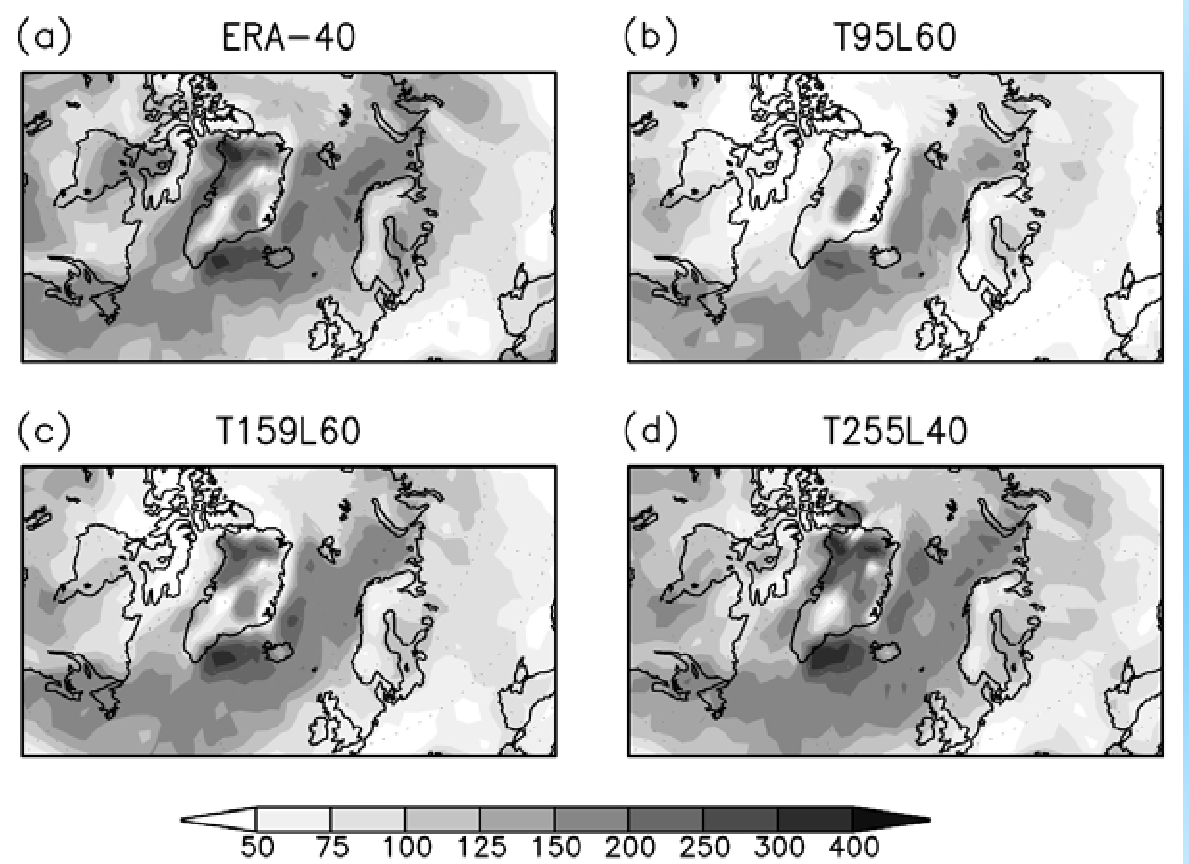

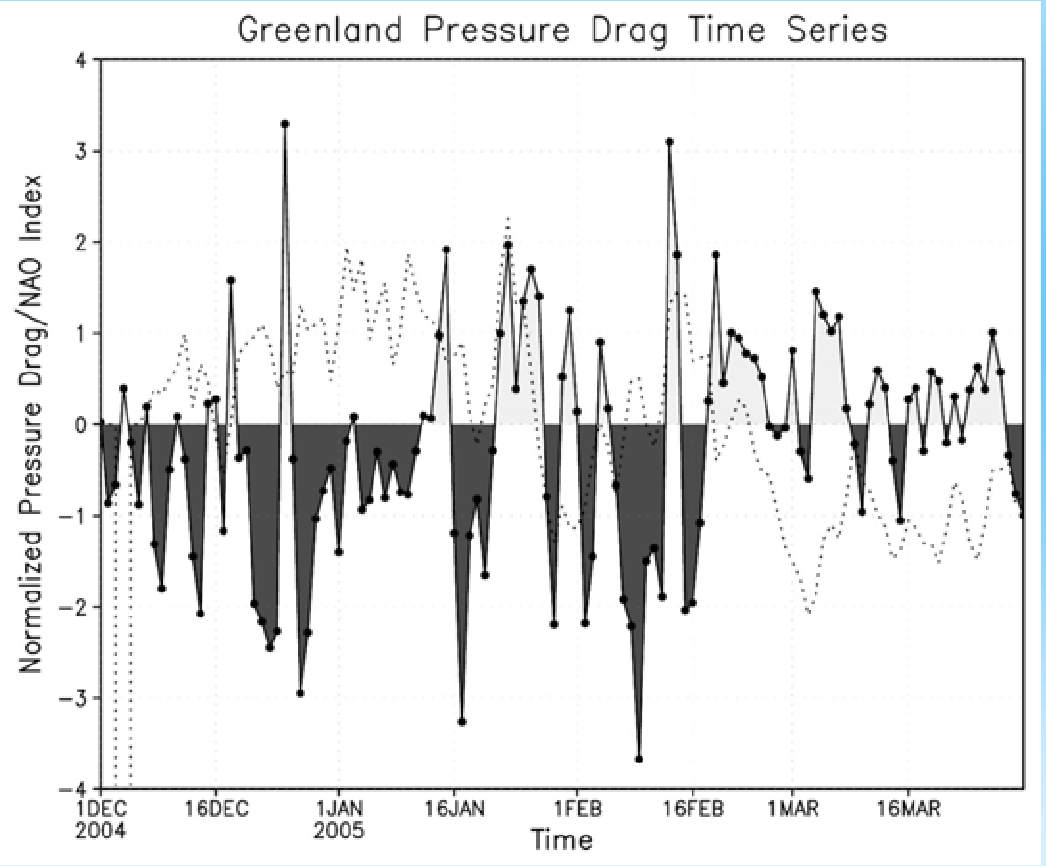

Greenland Pressure Drag Time Series
Normalized Pressure Drag/NAO Index
4
3
2
1
0
−1
−2
−3
−4
1DEC
2004
16DEC
1JAN
2005
16JAN
1FEB
16FEB
1MAR
16MAR
Time

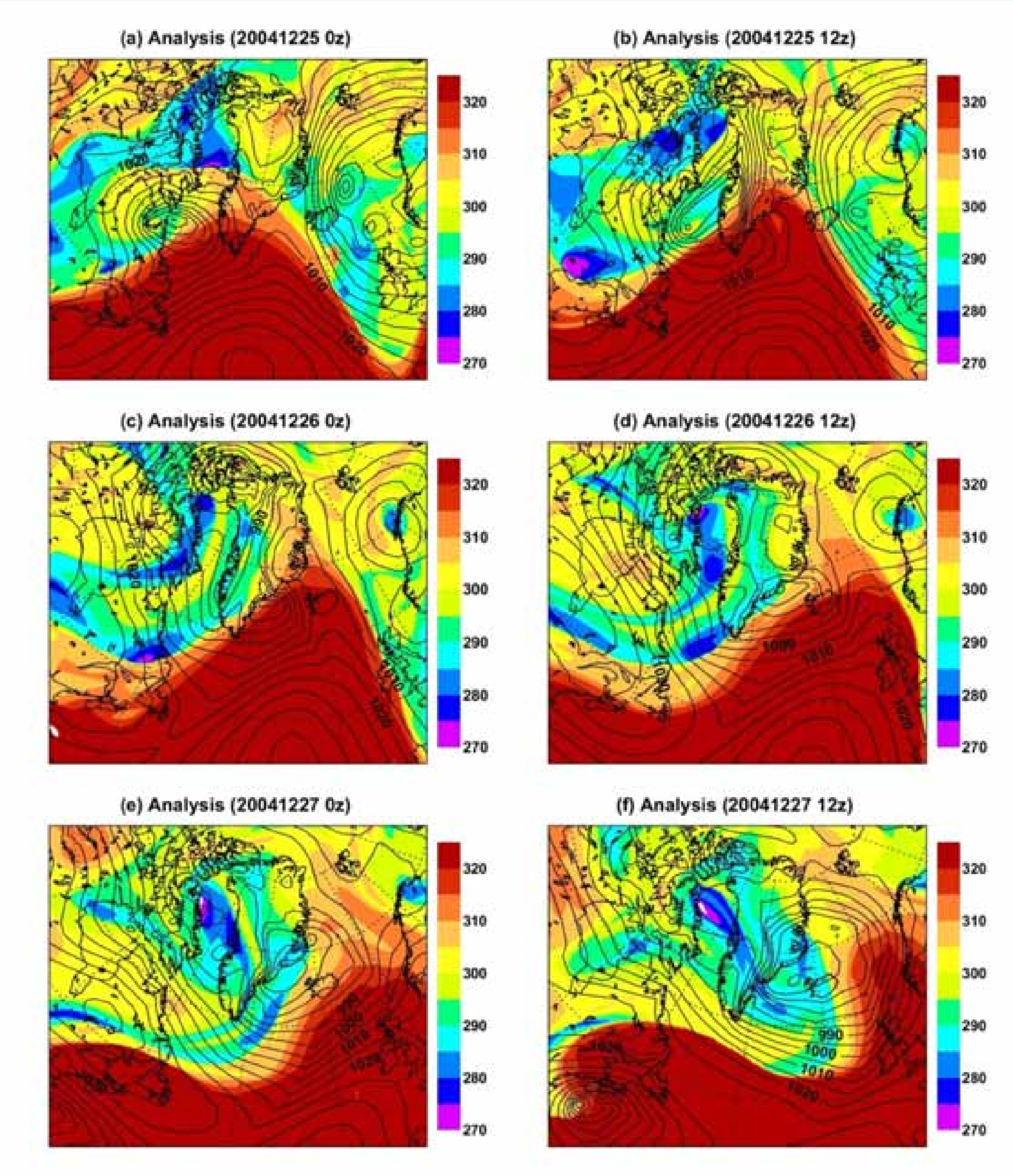


potential temperature at tropopause PV2 surface

and sea level pressure

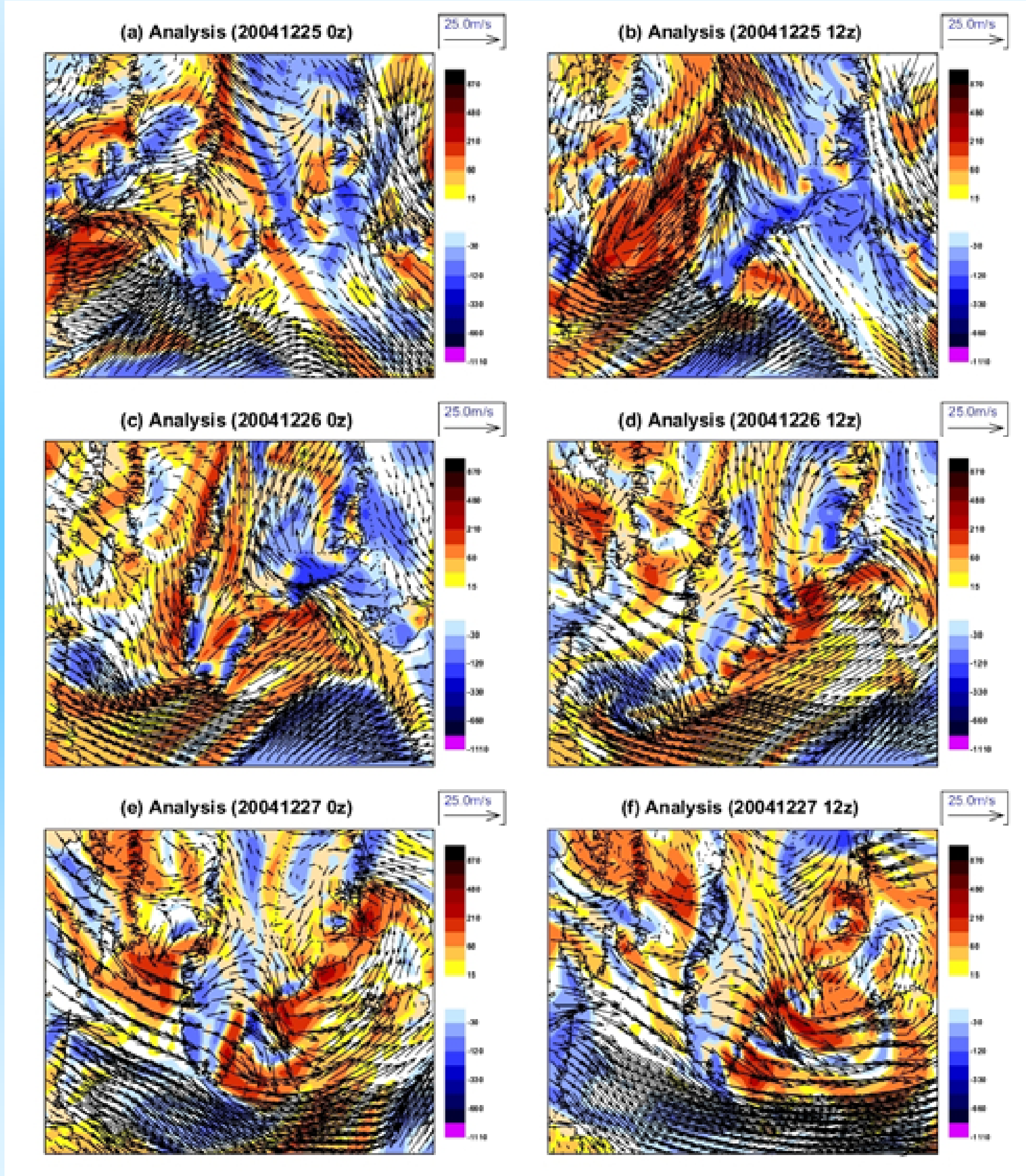
(a) Analysis (20041225 0z)
(b) Analysis (20041225 12z)
(c) Analysis (20041226 0z)
(d) Analysis (20041226 12z)
(e) Analysis (20041227 0z)
(f) Analysis (20041227 12z)
25.0m/s

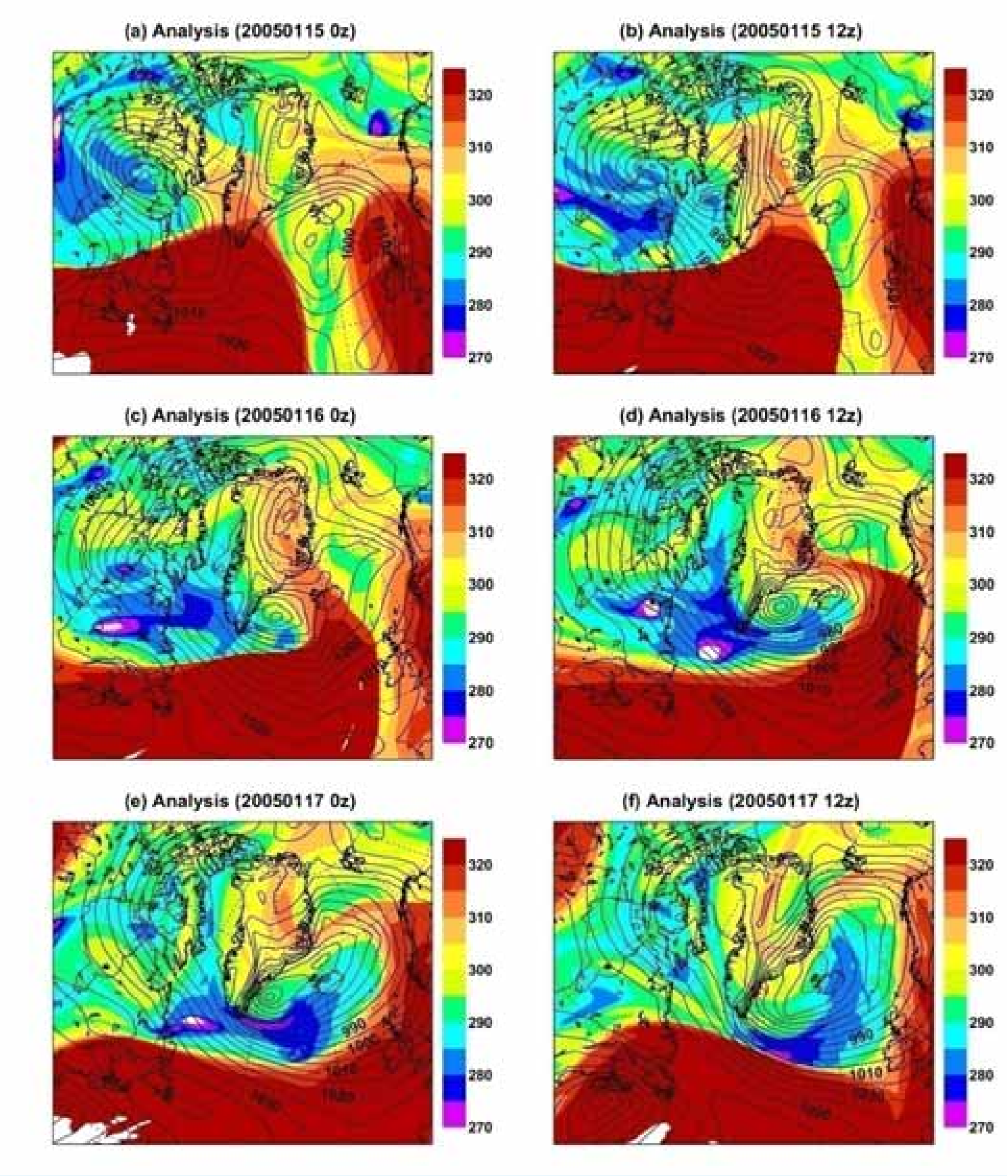
(a) Analysis (20050115 0z)
(b) Analysis (20050115 12z)
(c) Analysis (20050116 0z)
(d) Analysis (20050116 12z)
(e) Analysis (20050117 0z)
(f) Analysis (20050117 12z)
320
310
300
290
280
270
1000
1010
990

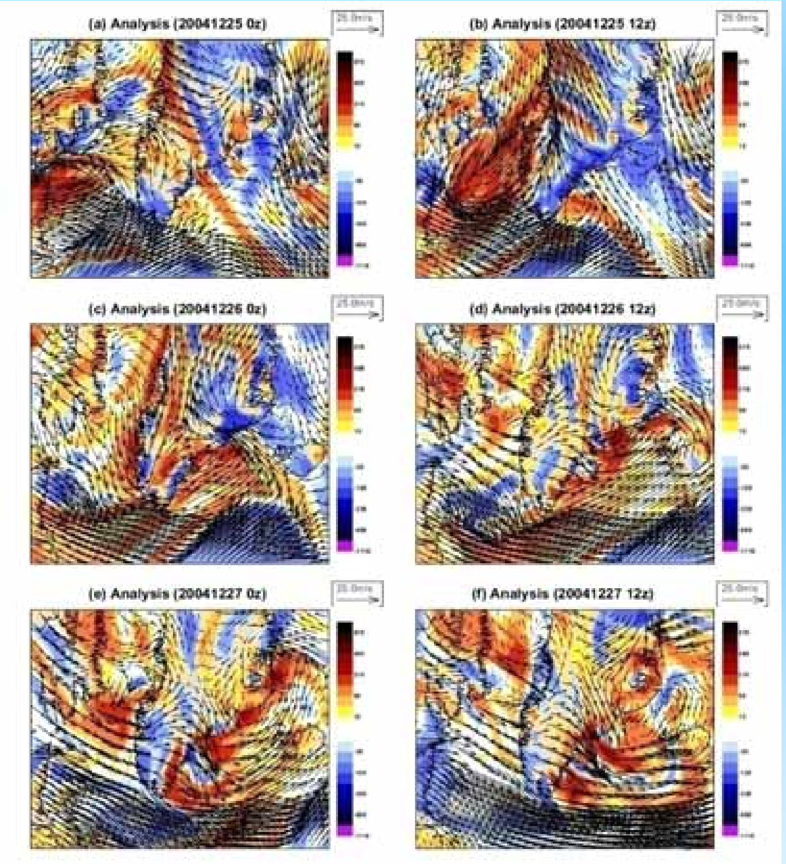
(a) Analysis (20041225 0z)
(b) Analysis (20041225 12z)
(c) Analysis (20041226 0z)
(d) Analysis (20041226 12z)
(e) Analysis (20041227 0z)
(f) Analysis (20041227 12z)

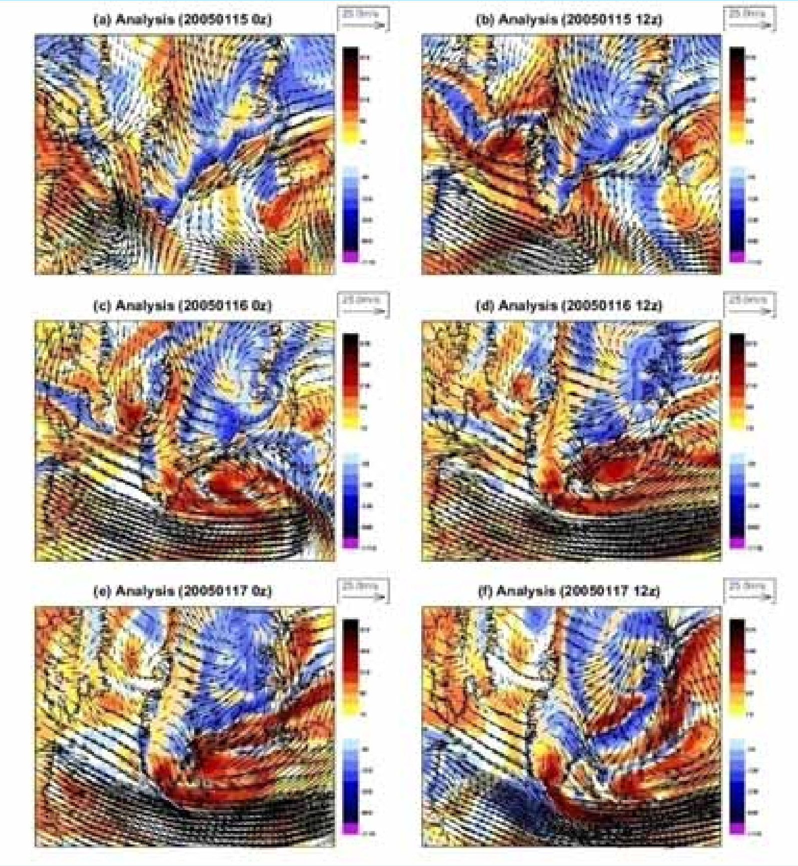
(a) Analysis (20050115 0z)
(b) Analysis (20050115 12z)
(c) Analysis (20050116 0z)
(d) Analysis (20050116 12z)
(e) Analysis (20050117 0z)
(f) Analysis (20050117 12z)

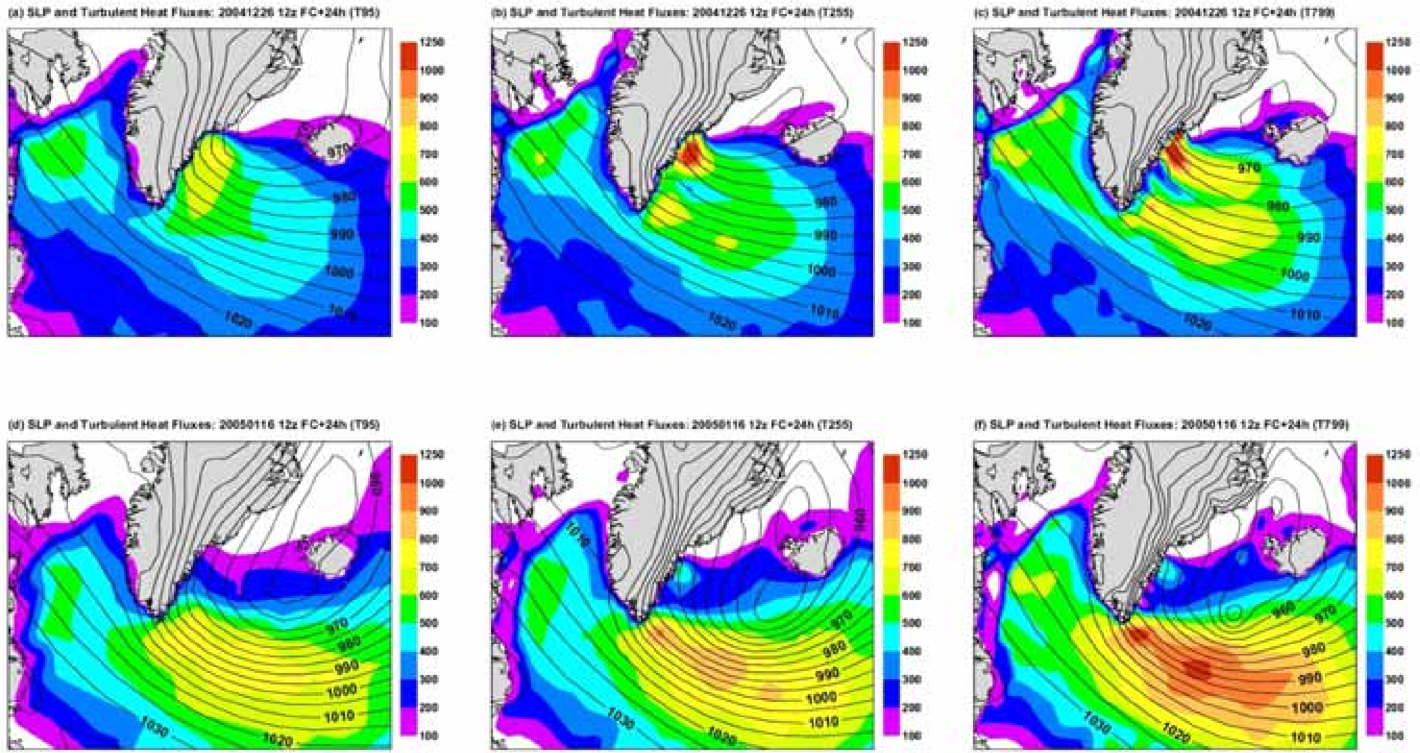
(a) SLP and Turbulent Heat Fluxes: 20041226 12z FC+24h (T95)
(b) SLP and Turbulent Heat Fluxes: 20041226 12z FC+24h (T255)
(c) SLP and Turbulent Heat Fluxes: 20041226 12z FC+24h (T799)
(d) SLP and Turbulent Heat Fluxes: 20050116 12z FC+24h (T95)
(e) SLP and Turbulent Heat Fluxes: 20050116 12z FC+24h (T255)
(f) SLP and Turbulent Heat Fluxes: 20050116 12z FC+24h (T799)

**Downslope winds increase wavedrag (by Bernoulli) here in a layer of $CO_2$**

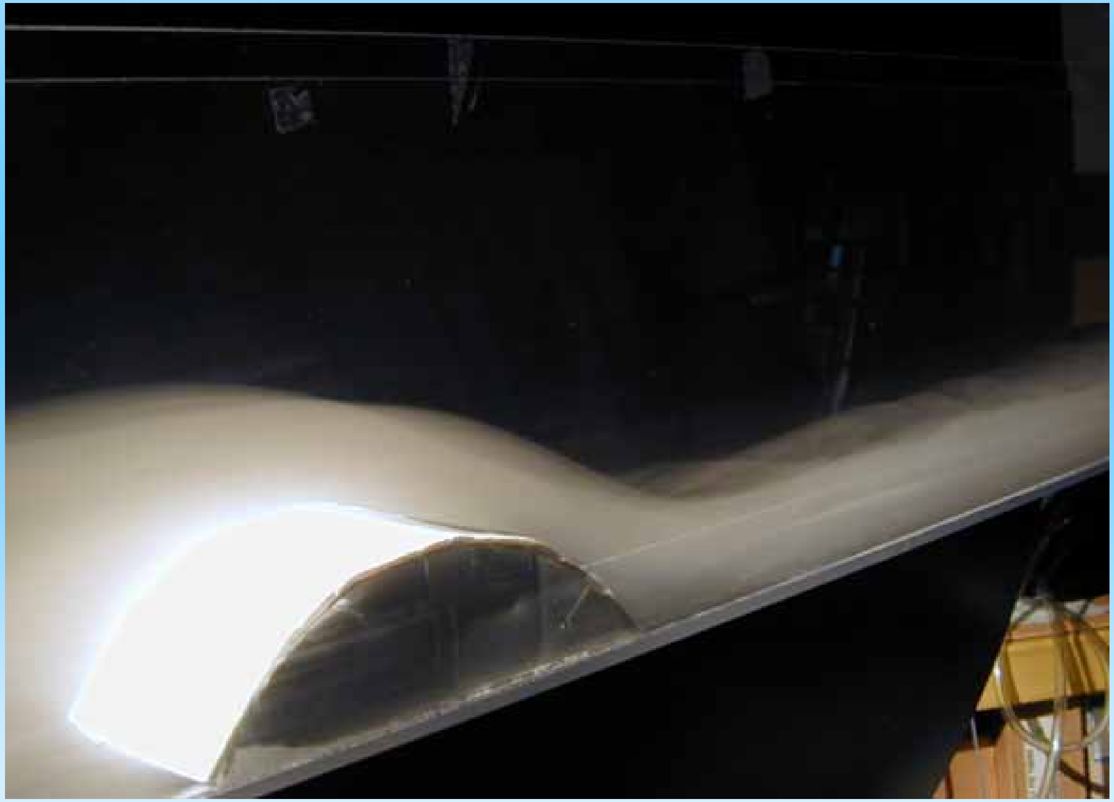

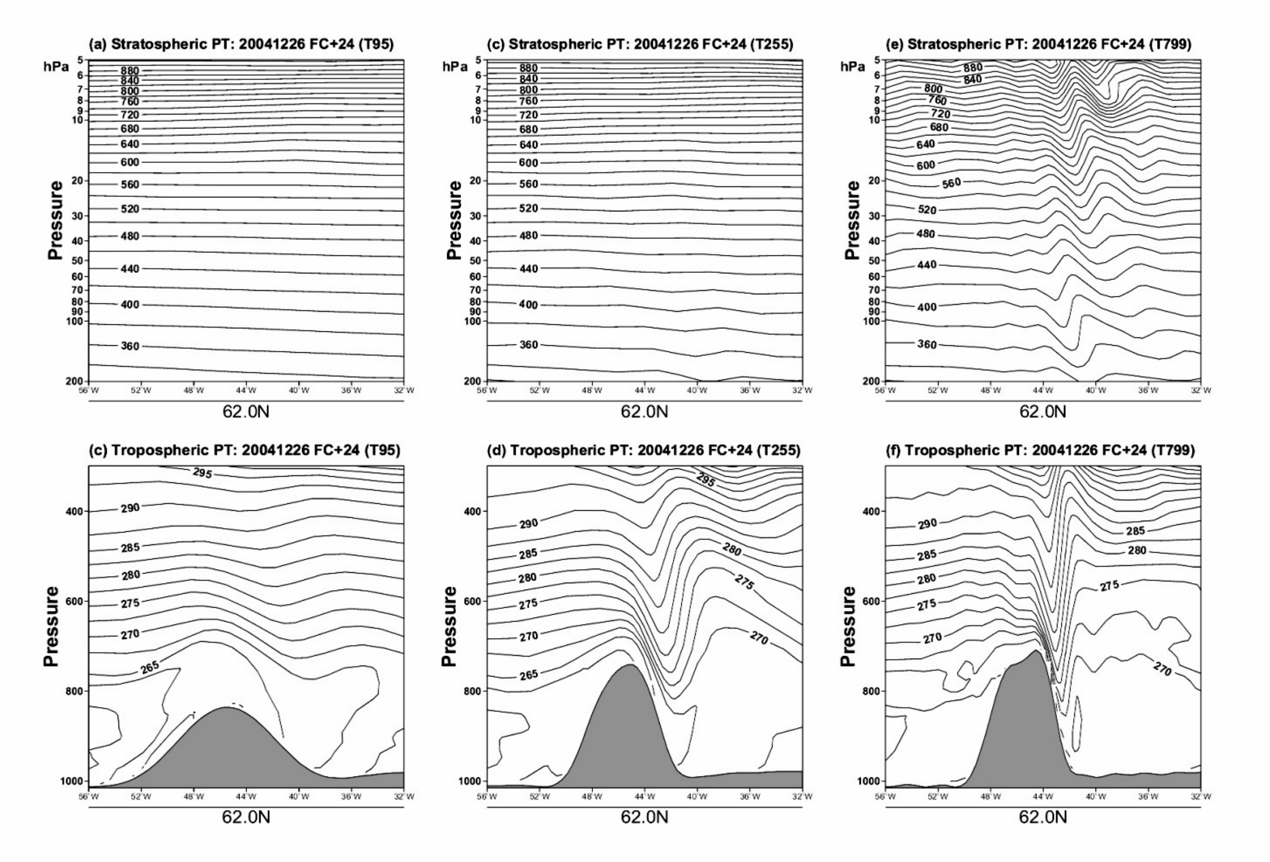
(a) Stratospheric PT: 20041226 FC+24 (T95)
(c) Stratospheric PT: 20041226 FC+24 (T255)
(e) Stratospheric PT: 20041226 FC+24 (T799)
(c) Tropospheric PT: 20041226 FC+24 (T95)
(d) Tropospheric PT: 20041226 FC+24 (T255)
(f) Tropospheric PT: 20041226 FC+24 (T799)
hPa
Pressure
62.0N

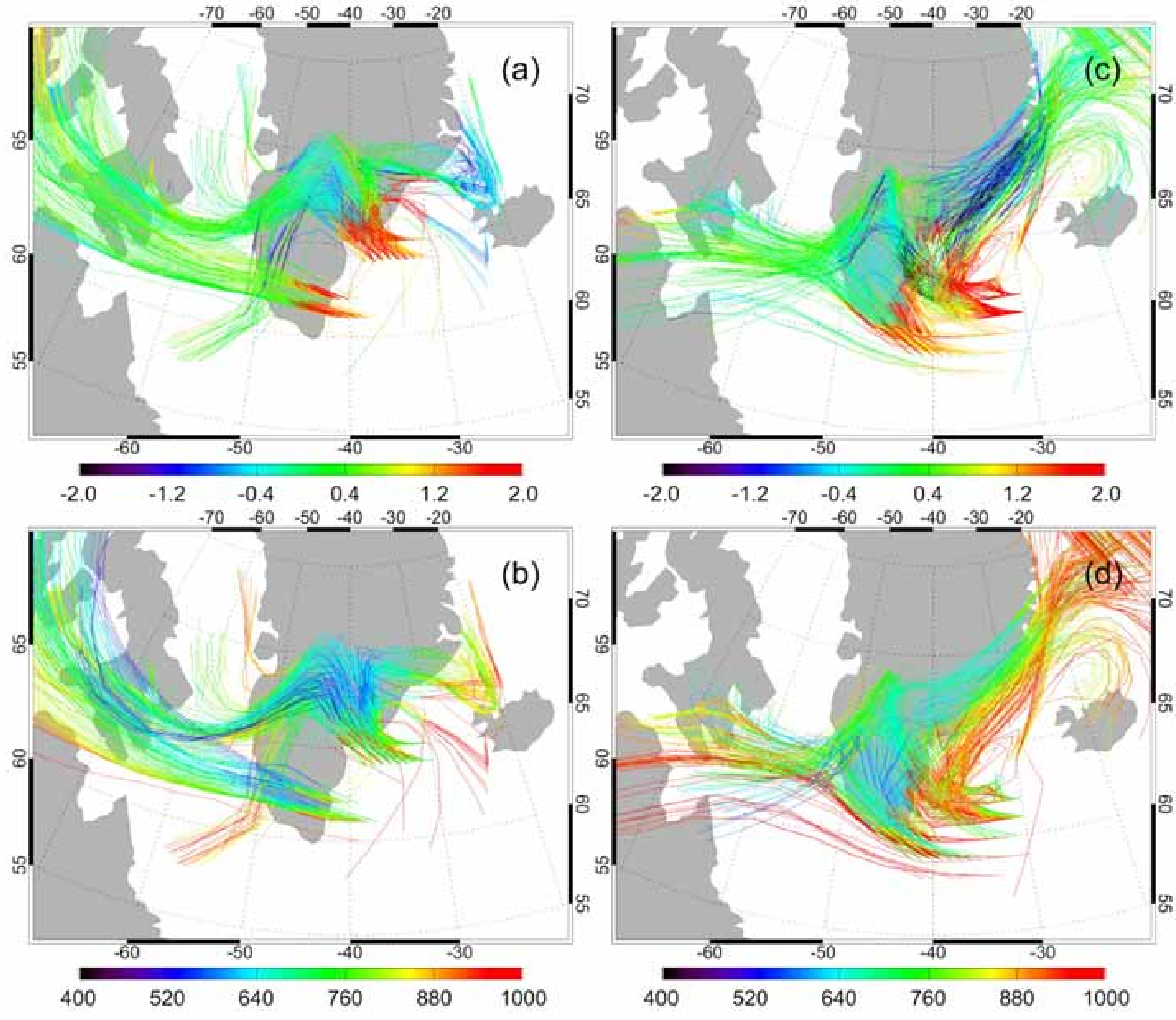

(a)
(b)
(c)
(d)
-70 -60 -50 -40 -30 -20
-60 -50 -40 -30
65 60 55
70 65 60 55
-2.0 -1.2 -0.4 0.4 1.2 2.0
400 520 640 760 880 1000

Mel Shapiro's Greenland flights

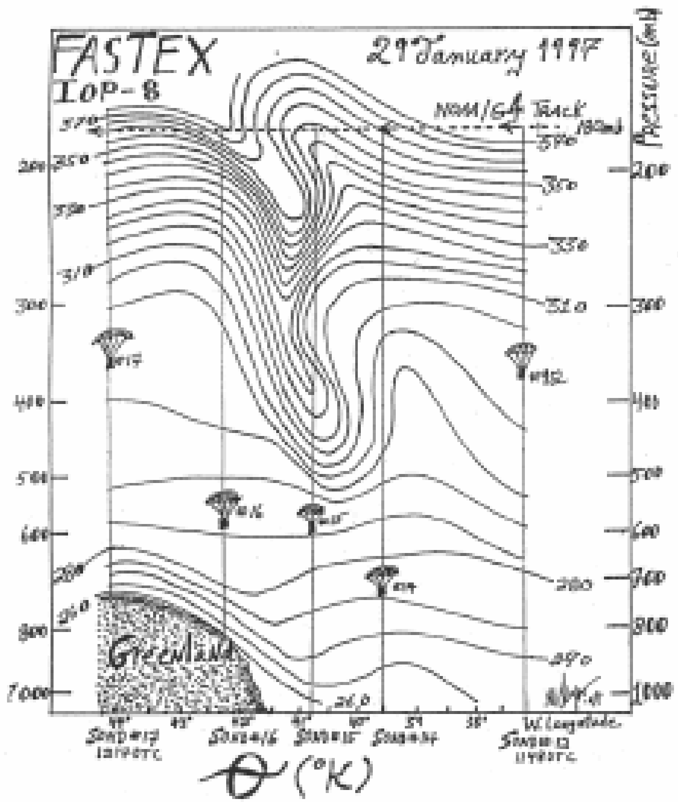


Fig. 5. Cross section of potential temperature (K) at ~1200 UTC 29 January 1997 derived from dropsondes (numbered 12-17) from the NOAA/G-4 aircraft.

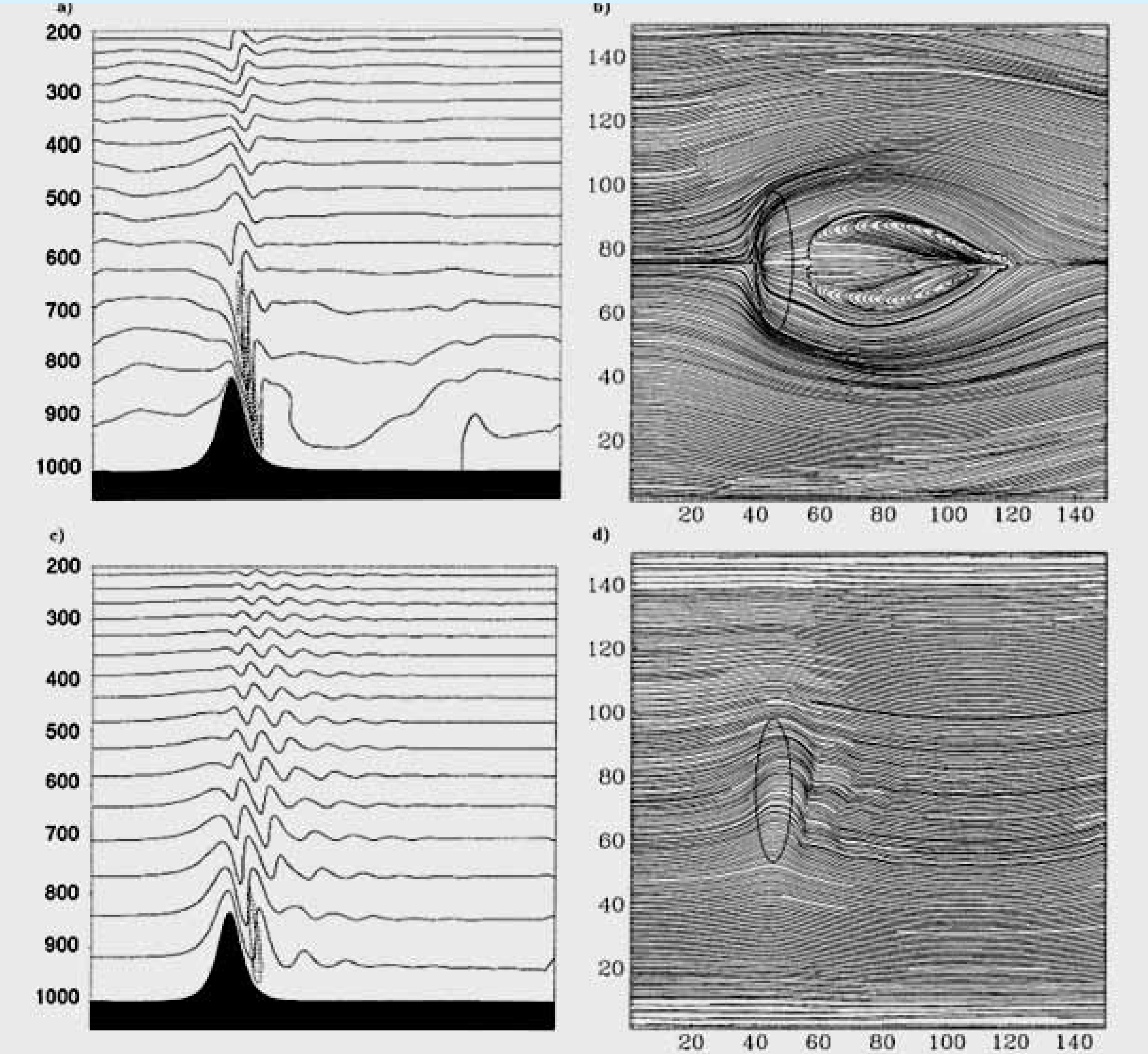


FIG. 1. Comparison of simulations excluding and including the Coriolis force. (a) A cross section of a flow with $\hat{h} = 1.5$ and Ro = ∞, taken at the axis of symmetry at $t^* = 34.56$ showing potential temperature (K, solid) and turbulent kinetic energy (J kg$^{-1}$, dashed). The isentrope contour interval is 2 K and the TKE contour interval 1 J kg$^{-1}$. (b) Streamlines at the surface at the same time. The topography is shown at 0.35$h$. (c), (d) As in (a), (b) but with Ro = 0.42.

Ro = ∞
Nh/U = 1.5

Ro = 0.42
Nh/U = 1.5

*Petersen, Olaffson, Kristjannson JAS2003*

Schär (*JAS 93*): PV is transported along the intersections of the Bernoulli-function and isentropic surfaces in a statistically steady flow….

$$PV\ flux: \vec{J} = \nabla\theta \times \nabla B$$

$$B = enthalpy + \tfrac{1}{2}|\vec{u}|^2 + \Phi$$

$$\approx c_p T + \tfrac{1}{2}|\vec{u}|^2 + gz$$

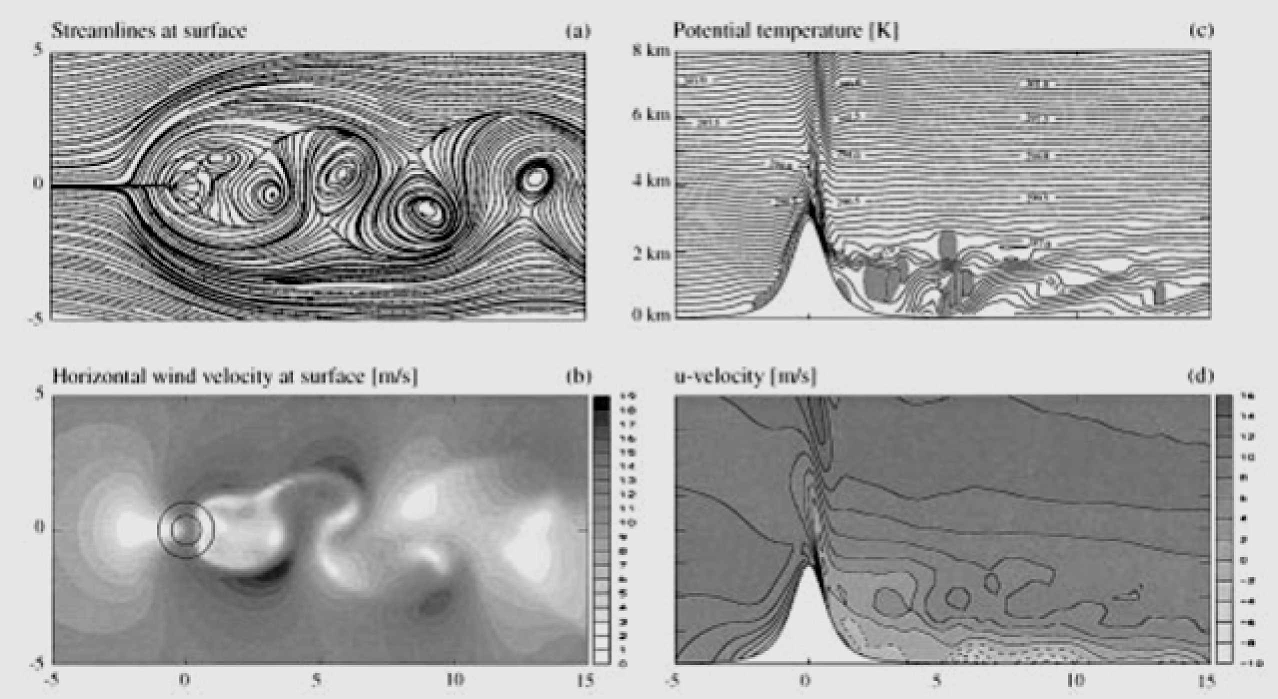


*Schär & Durran JAS 97*

also: tip horiz vorticity to make vertical vorticity *Rottuno et al. JAS 99*

Ertel potential voticity generation by breaking lee gravity wavesL the PV generation as well as the gravity-wave momentum flux alter the geostrophic circulation

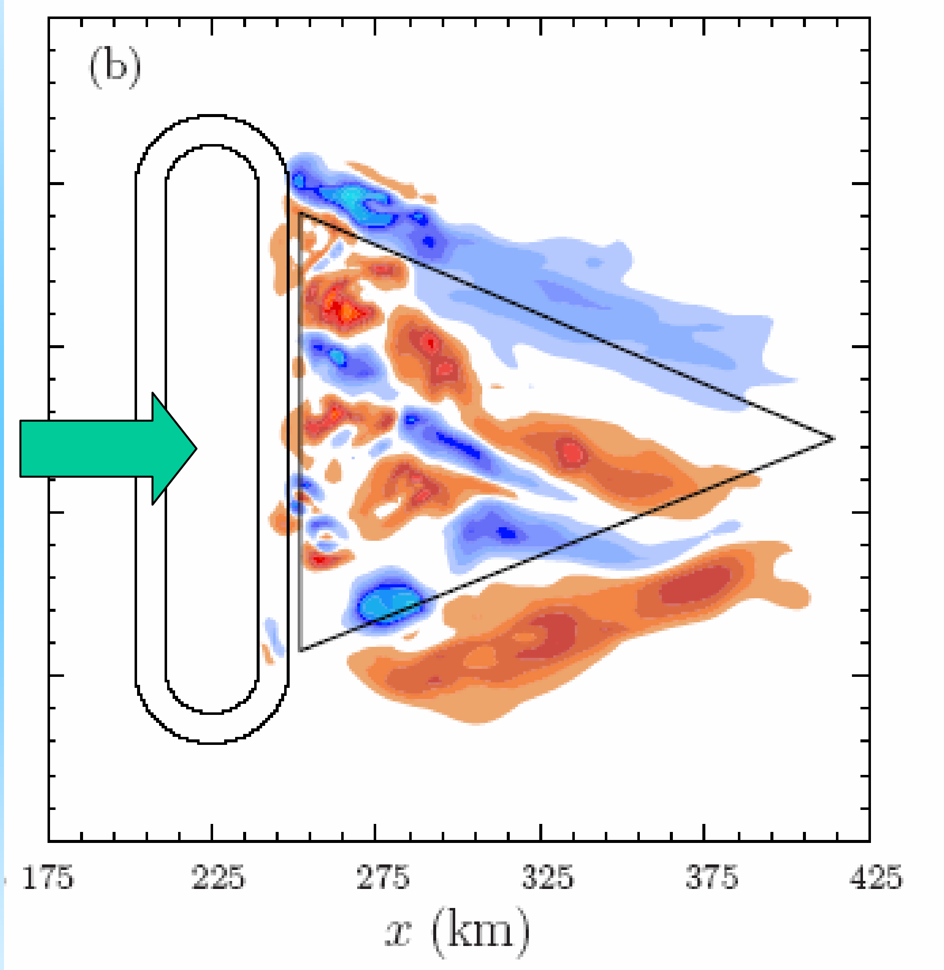


$$\frac{\partial q}{\partial t} + \nabla \cdot \mathbf{J} = 0,$$

$$\mathbf{J} = \nabla\theta \times \nabla B,$$

*Chen, Hakim & Durran, JAS 2007 subm*

PV and zonal flow generation in flow over a 1.5 km high mountain

(dipole of PV, decelerated wake)

*Chen, Hakim & Durran, JAS 2007 in press*

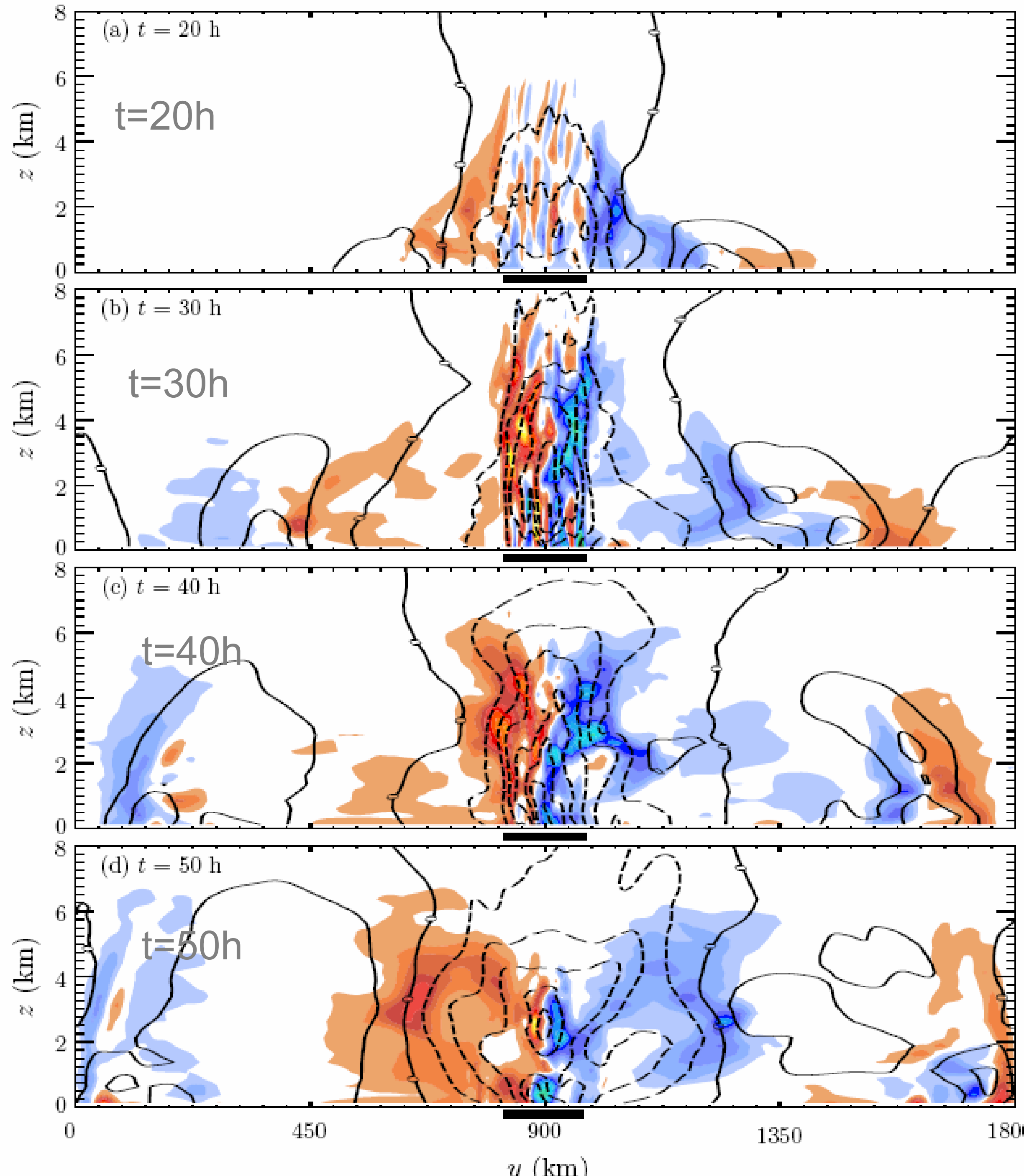

*Orographic gravity waves over Greenland observed: Limpasuvan et al.  JGR 2007*

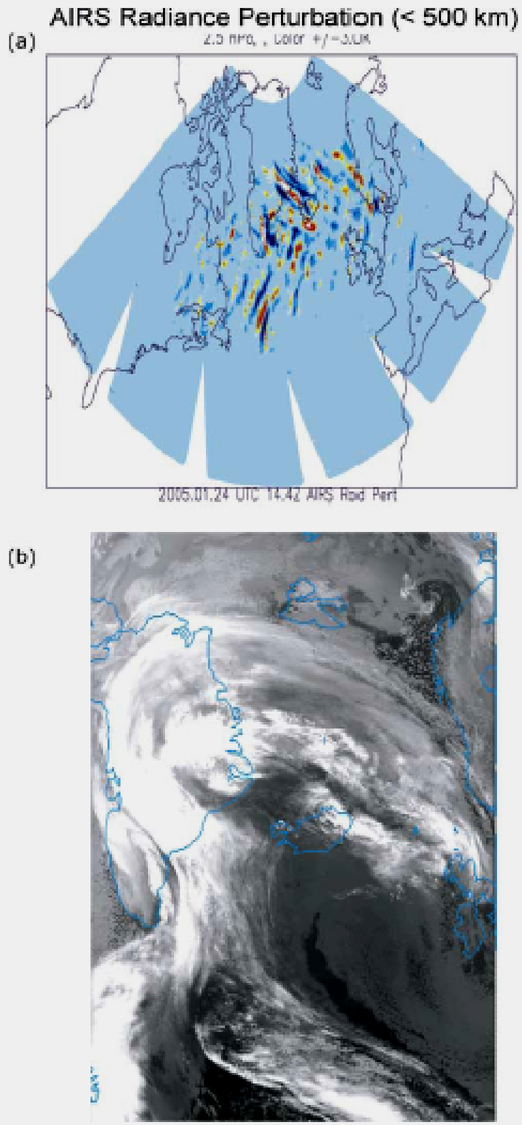


Figure 1.  (a) AIRS observations (ascending orbits) at 2.5 hPa of radiance perturbations (of horizontal scales shorter than 500 km). The approximate equivalent temperature amplitude is noted in the subtitle. (b) Infrared image from the Defense Meteorological Satellite Program at 0913 UTC 24 January 2005.

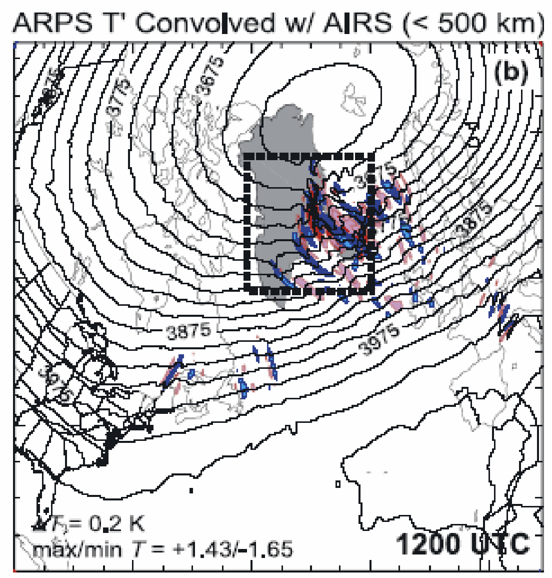


perturbations simulation at 2.5 hPa (contour interval

D10115 LIMPASUVAN ET AL.: STRATOSPHE

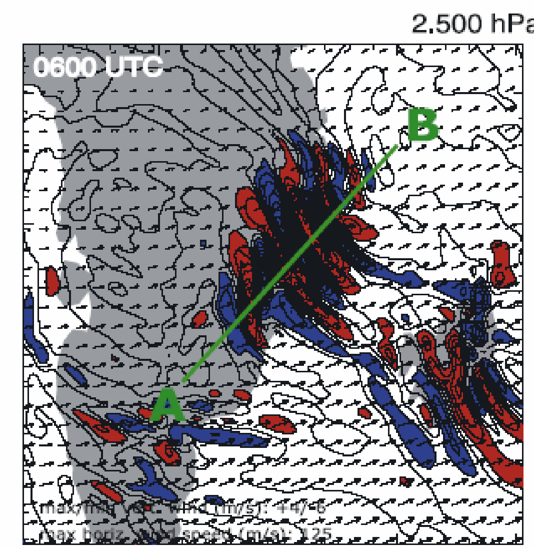

# Overturning circulations

•

Oceanic overturning circulations: coexisting with ‘horizontal gyres of wind-forced circulation

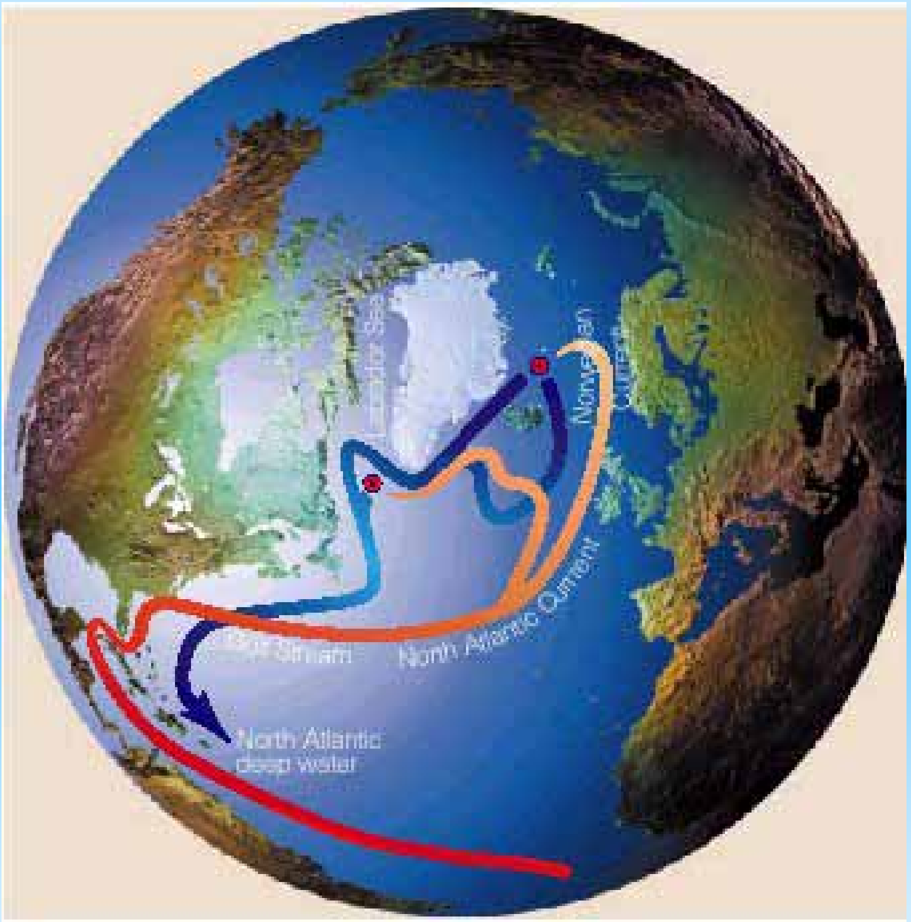


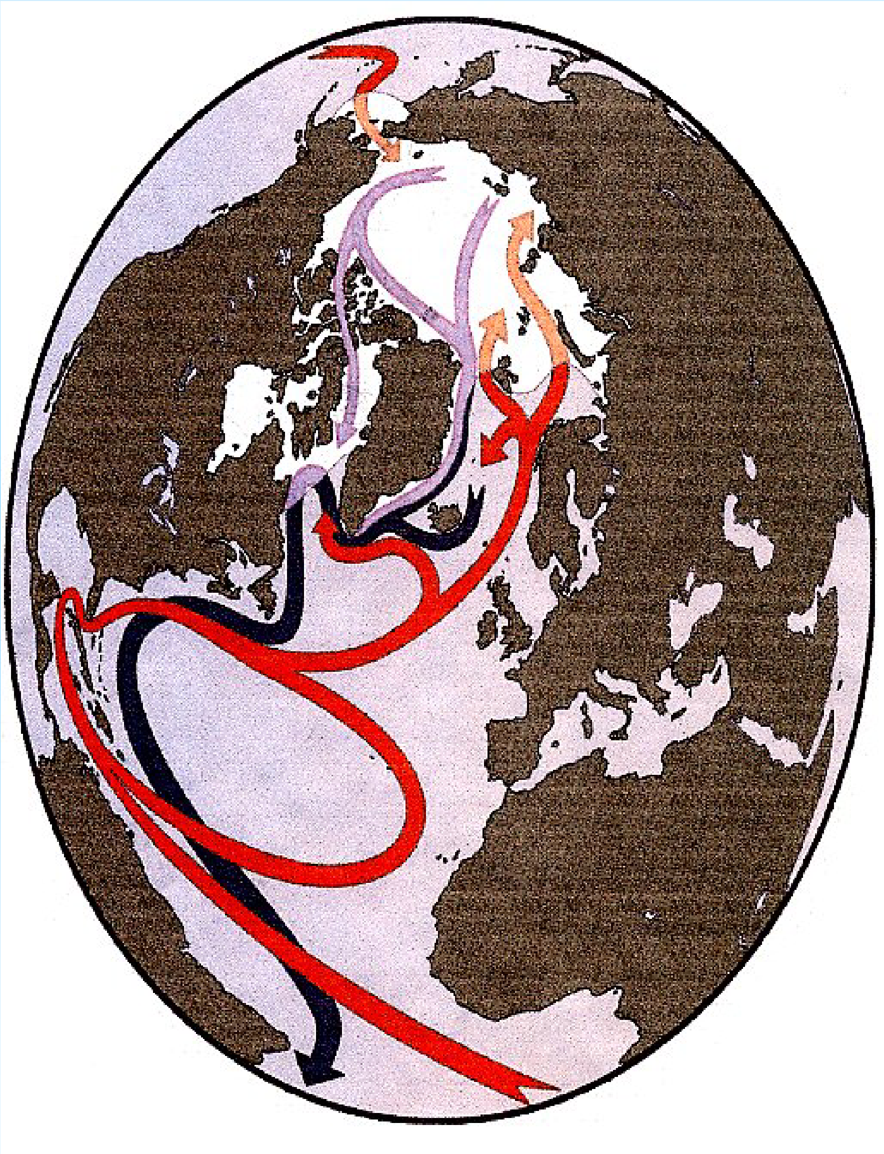

- MOCs have an easier time in the oceans than in the atmosphere:

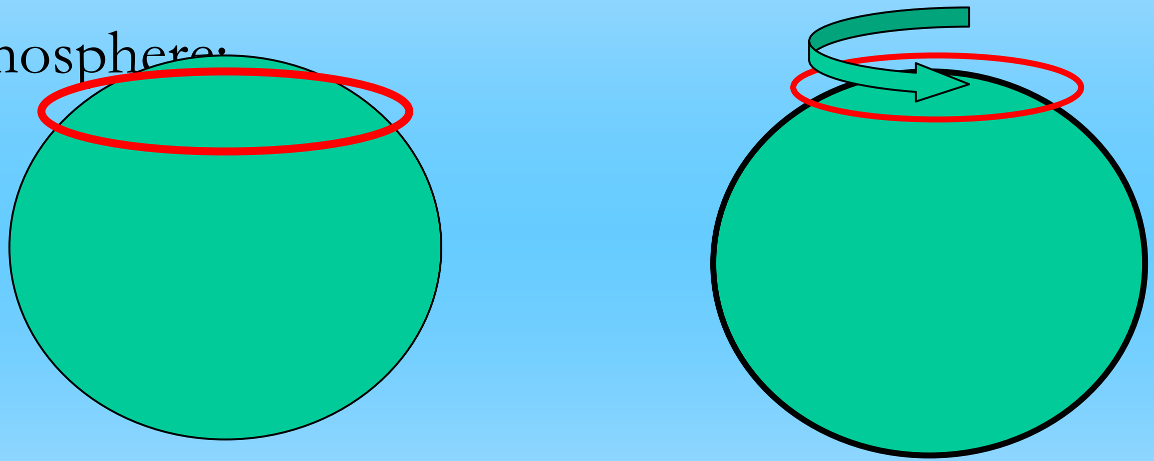

*a ring of air moved 1000 km north gains westerly velocity of 100 m sec$^{-1}$ There is not enough energy available to utilize this mode: the Hadley cell is limited in north-south extent. Forces (eddy momentum flux from PV stirring) and non-symmetric circulation are required to support extensive meridional excursion.*

# channels and conduits for heat- and fresh-water transport

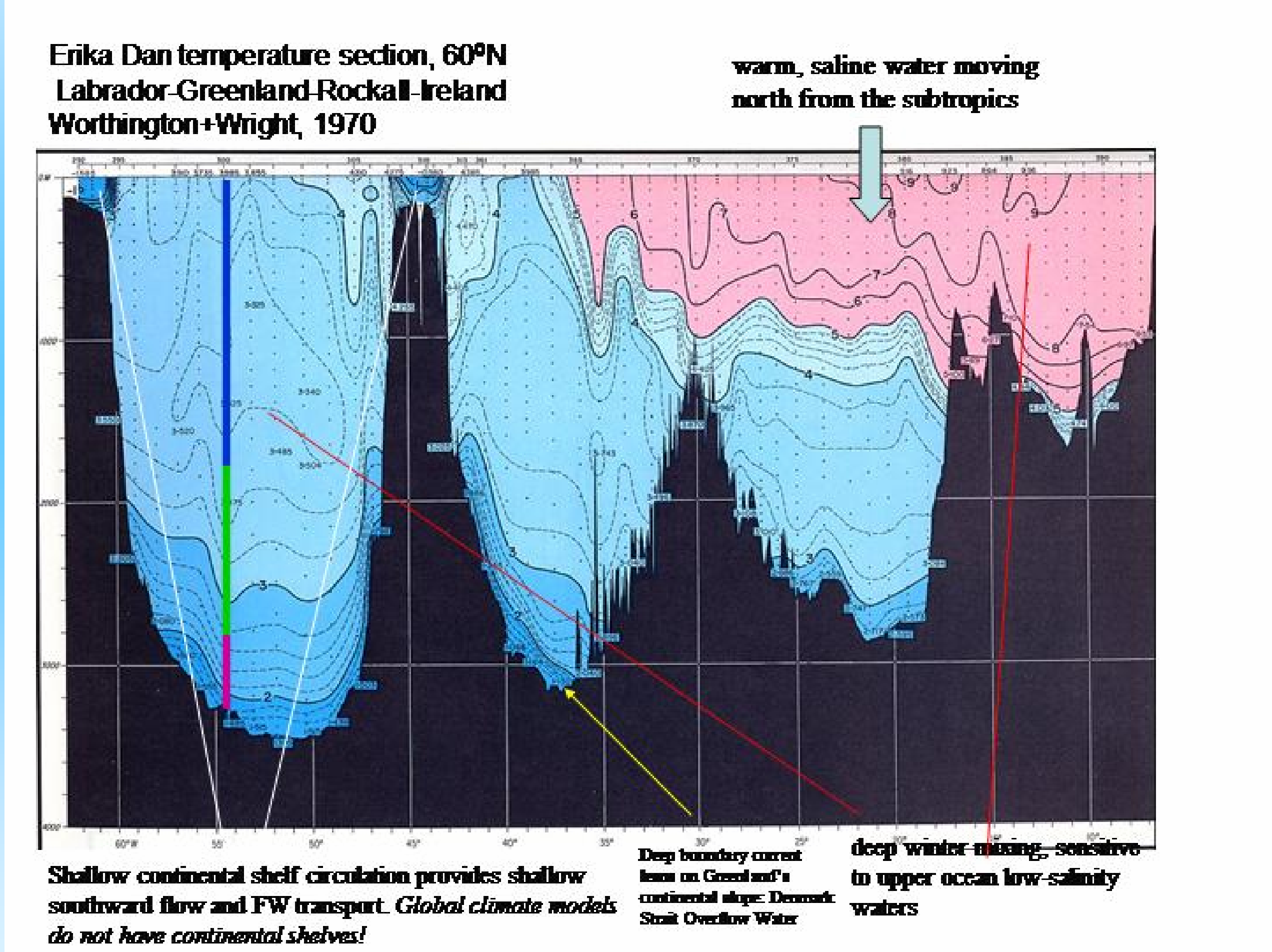

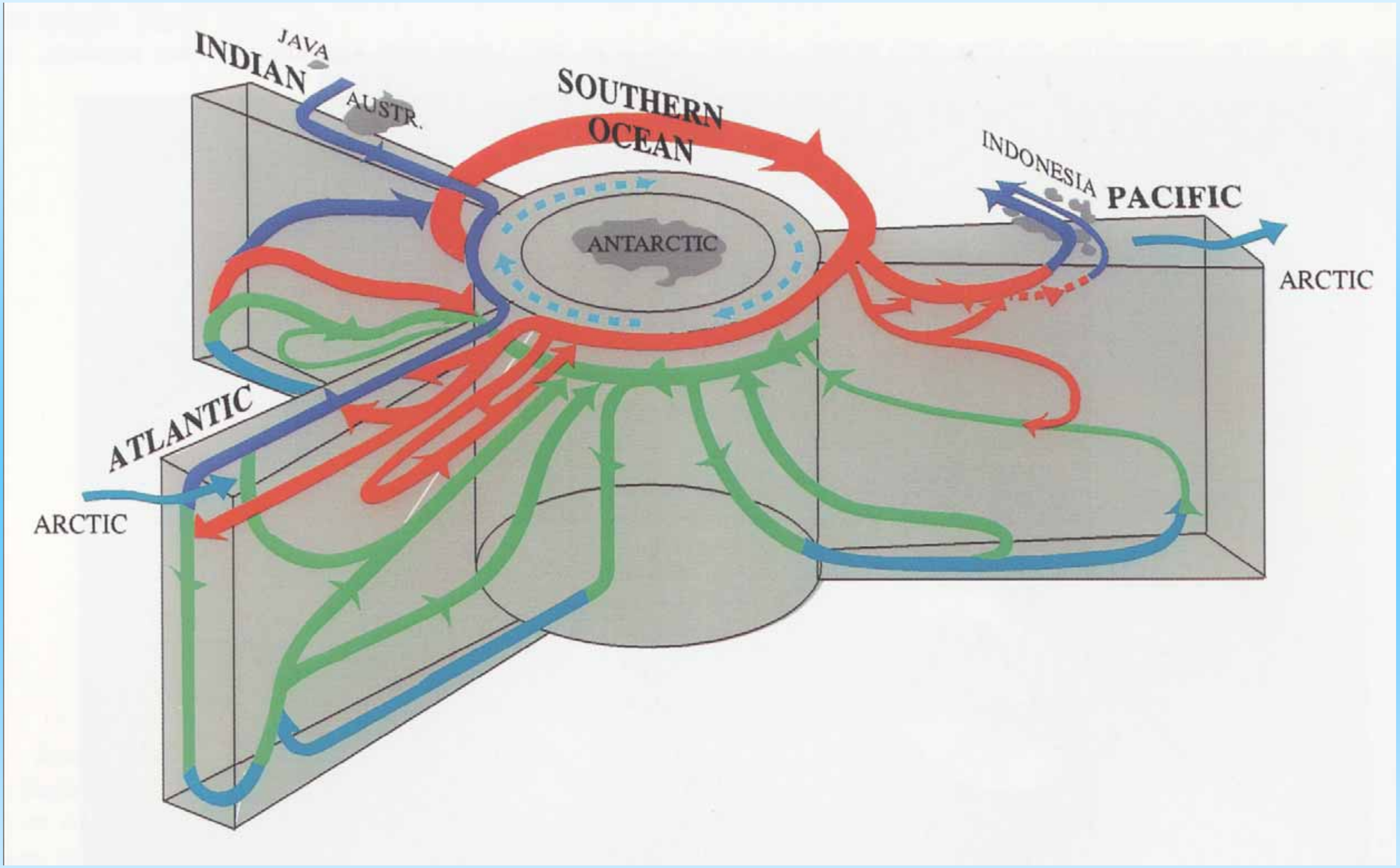

JAVA
INDIAN
AUSTR.
SOUTHERN
OCEAN
INDONESIA
PACIFIC
ANTARCTIC
ARCTIC
ATLANTIC
ARCTIC

Lateral penetration of convected water masses: Gradual diffusive closure of nearly balanced circulations:

(o) the linear heat-up problem

(i) geostrophic adjusment followed by

(ii) Elliassen-Sawyer overturning

(iii)~ 'slow diffusion'

(iv) $\beta$-plumes

A baroclinic vortex created by injecting water at mid-depth into a stratification

Note purple dye shows azimuthal velocity exists above and below the water mass!

The MOC (meridional circ) driving 3 vortices

PV inversion: using a model of convective destruction of PV. The modelled or diagnosed PV field is associated with a field of azimuthal circulation, displaced mass, and interacts with the meridional overturning circulation

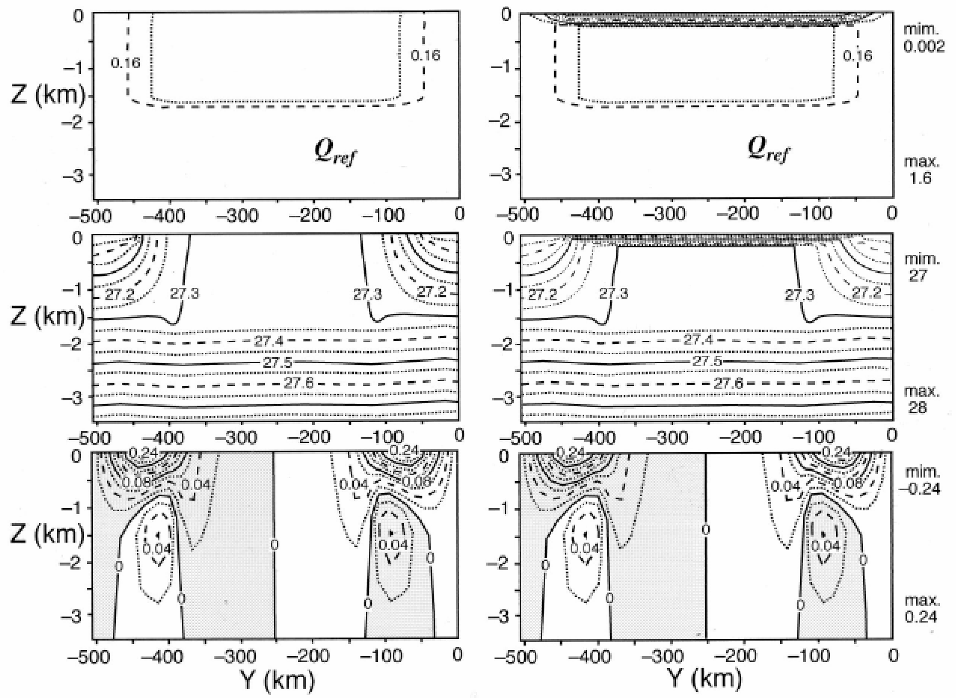


**Figure 37.** PV inversion for a mixed patch with (a) inhomogeneous and (b) homogenous boundary conditions at the surface. PV distribution, isopycnals, and currents are plotted. In Figure 37a the potential density at the sea surface is specified and an idealized interior PV anomaly inverted to give the hydrography and azimuthal velocity of a baroclinic vortex. In Figure 37b an interior PV field identical to that of Figure 37a is used, but now the cold surface is represented by a sheet of high PV just beneath the upper boundary, which is prescribed to be an isopycnal surface. Note that in Figure 37b, unlike Figure 37a, the isopycnals cannot cut the upper surface, which itself is an isopycnal.

viscous overturning in a rotating cylider:
the radial/vertical plane transmits stress from the top plate (which is at rest in the laboratory frame) and the bottom of the cylinder (which is rotating)

The Ekman layers are very thick.

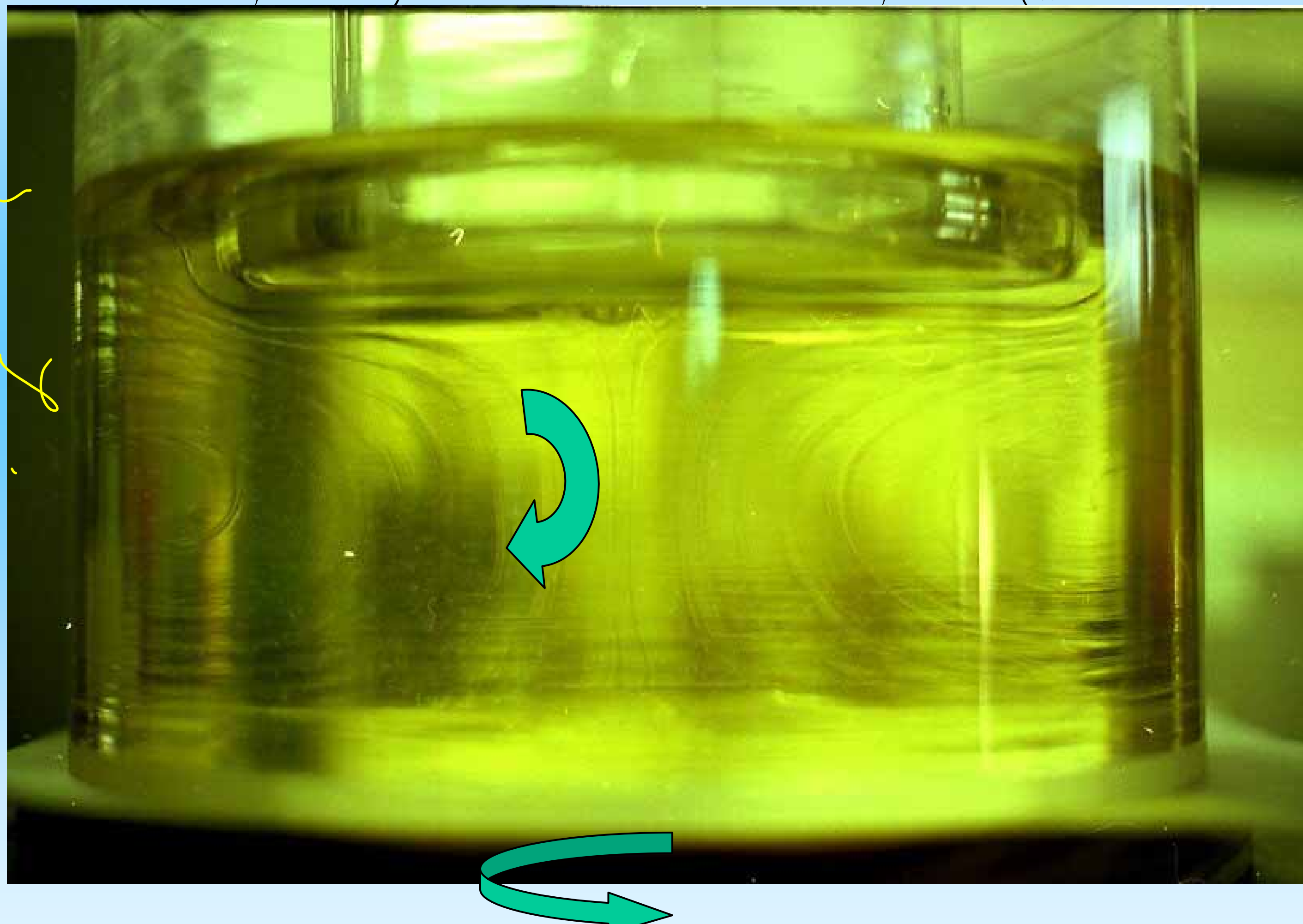

*sugar syrup*

Overturning cells in an annulus of fluid between concentric cylinders (the inner cyclinder is rotating, the outer cylinder is stationary (Taylor-Couette flow).

The cells transmit torque between the solid cylinders more strongly than would pure viscous diffusion.

(The same 2D equations govern thermal convection, and the Nusselt number expresses the analogous increase in heat flux above the diffusive rate).

MOCs organized by double diffusion

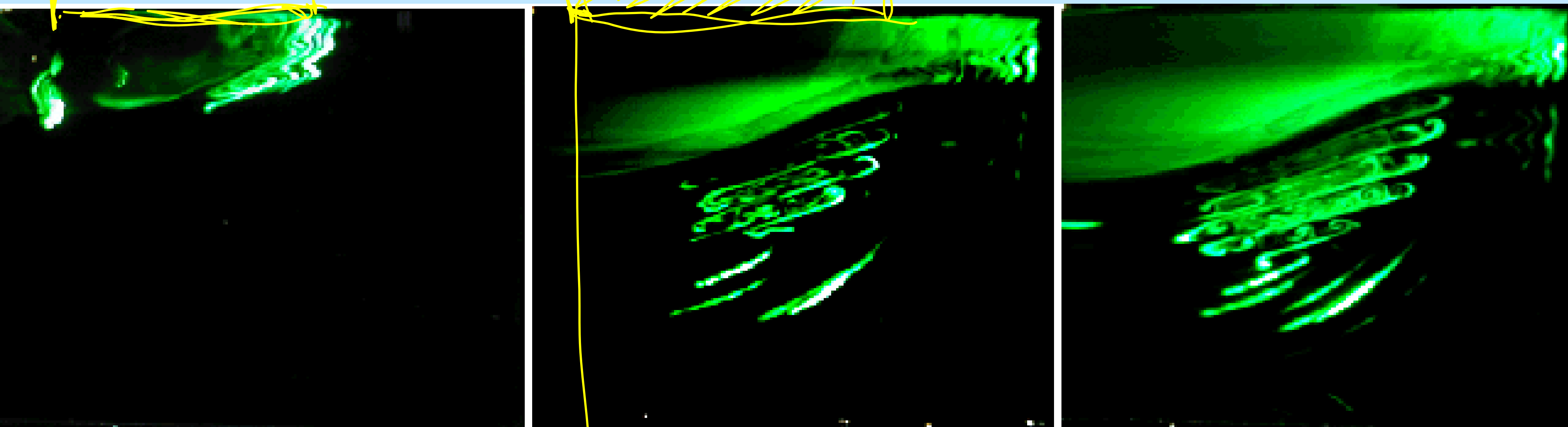


disk drives an anticyclone (warm eddy) in uniformly stratified fluid

Sink-driven flow in a rotating, stratified fluid: the cyclonic spin of the fluid would be resisted by bottom Ekman friction (and all radial inflow concentrated there in this tornado vortex); However, stable stratification resists and forces continuing MOC within the fluid. The azimuthal velocity

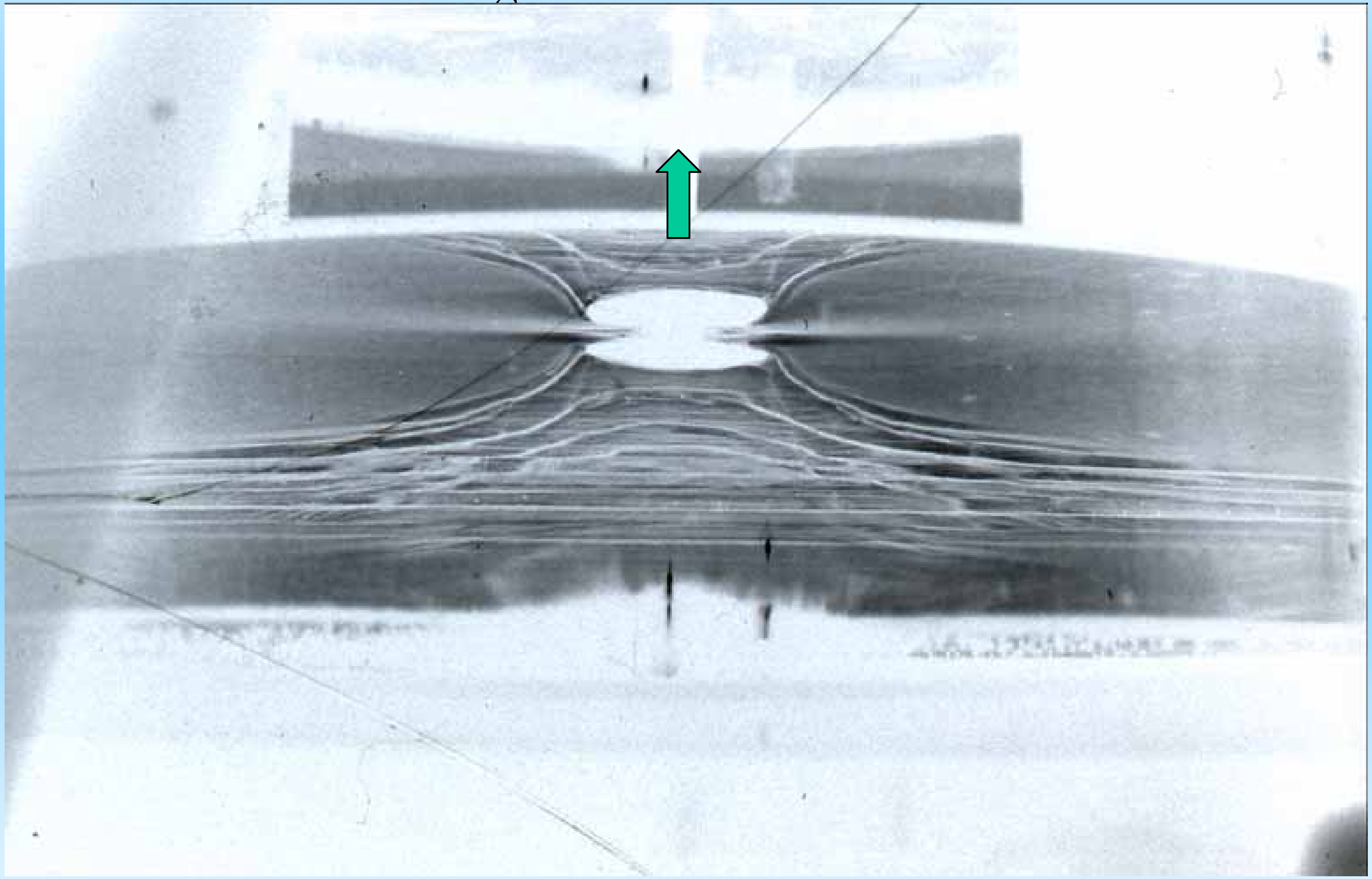

*GFD lab, Univ of Washington*

# Dense plume flowing down a sloping valley in a rotating fluid
(model of dense downslope flows in the Weddell Sea)

Elin Darelius, Univ of

*particle paths are helical, with Ekman driven meridional overturning transmitting the boundary stress into the fluid. (Looking up the sloping valley)*

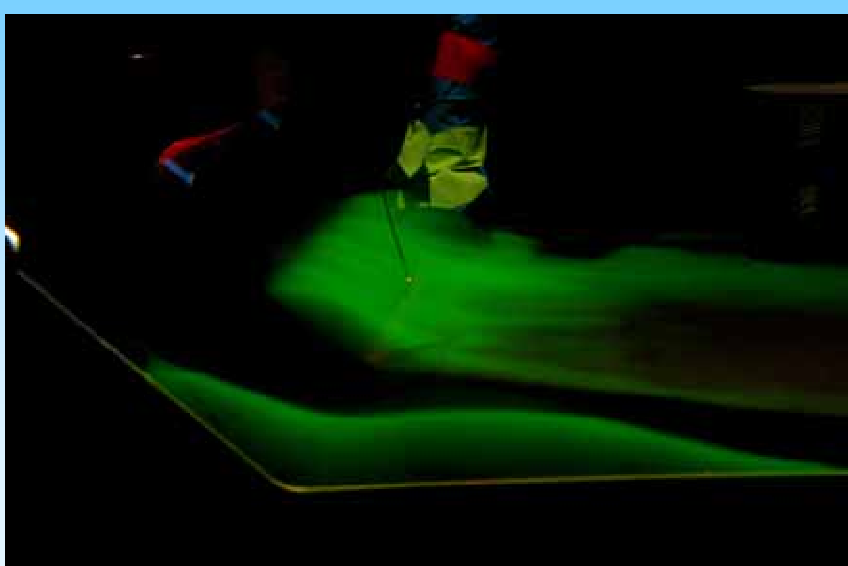


Figure 17: *The "Ekman Helix" traced out by dye injected in the bottom boundary layer seen a) up the canyon and b) from above. The secondary circulation causes a particle to follow a helix like path down the canyon.*

*Lumpkin & Speer's* JPO 03 discussion of the Atlantic MOC, here plotted against potential density and latitude. Even though we know there is much east-west structure (boundary currents, horizontal gyres as in Reid's maps) the zonally averaged MOC 'looks like' the simple 2-dimensional box models, for example Winton's

*S*

*$O_2$*

*sea surface*

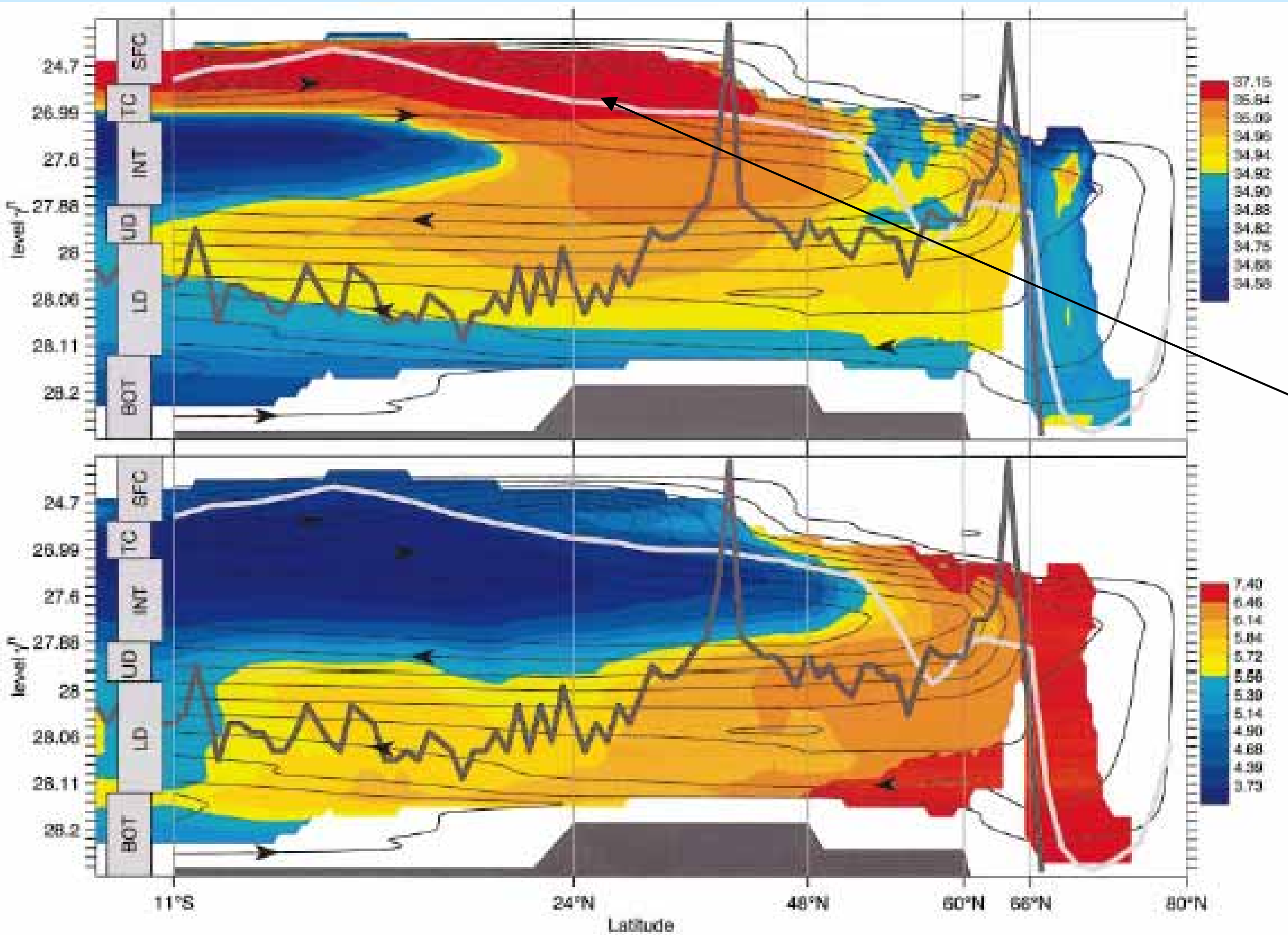


FIG. 9. Side view of the North Atlantic meridional overturning, contoured in 2-Sv intervals, superimposed on zonally averaged (top) salinity and (bottom) oxygen (mL L⁻¹) calculated from climatology (Gouretski and Jancke 1998). Light gray curve: densest outcropping layer, estimated from COADS climatology. Dark gray curve: crest of the Mid-Atlantic Ridge, including the Azores Plateau and Iceland.

*Lumpkin & Speer JPO 2003*

Figure 4. Vertical-meridional section of salinity at 24°W in the South Atlantic. Data sources are as in Fig. 2, and the heavy dashed lines are the potential density surfaces highlighted in that figure. The salinity minimum diving down at 52°S and heading north is AAIW. The salinity maximum below that, starting from the South Atlantic and rising and growing weaker into the Weddell Sea is NADW. The highlighted density surfaces were chosen to include this salinity maximum.

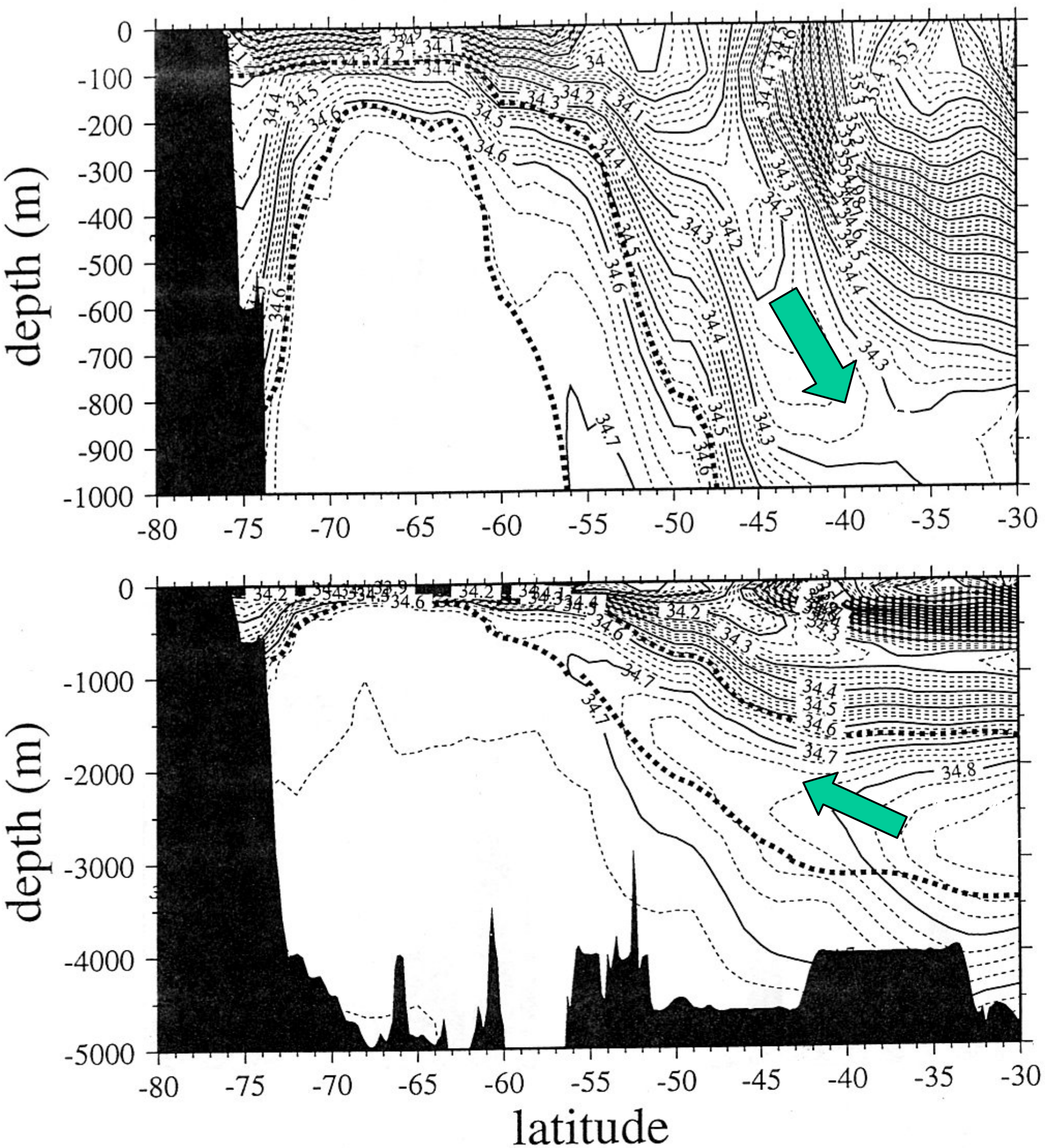


*The ACC is the only ocean current with The Problem (how to flow meridionally, given the absolute angular momentum constraint)..yet it has ample topographic bottom slopes to lean on: these clearly balance the zonal wind stress that drives this greatest of all ocean currents*

*meridional circulation implied by tracers in the Antarctic Circumpolar Current MacCready & Rhines*

# Oceanic meridional overturning strength vs. meridional baroclinic dynamic height gradient in HADCM3

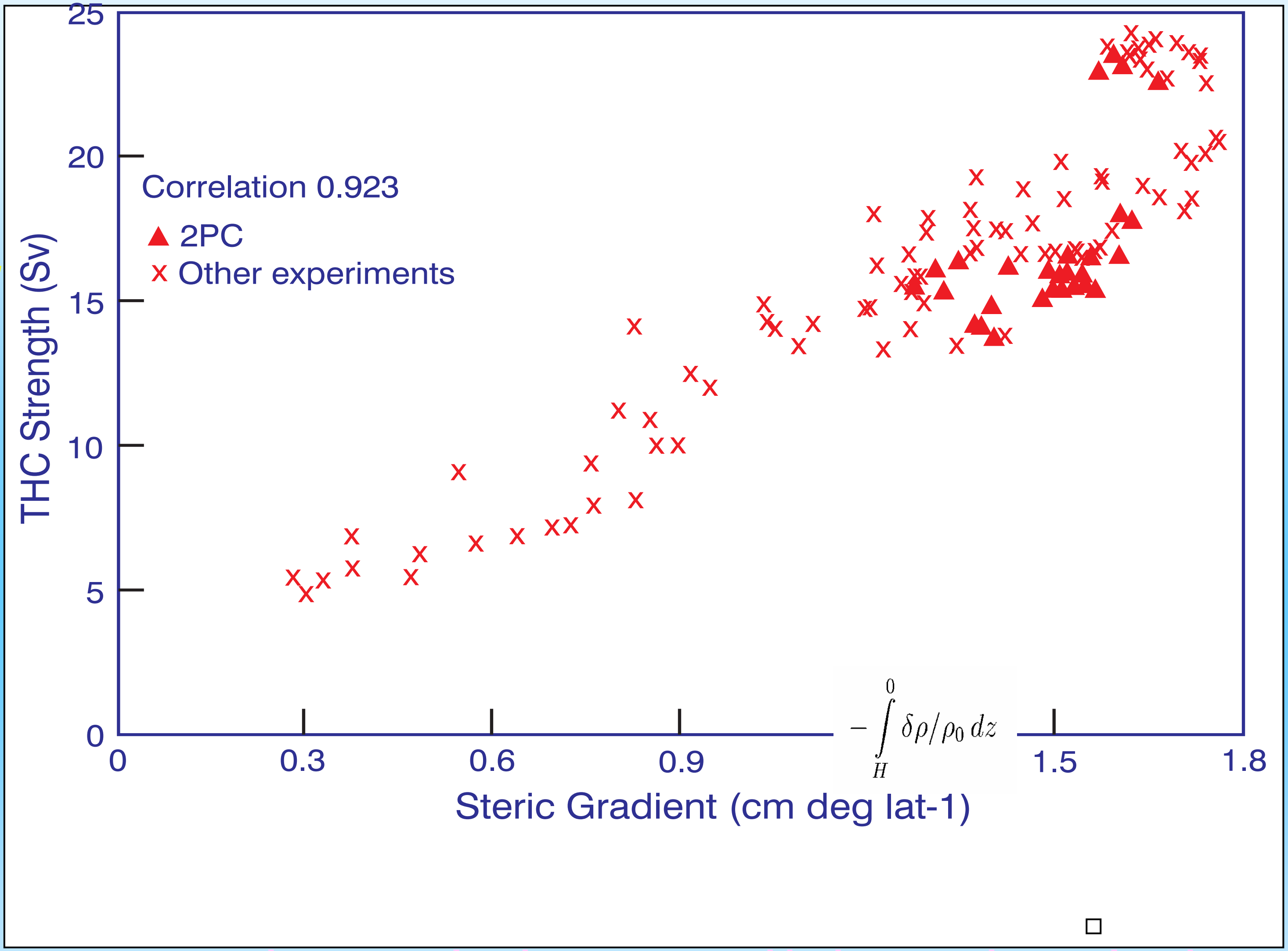


*A change in the MOC transport may be associated with some measurable change in the meridional density gradient. HadCM3 finds a very close correlation between Atlantic overturning rate and the S-N gradient of steric height from 30S - 60N through the W Atlantic. But, there is a possible oversensitivity of models to subpolar buoyancy/Labrador Sea described next.*

Spall, JPO 2004 Cooled Basin with shelf forced by inlet dense water plume: the 'MOC' of the basin is largely achieved with eddy mixing from the shelf-edge/

HERE THE MOC (AVERAGED AROUND CIRCLES) IS DOMINATED BY EDDY FLUXES

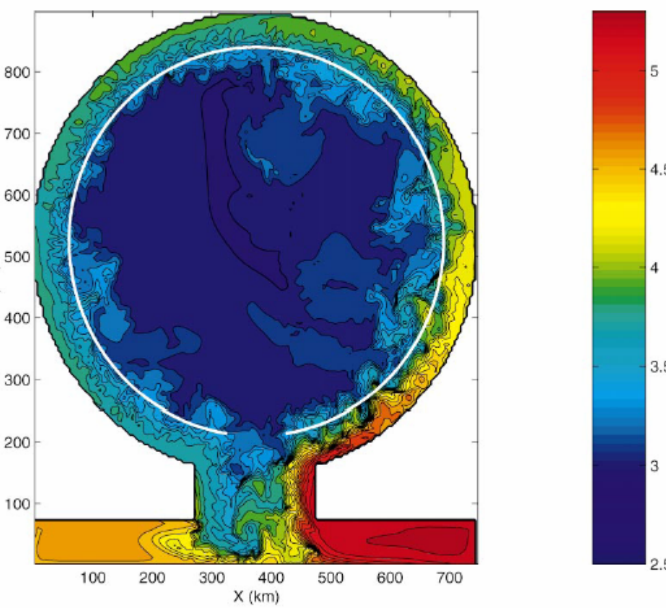


Fig. 6. Upper-level temperature (°C) at the end of the cooling period in year 22; contour interval = 0.1.

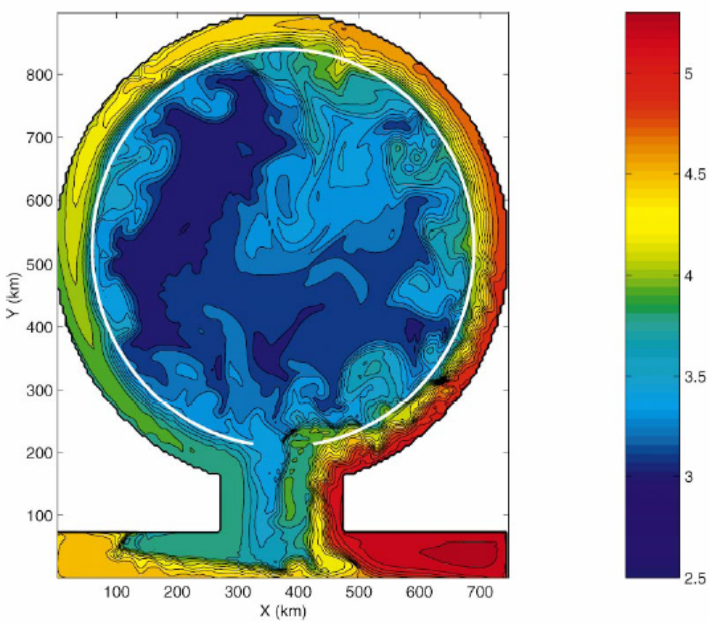


Fig. 8. Upper-level temperature (°C) at the end of month 4 in year 22; contour interval = 0.1.

The connection between primary horizontal circulation and the meridional overturning for a symmetric vortex or 2D circulation is expressed by the Eliassen-Sawyer equation (see Hoskins & Draghicci, 1972)

*As with the equations for Rayleigh-Benard convection, the overturning streamfunction and horizontal vorticity is of interest. In an axi-symmetric or 2D 'zonal channel' simulation the connection between primary horizontal circulation and the meridional overturning*

*for a symmetric vortex or 2D circulation is expressed by the Eliassen-Sawyer equation*

*(see Hoskins & Draghici, 1972)*

$$F_2^2 \frac{\partial^2 \psi}{\partial z^2} - 2S_2^2 \frac{\partial^2 \psi}{\partial z \partial y} + N^2 \frac{\partial^2 \psi}{\partial y^2} = -2Q_2^g \qquad (5)$$

where $N^2 = b_z$, $S_2^2 = -b_y = f u_{gz}$, $F_2^2 = f(f - u_{gy})$, and $Q_2^g$ is the $y$-component of the $Q$-vector

$$\mathbf{Q}^g = (Q_1^g, Q_2^g) = \left( -\frac{\partial \mathbf{u}_g}{\partial x} \cdot \nabla b, -\frac{\partial \mathbf{u}_g}{\partial y} \cdot \nabla b \right) \qquad (6)$$

introduced by *Hoskins et al.* [1978]. A geostrophic flow with a nonzero $Q$-vector will modify the magnitude of the horizontal buoyancy gradient following the equation

$$\frac{D}{Dt} |\nabla_h b|^2 = \mathbf{Q}^g \cdot \nabla_h b \qquad (7)$$

*Hoskins,Draghici &Davies QJRMS 78*

*Thomas, Tandon & Mahadavon, Revs Geophys to appear 2007*

Green's function for the E-S equation (*see Thomas et al. op cit.*)

This is one of a class of 'slow diffusion' equations in which a compact region of convection or mixing propagates outward through an interactive adjustment of the thermal balance a

like a series of geostrophic adjustment problems

$$G = \frac{1}{4\pi\sqrt{fq_{2D}}} \log|\mathrm{Arg}|$$

where

$$\mathrm{Arg} = \frac{[(y-\mathcal{Y}) - (z-\mathcal{Z})S_2^2/F_2^2]^2}{L_{SG}^2} + \frac{(z-\mathcal{Z})^2}{H^2}$$

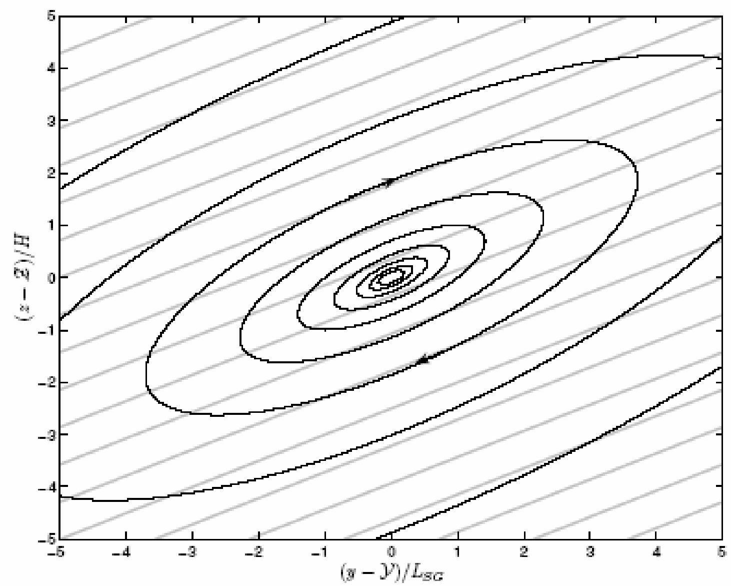


Figure 3. Ageostrophic secondary circulation $G$ driven by a negative point source $Q$-vector, $Q_2^g < 0$, at $y = \mathcal{Y}, z = \mathcal{Z}$. Isopycnals (gray contours) slant upward to the north due to a southward buoyancy gradient. For this frontogenetic forcing, $\mathbf{Q}^g \cdot \nabla_h b > 0$, the circulation is thermally direct and tends to restratify the fluid.

3D frontal instability induced by wind leads to downwelling by bolus flux, PV destruction

*Thomas et al. 2007 Revs Geophys submitted*

$$\int \int_{z=z_b}^{z=z_t} q''v''\mathrm{d}z\mathrm{d}x \sim \iint_A \nabla_h b \times \mathbf{F} \cdot \hat{k}\Big|_{z=0} \mathrm{d}y\mathrm{d}x, \qquad (27)$$

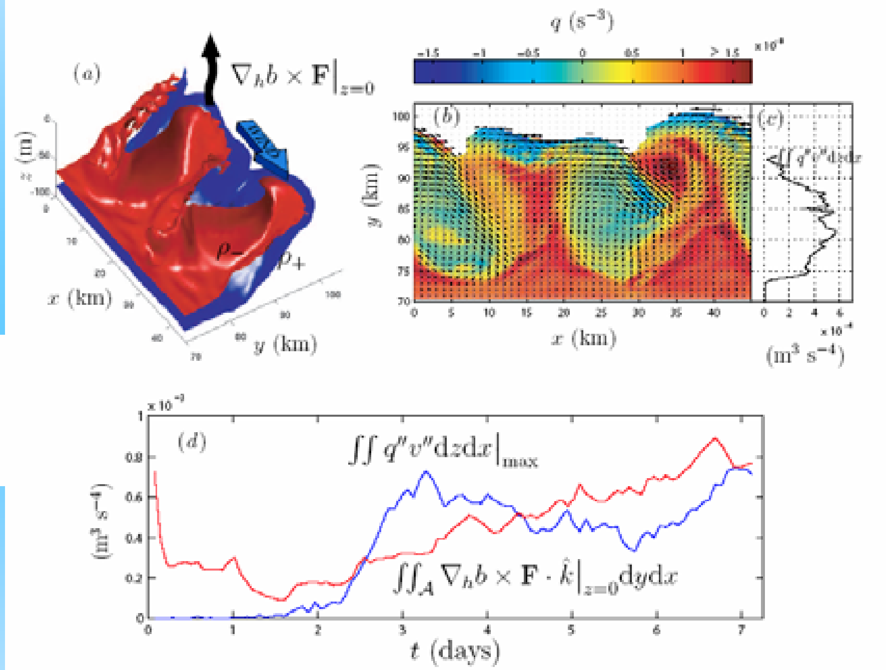


Figure 5. An example of submesoscale eddy PV fluxes driven by winds. (*a*) Down-front winds of strength 0.2 N m$^{-2}$ forcing a front induce an upward frictional PV flux, triggering frontal instabilities that distort the bounding frontal isopycnal surfaces $\rho_-$ (red) and $\rho_+$ (blue) ($\Delta\rho = \rho_+ - \rho_- = 0.2$ kg m$^{-3}$), shown here $t = 4.1$ days after the onset of the winds. (*b*) Isopycnal map of the PV (shades) and velocity (vectors) averaged in the vertical over the isopycnal layer shown in (*a*), illustrates the manner in which the instabilities subduct low PV from the surface while upwelling high PV from the pycnocline. (c) The correlation of the velocity and PV fields results in a net positive meridional eddy PV flux along the isopycnal layer $\iint q''v''\mathrm{d}z\mathrm{d}x > 0$. (*d*) A timeseries of the maximum value of the eddy PV flux with respect to $y$ (blue) and the frictional PV flux integrated over the outcrop area (red) reveal that the two fluxes scale with one another after the initial growth of the instabilities, i.e. $t > 3$ days.

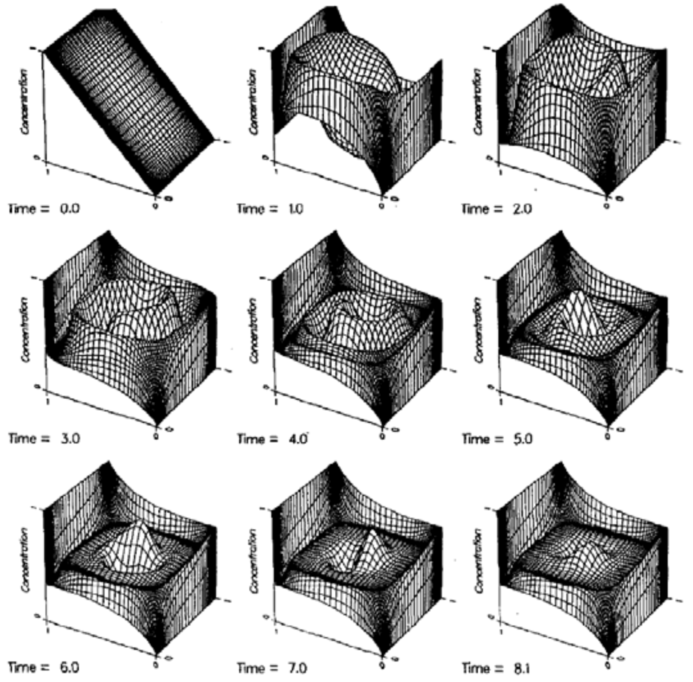


*Figure 10* The spin-up of a passive tracer in a gyre circulation with Péclet number of $2.5 \times 10^3$, based on the basin scale and interior velocity (Musgrave 1985). The ridge of high values does not follow the streamlines but represents the winding up of the initial conditions. A weak diffusive spiral crossing $\psi$-lines remains in the steady state upon the homogenized plateau. The injected boundary values can be followed through the western-boundary current, but they are quickly assimilated by horizontal mixing. The large tracer flux through the system depends on thin boundary layers, which are treated with a stretched grid.

Atmosphere-ocean coupling: heat, moisture fluxes, wind-stress

Meridional energy transport in the climate system

Is the ocean heat transport important to climate?

*Lau's JAS 1979* winter diabatic heating of the 700mb-1000mb lower atmosphere.  Peak values are 100-150 watts/m² in the subtropical storm track regions

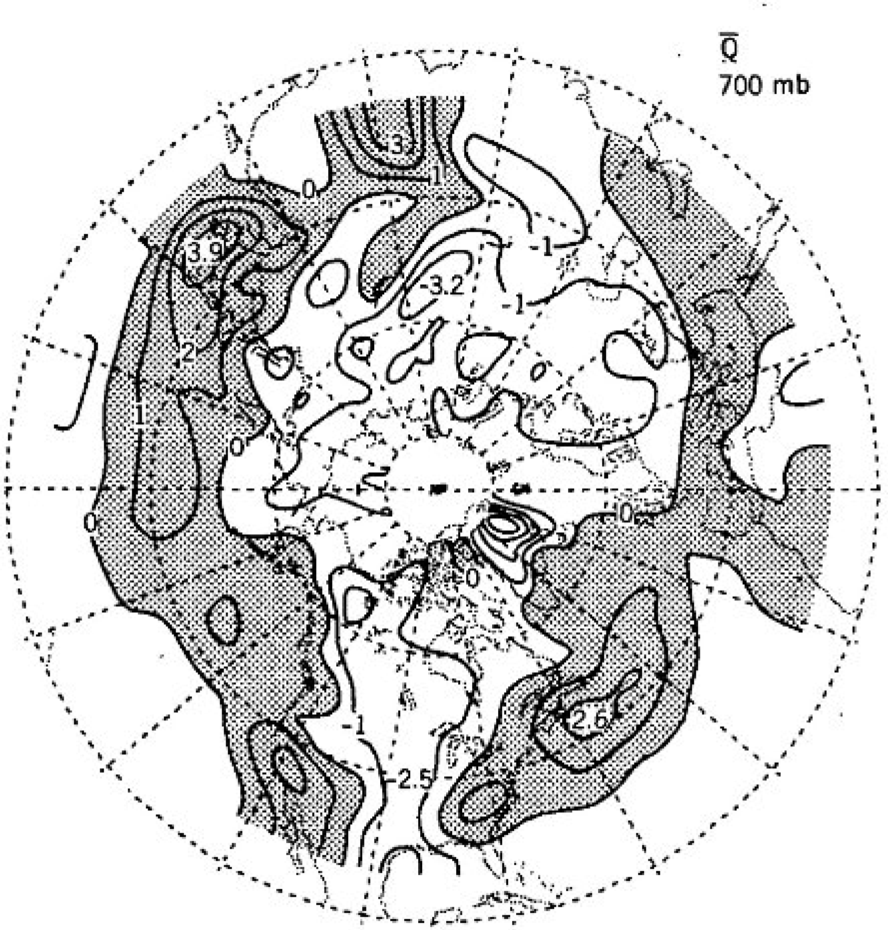


FIG. 21. Distribution of diabatic heating rate $\bar{Q}$ at 700 mb. Contour interval 1°C day$^{-1}$.

Held et al. (J.Clim.02) 100mb-1000mb diabatic heating for January

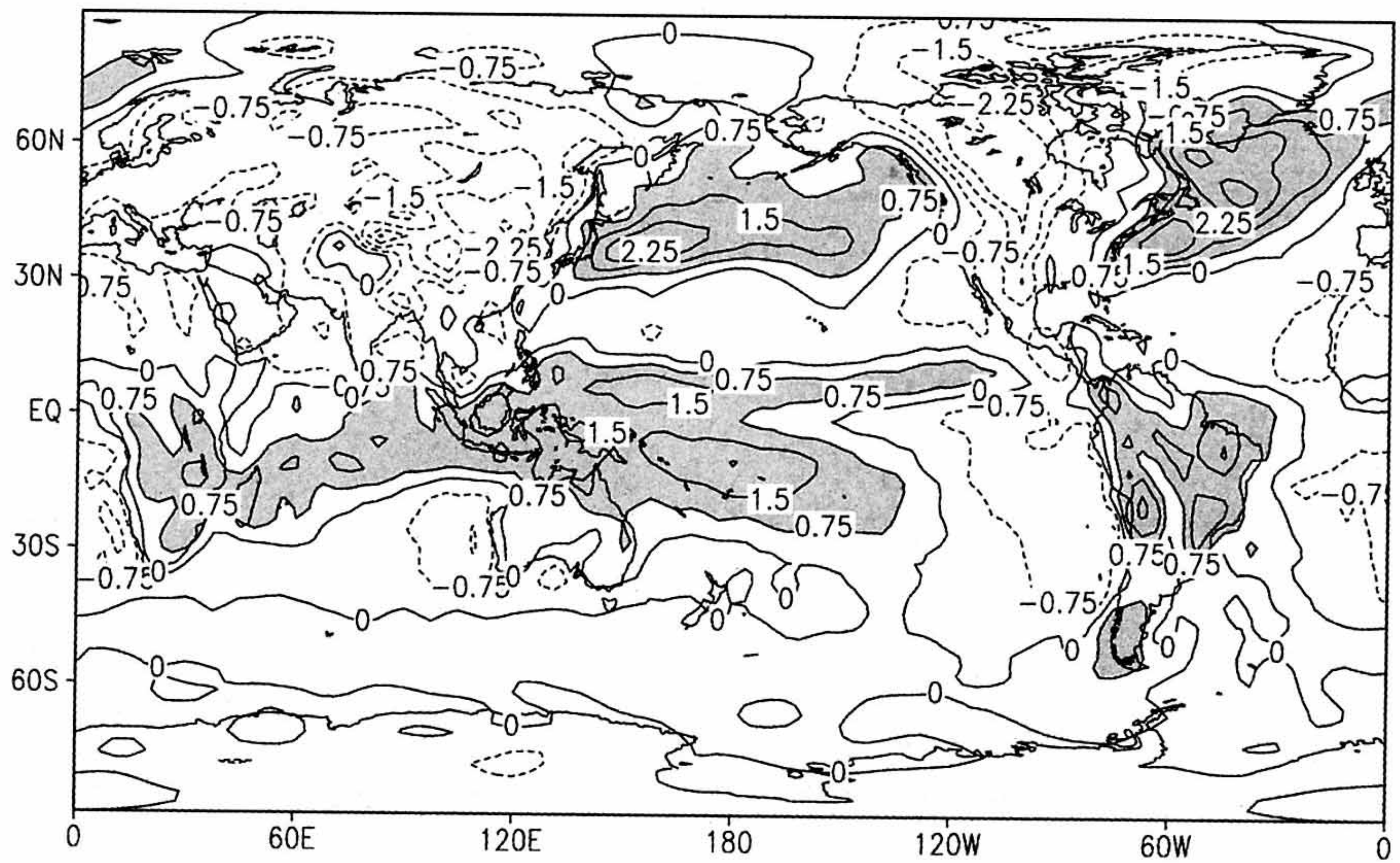


FIG. 8. The column-averaged diabatic heating field in Jan obtained from the NCEP–NCAR reanalysis as described in the appendix. The contour interval is 0.5 K day$^{-1}$.

Qnet, net atmosphere-ocean heat flux, watts/m$^2$ (Keith Tellus 95)
(annual average)

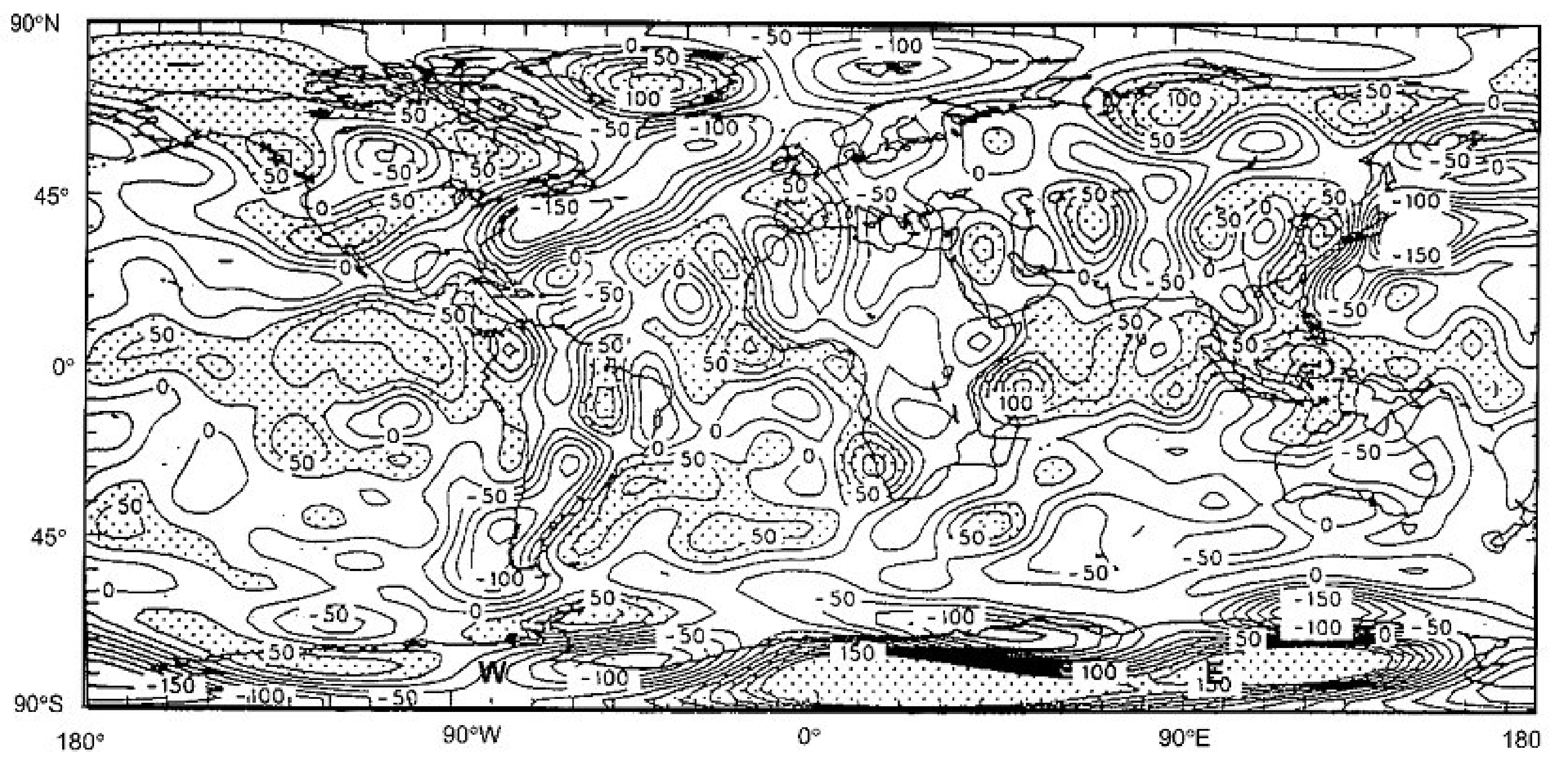


It should be noted that because the sun heats the ocean, O, but does not cool the atmosphere, A, the most useful maps of Qnet for A will differ those for O by the short-wave insolation.

(from *Thompson+Wallace J Clim 2000*)

30 year trend in advection of time-averaged
 winter temperature (925-500 Hpa av.)
..anomalous velocity and advection, cooling the ocean while warming the land in both Atlantic and Pacific sectors. Could these oceanic advective heat sources be the root cause of this contribution to global warming over Eurasia?

$$U \partial T / \partial x$$

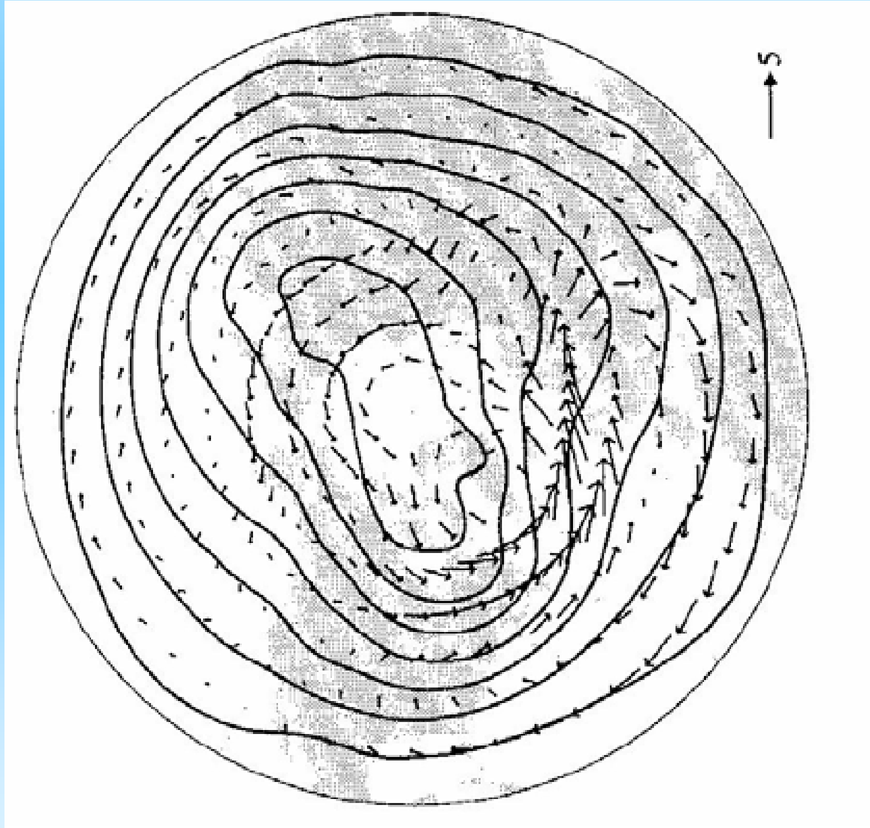


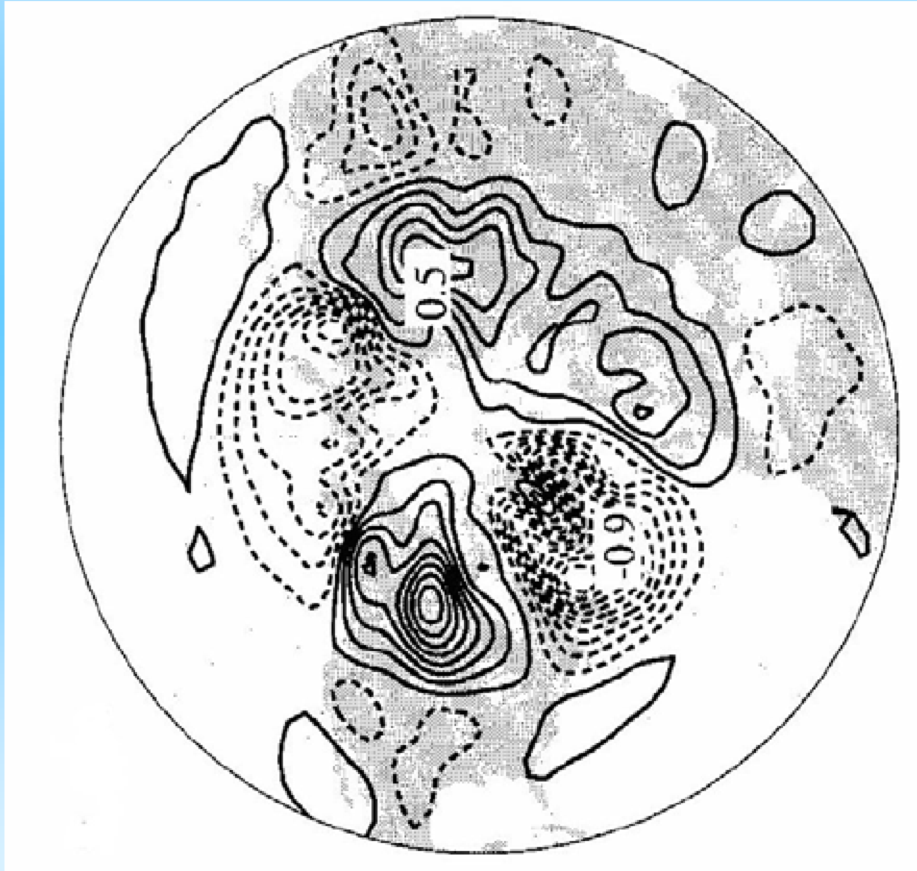

# THE END

An evacuated glass vessel with water in it illustrates the Clausius-Clapyron relation between vapor pressure of water and temperature. The water is pushed from the vessel in my hand to the ‘cold ball’, and the vapor pressure difference between the two ends is close to the hydrostatic pressure measured by the column’s vertical displacement. One can fill out the curve and see the greater sensitivity (to temperature) of water vapor production at high, ‘tropical’ temperature. This all works because we shake the vessel so that a thin film of water lies under my warm hand. It illustrates a key variable in the climate system.

When shaken this water ‘clinks’ like metal,vapor cavities opening up and slamming shut.

- **FDEPS Lectures,  November 2007**
- P.B. Rhines, Oceanography and Atmospheric Sciences, University of Washington
- Rhines@ocean.washington.edu
- www.ocean.washington.edu/research/gfd
-
- These lectures will address the dynamics of oceans and atmospheres, as seen through theory,  laboratory simulation and field observation. We will look particularly at high latitudes and climate dynamics of the ocean circulation coupled to the atmospheric storm tracks.  We will emphasize the dynamics that is difficult to represent in numerical circulation models. We will discuss properties of oceans and atmospheres that are both fundamental, unsolved questions of physics, and are also important, unsolved problems of global environmental change.
- **Lecture 1**:
- Is the ocean circulation important to global climate ? Does dense water drive the global conveyor circulation? Fundamental questions about oceans and atmospheres that are currently under debate.
-
- The field theory for buoyancy and potential vorticity.
- Basic propagators: Rossby waves and geostrophic adjustment.
- Potential vorticity: inversion and flux.
- **Lecture 2**:
- How do waves and eddies shape the general circulation, gyres and jet streams?
- Almost invisible overturning circulations.
- Lessons from Jupiter and Saturn.
- The peculiar role of mountains, seamounts and continental-slope topography.
- **Lecture 3**:
- Dynamics of ocean gyres and their relation with the global conveyor circulation.
- Water-mass transport, transformation and air-sea exchange of  heat and fresh water.
- Ocean overflows and their mixing.
- Decadal trends in the global ocean circulation.
- **Lecture 4**:
- Heat, fresh-water, ice:  convection in oceans and atmospheres and the texture of  geophysical fluids.
- **Lecture 5**:
- Teaching young students about the global environment using the GFD laboratory: science meets energy and environment in the lives of Arctic natives
- **Seminar**:
- *Exploring high-latitude ocean climate with Seagliders and satellites*

# Kelvin waves, inertial waves in shallow rotating fluid

# geostrophic adjustment: scenes from the North Pacific subtropical front region: Gregg, Brainerd, Hosegood, Alford

## Mixing Versus Mixed Layers

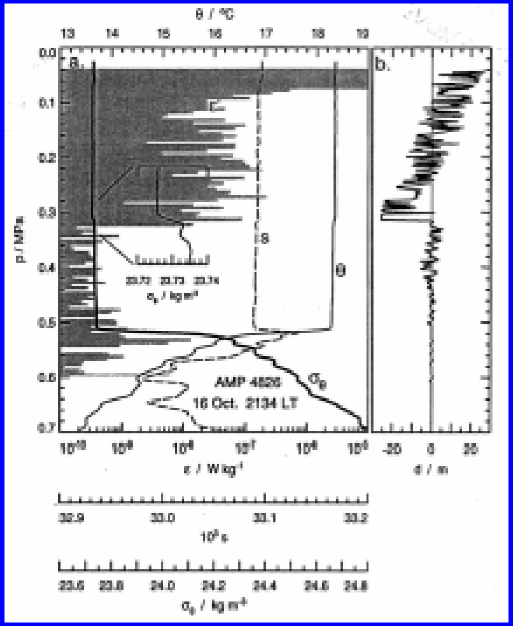


Brainerd & Gregg (1995)

- Mixed Layers: Relatively homogenous relative to deeper water, e.g., $\Delta\sigma_\theta \lesssim 0.1$ kg m$^{-3}$
- Mixing Layers: active turbulence generated at the surface, e.g., $\Delta(\log_{10}\epsilon) \leq 2$
- In this example, mixing drops where $\Delta\sigma_\theta \approx 0.001$ kg m$^{-3}$
- Mixed layers may not have been mixing for hours to days
- To compare with Ferarri & Rudnick, we considered mixed layers

3

– Because insolation accounted for only $\approx 60\%$ of restratification during a diurnal ML cycle observed with continuous microstructure profiling, Brainerd & Gregg (1993) inferred that observed $\theta S$ changes resulted from 'slumping'

– Rudnick & Ferrari (1999) and Ferrari & Rudnick (2000) reported that 20 m to 10 km ML $T$ & $S$ gradients have compensating density effects

## Rudnick & Ferrari (1999) Wavelet Coefficients

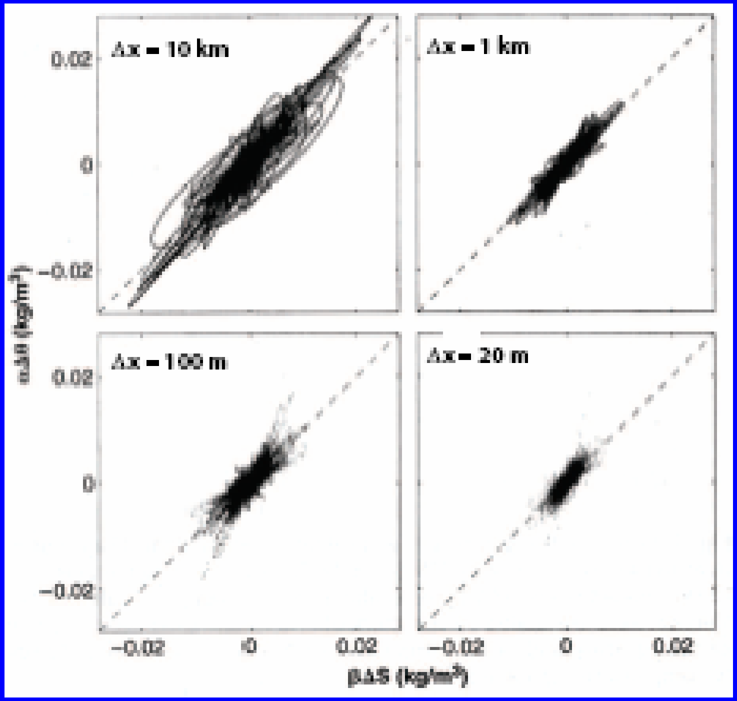


- Morlet wavelet: $e^{(x^2/2)}e^{2\sqrt{2}\pi jx}$
- Constant-depth run at 50 m
- Max variability 0.02 $\mathrm{kg\,m^{-3}}$
- All are close to $R_\rho = 1$, density compensation

Rudnick & Ferrari (1999)

# Evolution of Density Surfaces in Float-centered Coordinatess

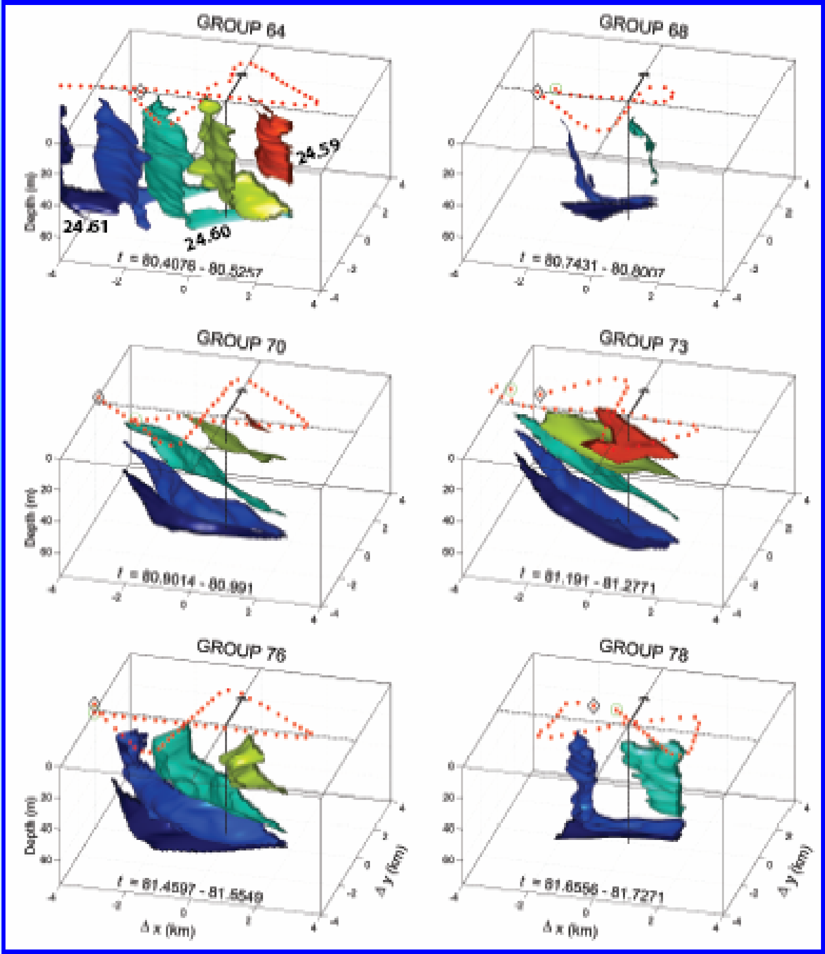


- Group 64: Convecting with vertical isopycnals
- Group 68: Slumping began just before convection ended
- Group 70: Mixed layer restratified 5.2 hours after convection ended
- Group 73: Light water added at surface
- Group 76: 8 hrs of convection homogenized top half of ML
- Group 78: 12 hrs of convection homogenized all of ML

Hosegood, Gregg, Alford (2007)

## Mixed Layer Evolution at 28 °N

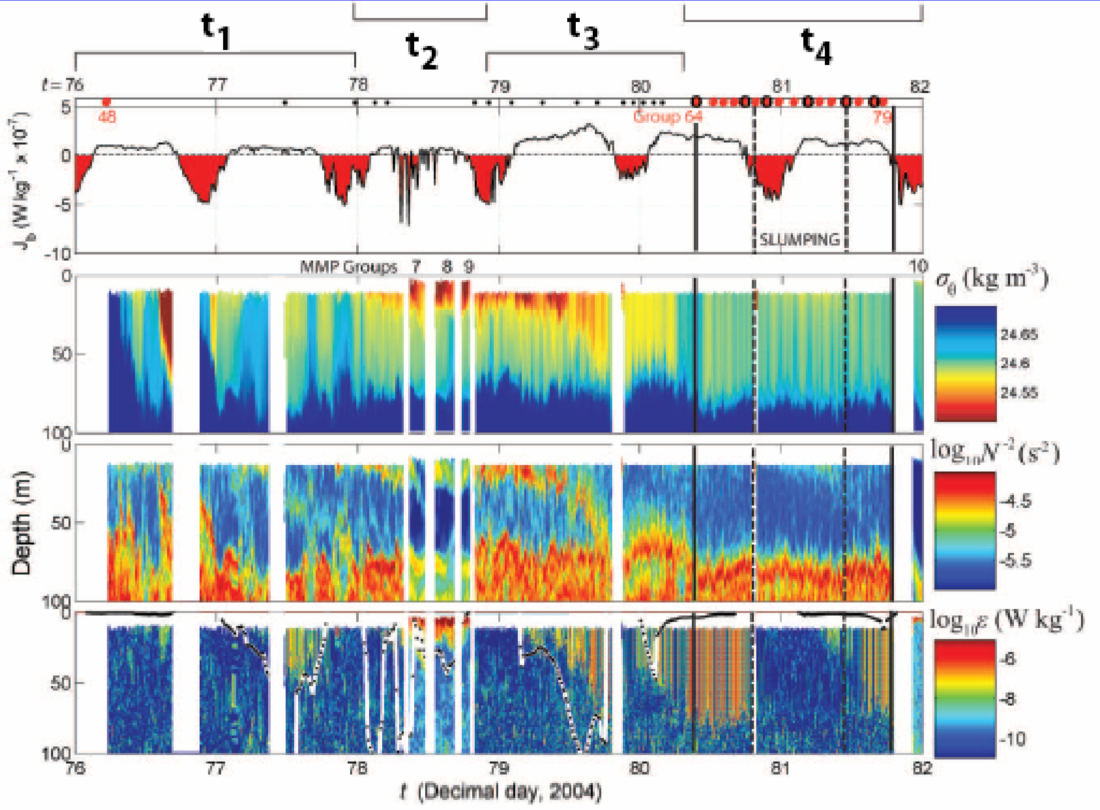


- t1: $h_m = 20 - 80$ m, light winds, weak convection
- t2: Heavy rain capped remnant ML
- t3: Winds & cold air deepened ML to 80 m
- t4: ML 'slumped' without rain or wind

Hosegood, Gregg, Alford (2007)

- $\epsilon$ estimated from scales of density overturns
- SWIMS data available below 15 m, missed restratification start during $t_4$

## Comparison with Tandon & Garrett (1994, 1995)

- Storm-driven homogenization of surface water with a horizontal buoyancy gradient, $b_x$, leaves a mixed layer with vertical isopycnals
- Geostrophic adjustment after the storm generates near-inertial motions that displace the isopycnals about their average position

$$\zeta = \frac{b_x(z + H/2)}{f^2}(1 - \cos ft)$$

- Resulting in an oscillating stratification: $N^2 = \frac{b_x^2(1-\cos ft)}{f^2}$

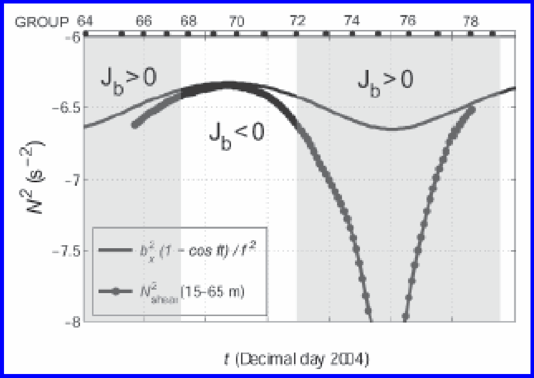


– The model does not consider a diurnal cycle after the storm

# Wavelet Coefficients Scaled by Density Contribution of $T'$, $S'$

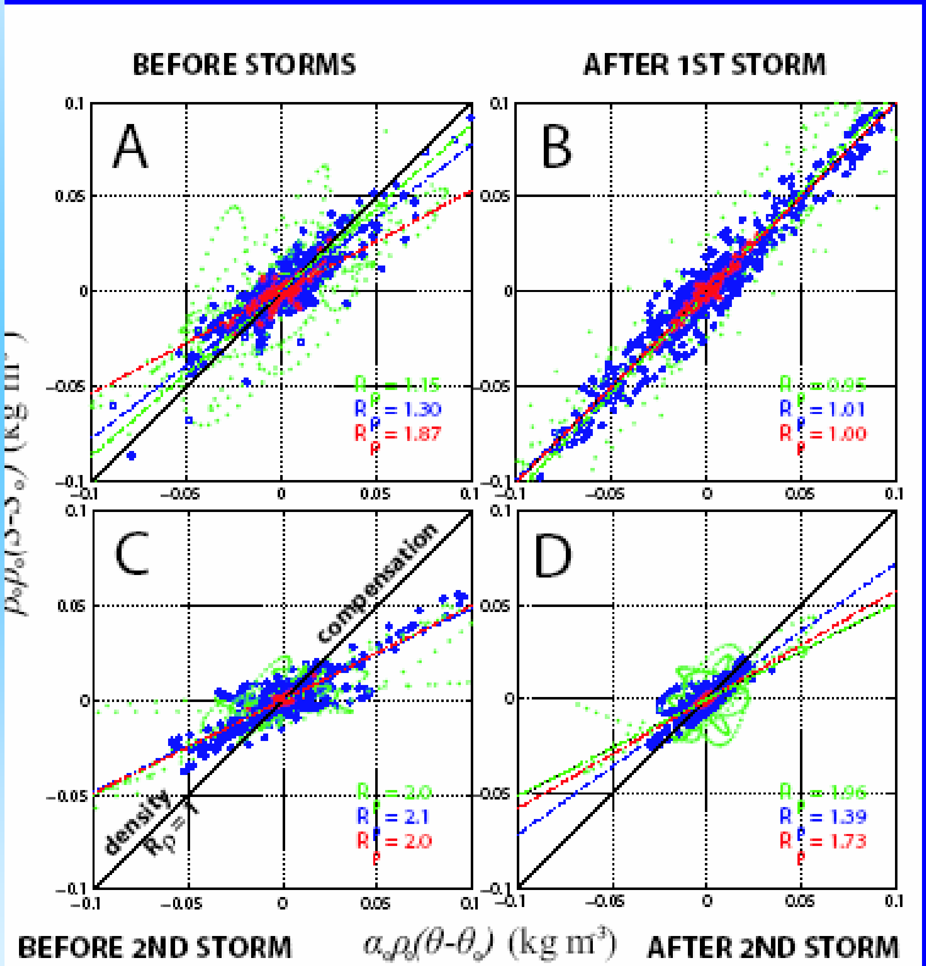


- Morlet wavelet: $e^{(x^2/2)}e^{2\sqrt{2}\pi jx}$
- Data interpolated to 20 m
- Scales are 2 km (red), 5 km (blue) and 10 km (green)
- Dash-dot lines are fits with slopes at lower right
- A & B tend to $R_\rho = 1$, consistent with northern front
- C & D tend to $R_\rho = 2$, $T$-dominated, consistent with southern front
- D conditions closest to those of Ferrari & Rudnick